IDENTIFICATION OF A NOVEL REGULATOR OF NOTCH SIGNALING IN VULVA DEVELOPMENT AND EXOGENOUS FACTORS AFFECTING GERMLINE STEM CELL PROLIFERATION IN *CAENORHABDITIS ELEGANS*

by

MADHUMATI MUKHERJEE

(Under the Direction of Edward T Kipreos)

ABSTRACT

Caenorhabditis elegans vulva development primarily requires interactions between Ras and Notch signaling pathways. Three vulval precursor cells (VPCs), P5.p, P6.p and P7.p are patterned by an epidermal growth factor (EGF) mediated 'inductive' signal and a LIN-12/Notch-mediated 'lateral' signal. The inductive signal activates the Ras–MAPK pathway in P6.p which induces 1° cell fate. The subsequent expression of Notch ligands in P6.p induces the 2° cell fate in the adjacent P5.p and P7.p cells by activating the LIN-12/Notch pathway in these cells. For proper vulval cell fate patterning, Ras inhibits Notch in the 1° cell, and Notch down-regulates Ras in the 2° cells. Excessive numbers of (or a lack of) 1° or 2° cells result in abnormal vulval phenotype. We see that inactivation of the substrate recognition subunit (SRS) LRR-1, of the cullin-RING ubiquitin ligase 2 (CRL2) complex, results in a multivulva (Muv) phenotype (~1%). We show that that LRR-1 functions in regulating vulval development by inhibiting Notch signaling via negatively regulating the transcription factor DAF-12.

C. elegans germ cells proliferate in an adult stem cell niche. In this study, we developed and utilized a primary tissue culture system that can maintain cultures of *C. elegans* germline

stem cells to identify bacterial folates as a positive regulator of germ cell proliferation. Folates are a family of B-complex vitamins. Here we show that the folate 10-formyl-THF-$Glu_{(n)}$ and the folate precursor compound dihydropteroate stimulates germ cell proliferation, while the majority of bacterial folate species cannot. The stimulation of germ cell proliferation by 10-formyl-THF-$Glu_{(n)}$ does not correlate with its role as a vitamin, as other folates that cannot stimulate germ cells are more effective in rescuing folate deficiency. Further, the folate-related compound dihydropteroate stimulates germ cell proliferation despite being incapable of participating in one-carbon metabolism. The folate receptor homolog FOLR-1 is required for the germ cell stimulatory activity, but is not essential for providing folates as vitamins. This work defines a subset of bacterial folates as exogenous signals that modulates germ cell proliferation. We also identify the steroid hormone dafachronic acid as a negative regulator of stem cell proliferation.

INDEX WORDS: *C. elegans*, vulva, LIN-12/Notch, LRR-1, DAF-12, germ stem cells, folates, FOLR-1, Dafachronic acid

IDENTIFICATION OF A NOVEL REGULATOR OF NOTCH SIGNALING IN VULVA DEVELOPMENT AND EXOGENOUS FACTORS AFFECTING GERMLINE STEM CELL PROLIFERATION IN *CAENORHABDITIS ELEGANS*

by

MADHUMATI MUKHERJEE

B.TECH., West Bengal University of Technology, India, 2007

M.S., West Virginia University, 2010

A Dissertation Submitted to the Graduate Faculty of The University of Georgia in Partial Fulfillment of the Requirements for the Degree

DOCTOR OF PHILOSOPHY

ATHENS, GEORGIA

2016

IDENTIFICATION OF A NOVEL REGULATOR OF NOTCH SIGNALING IN VULVA DEVELOPMENT AND EXOGENOUS FACTORS AFFECTING GERMLINE STEM CELL PROLIFERATION IN *CAENORHABDITIS ELEGANS*

by

MADHUMATI MUKHERJEE

Major Professor:	Edward T Kipreos
Committee:	Michael J McEachern R Kelly Dawe Douglas B Menke Scott T Dougan

Electronic Version Approved:

Suzanne Barbour
Dean of the Graduate School
The University of Georgia
August 2016

DEDICATION

I dedicate this dissertation and long years of hard work in science to my father Mr. Dibyendu Mukherjee. Thank you for giving me the opportunity to travel so far away from home so that I could achieve my dreams. Thank you for teaching me the value of hard work, patience and perseverance. Thank you for having faith in me and giving me constant encouragement, support and invaluable advice whenever I needed it.

ACKNOWLEDGEMENTS

I would like to thank my advisor Dr. Edward T. Kipreos for his guidance that has helped me hone my experimental, scientific reasoning and critical thinking skills and my ability to be an independent researcher. I would like to thank all my committee members for their advice over the years, keeping me on track in my graduate career and evaluating this dissertation. I would like to thank the past and present members of the Kipreos lab for your camaraderie, mentorship and thoughtful discussions on my projects.

My friends in Athens, GA for the last six years without whom, experiencing graduate school would not be the same. My family both in India and West Virginia, and my little brother, who mean the world to me. And finally, my husband Dr. Jared L. Wilmoth, who has been with me all these years during my PhD, and continues to support me in everything.

TABLE OF CONTENTS

Page

LIST OF TABLES

Page

LIST OF FIGURES

Page

CHAPTER 1

INTRODUCTION AND LITERATURE REVIEW

Organization of the dissertation

Sydney Brenner introduced *Caenorhabditis elegans* as a model system to the genetics community more than 40 years ago (Brenner, 1974). Since then, this roundworm has served as an invaluable tool to understand developmental biology, behavior, cell biology and physiological processes of metazoans (Wang and Sherwood, 2011). In this dissertation I present my findings on factors that regulate two difference aspects of *Caenorhabditis elegans* development- the vulva and the germline. In Chapter 1, I review the relevant literature needed to understand the signaling events and development of both these paradigms. In the first section of this chapter, I highlight important literature on the following topics that are relevant for Chapter 2: *ubiquitin mediated protein degradation*, *Cullin-Ring Ubiquitin Ligases and LRR-1* and *C. elegans vulva development (and signaling events that regulate vulva development with special significance to the Notch signaling pathway)*. Following that I present a review of the literature relevant for Chapter 3 and 4 and the topics include: *the C. elegans germline (its organization and signals regulating the germline development)*, *folates* as well as *steroid hormone signaling and dafachronic acid*.

Chapter 2 describes the ubiquitin ligase $CRL2^{LRR-1}$ as a negative regulator in Notch signaling in *C. elegans* vulva development. Chapter 3 outlines a novel cell culture media that can maintain *C. elegans* germ stem cells and describes identification of novel bacterial folates

that can stimulate germ stem cell proliferation in vivo and in vitro. Chapter 4 describes dafachronic acid as a negative regulator in germ stem cell proliferation. In Chapter 5, I discuss the implications, conclusions and future directions of the studies described in the dissertation.

Ubiquitin mediated protein degradation

Protein degradation plays a pivotal role in regulating protein homeostasis in diverse cellular processes. Ubiquitin mediated protein degradation is the key mechanism that is utilized to degrade variety of substrate proteins in the cell (Ciechanover, 1994; Rock KL, 1994). Ubiquitin (Ub) is a highly conserved 76 amino acid polypeptide, is found to express ubiquitously (Ciechanover, 1994), gets attached to proteins which the help of three enzymes (E1-E3) (Glickman and Ciechanover, 2002; Pickart, 2001). A ubiquitin-activating enzyme (E1) binds to a Ub moiety with a help of hydrolysis of one ATP; the activated Ub gets transferred to an E2 enzyme which is the ubiquitin-conjugating enzyme; the E2 brings the Ub to the substrate by binding to the E3 enzyme which is the ubiquitin-ligase, which is also responsible for binding the substrate protein (Kipreos, 2005b). E2 can either directly transfer the Ub to the substrate or in certain cases when a HECT-domain E3 is involved, transfers it to the HECT-E3 which then adds the Ub to the substrate (Kipreos, 2005b). A single Ub attached to a protein (monoubiquitination) can change its localization or function (Hicke, 2001), whereas attachment of multiple Ub moieties (poly-ubiquitination) are required to tag the protein for degradation, and can also alter function or localization (Pickart and Cohen, 2004). Poly-ubiquitination is achieved by either multiple rounds of E2 interaction with the substrate and E3, or by a fourth enzyme E4, which is a ubiquitin chain assembly factor (Koegl et al., 1999). A poly-ubiquitinated protein is targeted for degradation through the 26S proteasome (Pickart and Cohen, 2004).

Cullin-Ring Ubiquitin Ligases and LRR-1

Cullin-RING ubiquitin ligases (CRLs) are the largest known class of E3s (Bosu and Kipreos, 2008; Petroski and Deshaies, 2005). In metazoa, there are five main types of Cullins, which are each capable of forming distinct CRL complexes: SCF complexes (CUL1 based) and CRL2-5 complexes (CUL2-5 based), respectively. CRLS complexes have a RING H2 finger protein, a substrate recognition subunit (SRS) and an adapter protein (except in CUL3) that helps the SRS attached to the complex (Bosu and Kipreos, 2008). The CUL2 based complex (CRL2), which is the focus of this project, consists of four subunits: the cullin CUL2; the RING H2 finger protein Roc1/Rbx1; the adaptor Elongin C that is bound to Elongin B; and multiple SRSs that binds substrates (Bosu and Kipreos, 2008; Petroski and Deshaies, 2005).

LRR-1 is a leucine rich repeat protein, which was shown to be a substrate recognition subunit (SRS) for a *C. elegans* $CRL2^{LRR-1}$ complex (Starostina et al., 2010). The mammalian ortholog of LRR-1, LRR1, was also shown to interact with CUL2 as an SRS (Kamura et al., 2004). LRR-1 interacts with Elongin C (ELC-1), the adapter protein for the CRL2 complex. The *lrr-1(tm3543)* mutant is a recessive deletion null allele, which is predicted to generate a truncated LRR-1 protein lacking 66% of the C-terminal residues. *lrr-1* is an essential gene (Piano et al., 2002) and the null mutant has to be maintained as a heterozygote. *lrr-1* homozygous progeny from *lrr-1(tm3543)* heterozygous parents, become sterile adults. *lrr-1* homozygotes have a protruding vulva phenotype and only produce about 15 vulva cells compared to 22 in wild-type animals (Starostina et al., 2010).

***C. elegans* vulva development**

Overview of C. elegans vulva patterning

The development of the hermaphrodite vulva involves a set of six equipotent vulval precursor cells (VPCs), P3.p-P8.p, and a gonadal anchor cell (AC) (Fig. 1.1A) (Sternberg, 2005). The VPCs adopt a precise spatial pattern from anterior to posterior: 3°-3°-2°-1°-2°-3°. This highly invariant pattern is established primarily by two signals: (1) An inductive signal from the AC acts in a graded fashion and prompts the VPC closest to it (P6.p) to adopt a 1° cell fate; and (2) a lateral signal from P6.p prompts the neighboring P5.p and P7.p cells to assume 2° fates. The remaining VPCs, P3.p, P4.p and P8.p, assume non-vulval 3° fates (Sternberg, 2005) (Fig. 1.1B). Once the VPCs are specified, P5.p, P6.p, and P7.p undergo 3 rounds of division to produce the adult vulval tissue, which consists of 22 nuclei. The 3° cells generate two daughter nuclei, which fuse with the large hypodermal synctium (hyp7) (Sternberg, 2005; Sternberg and Horvitz, 1989).

Ras and Notch signaling patterns the developing vulva

A combination of Ras and Notch signaling results in the invariant 2°-1°-2° pattern seen in the wild-type *C. elegans* vulva (Fig.1.1C). The AC in the gonad is the key organizer of vulval development and morphogenesis. The AC produces an epidermal growth factor (EGF)-like ligand LIN-3, which serves as the "inductive" signal to stimulate LET-23/EGFR and the Ras pathway in the VPC closest to it (P6.p) (Sternberg, 2005). *let-23* encodes a receptor tyrosine kinase that transduces the inductive signal into a downstream cascade involving the Ras–MAP kinase pathway. LET-60 is the *C. elegans* Ras protein that activates LIN-45/Raf, which in turn activates MEK-2/MEK, which activates MPK-1/ERK (MAP kinase). The inductive signal through the Ras pathway leads to changes in gene expression downstream of the MAP kinase

cascade resulting in P6.p adopting a 1° fate, but the precise mechanism of 1° fate specification is unknown (Sundaram, 2006).

The *lin-12* gene codes for a Notch transmembrane receptor (Yochem et al., 1988) that is activated by multiple Delta/Serrate/LAG-2 (DSL) ligands (Chen and Greenwald, 2004). Notch signaling mediates cell-cell interaction during developmental processes in many organisms, including the *C. elegans* vulva development (Lai, 2004). The DSL ligands involved in vulval development comprise LAG-2, APX-1 as well as the soluble, secreted ligand DSL-1, all of which play redundant roles during vulva development (Chen and Greenwald, 2004).

LIN-12/Notch has two roles in vulva development. LIN-12 first specifies the AC through interactions between two cells in the somatic gonad, Z1.ppp and Z4.aaa. One of these cells becomes the future AC and the other becomes a vulval uterine (VU) cell through LIN-12 and LAG-2 mediated signaling (Greenwald, 2005). Initially both the precursor cells express both *lin-12* and *lag-2* transcripts; stochastic differences in the activity of LIN-12 between the two cells initiates a feedback mechanism, whereby LIN-12 activation by LAG-2 in the presumptive VU cell positively transcribes *lin-12* and downregulates *lag-2* transcription (Wilkinson et al., 1994). Loss-of-function mutations of *lin-12* causes two ACs to be specified and gain-of-function mutations of *lin-12* causes two VUs to form (Seydoux and Greenwald, 1989; Wilkinson et al., 1994).

In the VPCs, LIN-12/Notch promotes the 2° cell fate. Upon receiving the inductive signal, P6.p transcribes the Notch/DSL ligands that activate LIN-12/Notch receptor in P5.p and P7.p (Chen and Greenwald, 2004). A key step in this process is the endocytosis-mediated downregulation of the LIN-12 receptor in response to LET-23–Ras activation in P6.p to allow the DSL ligands to be active (Shaye and Greenwald, 2002). In the P5.p and P7.p cells, which

receive the DSL signal, ligand binding by LIN-12 leads to γ-secretase mediated cleavage of the LIN-12 receptor and release of the Notch intracellular domain (NICD) (Kopan and Ilagan, 2009). NICD then travels to the nucleus where it associates with the CSL (CBF1/Su(H)/LAG-1) transcription factor LAG-1. The hetero-complex of LIN-12 and LAG-1 drives the expression of various lateral signal target (*lst*) genes, which specify 2° cell fate (Berset et al., 2001; Kopan and Ilagan, 2009; Yoo et al., 2004). However, the precise mechanism by which this fate is decided is still unknown. The lst genes *lip-1*, *ark-1*, *dpy-23* are also of Ras-MAPK inhibitor genes that help maintain 2° cell fate in P5.p and P7.p (Greenwald, 1997, 2005; Kimble and Simpson, 1997).

Mutations in either the Ras–MAPK and LIN-12/Notch pathway are responsible for abnormal vulval phenotypes (Fig. 1.1D). Mutations that decrease EGF–Ras–MAPK signaling (e.g., in *lin-3, let-23,* and *let-60*) gives rise to a Vulvaless (Vul) phenotype, as all cells become 3º (Aroian et al., 1990; Beitel et al., 1990; Han et al., 1990; Hill and Sternberg, 1992; Sternberg, 2005). In fertile Vul hermaphrodites, eggs hatch inside the mother and eventually escape after the death of the mother, caused by the hatched larvae eating the insides of the mother (Sternberg, 2005). Gain-of-function alleles of genes in the Ras pathway cause Multivulva (Muv) phenotype wherein additional VPCs assume the 1º fate (Beitel et al., 1990; Han and Sternberg, 1990; Hill and Sternberg, 1992; Katz et al., 1996). *lin-12* gain-of-function mutations cause additional VPCs to adopt the 2º fate causing a Muv phenotype, as well as a failure to specify an anchor cell. Conversely, *lin-12* null alleles fail to exhibit 2º fate (Greenwald et al., 1983; Sternberg, 2005).

Regulation of LIN-12/Notch activity

LIN-12/Notch needs to be cleaved and sorted before it can carry out signaling. *C. elegans* has two Notch receptors (LIN-12 and GLP-1), *Drosophila* has one and humans have

four Notch paralogs (Chillakuri et al., 2012). N terminal domains of all Notch proteins have a number of epidermal growth factor (EGF)-like repeats which mediate interaction with the ligand (Kopan and Ilagan, 2009). The EGF-repeat region is followed by a negative regulatory region (NRR), which is composed of cysteine rich Lin12-Notch repeats (LNR) and a hetero-dimerization domain (HD). This region is close to the plasma membrane and is necessary for preventing activation of the Notch receptor in the absence of a ligand by hiding the S2 cleavage site from the ADAM metalloprotease (Chillakuri et al., 2012; Kopan and Ilagan, 2009; Sanchez-Irizarry et al., 2004). *sup-17* codes for the *C. elegans* ADAM family protease (Greenwald, 1998). In mammals, TACE, a paralog of SUP-17, has been shown to cleave Notch in biochemical assays (Brou et al., 2000). Next to the NRR region is a single transmembrane domain (TMD), followed by the Notch intracellular domain (NICD) (Chillakuri et al., 2012). The S3 cleavage site lies within the TMD where γ-secretase cleaves and releases the NICD (Chillakuri et al., 2012). Presilin is thought to be a core component of the γ-secretase protease complex (Kopan and Goate, 2000). *sel-12* and *hop-1* are two *C. elegans* presenilin genes that act redundantly to facilitate LIN-12/Notch signaling (Li and Greenwald, 1997; Westlund et al., 1999).

The newly synthesized Notch receptor has to travel from the endoplasmic reticulum (ER) to the Golgi, from where it matures and has to then reach the plasma membrane to be expressed as a cell-surface receptor (Andersson et al., 2011). In *C. elegans*, two negative regulators of LIN-12/Notch are involved in making sure that only a mature receptor reaches the cell surface. *sel-9* codes for a p24 like protein, and is hypothesized to prevent mis-folded LIN-12 and GLP-1 proteins from reaching the Golgi (Wen and Greenwald, 1999). *sel-2* codes for the *C. elegans* homolog of two mammalian proteins Neaurobeachin and LRBA which are involved in endosomal trafficking of LIN-12/Notch in polarized epithelial cells such as the VPCs, that

ensures the proper delivery of LIN-12/Notch to the lysosomes and maintaining an appropriate steady-state level of protein on the cell surface (de Souza et al., 2007).

EGFR-Ras-MAPK-mediated downregulation of the LIN-12/Notch receptor in the presumptive 1º vulval cell is crucial for proper activation of lateral signaling (Shaye and Greenwald, 2002). The intracellular region of the Notch receptor contains a downregulation target signal sequence or DTS, in which a di-leucine motif is responsible for proper endocytic trafficking of the Notch receptor and lysine residues near the DTS are required for its degradation (Shaye and Greenwald, 2002). In *C. elegans*, the internalization of Notch receptor also requires phosphorylation of serine/threonine residues near the DTS. This is contrast to what has been shown in *Drosophila*, which lacks a di-leucine motif and NEDD4 is required to ubiquitinate Notch receptor at a terminal PPXY site (Sakata et al., 2004). Deletion of the DTS in LIN-12 results in mis-localization of the Notch receptor to the apical membrane of the vulva cells and a compromised lateral signaling (Shaye and Greenwald, 2002).

LIN-12/Notch is negatively regulated by *sel-10*, which was identified in a genetic screen for suppressors of *lin-12* hypomorphs in *C. elegans* (Hubbard et al., 1997; Sundaram and Greenwald, 1993). SEL-10 is a member of the F-Box/WD40 repeat containing protein that works in an SCF (CUL1-containing) complex and directly binds NICD (Hubbard et al., 1997). The Mammalian ortholog of SEL-10, Fbw7, has been shown to promote ubiquitin-mediated turnover of NICD after phosphorylation of the PEST domain (Gupta-Rossi et al., 2001; Oberg et al., 2001; Wu et al., 2001). The cyclin dependent kinase CDK8 is responsible for hyper-phosphorylating NICD in its C-terminal PEST domain, which then makes the phosphorylated NICD a target for ubiquitin-mediated degradation by Fbw7 through the proteasome (Fryer et al., 2002; Fryer et al., 2004). NICD degradation disassembles the Notch transcriptional complex

thereby quenching all downstream signals (Kopan and Ilagan, 2009; Weng et al., 2004). This is an interesting mechanism to prevent unnecessary activation of Notch signaling, as continued Notch activity can be deleterious to the cell (Kopan and Ilagan, 2009). It is therefore not surprising that mutations in the C-terminal domain that stabilize the NICD cause are found in cancerous tissues such as in T-cell acute lymphoblastic leukemia (T-ALL) in humans (Weng et al., 2004).

The *C. elegans* germline

Germline development and organization

The germ line in *C. elegans* is specified from one primordial germ cell (PGC) called P4, which is segregated during embryogenesis. The P4 is also called the "germline founder cell" as it eventually gives rise to all the germ cells in the body, and does not contribute to the soma (Hubbard and Greenstein, 2005; Kimble and Crittenden, 2005). P4 divides in the embryo to give rise to Z2 and Z3 cells, which begin to divide in the mid-L1 larval stage under favorable growth conditions. After an exponential increase in germ cell numbers through the L1 and L2 larval stages, the proximal germ cells enter meiosis. This differentiates the germline into a distal region, which maintains a pool of proliferating mitotic cells, and a proximal region containing meiotic cells (Kimble and Crittenden, 2005). The germline in *C. elegans* is syncytial with each nuclei enclosed partially by a plasma membrane allowing a common opening to the central cytoplasm called the rachis (Hirsh et al., 1976). Each nucleus with its surrounding cytoplasm and membrane is referred to as a "germ cell". In spite of the germ cells being syncytial, the individual cells do not seem to communicate to each other, as they do not undergo synchronous cell divisions (Hubbard and Greenstein, 2005). Having a germline syncytium poses challenges

to studying the biology of the germ stem cells, as experiments involving transplantation and repopulation, as well as lineage tracing of germ cells is difficult to perform (Hansen and Schedl, 2013).

The adult germline in the hermaphrodite is divided into two gonadal arms and the males have only one gonad arm (Kimble and White, 1981). The proliferative cells are maintained in the distal region, which is also referred to as the *mitotic* or *proliferative* zone. In an adult hermaphrodite (24 hrs post adulthood), this distance is measured to be about 20 cell diameters from the distal end, housing about 200-250 cells (Michaelson et al., 2010). These cells are the mitotic stem cell population of the germline that self-renew and can differentiate into sperm and oocytes in an adult hermaphrodite (Eckmann et al., 2002; Hansen et al., 2004b; Kimble and Crittenden, 2005; Lamont et al., 2004). As the cells leave the proliferative zone, they enter a *transition zone*, which has some mitotic and some meiotic cells, where the chromosomes start pairing, giving the cells a characteristic crescent-shape (Crittenden et al., 2006; Dernburg et al., 1998; Francis et al., 1995). This region is also called the "meiotic entry region" (Hansen et al., 2004a). Proximal to the transition zone, the germ cells go through meiotic prophase and differentiate to yield mature oocyte and sperm (Boag et al., 2005; Kimble and Crittenden, 2007; Kipreos, 2005a) (Fig 1.2).

The stem cell niche and Notch signaling control germline proliferation

Like stem cell populations in many organisms, the *C. elegans* germline stem cells are maintained within a niche specified by a single somatic gonadal cell called the distal tip cell (DTC), which maintains the proliferative pool of germ cells (Kimble and White, 1981). A single DTC is present at the distal end of each gonad arm in the hermaphrodite. Laser ablation of the DTCs

causes all germ cells to differentiate, whereas mis-location of DTC can cause ectopic germline proliferation (Kimble and White, 1981). The DTC has elaborate cytoplasmic extensions (similar to cytonemes) that reach out over the proliferative zone and end before the meiotic zone begins (Byrd et al., 2014; Kimble and Seidel, 2013). Proximity of the germ cell to the region defined by the DTC extensions determines whether they proliferative or differentiate; germ cells close to the DTC remain undifferentiated whereas those further away enter meiosis (Crittenden et al., 2006; Kimble and White, 1981; McGovern et al., 2009).

GLP-1/Notch signaling in the DTC-defined niche maintains germ stem cell proliferation (Kimble and Crittenden, 2005). GLP-1 is the Notch receptor, which is expressed on the surface of germ cells and is activated by the Notch ligand LAG-2, which is expressed in the DTC (Crittenden et al., 1994; Henderson et al., 1994; Nadarajan et al., 2009; Tax et al., 1994). Upon activation, GLP-1/Notch initiates Notch signaling similar to what has been described in many organisms (Kopan and Ilagan, 2009). The cleaved NICD of GLP-1 binds to the CSL DNA binding protein LAG-1 and its transcriptional partners LAG-3/SEL-8 and activates transcription (Christensen et al., 1996; Doyle et al., 2000; Petcherski and Kimble, 2000). *glp-1* loss-of-function mutations as well as those that inhibit the Notch signaling, cause all germ cells to enter meiosis (Austin and Kimble, 1987; Doyle et al., 2000; Lambie and Kimble, 1991; Petcherski and Kimble, 2000). Conversely, in *glp-1* gain-of-function mutants, the proliferative zone extends throughout the gonad and animals display germline tumors (Berry et al., 1997). GLP-1 activates the ERK/MAPK inhibitor *lip-1* (Berset et al., 2001; Lee et al., 2006), which is required for germline proliferation; the RNA binding protein *fbf-2* (Lamont et al., 2004) (discussed below); as well as *lst-1* and *sygl-1*, which maintain the mitotic pool of germ cells (Kershner et al., 2014). *lst-1* (*lateral signal target*) encodes a Nanos-like RNA binding protein, but unlike canonical

Nanos, only has one zinc-finger domain (Curtis et al., 1997; Kershner et al., 2014) whereas *sygl-1* (*synthetic glp*) did not have any predicted domains, making both of them somewhat novel proteins that regulate germ stem cells (Kershner et al., 2014). Both *lst-1* and *sygl-1* are expressed in response to GLP-1/Notch signaling and are required redundantly to maintain stem cell state (Kershner et al., 2014).

Several RNA-binding proteins contribute to regulating the mitotic vs. meiotic fate of the germ cells. The main contributors are GLD-1, GLD-2, GLD-3, FBF-1, FBF-2, and NOS-3 (Kimble and Crittenden, 2005). GLD-1 binds to the 3' UTR of *glp-1* mRNA and downregulates *glp-1* translation in the cells entering meiosis; therefore *glp-1* protein expression is restricted only to mitotic cells (Crittenden et al., 1994; Marin and Evans, 2003). GLD-2 is a cytoplasmic poly-A polymerase (Wang et al., 2002) that works in a complex together with GLD -3, a Bicaudal C-related protein, to promote meiotic entry (Eckmann et al., 2004). The FBF proteins belong to the PUF family of RNA binding proteins (Pumilo and FBF) (Wickens et al., 2002; Zhang et al., 1997) that are known to bind the 3'UTRs of the *gld-1* and *gld-3* mRNAs and repress their translation (Crittenden et al., 2002; Eckmann et al., 2004; Wickens et al., 2002). The 5' UTR of *fbf-2* possesses LAG-1 binding sites making it a direct transcriptional target of GLP-1/Notch signaling (Lamont et al., 2004). FBF-1 and FBF-2 can repress each other, as the 3'UTRs of both genes have FBF binding sites (Lamont et al., 2004). Both FBF-1 and FBF-2 have redundant but distinct roles in maintaining mitotic signature of the germ stem cells; loss of either FBF alone has no obvious effect on the germ stem cell identity, but removal of both FBF-1 and FBF-2 causes all germ stem cells to enter meiosis and differentiate (Crittenden et al., 2002; Kimble and Seidel, 2013; Lamont et al., 2004). NOS-3 is related to the *Drosophila* translational

regulator Nanos that indirectly activates GLD-1 to favor meiotic entry of germ cells (Hansen et al., 2004a; Kraemer et al., 1999).

Nutritional signals regulate germline development

Germline development in *C. elegans* is tightly linked to environmental signals and these are relayed by a variety of signaling pathways including Insulin/IGF signaling (IIS), AMPK, TGFβ, and TOR–S6K, as well as nuclear hormone pathways (Hubbard et al., 2013). In the wild, *C. elegans'* life cycle has a feast-or-famine quality, in which animals will feast on the bacteria in rotting fruit or stems when available, and then their progeny will wait for the next rotting fruit (Hubbard et al., 2013). In the laboratory, *C. elegans* is fed a monoxenic diet of the B-type *E. coli* OP50 (MacNeil et al., 2013). When food is plentiful, the proliferative zone in the germline develops rapidly in the L3 and L4 stages and reaches approximately 200 cells per gonad arm by the end of the L4 stage (Hansen et al., 2004a; Killian and Hubbard, 2005). This rapid growth of the germ stem cell population under feasting conditions is relayed by IIS and its receptor *daf-2*/Insulin-IGF-like receptor (IIR), which promotes larval germ cell cycle (Michaelson et al., 2010). Two prominent ligands *ins-3* and *ins-33* bind to the insulin receptor DAF-2 to inhibit the activity of the DAF-16/FOXO transcription factor via the canonical PI3K pathway (Michaelson et al., 2010). TGFβ, on the other hand, has no effect on germ cell cycle control but works on the DTC to control germ cell proliferation in a non-cell autonomous manner (Dalfo et al., 2012). The TGFβ ligand (DAF-7) is expressed in sensory neurons, and binds to its receptor (DAF-1) that is expressed in the DTC. TGFβ signaling in the DTC inhibits the activity of the Co-Smad/Sno-Ski (DAF-3/DAF-5), thereby promoting germ cell proliferation (Dalfo et al., 2012).

Food deprivation severely impairs the ability of the *C. elegans* germline to accumulate germline progenitor cells in the larval stages (Korta et al., 2012). TOR (Target of Rapamycin) is a serine/threonine kinase that is known to incorporate cues from food availability and control cell division; TOR function is conserved from yeast to mammals (Hubbard et al., 2013). Under nutrient rich conditions, TOR and its signaling partners RAPTOR (regulatory associated protein of TOR) and S6K (p70 ribosomal S6 kinase) function in a germ cell autonomous fashion to maintain the pool of germline progenitor cells by promoting larval germ cell proliferation and inhibiting differentiation (Korta et al., 2012). Bacterial deprivation (i.e., food deprivation) severely reduces the number of germline progenitor cells; loss of the TOR or RAPTOR homolog causes a similar loss of germline progenitor cells, a mechanism that is dependent on the SK6 homolog (Korta et al., 2012). The TOR pathway was shown to work independently of GLP-1/Notch signaling to maintain the proliferative germ cell pool (Hubbard et al., 2013).

Folates

Folates and one carbon metabolism

Folates are a class of closely related B-group vitamins that are synthesized by bacteria, plants, fungi, protozoa, and archae (Rossi et al., 2011). Folates are required in the one-carbon metabolism cycle in every living organism to produce nucleosides, several amino acids, and the methyl donor S-adenosyl methionine (Selhub, 2002). Folates are composed of a pteridine ring, para-aminobenzoic acid (PABA), and one or more glutamate residues (Nazki et al., 2014). Animals cannot synthesize folates (Brzezinska et al., 2000) and therefore must acquire them either through their diet or microbiota. Folate deficiency causes improper functioning of the one-carbon metabolism pathway leading to developmental abnormalities such as failure to close

the neural tube, and pathologies that include cancer and cardiovascular diseases (Stover, 2004). The United States, Canada, and Chile mandated fortification of grains and cereals with the synthetic folate folic acid in 1998, 1999 and 2000, leading to a significant decrease in the incidences of neural tube birth defects in these countries (Eichholzer et al., 2006; Obican et al., 2010). The role of folates in cancer is complex. Folates are important to maintain genome stability, by preventing chromosome breakage and hypomethylation of DNA; low folate levels lower the synthesis of S-adenosyl methionine (SAM) which is critical for DNA methylation, and folates are also required for converting dUMP to dTMP (Fenech, 2001). Therefore genomic instability due to lack of folates may lead to neoplastic formation (Sieber et al., 2005). On the other hand, high folate levels appear to promote cancer progression of existing neoplastic tissues (Kim, 2003). Antifolates such as methotrexate have been long used as drug targets for cancers such as lymphoblastic leukemia, osteogenic sarcoma, and breast cancer (Goldman et al., 2010).

Folate carriers, transporters and receptors

The reduced folate carrier (RFC) is the major transporter for reduced folates in human cells and is ubiquitously expressed in all tissues. RFCs carry folates across membranes via counter transport of organic anions (Matherly and Goldman, 2003; Matherly et al., 2007). RFCs primarily transport 5-methyl tetrahydrofolate (5m-THF), which is the major circulating form of folate, but have much lower affinity for folic acid. RFCs have high affinity for antifolate drugs such as methotrexate (MTX), aminopterin (AMT), etc. (Matherly et al., 2007). RFCs perform specialized functions such as absorption across intestinal/colonic epithelia, transport across basolateral membrane of renal proximal tubules, as well as folate transport across the blood-brain barrier (Matherly and Hou, 2008). Although RFC is expressed throughout the intestine, and

plays a significant role in folate absorption, a second folate transporter, the PCFT (proton coupled folate tranporter), is the major folate transporter in the acidic environment of the small intestine (Matherly and Hou, 2008). The human RFC is a membrane protein predicted to have 12 transmembrane spanning domains (Ferguson and Flintoff, 1999; Sirotnak and Tolner, 1999). *C. elegans* has three RFC homologs, FOLT-1, FOLT-2, and FOLT-3 (Balamurugan et al., 2007). Loss-of-function in FOLT-1/RFC causes drastically reduced germ cell numbers and sterility in *C. elegans* as well as embryonic lethality in mouse RFC1 knockouts (Austin et al., 2010; Zhao et al., 2001), whereas RNAi inactivation of FOLT-2 and FOLT-3 has no phenotypes in *C. elegans* (wormbase.org). Expressing FOLT-1 in mammalian cells demonstrated uptake of folic acid, while expressing FOLT-2 did not show any folate transport activity (Balamurugan et al., 2007).

PCFT is the major absorber of dietary folates and is expressed in the acidic environments of the small intestine in mammals. Mutations in PCFT have been linked to hereditary folate malabsoption (HFM) syndrome. In addition to the small intestine, PCFT is widely expressed in the kidney and liver as well as in tumor microenviroments. As PCFT is not ubiquitously expressed like RFC, it has been studied as a target for selectively delivering antifolates to combat solid tumors (Desmoulin et al., 2012). PCFT is also a membrane protein having 12 transmembrane domains and functions as a proton-folate symporter that couples the uphill transport of folates to the downhill transport of protons in an acidic environment (Desmoulin et al., 2012). *C. elegans* has two orthologs of PCFT, Y4C6B.5 and Y43F8A.5 (Shaye and Greenwald, 2011) named *pcft-1* and *pcft-2*, neither of which have phenotypes upon RNAi inactivation.

Folate Receptors (FRs) bind folic acid and many reduced folates with high affinity. FRs predominantly function in transcytosis of folates across cell barriers, such as placenta to the fetus,

and in the kidney to reabsorb folates from glomerular filtrates (Desmoulin et al., 2012; Grapp et al., 2013; Selhub et al., 1987). There are four distinct isoforms of human FRs, namely FRα, FRβ FRγ, and FRδ (Ledermann et al., 2015). FRα, FRβ, and FRδ are cell surface GPI-anchored glycoproteins, and FRγ is a secretory protein with unknown function (Elnakat and Ratnam, 2004; Ledermann et al., 2015). C17G1.1 (named FOLR-1) in *C. elegans* is the closest homolog to the human FRγ, sharing 12% identity and 25.5% homology. FOLR-1 is predicted to have a signal peptide and transmembrane domain (Cserzo et al., 2002; Petersen et al., 2011; Suh and Hutter, 2012). FRs bind to folates and bring them into the cell by endocytosis of the ligand-bound receptors. Acidification of the endosomes leads to release of the ligand from the receptors and their subsequent entry into the cytoplasm is dependent on a transport process in which PCFT is thought to play a role allowing folates to escape from acidified endosomes (Desmoulin et al., 2012). FRα has a high affinity for folic acid. FRα is expressed is all normal tissues as well as overexpressed in many cancers including those in the ovary, uterus, kidney, endometrium, lung, breast, bladder, and pancreas (Antony, 1996; Kelemen, 2006; Parker et al., 2005). FRβ and FRγ are overexpressed in hematologic malignancies, chronic myelogenous leukemia (CML) and acute myelogenous leukemia (Ledermann et al., 2015).

The overexpression of FRα in cancerous cells is thought to bring in excess folates to provide for one-carbon metabolism (Antony, 1996; Kamen and Smith, 2004; Kelemen, 2006; Zhao et al., 2009). However, in ovarian cancer cells where FRα is highly overexpressed, it is responsible for bringing in less circulating folates into the cells (~20%), than RFCs (>70%) (Corona et al., 1998). In spite of being the major contributor of folate uptake, RFCs are not linked to cancer progression; in fact, overexpressing RFCs reduces cancer cell proliferation, migration and invasiveness in ovarian cancer cell lines, whereas FRα is required to promote

proliferation, migration in these cells (Siu et al., 2012). Therefore FRα potentially promotes cancer migration in a manner independent of one-carbon metabolism.

Steroid hormone signaling and Dafachronic acid

Hormones are known to play critical developmental and physiological roles in metazoans. Steroid hormones regulate multiple facets of growth and development, reproduction as well as ageing. Certain steroid hormones and their binding partners have been identified in *C. elegans,* which closely resembles those in humans (Aguilaniu et al., 2016; Antebi, 2015).

The reproductive life cycle of *C. elegans* is tightly linked to the environment and the steroid hormone pathway plays a crucial role in sensing cues from favorable or harsh environments and directing developmental decisions accordingly (Antebi, 2013b). Specifically, when conditions are favorable, *C. elegans* goes through its normal life cycle of 4 larval stages and enters reproductive adulthood, producing progeny over three days, and then living as an adult for another 2 weeks (Antebi, 2013b). However, under harsher conditions, for example when food is scarce, temperatures are high, or overcrowding occurs (Butcher et al., 2007; Golden and Riddle, 1984), L2-stage larvae enter into an alternate third larval stage called Dauer diapause, where they remain quiescent, often for months, until conditions are favorable again (Cassada and Russell, 1975).

Genetic identification of constitutive dauer forming (Daf-c) and dauer defective (Daf-d) mutants paved the way for characterizing the molecular mechanisms governing the developmental decisions of the dauer larvae (Riddle et al., 1981). Under replete conditions, the insulin/IGF (IIS), TGFβ, and cGMP signaling pathways promote the production of bile acid-like hormones called Dafachronic acid (DA) (Fielenbach and Antebi, 2008; Li et al., 2003; Motola et

al., 2006; Ren et al., 1996). TGFβ regulates Smad/Co-Smad transcriptional targets and the IIS signaling inhibits the DAF-16/FOXO transcription factor (Antebi, 2013b). Both these pathways converge to regulate the gene *daf-9*, which codes for a cytochrome P450 (CY450), an enzyme involved in catalyzing the final step leading to the production of two DAs Δ^4-dafachronic acid and Δ^7-dafachronic acid (Antebi, 2013b). Another gene *daf-36*, which codes for a Rieske oxygenase catalyzes the first step in the biosynthesis of Δ^7-DA, where cholesterol is converted to an intermediate molecule 7-dehydrocholesterol (Rottiers et al., 2006; Wollam et al., 2011; Yoshiyama-Yanagawa et al., 2011), which is ultimately converted to Δ^7-DA (Motola et al., 2006). A comprehensive study aimed at detecting DAs identified several novel forms of Δ^7-DA as well as $\Delta^{1,7}$-DA and Δ^0-DA, but failed to detect any Δ^4, suggesting that Δ^4 may be present at very low levels in the worm (Mahanti et al., 2014).

DAs bind to the nuclear hormone receptor DAF-12, which is closely related to the mammalian Vitamin D receptor (VDR), Liver X receptor (LXR), Farnesoid X (FXR) receptor, and Pregnane X receptor (PXR) (Antebi et al., 2000; Mooijaart et al., 2005). NHRs are mostly localized to the nucleus and have both ligand binding and DNA binding domains. They act as transcription factors and repress or activate downstream developmental signaling events (Antebi, 2006). DA binding to DAF-12 activates transcription of genes that allow the worm to transition into reproductive adulthood (Antebi et al., 2000). However, under unfavorable conditions, un-liganded DAF-12 is bound by its co-repressor DIN-1S/SHARP (short isoform of DIN-1), thereby allowing dauer specific programs to be turned on (Aguilaniu et al., 2016; Ludewig et al., 2004). Similar to mammalian LXR which promotes feed-forward biosynthesis of bile acids, DAF-12 is also involved in regulating *daf-9* expression in the hypodermis and thereby the production of DAs (Wollam and Antebi, 2011).

The endocrine signaling events that regulate dauer decision are also involved in regulating the lifespan of the nematode (Antebi, 2013b). Decreasing the IIS pathway (*daf-2* mutants) leads to activation of the DAF-16 transcription factor leading to longer lifespan in worms, flies, and mice (Kenyon, 2010). Mutations in the DAF-12 homologs LXR and VDR have also been associated with premature aging in mice and humans respectively (Keisala et al., 2009; Mooijaart et al., 2007). Steroid signaling has been shown to promote longevity in *C. elegans* mutants that lack the gonadal germline (Hsin and Kenyon, 1999). The longevity effect requires the somatic gonad, as well as DAF-16 (Hsin and Kenyon, 1999). The requirement of the somatic gonad suggests that DA is likely produced either in the somatic gonad or in tissues regulated by the somatic gonad (Aguilaniu et al., 2016). The DA biosynthetic pathway genes *daf-9* and *daf-36* are also required for longevity in gonad-ablated *C. elegans* (Gerisch et al., 2007; Rottiers et al., 2006). Germline ablation leads to DAF-12 dependent up-regulation of the microRNAs *miR-241* and *miR-81*, which can activate DAF-16 thereby playing a role in lifespan extension (Bethke et al., 2009; Shen et al., 2012).

The availability of food no doubt plays an important role in regulating the life of the nematode. It was recently shown that *C. elegans* under dietary restricted conditions can synthesize DAs (Thondamal et al., 2014). This suggests that worms use an alternate pathway (other than insulin and TGF β signaling) to regulate *daf-9* mRNA levels as well as DA synthesis under dietary restricted conditions (Thondamal et al., 2014; Wollam et al., 2012). Weak *daf-9* mutants that are diet restricted do not live long in contrast to when there is no restriction of food, and an alternate non-canonical NHR, NHR-8 is required to mediate this effect (Thondamal et al., 2014). NHR-8 is involved in cholesterol and DA homeostasis and interacts with components of the IIS signaling pathway (Magner et al., 2013). Thondamal et. al demonstrated that dietary

restriction leads to the production of DAs that result in *nhr-8* dependent longevity in *C. elegans* by regulating the mTOR signaling pathway (Thondamal et al., 2014). Diet restriction also leads to a decrease in the number of proliferating germline nuclei, presumably because mTOR signaling is no longer active. Genetically reducing the germ cell numbers bypasses the need for steroid signaling in long-lived diet-restricted worms (Thondamal et al., 2014).

Removing the germline precursor cells in early the L1 larval stage extended lifespan in *C. elegans* by 60% (Hsin and Kenyon, 1999), but removing the somatic gonad as well reverses this effect, suggesting that the somatic gonad has signals that promote longevity while the germline generates signals that may antagonize longevity (Antebi, 2013a). The germline stem cells are thought to inhibit long life (Arantes-Oliveira et al., 2002). Mutations that decrease the number of proliferative germ cells, such as *glp-1* (Notch receptor) loss-of-function mutations extend lifespan, whereas those that increase the number of germ cells such as *gld-1* mutations, shortens lifespan (Arantes-Oliveira et al., 2002). Association of longevity with the germline seems to be evolutionarily conserved, as *Drosophila* mutants lacking germ stem cells also have extended lifespan (Flatt et al., 2008).

References

Aguilaniu, H., Fabrizio, P., and Witting, M. (2016). The Role of Dafachronic Acid Signaling in Development and Longevity in Caenorhabditis elegans: Digging Deeper Using Cutting-Edge Analytical Chemistry. Frontiers in endocrinology *7*, 12.

Andersson, E.R., Sandberg, R., and Lendahl, U. (2011). Notch signaling: simplicity in design, versatility in function. Development *138*, 3593-3612.

Antebi, A. (2006). Nuclear hormone receptors in C. elegans. WormBook, 1-13.

Antebi, A. (2013a). Regulation of longevity by the reproductive system. Experimental gerontology *48*, 596-602.

Antebi, A. (2013b). Steroid regulation of C. elegans diapause, developmental timing, and longevity. Current topics in developmental biology *105*, 181-212.

Antebi, A. (2015). Nuclear receptor signal transduction in C. elegans. WormBook, 1-49.

Antebi, A., Yeh, W.H., Tait, D., Hedgecock, E.M., and Riddle, D.L. (2000). daf-12 encodes a nuclear receptor that regulates the dauer diapause and developmental age in C. elegans. Genes Dev *14*, 1512-1527.

Antony, A.C. (1996). Folate receptors. Annual review of nutrition *16*, 501-521.

Arantes-Oliveira, N., Apfeld, J., Dillin, A., and Kenyon, C. (2002). Regulation of life-span by germ-line stem cells in Caenorhabditis elegans. Science (New York, NY *295*, 502-505.

Aroian, R.V., Koga, M., Mendel, J.E., Ohshima, Y., and Sternberg, P.W. (1990). The let-23 gene necessary for Caenorhabditis elegans vulval induction encodes a tyrosine kinase of the EGF receptor subfamily. Nature *348*, 693-699.

Austin, J., and Kimble, J. (1987). glp-1 is required in the germ line for regulation of the decision between mitosis and meiosis. Cell *51*, 589-599.

Austin, M.U., Liau, W.S., Balamurugan, K., Ashokkumar, B., Said, H.M., and LaMunyon, C.W. (2010). Knockout of the folate transporter folt-1 causes germline and somatic defects in C. elegans. BMC developmental biology *10*, 46.

Balamurugan, K., Ashokkumar, B., Moussaif, M., Sze, J.Y., and Said, H.M. (2007). Cloning and functional characterization of a folate transporter from the nematode Caenorhabditis elegans. American journal of physiology *293*, C670-681.

Beitel, G.J., Clark, S.G., and Horvitz, H.R. (1990). Caenorhabditis elegans ras gene let-60 acts as a switch in the pathway of vulval induction. Nature *348*, 503-509.

Berry, L.W., Westlund, B., and Schedl, T. (1997). Germ-line tumor formation caused by activation of glp-1, a Caenorhabditis elegans member of the Notch family of receptors. Development *124*, 925-936.

Berset, T., Hoier, E.F., Battu, G., Canevascini, S., and Hajnal, A. (2001). Notch inhibition of RAS signaling through MAP kinase phosphatase LIP-1 during C. elegans vulval development. Science *291*, 1055-1058.

Bethke, A., Fielenbach, N., Wang, Z., Mangelsdorf, D.J., and Antebi, A. (2009). Nuclear hormone receptor regulation of microRNAs controls developmental progression. Science *324*, 95-98.

Boag, P.R., Nakamura, A., and Blackwell, T.K. (2005). A conserved RNA-protein complex component involved in physiological germline apoptosis regulation in C. elegans. Development *132*, 4975-4986.

Bosu, D.R., and Kipreos, E.T. (2008). Cullin-RING ubiquitin ligases: global regulation and activation cycles. Cell division *3*, 7.

Brenner, S. (1974). The genetics of Caenorhabditis elegans. Genetics *77*, 71-94.

Brou, C., Logeat, F., Gupta, N., Bessia, C., LeBail, O., Doedens, J.R., Cumano, A., Roux, P., Black, R.A., and Israel, A. (2000). A novel proteolytic cleavage involved in Notch signaling: the role of the disintegrin-metalloprotease TACE. Molecular cell *5*, 207-216.

Brzezinska, A., Winska, P., and Balinska, M. (2000). Cellular aspects of folate and antifolate membrane transport. Acta biochimica Polonica *47*, 735-749.

Butcher, R.A., Fujita, M., Schroeder, F.C., and Clardy, J. (2007). Small-molecule pheromones that control dauer development in Caenorhabditis elegans. Nat Chem Biol *3*, 420-422.

Byrd, D.T., Knobel, K., Affeldt, K., Crittenden, S.L., and Kimble, J. (2014). A DTC niche plexus surrounds the germline stem cell pool in Caenorhabditis elegans. PloS one *9*, e88372.

Cassada, R.C., and Russell, R.L. (1975). The dauerlarva, a post-embryonic developmental variant of the nematode Caenorhabditis elegans. Dev Biol *46*, 326-342.

Chen, N., and Greenwald, I. (2004). The lateral signal for LIN-12/Notch in C. elegans vulval development comprises redundant secreted and transmembrane DSL proteins. Developmental cell *6*, 183-192.

Chillakuri, C.R., Sheppard, D., Lea, S.M., and Handford, P.A. (2012). Notch receptor-ligand binding and activation: insights from molecular studies. Seminars in cell & developmental biology *23*, 421-428.

Christensen, S., Kodoyianni, V., Bosenberg, M., Friedman, L., and Kimble, J. (1996). lag-1, a gene required for lin-12 and glp-1 signaling in Caenorhabditis elegans, is homologous to human CBF1 and Drosophila Su(H). Development *122*, 1373-1383.

Ciechanover, A. (1994). The Ubiquitin-Proteasome Proteolytic Pathway. Cell *79*, 13-21.

Corona, G., Giannini, F., Fabris, M., Toffoli, G., and Boiocchi, M. (1998). Role of folate receptor and reduced folate carrier in the transport of 5-methyltetrahydrofolic acid in human ovarian carcinoma cells. International journal of cancer *75*, 125-133.

Crittenden, S.L., Bernstein, D.S., Bachorik, J.L., Thompson, B.E., Gallegos, M., Petcherski, A.G., Moulder, G., Barstead, R., Wickens, M., and Kimble, J. (2002). A conserved RNA-binding protein controls germline stem cells in Caenorhabditis elegans. Nature *417*, 660-663.

Crittenden, S.L., Leonhard, K.A., Byrd, D.T., and Kimble, J. (2006). Cellular analyses of the mitotic region in the Caenorhabditis elegans adult germ line. Mol Biol Cell *17*, 3051-3061.

Crittenden, S.L., Troemel, E.R., Evans, T.C., and Kimble, J. (1994). GLP-1 is localized to the mitotic region of the C. elegans germ line. Development *120*, 2901-2911.

Cserzo, M., Eisenhaber, F., Eisenhaber, B., and Simon, I. (2002). On filtering false positive transmembrane protein predictions. Protein Eng *15*, 745-752.

Curtis, D., Treiber, D.K., Tao, F., Zamore, P.D., Williamson, J.R., and Lehmann, R. (1997). A CCHC metal-binding domain in Nanos is essential for translational regulation. EMBO J *16*, 834-843.

Dalfo, D., Michaelson, D., and Hubbard, E.J. (2012). Sensory regulation of the C. elegans germline through TGF-beta-dependent signaling in the niche. Curr Biol *22*, 712-719.

de Souza, N., Vallier, L.G., Fares, H., and Greenwald, I. (2007). SEL-2, the C. elegans neurobeachin/LRBA homolog, is a negative regulator of lin-12/Notch activity and affects endosomal traffic in polarized epithelial cells. Development *134*, 691-702.

Dernburg, A.F., McDonald, K., Moulder, G., Barstead, R., Dresser, M., and Villeneuve, A.M. (1998). Meiotic recombination in C. elegans initiates by a conserved mechanism and is dispensable for homologous chromosome synapsis. Cell *94*, 387-398.

Desmoulin, S.K., Hou, Z., Gangjee, A., and Matherly, L.H. (2012). The human proton-coupled folate transporter: Biology and therapeutic applications to cancer. Cancer biology & therapy *13*, 1355-1373.

Doyle, T.G., Wen, C., and Greenwald, I. (2000). SEL-8, a nuclear protein required for LIN-12 and GLP-1 signaling in Caenorhabditis elegans. Proceedings of the National Academy of Sciences of the United States of America *97*, 7877-7881.

Eckmann, C.R., Crittenden, S.L., Suh, N., and Kimble, J. (2004). GLD-3 and control of the mitosis/meiosis decision in the germline of Caenorhabditis elegans. Genetics *168*, 147-160.

Eckmann, C.R., Kraemer, B., Wickens, M., and Kimble, J. (2002). GLD-3, a bicaudal-C homolog that inhibits FBF to control germline sex determination in C. elegans. Dev Cell *3*, 697-710.

Eichholzer, M., Tonz, O., and Zimmermann, R. (2006). Folic acid: a public-health challenge. Lancet *367*, 1352-1361.

Elnakat, H., and Ratnam, M. (2004). Distribution, functionality and gene regulation of folate receptor isoforms: implications in targeted therapy. Adv Drug Deliv Rev *56*, 1067-1084.

Fenech, M. (2001). The role of folic acid and Vitamin B12 in genomic stability of human cells. Mutation research *475*, 57-67.

Ferguson, P.L., and Flintoff, W.F. (1999). Topological and functional analysis of the human reduced folate carrier by hemagglutinin epitope insertion. J Biol Chem *274*, 16269-16278.

Fielenbach, N., and Antebi, A. (2008). C. elegans dauer formation and the molecular basis of plasticity. Genes Dev *22*, 2149-2165.

Flatt, T., Min, K.J., D'Alterio, C., Villa-Cuesta, E., Cumbers, J., Lehmann, R., Jones, D.L., and Tatar, M. (2008). Drosophila germ-line modulation of insulin signaling and lifespan. Proc Natl Acad Sci U S A *105*, 6368-6373.

Francis, R., Barton, M.K., Kimble, J., and Schedl, T. (1995). gld-1, a tumor suppressor gene required for oocyte development in Caenorhabditis elegans. Genetics *139*, 579-606.

Fryer, C.J., Lamar, E., Turbachova, I., Kintner, C., and Jones, K.A. (2002). Mastermind mediates chromatin-specific transcription and turnover of the Notch enhancer complex. Genes & development *16*, 1397-1411.

Fryer, C.J., White, J.B., and Jones, K.A. (2004). Mastermind recruits CycC:CDK8 to phosphorylate the Notch ICD and coordinate activation with turnover. Molecular cell *16*, 509-520.

Gerisch, B., Rottiers, V., Li, D., Motola, D.L., Cummins, C.L., Lehrach, H., Mangelsdorf, D.J., and Antebi, A. (2007). A bile acid-like steroid modulates Caenorhabditis elegans lifespan through nuclear receptor signaling. Proc Natl Acad Sci U S A *104*, 5014-5019.

Glickman, M.H., and Ciechanover, A. (2002). The ubiquitin-proteasome proteolytic pathway: destruction for the sake of construction. Physiol Rev *82*, 373-428.

Golden, J.W., and Riddle, D.L. (1984). The Caenorhabditis elegans dauer larva: developmental effects of pheromone, food, and temperature. Dev Biol *102*, 368-378.

Goldman, I.D., Chattopadhyay, S., Zhao, R., and Moran, R. (2010). The antifolates: evolution, new agents in the clinic, and how targeting delivery via specific membrane transporters is driving the development of a next generation of folate analogs. Current opinion in investigational drugs *11*, 1409-1423.

Grapp, M., Wrede, A., Schweizer, M., Huwel, S., Galla, H.J., Snaidero, N., Simons, M., Buckers, J., Low, P.S., Urlaub, H.*, et al.* (2013). Choroid plexus transcytosis and exosome shuttling deliver folate into brain parenchyma. Nat Commun *4*, 2123.

Greenwald, I. (1997). Development of the Vulva. In C elegans II, D.L. Riddle, T. Blumenthal, B.J. Meyer, and J.R. Priess, eds. (Cold Spring Harbor (NY)).

Greenwald, I. (1998). LIN-12/Notch signaling: lessons from worms and flies. Genes & development *12*, 1751-1762.

Greenwald, I. (2005). LIN-12/Notch signaling in C. elegans. WormBook : the online review of C elegans biology, 1-16.

Greenwald, I.S., Sternberg, P.W., and Horvitz, H.R. (1983). The lin-12 locus specifies cell fates in Caenorhabditis elegans. Cell *34*, 435-444.

Gupta-Rossi, N., Le Bail, O., Gonen, H., Brou, C., Logeat, F., Six, E., Ciechanover, A., and Israel, A. (2001). Functional interaction between SEL-10, an F-box protein, and the nuclear form of activated Notch1 receptor. The Journal of biological chemistry *276*, 34371-34378.

Han, M., Aroian, R.V., and Sternberg, P.W. (1990). The let-60 locus controls the switch between vulval and nonvulval cell fates in Caenorhabditis elegans. Genetics *126*, 899-913.

Han, M., and Sternberg, P.W. (1990). let-60, a gene that specifies cell fates during C. elegans vulval induction, encodes a ras protein. Cell *63*, 921-931.

Hansen, D., Hubbard, E.J., and Schedl, T. (2004a). Multi-pathway control of the proliferation versus meiotic development decision in the Caenorhabditis elegans germline. Dev Biol *268*, 342-357.

Hansen, D., and Schedl, T. (2013). Stem cell proliferation versus meiotic fate decision in Caenorhabditis elegans. Advances in experimental medicine and biology *757*, 71-99.

Hansen, D., Wilson-Berry, L., Dang, T., and Schedl, T. (2004b). Control of the proliferation versus meiotic development decision in the C. elegans germline through regulation of GLD-1 protein accumulation. Development *131*, 93-104.

Henderson, S.T., Gao, D., Lambie, E.J., and Kimble, J. (1994). lag-2 may encode a signaling ligand for the GLP-1 and LIN-12 receptors of C. elegans. Development *120*, 2913-2924.

Hicke, L. (2001). Protein regulation by monoubiquitin. Nature reviews Molecular cell biology *2*, 195-201.

Hill, R.J., and Sternberg, P.W. (1992). The gene lin-3 encodes an inductive signal for vulval development in C. elegans. Nature *358*, 470-476.

Hirsh, D., Oppenheim, D., and Klass, M. (1976). Development of the reproductive system of Caenorhabditis elegans. Dev Biol *49*, 200-219.

Hsin, H., and Kenyon, C. (1999). Signals from the reproductive system regulate the lifespan of C. elegans. Nature *399*, 362-366.

Hubbard, E.J., and Greenstein, D. (2005). Introduction to the germ line. WormBook, 1-4.

Hubbard, E.J., Korta, D.Z., and Dalfo, D. (2013). Physiological control of germline development. Advances in experimental medicine and biology *757*, 101-131.

Hubbard, E.J., Wu, G., Kitajewski, J., and Greenwald, I. (1997). sel-10, a negative regulator of lin-12 activity in Caenorhabditis elegans, encodes a member of the CDC4 family of proteins. Genes & development *11*, 3182-3193.

Kamen, B.A., and Smith, A.K. (2004). A review of folate receptor alpha cycling and 5-methyltetrahydrofolate accumulation with an emphasis on cell models in vitro. Adv Drug Deliv Rev *56*, 1085-1097.

Kamura, T., Maenaka, K., Kotoshiba, S., Matsumoto, M., Kohda, D., Conaway, R.C., Conaway, J.W., and Nakayama, K.I. (2004). VHL-box and SOCS-box domains determine binding specificity for Cul2-Rbx1 and Cul5-Rbx2 modules of ubiquitin ligases. Genes & development *18*, 3055-3065.

Katz, W.S., Lesa, G.M., Yannoukakos, D., Clandinin, T.R., Schlessinger, J., and Sternberg, P.W. (1996). A point mutation in the extracellular domain activates LET-23, the Caenorhabditis elegans epidermal growth factor receptor homolog. Molecular and cellular biology *16*, 529-537.

Keisala, T., Minasyan, A., Lou, Y.R., Zou, J., Kalueff, A.V., Pyykko, I., and Tuohimaa, P. (2009). Premature aging in vitamin D receptor mutant mice. The Journal of steroid biochemistry and molecular biology *115*, 91-97.

Kelemen, L.E. (2006). The role of folate receptor alpha in cancer development, progression and treatment: cause, consequence or innocent bystander? International journal of cancer *119*, 243-250.

Kenyon, C.J. (2010). The genetics of ageing. Nature *464*, 504-512.

Kershner, A.M., Shin, H., Hansen, T.J., and Kimble, J. (2014). Discovery of two GLP-1/Notch target genes that account for the role of GLP-1/Notch signaling in stem cell maintenance. Proc Natl Acad Sci U S A *111*, 3739-3744.

Killian, D.J., and Hubbard, E.J. (2005). Caenorhabditis elegans germline patterning requires coordinated development of the somatic gonadal sheath and the germ line. Dev Biol *279*, 322-335.

Kim, Y.I. (2003). Role of folate in colon cancer development and progression. The Journal of nutrition *133*, 3731S-3739S.

Kimble, J., and Crittenden, S.L. (2005). Germline proliferation and its control. WormBook, 1-14.

Kimble, J., and Crittenden, S.L. (2007). Controls of germline stem cells, entry into meiosis, and the sperm/oocyte decision in Caenorhabditis elegans. Annu Rev Cell Dev Biol *23*, 405-433.

Kimble, J., and Seidel, H. (2013). C. elegans germline stem cells and their niche. In StemBook (Cambridge (MA)).

Kimble, J., and Simpson, P. (1997). The LIN-12/Notch signaling pathway and its regulation. Annual review of cell and developmental biology *13*, 333-361.

Kimble, J.E., and White, J.G. (1981). On the Control of Germ Cell Development in Caenorhabditis elegans. Dev Biol *81*, 208-219.

Kipreos, E.T. (2005a). C. elegans cell cycles: invariance and stem cell divisions. Nature reviews Molecular cell biology *6*, 766-776.

Kipreos, E.T. (2005b). Ubiquitin-mediated pathways in C. elegans. WormBook : the online review of C elegans biology, 1-24.

Koegl, M., Hoppe, T., Schlenker, S., Ulrich, H.D., Mayer, T.U., and Jentsch, S. (1999). A novel ubiquitination factor, E4, is involved in multiubiquitin chain assembly. Cell *96*, 635-644.

Kopan, R., and Goate, A. (2000). A common enzyme connects notch signaling and Alzheimer's disease. Genes & development *14*, 2799-2806.

Kopan, R., and Ilagan, M.X. (2009). The canonical Notch signaling pathway: unfolding the activation mechanism. Cell *137*, 216-233.

Korta, D.Z., Tuck, S., and Hubbard, E.J. (2012). S6K links cell fate, cell cycle and nutrient response in C. elegans germline stem/progenitor cells. Development *139*, 859-870.

Kraemer, B., Crittenden, S., Gallegos, M., Moulder, G., Barstead, R., Kimble, J., and Wickens, M. (1999). NANOS-3 and FBF proteins physically interact to control the sperm-oocyte switch in Caenorhabditis elegans. Curr Biol *9*, 1009-1018.

Lai, E.C. (2004). Notch signaling: control of cell communication and cell fate. Development *131*, 965-973.

Lambie, E.J., and Kimble, J. (1991). Two homologous regulatory genes, lin-12 and glp-1, have overlapping functions. Development *112*, 231-240.

Lamont, L.B., Crittenden, S.L., Bernstein, D., Wickens, M., and Kimble, J. (2004). FBF-1 and FBF-2 regulate the size of the mitotic region in the C. elegans germline. Dev Cell *7*, 697-707.

Ledermann, J.A., Canevari, S., and Thigpen, T. (2015). Targeting the folate receptor: diagnostic and therapeutic approaches to personalize cancer treatments. Ann Oncol *26*, 2034-2043.

Lee, M.H., Hook, B., Lamont, L.B., Wickens, M., and Kimble, J. (2006). LIP-1 phosphatase controls the extent of germline proliferation in Caenorhabditis elegans. EMBO J *25*, 88-96.

Li, W., Kennedy, S.G., and Ruvkun, G. (2003). daf-28 encodes a C. elegans insulin superfamily member that is regulated by environmental cues and acts in the DAF-2 signaling pathway. Genes Dev *17*, 844-858.

Li, X., and Greenwald, I. (1997). HOP-1, a Caenorhabditis elegans presenilin, appears to be functionally redundant with SEL-12 presenilin and to facilitate LIN-12 and GLP-1 signaling. Proceedings of the National Academy of Sciences of the United States of America *94*, 12204-12209.

Ludewig, A.H., Kober-Eisermann, C., Weitzel, C., Bethke, A., Neubert, K., Gerisch, B., Hutter, H., and Antebi, A. (2004). A novel nuclear receptor/coregulator complex controls C. elegans lipid metabolism, larval development, and aging. Genes Dev *18*, 2120-2133.

MacNeil, L.T., Watson, E., Arda, H.E., Zhu, L.J., and Walhout, A.J. (2013). Diet-induced developmental acceleration independent of TOR and insulin in C. elegans. Cell *153*, 240-252.

Magner, D.B., Wollam, J., Shen, Y., Hoppe, C., Li, D., Latza, C., Rottiers, V., Hutter, H., and Antebi, A. (2013). The NHR-8 nuclear receptor regulates cholesterol and bile acid homeostasis in C. elegans. Cell metabolism *18*, 212-224.

Mahanti, P., Bose, N., Bethke, A., Judkins, J.C., Wollam, J., Dumas, K.J., Zimmerman, A.M., Campbell, S.L., Hu, P.J., Antebi, A.*, et al.* (2014). Comparative metabolomics reveals endogenous ligands of DAF-12, a nuclear hormone receptor, regulating C. elegans development and lifespan. Cell metabolism *19*, 73-83.

Marin, V.A., and Evans, T.C. (2003). Translational repression of a C. elegans Notch mRNA by the STAR/KH domain protein GLD-1. Development *130*, 2623-2632.

Matherly, L.H., and Goldman, D.I. (2003). Membrane transport of folates. Vitamins and hormones *66*, 403-456.

Matherly, L.H., and Hou, Z. (2008). Structure and function of the reduced folate carrier a paradigm of a major facilitator superfamily mammalian nutrient transporter. Vitamins and hormones *79*, 145-184.

Matherly, L.H., Hou, Z., and Deng, Y. (2007). Human reduced folate carrier: translation of basic biology to cancer etiology and therapy. Cancer Metastasis Rev *26*, 111-128.

McGovern, M., Voutev, R., Maciejowski, J., Corsi, A.K., and Hubbard, E.J. (2009). A "latent niche" mechanism for tumor initiation. Proc Natl Acad Sci U S A *106*, 11617-11622.

Michaelson, D., Korta, D.Z., Capua, Y., and Hubbard, E.J. (2010). Insulin signaling promotes germline proliferation in C. elegans. Development *137*, 671-680.

Mooijaart, S.P., Brandt, B.W., Baldal, E.A., Pijpe, J., Kuningas, M., Beekman, M., Zwaan, B.J., Slagboom, P.E., Westendorp, R.G., and van Heemst, D. (2005). C. elegans DAF-12, Nuclear Hormone Receptors and human longevity and disease at old age. Ageing Res Rev *4*, 351-371.

Mooijaart, S.P., Kuningas, M., Westendorp, R.G., Houwing-Duistermaat, J.J., Slagboom, P.E., Rensen, P.C., and van Heemst, D. (2007). Liver X receptor alpha associates with human life span. The journals of gerontology *62*, 343-349.

Motola, D.L., Cummins, C.L., Rottiers, V., Sharma, K.K., Li, T., Li, Y., Suino-Powell, K., Xu, H.E., Auchus, R.J., Antebi, A.*, et al.* (2006). Identification of ligands for DAF-12 that govern dauer formation and reproduction in C. elegans. Cell *124*, 1209-1223.

Nadarajan, S., Govindan, J.A., McGovern, M., Hubbard, E.J., and Greenstein, D. (2009). MSP and GLP-1/Notch signaling coordinately regulate actomyosin-dependent cytoplasmic streaming and oocyte growth in C. elegans. Development *136*, 2223-2234.

Nazki, F.H., Sameer, A.S., and Ganaie, B.A. (2014). Folate: metabolism, genes, polymorphisms and the associated diseases. Gene *533*, 11-20.

Oberg, C., Li, J., Pauley, A., Wolf, E., Gurney, M., and Lendahl, U. (2001). The Notch intracellular domain is ubiquitinated and negatively regulated by the mammalian Sel-10 homolog. The Journal of biological chemistry *276*, 35847-35853.

Obican, S.G., Finnell, R.H., Mills, J.L., Shaw, G.M., and Scialli, A.R. (2010). Folic acid in early pregnancy: a public health success story. FASEB J *24*, 4167-4174.

Parker, N., Turk, M.J., Westrick, E., Lewis, J.D., Low, P.S., and Leamon, C.P. (2005). Folate receptor expression in carcinomas and normal tissues determined by a quantitative radioligand binding assay. Analytical biochemistry *338*, 284-293.

Petcherski, A.G., and Kimble, J. (2000). LAG-3 is a putative transcriptional activator in the C. elegans Notch pathway. Nature *405*, 364-368.

Petersen, T.N., Brunak, S., von Heijne, G., and Nielsen, H. (2011). SignalP 4.0: discriminating signal peptides from transmembrane regions. Nat Methods *8*, 785-786.

Petroski, M.D., and Deshaies, R.J. (2005). Function and regulation of cullin-RING ubiquitin ligases. Nature reviews Molecular cell biology *6*, 9-20.

Piano, F., Schetter, A.J., Morton, D.G., Gunsalus, K.C., Reinke, V., Kim, S.K., and Kemphues, K.J. (2002). Gene clustering based on RNAi phenotypes of ovary-enriched genes in C. elegans. Current biology : CB *12*, 1959-1964.

Pickart, C.M. (2001). Mechanisms underlying ubiquitination. Annual review of biochemistry *70*, 503-533.

Pickart, C.M., and Cohen, R.E. (2004). Proteasomes and their kin: proteases in the machine age. Nat Rev Mol Cell Biol *5*, 177-187.

Ren, P., Lim, C.S., Johnsen, R., Albert, P.S., Pilgrim, D., and Riddle, D.L. (1996). Control of C. elegans larval development by neuronal expression of a TGF-beta homolog. Science (New York, NY *274*, 1389-1391.

Riddle, D.L., Swanson, M.M., and Albert, P.S. (1981). Interacting genes in nematode dauer larva formation. Nature *290*, 668-671.

Rock KL, G.C., Rothstein L, Clark K, Stein R, Dick L, Hwang D, Goldberg AL (1994). Inhibitors of the proteasome block the degradation of most cell proteins and the generation of peptides presented on MHC class I molecules. Cell *78*, 761-771.

Rossi, M., Amaretti, A., and Raimondi, S. (2011). Folate production by probiotic bacteria. Nutrients *3*, 118-134.

Rottiers, V., Motola, D.L., Gerisch, B., Cummins, C.L., Nishiwaki, K., Mangelsdorf, D.J., and Antebi, A. (2006). Hormonal control of C. elegans dauer formation and life span by a Rieske-like oxygenase. Dev Cell *10*, 473-482.

Sakata, T., Sakaguchi, H., Tsuda, L., Higashitani, A., Aigaki, T., Matsuno, K., and Hayashi, S. (2004). Drosophila Nedd4 regulates endocytosis of notch and suppresses its ligand-independent activation. Current biology : CB *14*, 2228-2236.

Sanchez-Irizarry, C., Carpenter, A.C., Weng, A.P., Pear, W.S., Aster, J.C., and Blacklow, S.C. (2004). Notch subunit heterodimerization and prevention of ligand-independent proteolytic activation depend, respectively, on a novel domain and the LNR repeats. Molecular and cellular biology *24*, 9265-9273.

Selhub, J. (2002). Folate, vitamin B12 and vitamin B6 and one carbon metabolism. The journal of nutrition, health & aging *6*, 39-42.

Selhub, J., Emmanouel, D., Stavropoulos, T., and Arnold, R. (1987). Renal folate absorption and the kidney folate binding protein. I. Urinary clearance studies. The American journal of physiology *252*, F750-756.

Seydoux, G., and Greenwald, I. (1989). Cell autonomy of lin-12 function in a cell fate decision in C. elegans. Cell *57*, 1237-1245.

Shaye, D.D., and Greenwald, I. (2002). Endocytosis-mediated downregulation of LIN-12/Notch upon Ras activation in Caenorhabditis elegans. Nature *420*, 686-690.

Shaye, D.D., and Greenwald, I. (2011). OrthoList: a compendium of C. elegans genes with human orthologs. PloS one *6*, e20085.

Shen, Y., Wollam, J., Magner, D., Karalay, O., and Antebi, A. (2012). A steroid receptor-microRNA switch regulates life span in response to signals from the gonad. Science (New York, NY *338*, 1472-1476.

Sieber, O., Heinimann, K., and Tomlinson, I. (2005). Genomic stability and tumorigenesis. Semin Cancer Biol *15*, 61-66.

Sirotnak, F.M., and Tolner, B. (1999). Carrier-mediated membrane transport of folates in mammalian cells. Annual review of nutrition *19*, 91-122.

Siu, M.K., Kong, D.S., Chan, H.Y., Wong, E.S., Ip, P.P., Jiang, L., Ngan, H.Y., Le, X.F., and Cheung, A.N. (2012). Paradoxical impact of two folate receptors, FRalpha and RFC, in ovarian cancer: effect on cell proliferation, invasion and clinical outcome. PloS one *7*, e47201.

Starostina, N.G., Simpliciano, J.M., McGuirk, M.A., and Kipreos, E.T. (2010). CRL2(LRR-1) targets a CDK inhibitor for cell cycle control in C. elegans and actin-based motility regulation in human cells. Developmental cell *19*, 753-764.

Sternberg, P.W. (2005). Vulval development. WormBook : the online review of C elegans biology, 1-28.

Sternberg, P.W., and Horvitz, H.R. (1989). The combined action of two intercellular signaling pathways specifies three cell fates during vulval induction in C. elegans. Cell *58*, 679-693.

Stover, P.J. (2004). Physiology of folate and vitamin B12 in health and disease. Nutrition reviews *62*, S3-12; discussion S13.

Suh, J., and Hutter, H. (2012). A survey of putative secreted and transmembrane proteins encoded in the C. elegans genome. BMC genomics *13*, 333.

Sundaram, M., and Greenwald, I. (1993). Suppressors of a lin-12 hypomorph define genes that interact with both lin-12 and glp-1 in Caenorhabditis elegans. Genetics *135*, 765-783.

Sundaram, M.V. (2006). RTK/Ras/MAPK signaling. WormBook : the online review of C elegans biology, 1-19.

Tax, F.E., Yeargers, J.J., and Thomas, J.H. (1994). Sequence of C. elegans lag-2 reveals a cell-signalling domain shared with Delta and Serrate of Drosophila. Nature *368*, 150-154.

Thondamal, M., Witting, M., Schmitt-Kopplin, P., and Aguilaniu, H. (2014). Steroid hormone signalling links reproduction to lifespan in dietary-restricted Caenorhabditis elegans. Nat Commun *5*, 4879.

Wang, L., Eckmann, C.R., Kadyk, L.C., Wickens, M., and Kimble, J. (2002). A regulatory cytoplasmic poly(A) polymerase in Caenorhabditis elegans. Nature *419*, 312-316.

Wang, Z., and Sherwood, D.R. (2011). Dissection of genetic pathways in C. elegans. Methods in cell biology *106*, 113-157.

Wen, C., and Greenwald, I. (1999). p24 proteins and quality control of LIN-12 and GLP-1 trafficking in Caenorhabditis elegans. The Journal of cell biology *145*, 1165-1175.

Weng, A.P., Ferrando, A.A., Lee, W., Morris, J.P.t., Silverman, L.B., Sanchez-Irizarry, C., Blacklow, S.C., Look, A.T., and Aster, J.C. (2004). Activating mutations of NOTCH1 in human T cell acute lymphoblastic leukemia. Science *306*, 269-271.

Westlund, B., Parry, D., Clover, R., Basson, M., and Johnson, C.D. (1999). Reverse genetic analysis of Caenorhabditis elegans presenilins reveals redundant but unequal roles for sel-12 and hop-1 in Notch-pathway signaling. Proceedings of the National Academy of Sciences of the United States of America *96*, 2497-2502.

Wickens, M., Bernstein, D.S., Kimble, J., and Parker, R. (2002). A PUF family portrait: 3'UTR regulation as a way of life. Trends Genet *18*, 150-157.

Wilkinson, H.A., Fitzgerald, K., and Greenwald, I. (1994). Reciprocal changes in expression of the receptor lin-12 and its ligand lag-2 prior to commitment in a C. elegans cell fate decision. Cell *79*, 1187-1198.

Wollam, J., and Antebi, A. (2011). Sterol regulation of metabolism, homeostasis, and development. Annual review of biochemistry *80*, 885-916.

Wollam, J., Magner, D.B., Magomedova, L., Rass, E., Shen, Y., Rottiers, V., Habermann, B., Cummins, C.L., and Antebi, A. (2012). A novel 3-hydroxysteroid dehydrogenase that regulates reproductive development and longevity. PLoS Biol *10*, e1001305.

Wollam, J., Magomedova, L., Magner, D.B., Shen, Y., Rottiers, V., Motola, D.L., Mangelsdorf, D.J., Cummins, C.L., and Antebi, A. (2011). The Rieske oxygenase DAF-36 functions as a cholesterol 7-desaturase in steroidogenic pathways governing longevity. Aging Cell *10*, 879-884.

Wu, G., Lyapina, S., Das, I., Li, J., Gurney, M., Pauley, A., Chui, I., Deshaies, R.J., and Kitajewski, J. (2001). SEL-10 is an inhibitor of notch signaling that targets notch for ubiquitin-mediated protein degradation. Molecular and cellular biology *21*, 7403-7415.

Yochem, J., Weston, K., and Greenwald, I. (1988). The Caenorhabditis elegans lin-12 gene encodes a transmembrane protein with overall similarity to Drosophila Notch. Nature *335*, 547-550.

Yoo, A.S., Bais, C., and Greenwald, I. (2004). Crosstalk between the EGFR and LIN-12/Notch pathways in C. elegans vulval development. Science *303*, 663-666.

Yoshiyama-Yanagawa, T., Enya, S., Shimada-Niwa, Y., Yaguchi, S., Haramoto, Y., Matsuya, T., Shiomi, K., Sasakura, Y., Takahashi, S., Asashima, M.*, et al.* (2011). The conserved Rieske oxygenase DAF-36/Neverland is a novel cholesterol-metabolizing enzyme. J Biol Chem *286*, 25756-25762.

Zhang, B., Gallegos, M., Puoti, A., Durkin, E., Fields, S., Kimble, J., and Wickens, M.P. (1997). A conserved RNA-binding protein that regulates sexual fates in the C. elegans hermaphrodite germ line. Nature *390*, 477-484.

Zhao, R., Matherly, L.H., and Goldman, I.D. (2009). Membrane transporters and folate homeostasis: intestinal absorption and transport into systemic compartments and tissues. Expert reviews in molecular medicine *11*, e4.

Zhao, R., Russell, R.G., Wang, Y., Liu, L., Gao, F., Kneitz, B., Edelmann, W., and Goldman, I.D. (2001). Rescue of embryonic lethality in reduced folate carrier-deficient mice by maternal folic acid supplementation reveals early neonatal failure of hematopoietic organs. J Biol Chem *276*, 10224-10228.

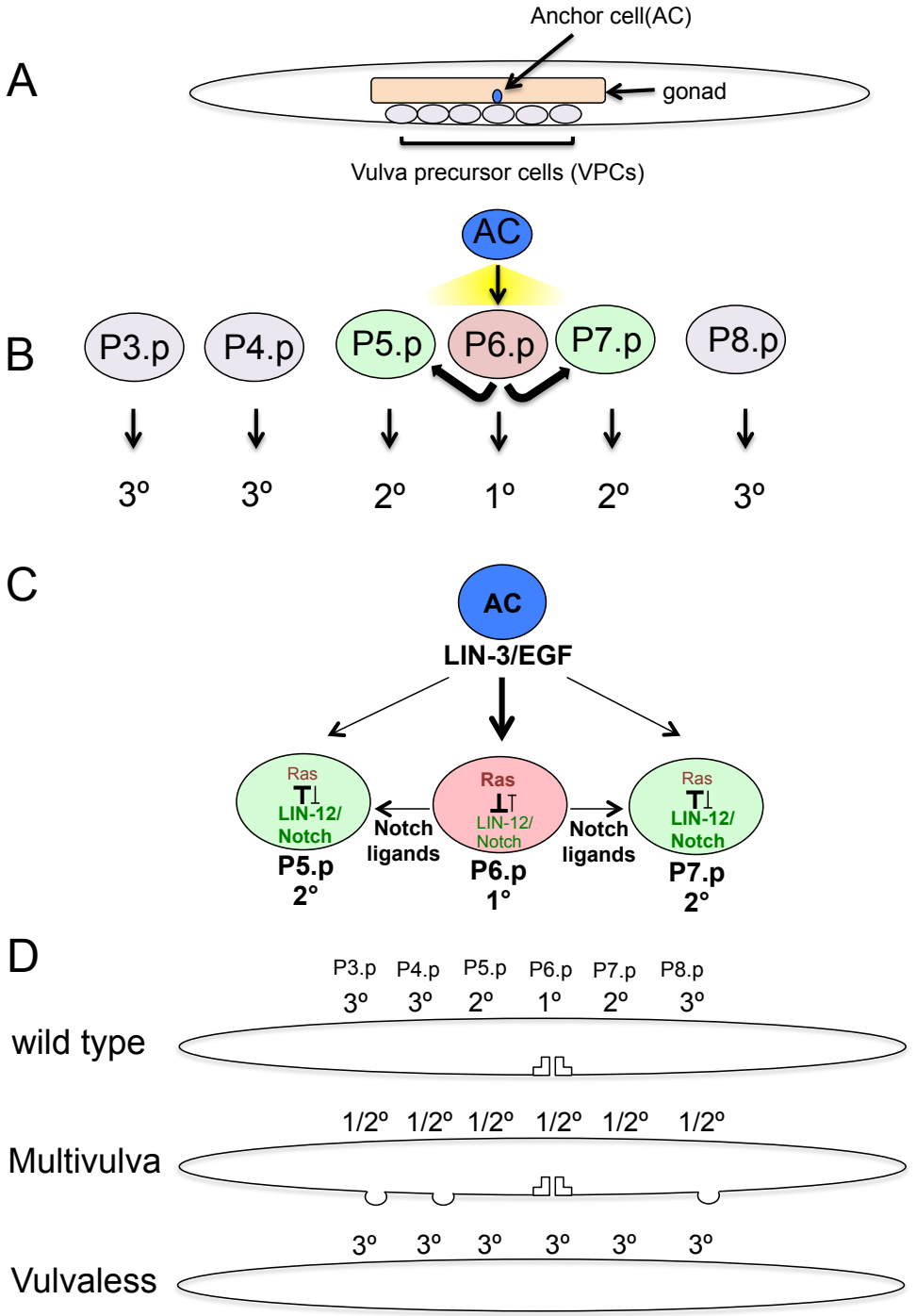
A
Anchor cell(AC)
gonad
Vulva precursor cells (VPCs)
B
AC
P3.p
P4.p
P5.p
P6.p
P7.p
P8.p
3º
3º
2º
1º
2º
3º
C
AC
LIN-3/EGF
Ras
LIN-12/
Notch
Notch
ligands
P5.p
2°
P6.p
1°
P7.p
2°
D
P3.p P4.p P5.p P6.p P7.p P8.p
3º 3º 2º 1º 2º 3º
wild type
1/2º 1/2º 1/2º 1/2º 1/2º 1/2º
Multivulva
3º 3º 3º 3º 3º 3º
Vulvaless

Figure 1.1 *C. elegans* vulval patterning and vulval phenotypes. (A) A *C. elegans* L2 stage animal showing the vulval precursor cells (VPCs), the gonad and the Anchor cell (AC) in the gonad. (B) A magnified version of the VPCs is depicted using the circles. A graded inductive signal (yellow) from the AC (blue) reaches the VPCs and P6.p adopts a 1º fate (red). The 1º cell signals its adjacent P5.p and P7.p to adopt 2º fates (green). The remaining VPCs P3.p, P4.p and P8.p become 3º cells (grey). (C) Ras and Notch signaling regulate the vulval fate patterning. The inductive signal from AC is an epidermal growth factor (EGF)-like signal LIN-3. LIN-3 upregulates the Ras pathway in P6.p making it the 1º cell. Ras leads to transcription of Notch ligands that activate the LIN-12/Notch pathway in P5.p and P7.p making them 2º cells. Ras downregulates LIN-12/Notch in the 1º cells and LIN-12/Notch downregulates Ras in the 2º cells. (Figures 1.1 A, B and D are modified from Kerry Kornfeld lab website http://kornfeldlab.wustl.edu/cellfate.htm).

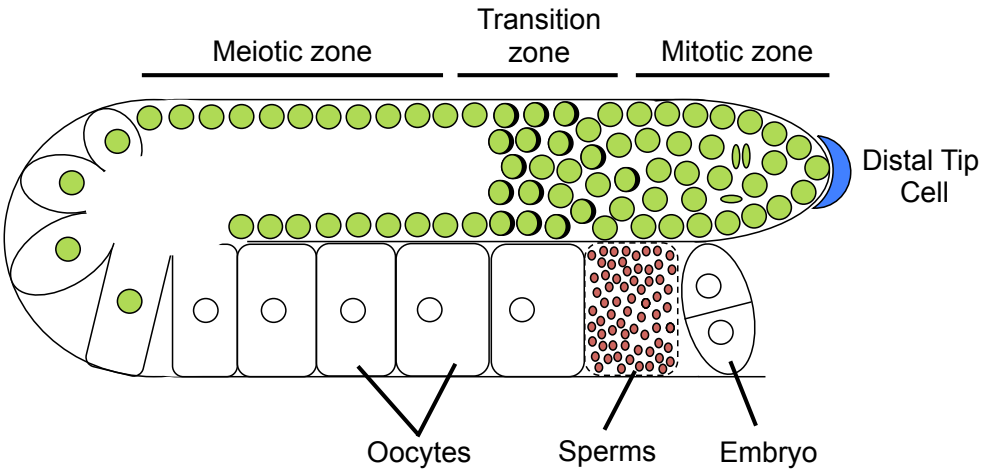

Figure 1.2 Organization of the *C. elegans* germline. A *C. elegans* hermaphrodite gonad arm is shown that has germ cells in the distal end and oocytes, sperms and an embryo in the proximal end. The somatic distal tip cell (DTC; blue) maintains the pool of proliferating germ cells within the mitotic region. As the germ cells move away from the DTC niche region, they enter the transition zone where some cells have entered meiosis (characterized by the crescent nuclei) while a few mitotic cells are also retained. Following the transition zone, the germ cells enter meiotic prophase I and eventually differentiate into ooctyes and sperms at the proximal end of the gonad. (Modified from Boag et al., 2005; Kipreos, 2005a).

CHAPTER 2

THE CRL2^{LRR-1} UBIQUITIN LIGASE NEGATIVELY REGULATES NOTCH SIGNALING DURING *CAENORHABDITIS ELEGANS* VULVA DEVELOPMENT [1]

[1] **Mukherjee M** and Kipreos E.T. To be submitted to *Developmental Dynamics*.

Abstract

The *Caenorhabditis elegans* vulva is one of the classic systems used to study interactions between the Ras and Notch signaling pathways. The vulva is patterned by a Ras-mediated 'inductive' signal and a Notch-mediated 'lateral' signal. Three vulval precursor cells, P5.p, P6.p and P7.p, form the mature vulva. Activation of the Ras pathway in P6.p induces the 1° cell fate in P6.p. The subsequent expression of Notch ligands in P6.p induces the 2° cell fate in the adjacent P5.p and P7.p cells by activating the Notch pathway in these cells. For proper 2°-1°-2° patterning, Ras inhibits Notch in the 1° cell, and Notch down-regulates Ras in the 2° cells. Defects in this mechanism lead to excessive numbers of (or a lack of) 1° or 2° cells, and thus abnormal vulva development. We observed that inactivation of the substrate recognition subunit (SRS) LRR-1, of the cullin-RING ubiquitin ligase 2 (CRL2) complex, results in a multivulva (Muv) phenotype (~1%). We found that the expression of the Notch-target gene *lip-1* is higher in *lrr-1* mutants compared to wild-type, whereas the expression of the Ras-target gene *egl-17* is unchanged. This suggests that Ras activity is not affected by loss of *lrr-1*, while Notch activity is upregulated. Genetic interaction experiments combining the *lrr-1* mutant with different mutants in the Ras and Notch pathways also revealed that the Notch pathway is overactive in *lrr-1* mutants. Detailed analysis of the expression of Notch proteins showed us that in P6.p, loss of *lrr-1* leads to an increase in the levels of both full-length Notch receptor as well as the cleaved transcriptional activator Notch intracellular domain (NICD). The ubiquitin ligase SCF^{SEL-10} is known to degrade NICD, and *sel-10* mutants have higher levels of NICD than *lrr-1* mutants. Interestingly, *lrr-1* mutants have higher levels of expression of certain Notch-regulated genes. These experiments suggest that loss of $CRL2^{LRR-1}$ increases the expression of Notch target genes downstream of the generation of the NICD. Using the modENCODE ChIP-seq database we

identified DAF-12 as a transcription factor that binds the gene regulatory sequences of these Notch target genes. Inactivation of DAF-12 reduces Notch target gene expression, indicating that it normally promotes their expression. The level of DAF-12::GFP increases in *lrr-1* mutants, suggesting that LRR-1 inhibits Notch signaling by negatively regulating the transcription factor DAF-12.

Introduction

Notch genes encode cell surface receptors that were first discovered nearly a century ago as a notched winged phenotype in *Drosophila* (Allenspach et al., 2002). Notch and its signaling components, which consist of receptors, ligands, positive and negative regulators, transcription factors, are highly conserved from *Drosophila* to humans (Allenspach et al., 2002). Notch plays an extremely important role in metazoan development and this role has been well studied in the patterning of the wing and eye in *Drosophila* (Fortini and Artavanis-Tsakonas, 1993; Irvine and Vogt, 1997), vulval cell fate in *C. elegans* (Greenwald et al., 1983), neuronal fate decisions (Aguirre et al., 2010; Hitoshi et al., 2002) and mammalian angiogenesis (Liu et al., 2003). Misregulation or loss of Notch signaling has been implicated in various human developmental abnormalities and many cancers (Allenspach et al., 2002; Penton et al., 2012).

In *C. elegans*, LIN-12/Notch plays a critical role during vulva development as well as in the specification of the Anchor Cell (AC), which is required to produce an inductive signal for the vulval precursor cells (Greenwald, 2005). The VPCs, P3.p – P8.p cells, adopt a precise spatial pattern from anterior to posterior, 3°-3°-2°-1°-2°-3°, that is initiated in response to a graded inductive signal from the AC: the epidermal growth factor (EGF) ligand LIN-3 (Figure 2.1A). LIN-3 binds to the epidermal growth factor receptor (EGFR)/LET-23 and subsequently activates the Ras/LET-60–MAPK/MPK-1 pathway. MPK-1/MAPK phosphorylates two downstream substrates LIN-1 and LIN-31 in P6.p (Sternberg, 2005). LIN-1 is an ETS domain transcription factor that blocks induction of 1º fate (Beitel et al., 1995; Han et al., 1990). LIN-1 forms a complex with the forkhead-like transcription factor LIN-31 that inhibits 1º fate induction (Tan et al., 1998). The activation of the EGFR–Ras–MAPK pathway leads to phosphorylation of both LIN-1 and LIN-31 in the P6.p by MPK-1 thereby disrupting this repressive complex (Tan et

al., 1998). In the absence of the inductive signal, the LIN-1–LIN-31 repressor complex inhibits the *hox* gene *lin-39* (Guerry et al., 2007; Wagmaister et al., 2006). LIN-39 is required for the final execution of the 1º fate by regulating vulval proliferation and morphogenesis (Clandinin et al., 1997; Maloof and Kenyon, 1998; Pellegrino et al., 2011; Shemer and Podbilewicz, 2002).

High-level EGFR–Ras signaling in the P6.p cell leads to transcription of DSL (Delta/Serrate) ligands. The DSL ligands promote lateral signaling by activating LIN-12/Notch in the adjacent P5.p and P7.p cells; which induces the 2º fate in these cells (Chen and Greenwald, 2004). Additionally, a lower level of inductive signal in P5.p and P7.p has been proposed to upregulate an alternate Ras pathway via the Ras exchange factor RalGEF that shuttles Ras signaling from the Ras–MAPK pathway to the Ras–RalGEF–Ral pathway (Zand et al., 2011). The RalGEF–Ral pathway provides evidence in support of the proposed morphogen gradient model (Katz et al., 1995; Katz et al., 1996; Sternberg and Horvitz, 1986; Sternberg and Horvitz, 1989) where graded EGF supports 2º fate in P5.p and P6.p by activating the RalGEF–Ral pathway (Zand et al., 2011). However the direct targets by which this pathway promotes 2º fate have not yet been discovered (Zand et al., 2011).

In order for proper spatial patterning to occur, LIN-12/Notch signaling increases expression of genes that inhibit Ras–MAPK in the 2º cells (Berset et al., 2001; Berset et al., 2005; Yoo et al., 2004). Similarly, activation of Ras–MAPK in P6.p leads to endocytosis- and lysosome-mediated degradation of LIN-12/Notch receptor, as well as activation of 2º-fate antagonizing programs, thereby sealing the 1º fate in P6.p (Levitan and Greenwald, 1998; Shaye and Greenwald, 2002; Yoo and Greenwald, 2005). The VPCs P3.p, P4.p, and P8.p adopt 3º non-vulval fates and fuse to the large hypodermal synctium (hyp7) (Sternberg, 2005).

Altering the Ras–MAPK and LIN-12/Notch pathways can give rise to abnormal vulval phenotypes. Mutations that decrease EGF–Ras–MAPK signaling (e.g., in *lin-3, let-23, let-60*) give rise to a Vulvaless (Vul) phenotype, as all cells become 3º (Aroian et al., 1990; Beitel et al., 1990; Han et al., 1990; Hill and Sternberg, 1992; Sternberg, 2005). Conversely, gain-of-function alleles of EGF–Ras–MAPK genes cause a Multivulva (Muv) phenotype wherein extra VPCs assume the 1º fate (Beitel et al., 1990; Han and Sternberg, 1990; Hill and Sternberg, 1992; Katz et al., 1996). *lin-12* null alleles fail to specify the 2º fate. *lin-12* gain-of-function mutations cause all VPCs to adopt the 2º fate and display Muv phenotype (Greenwald et al., 1983; Sternberg, 2005). LIN-12/Notch is also required to specify the cell-fate decision between two cells in the somatic gonad, Z1.ppp and Z4.aaa. One of these cells becomes the future AC and the other becomes a vulval uterine (VU) cell through LIN-12 and LAG-2 mediated signaling (Greenwald, 2005). Initially both the precursor cells express both *lin-12* and *lag-2* transcripts; stochastic differences in the activity of *lin-12* between the two cells initiates a feedback mechanism, whereby LIN-12 activation by LAG-2 in the presumptive VU cell positively transcribes *lin-12* and downregulates *lag-2* transcription (Wilkinson et al., 1994). Loss-of-function of *lin-12* causes two ACs to be specified and a gain-of-function of *lin-12* causes two VUs to form (Seydoux and Greenwald, 1989; Wilkinson et al., 1994). In *lin-12* gain-of-function mutants, the absence of an AC means that the inductive EGF signal is not present, therefore the Muv phenotype observed is due to all VPCs assuming 2º fate (Greenwald et al., 1983).

Several negative regulators of both the Ras–MAPK and LIN-12/Notch pathway have been identified. Among the negative modulators of LIN-12/Notch, some directly target the receptor or its intracellular form (NICD) whereas others affect Notch-pathway components (Greenwald, 2005). SEL-10 is a negative regulator of NICD that was identified in a genetic

screen for suppressors of *lin-12* hypomorphs (Feldman et al., 1997; Hubbard et al., 1997; Skowyra et al., 1997; Sundaram and Greenwald, 1993b). SEL-10 is the *C. elegans* ortholog of the F-Box/WD40 repeat containing protein Fbw7 that is a part of the CRL E3 ubiquitin ligase Skp1/Cul1/Fbox (SCF) complex. $SCF^{SEL-10/Fbw7}$ promotes the ubiquitin-mediated degradation of NICD in both *C. elegans* and mammals (Gupta-Rossi et al., 2001; Hubbard et al., 1997; Oberg et al., 2001; Wu et al., 2001).

Unlike *lin-12* gain-of-function mutants, *sel-10* loss-of-function mutants do not have a multivulva phenotype, irrespective of the fact that the levels of NICD and full-length LIN-12 are significantly elevated in all six VPCs (Hubbard et al., 1997; Shaye and Greenwald, 2002). Full-length Notch signaling generates nuclear-localized NICD, whose transcriptional activity mediates the signaling. The observation that merely elevating NICD or full-length LIN-12/Notch levels are not sufficient to induce Notch signaling, and suggests either that other aspects of Notch signaling, such as co-activators, are not activated, or that mechanisms that downregulate Notch signaling are induced upon elevation of the LIN-12 full-length and NICD proteins. While *sel-10* mutants have no defect in vulval phenotype on their own (Jager et al., 2004; Sundaram and Greenwald, 1993a), they can exacerbate the Muv phenotype of mild gain-of-function alleles of *lin-12,* and suppress the two AC phenotype of *lin-12* hypomorphs (Hubbard et al., 1997).

In this study we describe LRR-1 as a negative regulator of Notch signaling in vulval cells. LRR-1 is a leucine rich repeat protein that functions as a substrate recognition subunit (SRS) for a cullin-RING ubiquitin ligase complex (CRL) (Starostina et al., 2010). CRLs are the largest known class of ubiquitin ligases (E3s) (Bosu and Kipreos, 2008; Petroski and Deshaies, 2005). In metazoa, there are five main types of cullins, which are capable of forming distinct CRL

complexes: SCF complexes (CUL-1 based) and CRL2-5 complexes (CUL2-5 based, respectively). The CUL-2 based complex (CRL2) consists of four subunits: the cullin CUL-2; the RING H2 finger protein Roc1/Rbx1; the adaptor Elongin C that is bound to Elongin B; and the substrate recognition subunit (SRS) that binds substrates (Bosu and Kipreos, 2008; Petroski and Deshaies, 2005). *C. elegans* LRR-1 interacts with Elongin C (ELC-1), the adapter protein for CRL2 and brings substrates to the $CRL2^{LRR-1}$ complex (Starostina et al., 2010). Loss of *lrr-1* produces a severe reduction in germ cell division that has been attributed to an increase in the levels of the CDK-inhibitor CKI-1 and the activation of a cell cycle checkpoint (Merlet et al., 2010; Starostina et al., 2010). Because of the germ cell proliferation defect, *lrr-1* mutants are sterile. *lrr-1* mutants also exhibit a protruding vulva phenotype that results from a failure to produce the full complement of vulva cells; *lrr-1* mutants have an average of 15 vulva cells rather than the 22 vulva cells of wild type (Starostina et al., 2010). Here we show that $CRL2^{LRR-1}$ negatively regulates Notch signaling during vulva development, in part by negatively regulating the transcription factor DAF-12.

Materials and Methods

C. elegans alleles and general methods

C. elegans were maintained and cultured as previously described (Brenner, 1974). Strains were maintained at 20ºC unless otherwise mentioned. The following strains and alleles were used: N2, wild type, ET460 *lrr-1(tm3543)*/*mIn1* II, ET430 *lrr-1(tm3543)*/*mIn1* II; *him-8(me4)* IV, AH142 *zhIs4* [*lip-1p::gfp*] III, GS3582 *unc-4(e120)* II; *arIs92*[*egl-17p*::NLS-CFP-LacZ + *unc-4(+)* + *ttx-3*::GFP], ET534 *lrr-1(tm3543)*/*mIn1*; *zhIs4*, ET535 *lrr-1*(tm3543)/*mIn1*; *arIs92*, OP72 unc-119(ed3)III; *wgIs72*[*Plin12*::*lin-12*:: TY1:: EGFP:: 3xFLAG (92C12) + *unc-119(+)*],

zhIs39[bar-1p::nicd::gfp::unc-54 3'utr, unc-119(+)] II (gift from Alex Hajnal), *zhIs56[bar-1p::nicd::gfp*Δ*CT::unc-54 3'utr, unc-119(+)]*II (gift from Alex Hajnal), ET502 *sel-10(bc243)* V; *him-8(me4)* IV, ET536 *sel-10(bc243); zhIs39,* MD2241 bc1s58 [*ces-1p::ces-1::yfp*], PS80 *let-23(sy1);unc-4(e120)* II, SD366 *mpk-1(n2521) III*; *let-60(n1046)* IV, MT302 *lin-12(n302)* III, CB1417 *lin-3(e1417)* IV, AA120 *dhIs26*[*daf-12A*::GFP + *lin-15(+)*], MT11836 *ark-1(n3701)* IV, MT13032 *sli-1(n3538)* X, AH12 *gap-1(ga133)* X, GS60 *unc-32(e189);lin-12(n676n930)* III.

RNA interference (RNAi)

Feeding RNAi was performed on worms as described in (Kamath et al., 2001). RNAi feeding clones of *lrr-1*, *sel-10*, *daf-12*, *ces-1*, *lst-2*, *lst-3*, *lst-4*, *dpy-23, unc-101* were obtained from Ahringer library (Kamath and Ahringer, 2003) were grown in 2xYT media overnight with 100 μg/ml Carbenicillin (Gold Biotechnology). RNAi bacteria was induced by directly seeding overnight cultures on to 1X NGM plates containing 1 mM IPTG (Gold Biotechnology) and 100 μg/ml Carbenicillin. Bacteria containing the empty vector L440 were used as control RNAi.

Microscopy

Live imaging of *C. elegans* was performed with Zeiss Axioplan microscope with a Hamamatsu ORCA-ER CCD camera and Openlab 4.0.2 software (Agilent). Briefly, worms were mounted on a 2% agarose pad with 10 mM levamisole or tetramisole (Sigma). Normanski differential interference contrast (DIC) images were taken as described in (Sulston and Horvitz, 1977) GFP images for a particular genotype were all taken at the same exposure and Adobe Photoshop CS6 was used to measure fluorescence intensity.

Vulval phenotype analysis

lip-1p::GFP, *egl-17p*::CFP, *lin-12p*::*lin-12*::GFP, *bar-1p*::*nicd*::GFP, *bar-1p*::*nicd*::GFPΔCT, *daf-12p*::*daf-12*::GFP levels in the VPC were assayed at L2-L3 stage in the Pn.px cells by epifluorescence and DIC optics. L4 and adult animals were used to assay Vul and Muv phenotypes.

Quantitative real time RT-PCR (qRT-PCR)

Total RNA was isolated from different stages of worms using TRIzol reagent (Life Technologies) according to manufacturer's instructions. 0.5 μg total RNA was used to generate first strand cDNA using SuperScript III First-Strand Synthesis Kit (Life Technology) following manufacturer's instruction. qRT-PCR was performed in a 20 μl volume using SYBR Green Supermix (Bio-Rad) and analyzed using CFX Connect Real-Time PCR Detection System (Bio-Rad). The following primer sets were used to amplify the respective genes: *lst-1* forward: 5'GTGAAACTGTGCCAACGAGT 3', reverse: 5'CGAGCGTGTCCCATTTGTTC 3'; *lst-2*, forward: 5' GCAACACGATCAGCATTCCA 3', reverse: 5'ATGGCACTGTAGCTCCGTTT 3'; *lst-3*, forward: 5' *lst-4,* forward: 5' AGCTCTCGCCTACACTGCAT 3', reverse: 5'CGTCCTTCGCTGTCACGGA 3'; *dpy-23* forward: 5' CCACCAAATACATCCGGCGT 3', reverse: 5' TCATTCCGGCCATACGCTTT 3'; *lip-1* forward: 5' TCTGCCTACGAATGGGTTCAA 3', reverse: 5' CGAGGAGCCGAGGAAGGATA 3'; *daf-12*, forward: 5'ATGACTCCAACACATGGTTTT 3', reverse: 5' TTCTCCTGGCAGCTCTTCG 3' (Jeong et al., 2010); *rpl-19* (control), forward: 5' CGCGCAAAGGGAAACAACTT 3', reverse: 5'CTTGCGGCTCTCCTTGTTCT 3'. The mRNA level of each gene was normalized to *rpl-19* and relative fold change was calculated using the ΔΔCt method (Pfaffl method) (Pfaffl, 2001).

Statistical analysis

Graphs represent means with ± SEM (standard error of the mean). Two-tailed student's t-test was performed for the quantification of fluorescence in the VPCs. Chi-square test was used to analyze the percentage of Muv animals in Table 2.1. Asterisks indicate significance compared to wild type; * $P \leq 0.05$, ** $P \leq 0.01$, *** $P \leq 0.001$, ns= no significance, $P > 0.05$.

Results

lrr-1 mutants have an impenetrant Muv phenotype

The *lrr-1(tm3543)* mutant is a recessive deletion allele, which is predicted to generate a truncated LRR-1 protein lacking 66% of the C-terminal residues (Starostina et al., 2010). *lrr-1* homozygous mutants show an impenetrant Muv phenoype (0.9%, n=700) (Figure 2.1B).

Expression of 1° cell fate marker is normal in lrr-1 mutants

To determine if the inductive signal is properly perceived by the VPCs in *lrr-1* mutants, we analyzed the 1° cell fate marker *egl-17p*::CFP , which is a transcriptional target of the Ras-MAPK pathway (Yoo et al., 2004). *egl-17* encodes a homolog of mammalian fibroblast growth factor (FGF), and, together with the FGF receptor EGL-15 (Burdine et al., 1997; DeVore et al., 1995). The expression of *egl-17* in the VPCs acts as a cue to guide the proper positioning of the sex myoblasts, which migrate to the vulval region (Burdine et al., 1998). *egl-17* expression is dependent on the inductive signal LIN-3/EGF that arises from the somatic gonad and not on the LIN-12/Notch mediated lateral signal (Burdine et al., 1998). In response to the inductive signal, *egl-17p*::CFP is expressed in a graded fashion with strong expression in P6.p and weaker expression in P5.p and P7.p cells. In early L3 stage, the expression disappears from P5.p and

P7.p but persists in P6.p and its descendants (Yoo et al., 2004) (Figure 2.2A). We observed that the expression pattern of *egl-17p*::CFP in *lrr-1* mutants was identical to that in wild type hermaphrodites, with no difference in the level of expression in P6.p (Figure 2.2B,C). This suggests that the 1° vulval fate is unaffected in *lrr-1* mutants.

The expression of the LIN-12/Notch target lip-1 is elevated in lrr-1 mutant 1° and 2° VPCs

lip-1 encodes for a MAP kinase phosphatase (MKP) whose transcription is upregulated in P5.p and P7.p in response to the LIN-12/Notch-mediated lateral signal (Berset et al., 2001). LIP-1 is dual-specificity MKP similar to the human MKP-3/PYST1 (Berset et al., 2001), which can remove both activating phosphate groups from the threonine and tyrosine residues of an activated MAPK (Alessi et al., 1993; Groom et al., 1996; Guan and Butch, 1995; Muda et al., 1996). LIN-12/Notch transcribes *lip-1* by activating binding of the CSL (CBF/Suppressor of Hairless/LAG-1) transcription factor to the conserved LAG-1 binding sites on *lip-1* regulatory regions (Christensen et al., 1996). LIP-1 inactivates MPK-1 kinase activity in 2° cells to inhibit the 1º cell fate (Berset et al., 2001). *lip-1* is uniformly expressed at a low level in all VPCs until the L2 stage. In the early L3 stage, when the EGF signal is introduced from the AC, *lip-1* expression disappears from P6.p and its descendants, but is increased in P5.p and P7.p, thereby inhibiting the 1° fate in these cells (Figure 2.3A) (Berset et al., 2001). We used a *lip-1p*::GFP transcriptional reporter to assay the 2° fate in *lrr-1* homozygous mutants. We found that in *lrr-1* mutants, *lip-1p*::GFP expression perdures in P6.p and its descendants (Figure 2.3B) at significantly higher levels compared to wild-type animals, suggesting a failure to downregulate LIN-12/Notch signaling in these cells (Figure 2.3B,C). We also observed higher levels of *lip-*

1p::GFP expression in P5.p and P7.p, suggesting that LRR-1 acts to reduce the 2° cell fate marker in all three VPCs (Figure 2.3B,C).

The Muv phenotype of lrr-1 mutants is correlated with a failure to inhibit LIN-12/Notch signaling

Genetic interactions between *lrr-1* and mutants in the EGFR–Ras–MAPK and Notch pathways suggest that *lrr-1* mutant phenotypes arise from an increase in LIN-12/Notch activity. In the VPCs, Ras–MAPK and Notch signaling pathways are antagonistic (Sundaram, 2004). Disrupting any of multiple negative regulators of the Ras–MAPK pathway can increase Ras–MAPK signaling (Sundaram, 2006). Negative regulators of Ras–MAPK include: ARK-1, an Ack-related nonreceptor tyrosine kinase, that negatively regulates LET-23/EGFR (Hopper et al., 2000); GAP-1, a Ras GTPase activating protein (RasGAP), that inactivates LET-60/Ras by converting its active Ras-GTP form to inactive Ras-GDP (Hajnal et al., 1997); SLI-1, a homolog of the *Cbl* E3 ubiquitin ligase, that negatively regulates LET-23/EGFR and SEM-5(Grb2), the latter being the adapter protein that recruits a guanine exchange factor responsible for activating LET-60/Ras (Clark et al., 1992; Jongeward et al., 1995; Sundaram, 2006; Yoon et al., 1995); UNC-101, the AP1 subunit of the clathrin adaptor protein, which antagonizes the localization of LET-23/EGFR to the basolateral membrane in VPCs (Lee et al., 1994; Skorobogata et al., 2014); DPY-23, the AP2 subunit for clathrin adaptor protein (Pan et al., 2008; Yoo et al., 2004); and LST-4, a sorting nexin (Lu et al., 2011), whose orthologs have been implicated in the degradation of EGFR (Lin et al., 2002; Rapoport et al., 1997; Yoo et al., 2004). SLI-1, UNC-101, DPY-23, and LST-4, all negatively regulate LET-23/EGFR, presumably by promoting its endocytosis and/or degradation (Sundaram, 2006). The *lst (1-4)* genes, *dpy-23*, *lip-1*, *ark-1* are

classified as *lateral signal target* (*lst*) genes. These genes contain LAG-1 binding sites, which make them transcriptional targets for LIN-12/Notch (Berset et al., 2001; Yoo et al., 2004). Mutations in these negative regulators of EGFR–Ras–MAPK pathway by themselves do not cause a visible vulval phenotype (Berset et al., 2001; Berset et al., 2005; Sundaram, 2006). RNAi depletion of *lst-2*, *lst-3*, *lst-4*, *dpy-23*, *ark-1*, *gap-1*, *sli-1*, and *unc-101* mutants all suppressed the Muv phenotype of *lrr-1* mutants (Table 2.1).

There is evidence for two pathways downstream of Ras in the VPCs. In the 1° cell, Ras activates MPK-1/ERK, while in the 2° cells, Ras activates RalGEF, which activates the small GTPase Ral to promote the 2° cell (Zand et al., 2011). The mutant combination gain-of-function *let-60(n1046-gf)*/Ras with a null *mpk-1(n2521-lf)*/ERK mutation shuttles Ras activity to the RalGEF–Ral pathway, as the gain of function Ras is unable to activate the Ras–MAPK pathway because it is blocked by the *mpk-1* mutation (Zand et al., 2011). This mutant combination increases 2° cell fates in VPCs. Inactivation of *lrr-1* in the double mutant *let-60(n1046-gf)*/Ras, *mpk-1(n2521-lf)*/ERK increases the percentage of Muv from 1% to 11.5% (Table 2.1). This provides further evidence that loss of LRR-1 promotes ectopic 2° cell fate to produce the Muv phenotype.

The *let-23(sy1)* mutation deletes the last 6 amino acids in LET-23 causing mislocalization of the LET-23/EGFR receptor to the apical membrane, instead of its usual location in the basolateral membrane, causing a reduction of EGFR function and a Vul phenotype (Aroian et al., 1994; Aroian and Sternberg, 1991; Ferguson and Horvitz, 1985; Kaech et al., 1998). *lrr-1* RNAi inactivation of the *let-23(sy1)* induced a 5% Muv phenotype as well as partially suppressed the Vul phenotype, suggesting that reducing Ras–MAPK signaling enhances the Muv phenotype in *lrr-1* (Table 2.1).

Finally we wanted to determine if loss of *lrr-1* can increases the Muv phenotype independent of the EGF signaling. Therefore we used a *lin-12 (n302)* mutant that has mildly constitutive *lin-12* activity, and these animals lack an anchor cell (AC), which makes all of the VPCs adopt 3º fate due to the absence of inductive signal. However, due to the mildly elevated *lin-12* activity, a small percentage of mutants display Muv phenotype where all VPCs adopt 2º fates (Greenwald et al., 1983). In a *lin-12(n302)* mutant background, loss of a negative regulator of *lin-12* results in increased *lin-12* activity, which induces all six VPCs to adopt the 2º fate and display a Muv phenotype (Sundaram and Greenwald, 1993b). We observed that *lrr-1* RNAi on a weak gain-of-function *lin-12(n302)* mutant increases its Muv percentage from 7% in the single mutant to almost 25% (Table 2.1). Taken together, these results suggest that *lrr-1* mutant phenotype arises from an increase in LIN-12/Notch signaling in the VPCs resulting in a Muv phenotype.

LRR-1 negatively regulates LIN-12 full-length and Notch intracellular domain (NICD) protein levels in VPCs.

We wanted to determine whether the loss of LRR-1 affected the levels of full length LIN-12/Notch or LIN-12 NICD. We followed the accumulation of full-length Notch protein using a transgenic strain expressing *lin-12p*::*lin-12*::GFP, where the GFP is inserted in-frame within the C-terminal of LIN-12. We observed that the membrane localized full-length LIN-12::GFP was elevated in the P6.p cell in *lrr-1(RNAi)* animals compared to control RNAi animals (Figure 2.4A, B). To follow NICD protein levels we used the *bar-1p::nicd*::GFP strain, where NICD expression is driven uniformly in all VPCs by the *bar-1*/β-catenin promoter (Nusser-Stein et al., 2012). Because NICD::GFP is expressed in all VPCs, the P3.p, P4.p and P8.p cells adopt 2°

fates, and *bar-1p*::*nicd*::GFP transgenic animals have a multivulva phenotype. However, even in *bar-1p*::*nicd*::GFP transgenic animals, P6.p adopts a normal 1° fate, and NICD::GFP expression fades and becomes undetectable in P6.p and its descendants (Figure 2.5A) (Nusser-Stein et al., 2012). We observed that *lrr-1(RNAi)* animals have significantly elevated levels of NICD::GFP in P6.p, while the levels of NICD::GFP in P5.p and P7.p were not significantly higher than in control RNAi animals (Figure 2.5B,C). These results suggest that LRR-1 negatively regulates the levels of Notch full-length and the NICD proteins.

We wondered whether LRR-1 may directly interact with LIN-12 NICD. We co-expressed the two genes in human HEK293T cells. We did not observe any obvious interaction between NICD and LRR-1 in co-immunoprecipitation experiments, which would be expected if $CRL2^{LRR-1}$ directly targets the degradation of LIN-12 NICD (data not shown).

Loss of LRR-1 does not increase NICD levels in a sel-10 mutant background

SEL-10 is the *C. elegans* ortholog of the F-Box/WD40 repeat containing protein Fbw7 that is a part of a multi-subunit E3 ubiquitin ligase Skp1/Cul1/Fbox (SCF) complex (Feldman et al., 1997; Skowyra et al., 1997). The *sel-10* mutant was identified in a genetic screen for suppressor of *lin-12* hypomorphs (Feldman et al., 1997; Hubbard et al., 1997; Skowyra et al., 1997; Sundaram and Greenwald, 1993b). Mammalian Fbw7 and *C. elegans* SEL-10 promote the ubiquitin-mediated degradation of NICD (Gupta-Rossi et al., 2001; Hubbard et al., 1997; Oberg et al., 2001; Wu et al., 2001). Consistent with this role, we have seen that inactivation of *C. elegans sel-10* increases NICD levels.

If LRR-1 and SEL-10 regulate NICD levels independently, then one would expect that loss of both proteins would further increase NICD levels. To determine if loss of both LRR-1

and SEL-10 increases NICD more than singly, we combined *lrr-1* RNAi with a null allele of *sel-10(bc243)* that lacks the F-box domain (required to link it to the SCF complex) and all 7 WD40 repeats (Hubbard et al., 1997; Jager et al., 2004) in combination with *nicd*::GFP. We observed that RNAi depletion of *lrr-1* in *sel-10(bc243)* mutants did not cause a further increase in the levels of NICD (Figure 2.6). This suggests that LRR-1 does not regulate NICD independently of SEL-10.

NICD contains a nuclear localization signal (NLS) followed by a RAM domain (RBP-jκ association module) (Kopan and Ilagan, 2009). The RAM domain contains a DTS (downregulation target signal) that is necessary for Notch endocytosis (Shaye and Greenwald, 2002). Next to the RAM domain are the Ankyrin repeats (ANK) that are required to interact with the CSL transcription factors, followed by a PEST (proline/glutamic acid/serine/threonine-enriched) sequence. The PEST domain contains multiple phosphorylation sites, which are phosphorylated by cyclin C-dependent kinase (CDK8) (Fryer et al., 2004). Hyperphosphorylated NICD is ubiquitinated by Fbw7/SEL-10 (Fryer et al., 2004; Gupta-Rossi et al., 2001; Kopan and Ilagan, 2009; Oberg et al., 2001; Wu et al., 2001). Deleting the C terminal PEST domain of NICD (NICD-GFPΔCT) stabilizes NICD-GFPΔCT in P6.p and elevates it in P5.p and P7.p (Nusser-Stein et al., 2012). We observed that RNAi depletion of *lrr-1* does not increase NICD-GFPΔCT levels in the VPCs (Figure 2.7). These results suggest that LRR-1 affects NICD levels only if SEL-10-mediated degradation of NICD is functioning. This suggests that LRR-1 might function upstream of SEL-10 to promote its activity, and that in *lrr-1* mutants, the level of NICD increases due to a failure of SEL-10-mediated degradation of NICD.

Loss of LRR-1 has a larger impact on Notch target gene expression than loss of SEL-10

sel-10 loss-of-function elevates Notch signaling and enhances Muv phenotypes of *lin-12* hypermorphs, however *sel-10* mutants by themselves they do not have a Muv phenotype (Hubbard et al., 1997; Sundaram and Greenwald, 1993b). As *lrr-1* mutants have a Muv phenotype, we expected LRR-1 to regulate Notch signaling independently of *sel-10*. Supporting this hypothesis, we observed that *lrr-1* RNAi depletion in a *sel-10 (bc243)* null mutant (Jager et al., 2004) increased the percentage of Muv from 0% to 5.6%. The increase in the Muv phenotype from the knockdown of both genes presumably results in higher levels of Notch signaling, suggesting that LRR-1 might function independently of SEL-10 to regulate Notch mediated Muv phenotype.

Interestingly, when comparing the level of the Notch-regulated 2° cell marker *lip-1p*::GFP, we observed significantly higher levels in P5.p, P6.p and P7.p cells *lrr-1* mutants compared to wild type, while *sel-10(RNAi)* animals did not show a significant increase (Figure 2.8A, B). This suggests that loss of *lrr-1* activates the Notch-regulated 2° cell fate pathway, while loss of *sel-10* does not. Interestingly, *sel-10* RNAi increases the level of full-length LIN-12/Notch to a higher level than is observed in *lrr-1* mutants. This suggests that even though both NICD and full-length LIN-12 accumulate to higher levels upon inactivation of *sel-10* compared to *lrr-1* mutants, the loss of LRR-1 has a larger impact on the expression of the *lip-1p*::GFP Notch reporter than the loss of SEL-10.

We wanted to determine if the levels of other Notch target genes are also elevated in *lrr-1* mutants relative to *sel-10* mutants. We performed real-time quantitative RT-PCR on several of the *lst* genes, including *lip-1*. We found that the mRNA levels of *lst-2, lip-1*, and *dpy-23* were all more elevated in *lrr-1* mutants than in *sel-10* mutants; *lst-4* was only slightly higher than wild-

type; and *lst-1* and *lst-3* showed reduced mRNA levels in both *lrr-1* and *sel-10* mutants compared to the wild-type (Figure 2.9). These results suggest that a subset of genes promoting 2° cell fate and/or downregulating EGFR–Ras–MAPK are elevated in *lrr-1* mutants.

DAF-12 and CES-1 transcription factors are required for the elevated levels of lip-1p::GFP in lrr-1 mutants

In Notch signaling, once the Notch receptor is cleaved by γ-secretase (Kopan and Ilagan, 2009), the NICD translocates to the nucleus and initiates the transcription of downstream genes. NICD does not bind to genomic DNA directly, but instead binds as a heterodimer with the CSL (CBF1/Su(H)/LAG-1) transcription factor LAG-1, and its co-activator LAG-3 (Christensen et al., 1996). The *lst* genes (*ark-1, dpy-23, lst (1-4)*) are regulated by Notch signaling and were also shown to have LAG-1 binding sites (Berset et al., 2001; Yoo et al., 2004). We explored the possibility that the *lst* genes that were upregulated in *lrr-1* mutants share common transcription factor(s). We utilized the *C. elegans* ChIP-seq database available from the modENCODE Project to obtain a list of transcription factors that are bound to the regulatory regions of the *lst* genes (www.modencode.org) (Celniker et al., 2009; Gerstein et al., 2010). Binding of multiple transcription factors in homotypic clusters in the regulatory regions of eukaryotic genomes is associated with actively transcribed genes (Ezer et al., 2014; Gotea et al., 2010). We focused on transcription factors that had more binding sites in the genes that were upregulated in *lrr-1* mutants (*lip-1, lst-2,* and *dpy-23*) relative to the genes that were unchanged or downregulated in *lrr-1* mutants (*lst-1, lst-3, lst-4*). We identified over 50 candidate transcription factors binding to the regulatory region of these genes (Table 2.2). Two of the transcription factors met these criteria: DAF-12 had two binding sites in the regulatory regions of each of the three upregulated

genes but none in the downregulated genes; and the transcription factor CES-1 had more binding sites in the upregulated genes (7-10) and fewer in the downregulated genes (0-3).

DAF-12 is a steroid hormone receptor that is homologous to the vertebrate vitamin-D receptor (Antebi et al., 2000). The steroid hormone dafachronic acid (DA) acts as a ligand for DAF-12 to regulate its transcriptional activity (Antebi, 2013; Hochbaum et al., 2011). DAF-12 regulates heterochronic larval and adult development in part by regulating microRNAs (Antebi, 2013). *daf-12* encodes multiple isoforms, the A1 and A3 isoforms have both DNA- and ligand-binding domains, whereas the B isoform encodes lacks the DNA-binding domain (Antebi et al., 2000). We tested if DAF-12 contributes to the upregulation of *lip-1p*::GFP expression in *lrr-1* mutants. RNAi depletion of *daf-12* in *lrr-1* mutants expressing *lip-1p*::GFP significantly reduced *lip-1p*::GFP expression in P5.p and P6.p (Figure 2.10A). This suggests that DAF-12 contributes to the upregulation of *lip-1* expression in *lrr-1* mutants.

ces-1 (*ce*ll death *s*pecific-1) encodes a Snail family Zinc-finger protein that (Metzstein and Horvitz, 1999; Roark et al., 1995) promotes neuronal cell fates and prevents the cells from undergoing programmed cell death (Ellis and Horvitz, 1991). We did not see detectable *ces-1p::ces-1::yfp* expression in the VPCs, suggesting that its expression is very low in these cells (data not shown). Nevertheless, *ces-1 RNAi* in *lrr-1* mutants significantly reduced *lip-1p*::GFP levels in all three VPCs. (Figure 2.10B). A double RNAi depletion of *daf-12* and *ces-1 (RNAi)* in *lrr-1* mutants resulted in elimination of the elevated *lip-1p*::GFP levels in P6.p cells, and modestly decreased the levels in P5.p and P6.p relative to the individual RNAi depletions (Figure 2.10C). This suggests that in *lrr-1* mutants, both *daf-12* and *ces-1* are required for the increased expression of the Notch target gene *lip-1*.

DAF-12::GFP protein levels are increased in VPCs in lrr-1 mutants, but daf-12 mRNA levels are unchanged

DAF-12::GFP is localized primarily to the nucleus and is widely expressed in multiple tissues (Antebi et al., 1998; Antebi et al., 2000). In the vulva, *daf-12p::daf-12*::GFP is expressed in VPCs in the L2 stage at the Pn.px and Pn.pxx stage and then proceeds to fade in the adult vulva (Antebi et al., 2000). DAF-12::GFP expresses at approximately equal levels in the VPCs (Figure 2.11). *lrr-1* RNAi depletion causes a significant increase in DAF-12::GFP levels in P5.p, P6.p and P7.p (Figure 2.11A). Since *daf-12p::daf-12*::GFP is a fosmid containing the *daf-12* regulatory region, we wanted to determine whether the increase in *daf-12* levels was due to an increase in *daf-12* mRNA levels. We performed real-time quantitative RT-PCR and saw no change in the *daf-12* mRNA levels in *lrr-1* mutants versus wild type (Figure 2.11B). Therefore, the changes in DAF-12::GFP levels in *lrr-1* can be attributed to a post-transcriptional increase in DAF-12::GFP protein levels. In an attempt to address if LRR-1, as part of the $CRL2^{LRR-1}$ complex, targets the degradation of DAF-12, we asked whether LRR-1 can bind to DAF-12. We expressed myc-tagged DAF-12 protein with FLAG-tagged LRR-1 in human HEK293T cells to assess interaction by co-immunoprecipitation. However, we were unable to detect physical interaction in this assay (data not shown).

Discussion

We describe $CRL2^{LRR-1}$ as a new negative regulator of LIN-12/Notch signaling pathway. Loss of LRR-1 leads to an impenetrant (1%) multivulva phenotype, which is exacerbated in sensitized genetic backgrounds that increase LIN-12 activity. For example, in a *lin-12* mild gain-of-function mutant, *lrr-1 RNAi* increases the percentage of Muv animals from 7% to 25%, and in

combination with *sel-10 (null)* mutants the Muv percentage increases to 5%. Similarly, loss of the Notch effectors *lst-2, lst-3, lst-4* and *dpy-23* can suppress the Muv phenotype in *lrr-1* mutants. The increase in Notch activity in *lrr-1* is reflected in higher expression of the Notch reporter *lip-1p::gfp* in all three VPCs. Loss of *lrr-1* increases the levels of both full-length LIN-12/Notch and LIN-12 NICD. Although *cul-2* mutants do not show a Muv phenotype, *cul-2 (RNAi)* increases NICD::GFP expression similar to that in *lrr-1(RNAi)* animals (data not shown), thereby establishing a connection between the mutant phenotypes of *lrr-1* and *cul-2*.

Although not significant, *daf-12* and *ces-1* RNAi showed slight reduction in *lip-1p*::GFP levels in P5.p and P7.p in wild-type animals. DAF-12 and CES-1 has binding sites in the regulatory region of *lst-2*, *lst-4* and *dpy-23*, the other Notch targets whose mRNA levels are also upregulated in *lrr-1* mutants. Further investigation needs to be done to demonstrate whether *daf-12* and *ces-1* RNAi can also inhibit mRNA levels of these genes in wild-type as well as in *lrr-1* mutants. The function of both DAF-12 and CES-1 transcription factors inhibiting the levels of the Notch target gene *lip-1* in *lrr-1* mutants, demonstrates an added layer of regulation in the Notch signaling pathway

LIN-12/Notch is regulated by the feedback mechanism in *C. elegans* during the AC-VU cell fate decision (Greenwald et al., 1983; Wilkinson and Greenwald, 1995), where the HLH-2 transcription factor (the basic helix-loop-helix ortholog of the mammalian E2A) plays a key role in deciding which cell becomes the AC (Sallee and Greenwald, 2015). LIN-12 activation causes downregulation of HLH-2, which is necessary to inhibit *lag-2* transcription in the same cell, making it the AC cell (Sallee and Greenwald, 2015). *lin-12* is not yet known to be transcriptionally regulated in the VPCs, as a *lin-12* transcriptional reporter is expressed in all VPCs at equal levels from the L2 through the L3 stage (Wilkinson and Greenwald, 1995).

However, other mechanisms might exist whereby LIN-12/Notch receptor is stabilized at the protein level by the activity of its downstream target genes.

Although SEL-10 degrades NICD (Hubbard et al., 1997) and upregulates full-length LIN-12/Notch receptor levels in the VPC (Shaye and Greenwald, 2002), *sel-10* mutants do no exhibit a Muv phenotype on their own (Hubbard et al., 1997; Jager et al., 2004) but can exacerbate *lin-12* gain-of-function phenotypes (Hubbard et al., 1997). On the other hand *lrr-1* displays a Muv phenotype on its own as well as displays both high levels of NICD and LIN-12 full-length receptor. Moreover, *lrr-1* displays higher transcript levels of the Notch transcriptional target genes *lst-2*, *lst-4*, *lip-1* and *dpy-23* compared to *sel-10*. These results imply that LRR-1 acts downstream of SEL-10, at the level of regulating Notch gene transcription, which in turn may work to stabilize LIN-12 full-length as well as NICD protein levels in the VPCs of *lrr-1* mutants. Notch is known to positively regulate itself in several cancerous cell lines. Mutations in the C-terminal domain of Notch that prevent NICD degradation, are often found together with mutations in Fbw7 (human homolog of SEL-10) in T-cell acute lymphoblastic leukemia (T-ALL) (O'Neil et al., 2007; Thompson et al., 2007). In T-ALL cell lines, the Notch homolog NICD-3 mediated activation of the micro RNA *mir-233* was shown to repress Fbw7 levels (Borggrefe et al., 2016; Kumar et al., 2014). Interestingly, a direct Notch1 transcriptional target called Prolyl isomerase 1 (Pin1) was shown to positively reinforce Notch signaling in breast cancer cells by enhancing the γ-secretase mediated cleavage of Notch1 resulting in an increase in Notch1-ICD levels (Rustighi et al., 2009). Pin1 was shown to directly bind to phosphorylated Notch1 at conserved serine/threonine rich (STR) region to possibly bring about a conformational change in the Notch1 receptor so that γ-secretase can efficiently cleave it and release NICD1 (Rustighi et al., 2009). Notch regulates a plethora of target genes during

development, and in certain cases such as in tumorigenic cells, Notch target genes enhance Notch activity to continue a feed-forward cycle (Borggrefe et al., 2016; Rustighi et al., 2009). Identification and understanding the players in these feed-forward pathways will have tremendous implications in human cancer therapeutics.

Author Contributions

M.M conceived and performed experiments. M.M and E.T.K wrote the paper.

Acknowledgements

Some *C. elegans* strains were provided by the CGC, which is funded by NIH Office of Research Infrastructure Programs (P40 OD010440). Some strains were gifts from Alex Hajnal. Ying Cao performed some of the initial Muv analysis in Table 2.1. We thank Dr. Karl F Lechtreck for the use of the real-time PCR machine. This work was supported by the grant NIH/NIGMS (1R01GM074212) to ETK.

References

Aguirre, A., Rubio, M.E., and Gallo, V. (2010). Notch and EGFR pathway interaction regulates neural stem cell number and self-renewal. Nature *467*, 323-327.

Alessi, D.R., Smythe, C., and Keyse, S.M. (1993). The human CL100 gene encodes a Tyr/Thr-protein phosphatase which potently and specifically inactivates MAP kinase and suppresses its activation by oncogenic ras in Xenopus oocyte extracts. Oncogene *8*, 2015-2020.

Allenspach, E.J., Maillard, I., Aster, J.C., and Pear, W.S. (2002). Notch signaling in cancer. Cancer biology & therapy *1*, 466-476.

Antebi, A. (2013). Steroid regulation of C. elegans diapause, developmental timing, and longevity. Current topics in developmental biology *105*, 181-212.

Antebi, A., Culotti, J.G., and Hedgecock, E.M. (1998). daf-12 regulates developmental age and the dauer alternative in Caenorhabditis elegans. Development *125*, 1191-1205.

Antebi, A., Yeh, W.H., Tait, D., Hedgecock, E.M., and Riddle, D.L. (2000). daf-12 encodes a nuclear receptor that regulates the dauer diapause and developmental age in C. elegans. Genes Dev *14*, 1512-1527.

Aroian, R.V., Koga, M., Mendel, J.E., Ohshima, Y., and Sternberg, P.W. (1990). The let-23 gene necessary for Caenorhabditis elegans vulval induction encodes a tyrosine kinase of the EGF receptor subfamily. Nature *348*, 693-699.

Aroian, R.V., Lesa, G.M., and Sternberg, P.W. (1994). Mutations in the Caenorhabditis elegans let-23 EGFR-like gene define elements important for cell-type specificity and function. The EMBO journal *13*, 360-366.

Aroian, R.V., and Sternberg, P.W. (1991). Multiple Functions of let-23, a Caenorhabditis elegans Receptor Tyrosine Kinase Gene Required for Vulval Induction. Genetics *128*, 251-267.

Beitel, G.J., Clark, S.G., and Horvitz, H.R. (1990). Caenorhabditis elegans ras gene let-60 acts as a switch in the pathway of vulval induction. Nature *348*, 503-509.

Beitel, G.J., Tuck, S., Greenwald, I., and Horvitz, H.R. (1995). The Caenorhabditis elegans gene lin-1 encodes an ETS-domain protein and defines a branch of the vulval induction pathway. Genes & development *9*, 3149-3162.

Berset, T., Hoier, E.F., Battu, G., Canevascini, S., and Hajnal, A. (2001). Notch inhibition of RAS signaling through MAP kinase phosphatase LIP-1 during C. elegans vulval development. Science *291*, 1055-1058.

Berset, T.A., Hoier, E.F., and Hajnal, A. (2005). The C. elegans homolog of the mammalian tumor suppressor Dep-1/Scc1 inhibits EGFR signaling to regulate binary cell fate decisions. Genes & development *19*, 1328-1340.

Borggrefe, T., Lauth, M., Zwijsen, A., Huylebroeck, D., Oswald, F., and Giaimo, B.D. (2016). The Notch intracellular domain integrates signals from Wnt, Hedgehog, TGFbeta/BMP and hypoxia pathways. Biochimica et biophysica acta *1863*, 303-313.

Bosu, D.R., and Kipreos, E.T. (2008). Cullin-RING ubiquitin ligases: global regulation and activation cycles. Cell division *3*, 7.

Brenner, S. (1974). The genetics of Caenorhabditis elegans. Genetics *77*, 71-94.

Burdine, R.D., Branda, C.S., and Stern, M.J. (1998). EGL-17(FGF) expression coordinates the attraction of the migrating sex myoblasts with vulval induction in C. elegans. Development *125*, 1083-1093.

Burdine, R.D., Chen, E.B., Kwok, S.F., and Stern, M.J. (1997). egl-17 encodes an invertebrate fibroblast growth factor family member required specifically for sex myoblast migration in Caenorhabditis elegans. Proceedings of the National Academy of Sciences of the United States of America *94*, 2433-2437.

Celniker, S.E., Dillon, L.A., Gerstein, M.B., Gunsalus, K.C., Henikoff, S., Karpen, G.H., Kellis, M., Lai, E.C., Lieb, J.D., MacAlpine, D.M.*, et al.* (2009). Unlocking the secrets of the genome. Nature *459*, 927-930.

Chen, N., and Greenwald, I. (2004). The lateral signal for LIN-12/Notch in C. elegans vulval development comprises redundant secreted and transmembrane DSL proteins. Developmental cell *6*, 183-192.

Christensen, S., Kodoyianni, V., Bosenberg, M., Friedman, L., and Kimble, J. (1996). lag-1, a gene required for lin-12 and glp-1 signaling in Caenorhabditis elegans, is homologous to human CBF1 and Drosophila Su(H). Development *122*, 1373-1383.

Clandinin, T.R., Katz, W.S., and Sternberg, P.W. (1997). Caenorhabditis elegans HOM-C genes regulate the response of vulval precursor cells to inductive signal. Developmental biology *182*, 150-161.

Clark, S.G., Stern, M.J., and Horvitz, H.R. (1992). C. elegans cell-signalling gene sem-5 encodes a protein with SH2 and SH3 domains. Nature *356*, 340-344.

DeVore, D.L., Horvitz, H.R., and Stern, M.J. (1995). An FGF receptor signaling pathway is required for the normal cell migrations of the sex myoblasts in C. elegans hermaphrodites. Cell *83*, 611-620.

Ellis, R.E., and Horvitz, H.R. (1991). Two C. elegans genes control the programmed deaths of specific cells in the pharynx. Development *112*, 591-603.

Ezer, D., Zabet, N.R., and Adryan, B. (2014). Homotypic clusters of transcription factor binding sites: A model system for understanding the physical mechanics of gene expression. Computational and structural biotechnology journal *10*, 63-69.

Feldman, R.M., Correll, C.C., Kaplan, K.B., and Deshaies, R.J. (1997). A complex of Cdc4p, Skp1p, and Cdc53p/cullin catalyzes ubiquitination of the phosphorylated CDK inhibitor Sic1p. Cell *91*, 221-230.

Ferguson, E.L., and Horvitz, H.R. (1985). Identification and characterization of 22 genes that affect the vulval cell lineages of the nematode Caenorhabditis elegans. Genetics *110*, 17-72.

Fortini, M.E., and Artavanis-Tsakonas, S. (1993). Notch: neurogenesis is only part of the picture. Cell *75*, 1245-1247.

Fryer, C.J., White, J.B., and Jones, K.A. (2004). Mastermind recruits CycC:CDK8 to phosphorylate the Notch ICD and coordinate activation with turnover. Molecular cell *16*, 509-520.

Gerstein, M.B., Lu, Z.J., Van Nostrand, E.L., Cheng, C., Arshinoff, B.I., Liu, T., Yip, K.Y., Robilotto, R., Rechtsteiner, A., Ikegami, K*., et al.* (2010). Integrative analysis of the Caenorhabditis elegans genome by the modENCODE project. Science *330*, 1775-1787.

Gotea, V., Visel, A., Westlund, J.M., Nobrega, M.A., Pennacchio, L.A., and Ovcharenko, I. (2010). Homotypic clusters of transcription factor binding sites are a key component of human promoters and enhancers. Genome research *20*, 565-577.

Greenwald, I. (2005). LIN-12/Notch signaling in C. elegans. WormBook : the online review of C elegans biology, 1-16.

Greenwald, I.S., Sternberg, P.W., and Horvitz, H.R. (1983). The lin-12 locus specifies cell fates in Caenorhabditis elegans. Cell *34*, 435-444.

Groom, L.A., Sneddon, A.A., Alessi, D.R., Dowd, S., and Keyse, S.M. (1996). Differential regulation of the MAP, SAP and RK/p38 kinases by Pyst1, a novel cytosolic dual-specificity phosphatase. The EMBO journal *15*, 3621-3632.

Guan, K.L., and Butch, E. (1995). Isolation and characterization of a novel dual specific phosphatase, HVH2, which selectively dephosphorylates the mitogen-activated protein kinase. The Journal of biological chemistry *270*, 7197-7203.

Guerry, F., Marti, C.O., Zhang, Y., Moroni, P.S., Jaquiery, E., and Muller, F. (2007). The Mi-2 nucleosome-remodeling protein LET-418 is targeted via LIN-1/ETS to the promoter of lin-39/Hox during vulval development in C. elegans. Developmental biology *306*, 469-479.

Gupta-Rossi, N., Le Bail, O., Gonen, H., Brou, C., Logeat, F., Six, E., Ciechanover, A., and Israel, A. (2001). Functional interaction between SEL-10, an F-box protein, and the nuclear form of activated Notch1 receptor. The Journal of biological chemistry *276*, 34371-34378.

Hajnal, A., Whitfield, C.W., and Kim, S.K. (1997). Inhibition of Caenorhabditis elegans vulval induction by gap-1 and by let-23 receptor tyrosine kinase. Genes & development *11*, 2715-2728.

Han, M., Aroian, R.V., and Sternberg, P.W. (1990). The let-60 locus controls the switch between vulval and nonvulval cell fates in Caenorhabditis elegans. Genetics *126*, 899-913.

Han, M., and Sternberg, P.W. (1990). let-60, a gene that specifies cell fates during C. elegans vulval induction, encodes a ras protein. Cell *63*, 921-931.

Hill, R.J., and Sternberg, P.W. (1992). The gene lin-3 encodes an inductive signal for vulval development in C. elegans. Nature *358*, 470-476.

Hitoshi, S., Alexson, T., Tropepe, V., Donoviel, D., Elia, A.J., Nye, J.S., Conlon, R.A., Mak, T.W., Bernstein, A., and van der Kooy, D. (2002). Notch pathway molecules are essential for the maintenance, but not the generation, of mammalian neural stem cells. Genes & development *16*, 846-858.

Hochbaum, D., Zhang, Y., Stuckenholz, C., Labhart, P., Alexiadis, V., Martin, R., Knolker, H.J., and Fisher, A.L. (2011). DAF-12 regulates a connected network of genes to ensure robust developmental decisions. PLoS genetics *7*, e1002179.

Hopper, N.A., Lee, J., and Sternberg, P.W. (2000). ARK-1 inhibits EGFR signaling in C. elegans. Molecular cell *6*, 65-75.

Hubbard, E.J., Wu, G., Kitajewski, J., and Greenwald, I. (1997). sel-10, a negative regulator of lin-12 activity in Caenorhabditis elegans, encodes a member of the CDC4 family of proteins. Genes & development *11*, 3182-3193.

Irvine, K.D., and Vogt, T.F. (1997). Dorsal-ventral signaling in limb development. Current opinion in cell biology *9*, 867-876.

Jager, S., Schwartz, H.T., Horvitz, H.R., and Conradt, B. (2004). The Caenorhabditis elegans F-box protein SEL-10 promotes female development and may target FEM-1 and FEM-3 for degradation by the proteasome. Proceedings of the National Academy of Sciences of the United States of America *101*, 12549-12554.

Jeong, M.H., Kawasaki, I., and Shim, Y.H. (2010). A circulatory transcriptional regulation among daf-9, daf-12, and daf-16 mediates larval development upon cholesterol starvation in Caenorhabditis elegans. Developmental dynamics : an official publication of the American Association of Anatomists *239*, 1931-1940.

Jongeward, G.D., Clandinin, T.R., and Sternberg, P.W. (1995). sli-1, a negative regulator of let-23-mediated signaling in C. elegans. Genetics *139*, 1553-1566.

Kaech, S.M., Whitfield, C.W., and Kim, S.K. (1998). The LIN-2/LIN-7/LIN-10 complex mediates basolateral membrane localization of the C. elegans EGF receptor LET-23 in vulval epithelial cells. Cell *94*, 761-771.

Kamath, R.S., and Ahringer, J. (2003). Genome-wide RNAi screening in Caenorhabditis elegans. Methods *30*, 313-321.

Kamath, R.S., Martinez-Campos, M., Zipperlen, P., Fraser, A.G., and Ahringer, J. (2001). Effectiveness of specific RNA-mediated interference through ingested double-stranded RNA in Caenorhabditis elegans. Genome biology *2*, RESEARCH0002.

Katz, W.S., Hill, R.J., Clandinin, T.R., and Sternberg, P.W. (1995). Different levels of the C. elegans growth factor LIN-3 promote distinct vulval precursor fates. Cell *82*, 297-307.

Katz, W.S., Lesa, G.M., Yannoukakos, D., Clandinin, T.R., Schlessinger, J., and Sternberg, P.W. (1996). A point mutation in the extracellular domain activates LET-23, the Caenorhabditis elegans epidermal growth factor receptor homolog. Molecular and cellular biology *16*, 529-537.

Kopan, R., and Ilagan, M.X. (2009). The canonical Notch signaling pathway: unfolding the activation mechanism. Cell *137*, 216-233.

Kumar, V., Palermo, R., Talora, C., Campese, A.F., Checquolo, S., Bellavia, D., Tottone, L., Testa, G., Miele, E., Indraccolo, S.*, et al.* (2014). Notch and NF-kB signaling pathways regulate miR-223/FBXW7 axis in T-cell acute lymphoblastic leukemia. Leukemia *28*, 2324-2335.

Lee, J., Jongeward, G.D., and Sternberg, P.W. (1994). unc-101, a gene required for many aspects of Caenorhabditis elegans development and behavior, encodes a clathrin-associated protein. Genes & development *8*, 60-73.

Levitan, D., and Greenwald, I. (1998). LIN-12 protein expression and localization during vulval development in C. elegans. Development *125*, 3101-3109.

Lin, Q., Lo, C.G., Cerione, R.A., and Yang, W. (2002). The Cdc42 target ACK2 interacts with sorting nexin 9 (SH3PX1) to regulate epidermal growth factor receptor degradation. The Journal of biological chemistry *277*, 10134-10138.

Liu, Z.J., Shirakawa, T., Li, Y., Soma, A., Oka, M., Dotto, G.P., Fairman, R.M., Velazquez, O.C., and Herlyn, M. (2003). Regulation of Notch1 and Dll4 by vascular endothelial growth factor in arterial endothelial cells: implications for modulating arteriogenesis and angiogenesis. Molecular and cellular biology *23*, 14-25.

Lu, N., Shen, Q., Mahoney, T.R., Liu, X., and Zhou, Z. (2011). Three sorting nexins drive the degradation of apoptotic cells in response to PtdIns(3)P signaling. Molecular biology of the cell *22*, 354-374.

Maloof, J.N., and Kenyon, C. (1998). The Hox gene lin-39 is required during C. elegans vulval induction to select the outcome of Ras signaling. Development *125*, 181-190.

Merlet, J., Burger, J., Tavernier, N., Richaudeau, B., Gomes, J.E., and Pintard, L. (2010). The CRL2LRR-1 ubiquitin ligase regulates cell cycle progression during C. elegans development. Development *137*, 3857-3866.

Metzstein, M.M., and Horvitz, H.R. (1999). The C. elegans cell death specification gene ces-1 encodes a snail family zinc finger protein. Molecular cell *4*, 309-319.

Muda, M., Boschert, U., Dickinson, R., Martinou, J.C., Martinou, I., Camps, M., Schlegel, W., and Arkinstall, S. (1996). MKP-3, a novel cytosolic protein-tyrosine phosphatase that exemplifies a new class of mitogen-activated protein kinase phosphatase. The Journal of biological chemistry *271*, 4319-4326.

Nusser-Stein, S., Beyer, A., Rimann, I., Adamczyk, M., Piterman, N., Hajnal, A., and Fisher, J. (2012). Cell-cycle regulation of NOTCH signaling during C. elegans vulval development. Molecular systems biology *8*, 618.

O'Neil, J., Grim, J., Strack, P., Rao, S., Tibbitts, D., Winter, C., Hardwick, J., Welcker, M., Meijerink, J.P., Pieters, R.*, et al.* (2007). FBW7 mutations in leukemic cells mediate NOTCH pathway activation and resistance to gamma-secretase inhibitors. The Journal of experimental medicine *204*, 1813-1824.

Oberg, C., Li, J., Pauley, A., Wolf, E., Gurney, M., and Lendahl, U. (2001). The Notch intracellular domain is ubiquitinated and negatively regulated by the mammalian Sel-10 homolog. The Journal of biological chemistry *276*, 35847-35853.

Pan, C.L., Baum, P.D., Gu, M., Jorgensen, E.M., Clark, S.G., and Garriga, G. (2008). C. elegans AP-2 and retromer control Wnt signaling by regulating mig-14/Wntless. Developmental cell *14*, 132-139.

Pellegrino, M.W., Farooqui, S., Frohli, E., Rehrauer, H., Kaeser-Pebernard, S., Muller, F., Gasser, R.B., and Hajnal, A. (2011). LIN-39 and the EGFR/RAS/MAPK pathway regulate C. elegans vulval morphogenesis via the VAB-23 zinc finger protein. Development *138*, 4649-4660.

Penton, A.L., Leonard, L.D., and Spinner, N.B. (2012). Notch signaling in human development and disease. Seminars in cell & developmental biology.

Petroski, M.D., and Deshaies, R.J. (2005). Function and regulation of cullin-RING ubiquitin ligases. Nature reviews Molecular cell biology *6*, 9-20.

Pfaffl, M.W. (2001). A new mathematical model for relative quantification in real-time RT-PCR. Nucleic acids research *29*, e45.

Rapoport, I., Miyazaki, M., Boll, W., Duckworth, B., Cantley, L.C., Shoelson, S., and Kirchhausen, T. (1997). Regulatory interactions in the recognition of endocytic sorting signals by AP-2 complexes. The EMBO journal *16*, 2240-2250.

Roark, M., Sturtevant, M.A., Emery, J., Vaessin, H., Grell, E., and Bier, E. (1995). scratch, a pan-neural gene encoding a zinc finger protein related to snail, promotes neuronal development. Genes & development *9*, 2384-2398.

Rustighi, A., Tiberi, L., Soldano, A., Napoli, M., Nuciforo, P., Rosato, A., Kaplan, F., Capobianco, A., Pece, S., Di Fiore, P.P.*, et al.* (2009). The prolyl-isomerase Pin1 is a Notch1 target that enhances Notch1 activation in cancer. Nature cell biology *11*, 133-142.

Sallee, M.D., and Greenwald, I. (2015). Dimerization-driven degradation of C. elegans and human E proteins. Genes & development *29*, 1356-1361.

Seydoux, G., and Greenwald, I. (1989). Cell autonomy of lin-12 function in a cell fate decision in C. elegans. Cell *57*, 1237-1245.

Shaye, D.D., and Greenwald, I. (2002). Endocytosis-mediated downregulation of LIN-12/Notch upon Ras activation in Caenorhabditis elegans. Nature *420*, 686-690.

Shemer, G., and Podbilewicz, B. (2002). LIN-39/Hox triggers cell division and represses EFF-1/fusogen-dependent vulval cell fusion. Genes & development *16*, 3136-3141.

Skorobogata, O., Escobar-Restrepo, J.M., and Rocheleau, C.E. (2014). An AGEF-1/Arf GTPase/AP-1 ensemble antagonizes LET-23 EGFR basolateral localization and signaling during C. elegans vulva induction. PLoS genetics *10*, e1004728.

Skowyra, D., Craig, K.L., Tyers, M., Elledge, S.J., and Harper, J.W. (1997). F-box proteins are receptors that recruit phosphorylated substrates to the SCF ubiquitin-ligase complex. Cell *91*, 209-219.

Starostina, N.G., Simpliciano, J.M., McGuirk, M.A., and Kipreos, E.T. (2010). CRL2(LRR-1) targets a CDK inhibitor for cell cycle control in C. elegans and actin-based motility regulation in human cells. Developmental cell *19*, 753-764.

Sternberg, P.W. (2005). Vulval development. WormBook : the online review of C elegans biology, 1-28.

Sternberg, P.W., and Horvitz, H.R. (1986). Pattern formation during vulval development in C. elegans. Cell *44*, 761-772.

Sternberg, P.W., and Horvitz, H.R. (1989). The Combined Action of Two Intercellular Signaling Pathways Specifies Three Cell Fates during Vulval Induction in C. elegans. Cell *58*, 679-693.

Sulston, J.E., and Horvitz, H.R. (1977). Post-embryonic cell lineages of the nematode, Caenorhabditis elegans. Developmental biology *56*, 110-156.

Sundaram, M., and Greenwald, I. (1993a). Suppressors of a lin-12 hypomorph define genes that interact with both lin-12 and glp-1 in Caenorhabditis elegans. Genetics *135*, 765-783.

Sundaram, M., and Greenwald, I. (1993b). Suppressors of a lin-12 hypomorph define genes that interact with both lin-12 and glp-1 in Caenorhabditis elegans. Genetics *135*, 765-783.

Sundaram, M.V. (2004). Vulval development: the battle between Ras and Notch. Current biology : CB *14*, R311-313.

Sundaram, M.V. (2006). RTK/Ras/MAPK signaling. WormBook : the online review of C elegans biology, 1-19.

Tan, P.B., Lackner, M.R., and Kim, S.K. (1998). MAP kinase signaling specificity mediated by the LIN-1 Ets/LIN-31 WH transcription factor complex during C. elegans vulval induction. Cell *93*, 569-580.

Thompson, B.J., Buonamici, S., Sulis, M.L., Palomero, T., Vilimas, T., Basso, G., Ferrando, A., and Aifantis, I. (2007). The SCFFBW7 ubiquitin ligase complex as a tumor suppressor in T cell leukemia. The Journal of experimental medicine *204*, 1825-1835.

Wagmaister, J.A., Miley, G.R., Morris, C.A., Gleason, J.E., Miller, L.M., Kornfeld, K., and Eisenmann, D.M. (2006). Identification of cis-regulatory elements from the C. elegans Hox gene lin-39 required for embryonic expression and for regulation by the transcription factors LIN-1, LIN-31 and LIN-39. Developmental biology *297*, 550-565.

Wilkinson, H.A., Fitzgerald, K., and Greenwald, I. (1994). Reciprocal changes in expression of the receptor lin-12 and its ligand lag-2 prior to commitment in a C. elegans cell fate decision. Cell *79*, 1187-1198.

Wilkinson, H.A., and Greenwald, I. (1995). Spatial and temporal patterns of lin-12 expression during C. elegans hermaphrodite development. Genetics *141*, 513-526.

Wu, G., Lyapina, S., Das, I., Li, J., Gurney, M., Pauley, A., Chui, I., Deshaies, R.J., and Kitajewski, J. (2001). SEL-10 is an inhibitor of notch signaling that targets notch for ubiquitin-mediated protein degradation. Molecular and cellular biology *21*, 7403-7415.

Yoo, A.S., Bais, C., and Greenwald, I. (2004). Crosstalk between the EGFR and LIN-12/Notch pathways in C. elegans vulval development. Science *303*, 663-666.

Yoo, A.S., and Greenwald, I. (2005). LIN-12/Notch activation leads to microRNA-mediated down-regulation of Vav in C. elegans. Science *310*, 1330-1333.

Yoon, C.H., Lee, J., Jongeward, G.D., and Sternberg, P.W. (1995). Similarity of sli-1, a regulator of vulval development in C. elegans, to the mammalian proto-oncogene c-cbl. Science *269*, 1102-1105.

Zand, T.P., Reiner, D.J., and Der, C.J. (2011). Ras effector switching promotes divergent cell fates in C. elegans vulval patterning. Developmental cell *20*, 84-96.

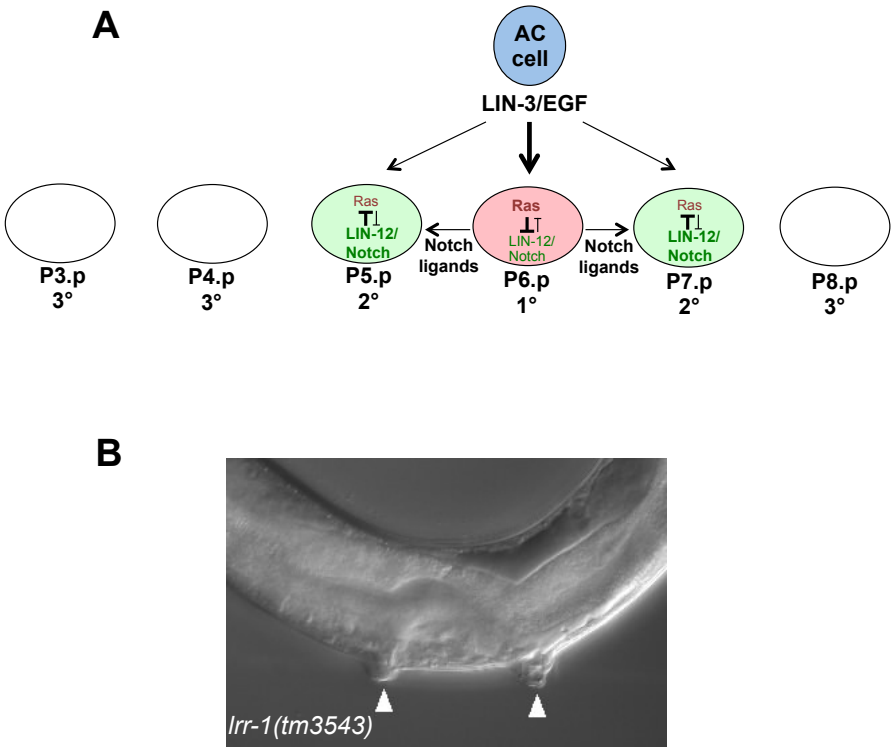

Figure 2.1 A simplified diagram of the signaling events that pattern the *C. elegans* vulval development and *lrr-1 (tm3543)* multivulva (Muv) phenotype. (A) Ras and Notch signaling regulate the vulval fate patterning. The inductive signal from AC is an epidermal growth factor (EGF)-like signal LIN-3. LIN-3 upregulates the Ras pathway in P6.p making it the 1º cell. Ras leads to transcription of Notch ligands that activate the LIN-12/Notch pathway in P5.p and P7.p making them 2º cells. Ras downregulates LIN-12/Notch in the 1º cells and LIN-12/Notch downregulates Ras in the 2º cells. P3.p, P4.p and P8.p assume 3º cell fates (white). (B) DIC image of an adult *lrr-1 (tm3543)* homozygous animal showing 2 vulval protrusions (white arrowheads).

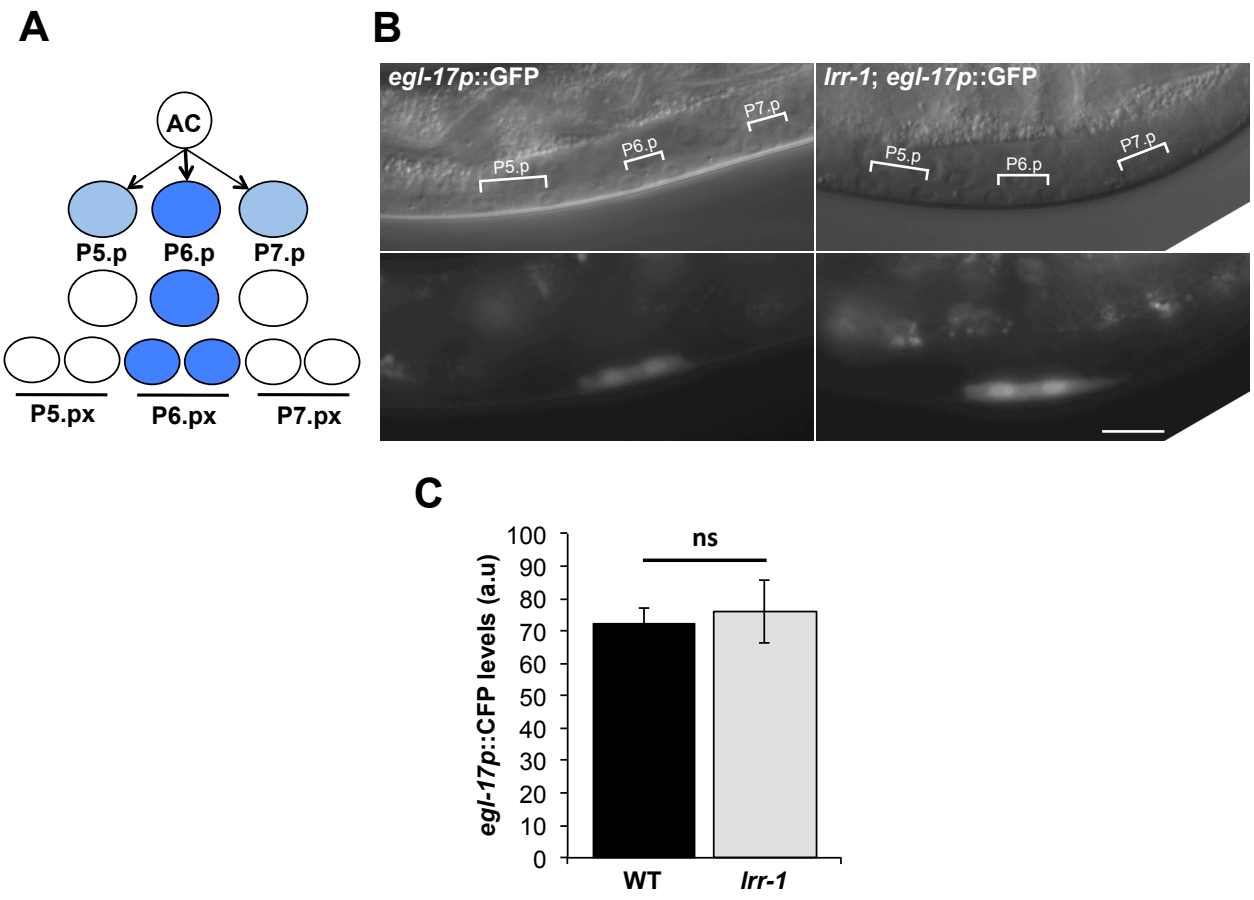

Figure 2.2 1º cell fate marker *egl-17p*::CFP expression in *lrr-1(tm3543)* is similar to wild type. (A) Schematic diagram of the wild-type expression pattern of the 1º cell marker *egl-17p*::CFP. In response to the graded inductive signal during early L3 larval stage, *egl-17p*::CFP expresses strongly in P6.p and weakly in P5.p and P7.p. Later, during the mid-L3 larval stage, expression of *egl-17p*::CFP disappears in P5.p and P7.p but persists in P6.p and its descendants. (B) DIC (top panels) and fluorescent (bottom panels) images showing *egl-17p*::CFP wild-type expressions (left panels) and in *lrr-1(tm3543)* mutant (right panels) in the Pn.px-stage VPC lineage cells. *egl-17p*::CFP expresses only in P6.p descendent cells but not in P5.p and P7.p descendants. Scale bar represents 20 μM for all panels. (C) Quantification of *egl-17p*::CFP expression (arbitary units, a.u.) in P6.p cells in wild type and *lrr-1(tm3543)* mutants. For all

figures: error bars indicate standard error of the mean; asterisks indicate significance compared to wild type, *P ≤ 0.05, **P ≤ 0.01, ***P ≤ 0.001, ns = no significance, P>0.05; statistical methods are described in Materials and Methods section.

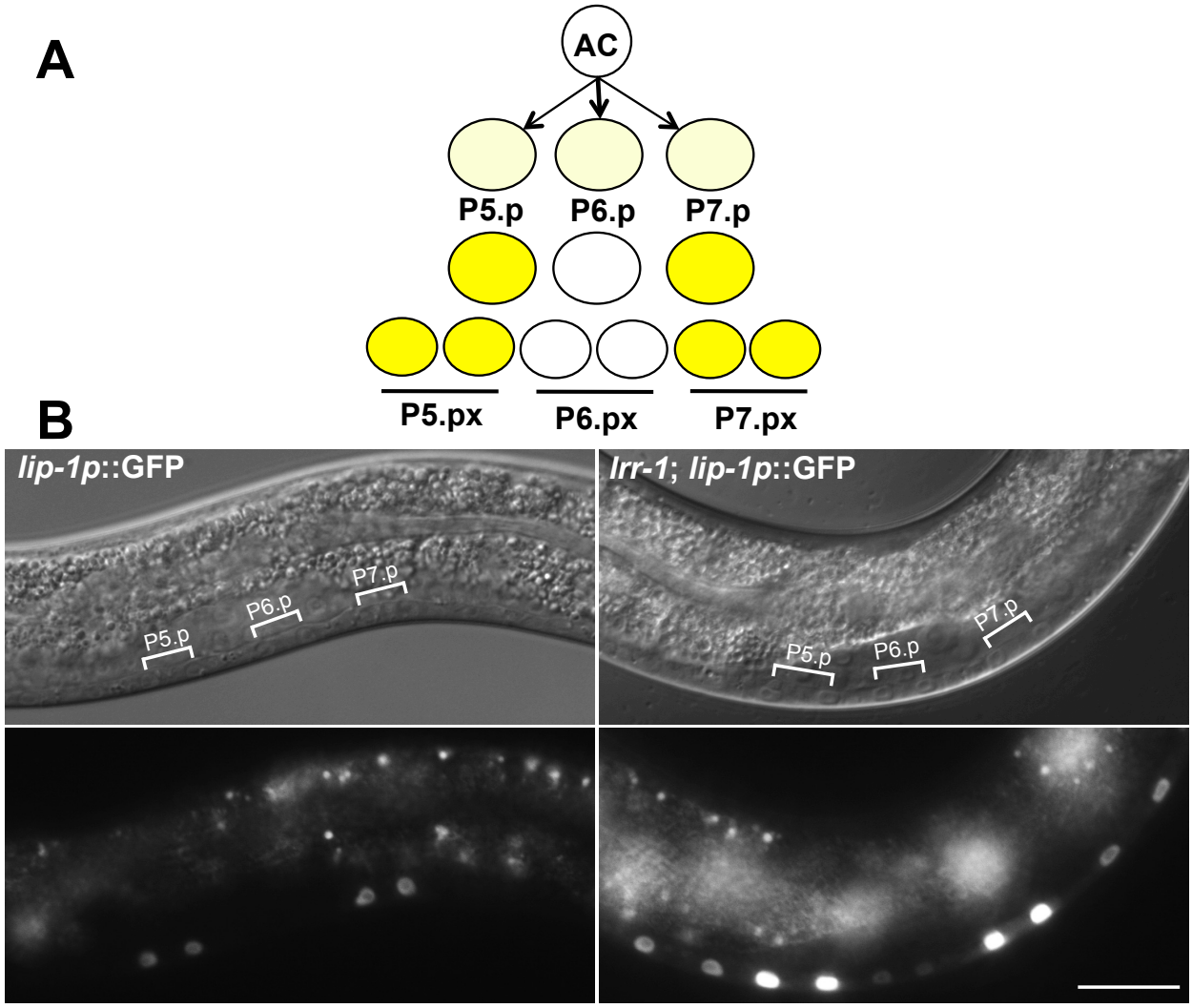
A
AC
P5.p
P6.p
P7.p
P5.px
P6.px
P7.px
B
lip-1p::GFP
lrr-1; lip-1p::GFP
P5.p
P6.p
P7.p
C
lip-1p::GFP levels (a.u)
100
90
80
70
60
50
40
30
20
10
0
***
***
***
WT
lrr-1
WT
lrr-1
WT
lrr-1
P5
P6
P7

Figure 2.3 2º cell fate marker *lip-1p*::GFP expression is elevated in *lrr-1(tm3543)* mutants. (A) Schematic diagram of the wild-type expression pattern of the 2º cell marker *lip-1p*::GFP. *lip-1p*::GFP expresses at low levels in all three VPC (Berset et al., 2001). After the inductive signal, the expression in P6.p disappears but persists in P5.p and P7.p and their descendants. *lip-1p*::GFP also expresses in the daughters of P3.p, P4.p and P8.p after they fuse with the hyp7. (B) DIC (top panels) and fluorescent images (bottom panels) showing *lip-1p*::GFP in wild-type (left panels) and in *lrr-1(tm3543)* (right panels) animals at Pn.p and Pn.px stage with *lip-1p*::GFP expression. P6.p and its descendants show persistent and elevated levels of *lip-1p*::GFP in *lrr-1(tm3543)*. Although not obvious in this image, wild-type animals do have faint expression of *lip-1p*::GFP in the P4.p and P8.p cells (P3.p not in frame for either wild-type or *lrr-1* mutants). Scale bar represents 20 μM for all panels. (C) Quantification of *lip-1p*::GFP expression in P5.p, P6.p and P7.p cells in wild type and *lrr-1(tm3543)*. An average of Pn.pa and Pn.pp is shown for each of the three VPCs in arbitrary units (a.u).

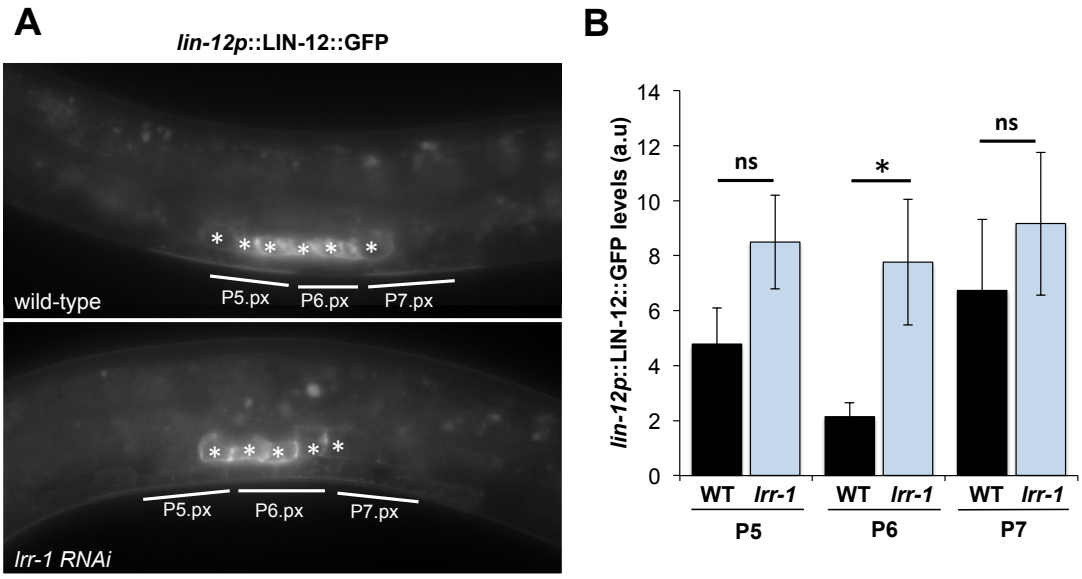

Figure 2.4 Localization and expression of the full-length LIN-12/Notch protein is elevated in P6.p in *lrr-1(RNAi)* animals. (A) The level of a lin-12 promoter driven full-length LIN-12/Notch protein expression using the transgene *lin-12p*::LIN-12::GFP, is seen at the apical membrane of the P5.p, P6.p and P7.p descendants in wild-type and *lrr-1 (RNAi)* animals. *lrr-1(RNAi)* animals (bottom panel) have elevated levels of *lin-12p*::LIN-12::GFP in P6.p compared to wild-type (top panel). White asterisks indicate *lin-12p*::LIN-12::GFP expression in the uterus. (B) Quantification of *lin-12p*::LIN-12::GFP expression at the apical membrane of P5.p, P6.p and P7.p cells in wild-type (WT) and *lrr-1(RNAi)* animals.

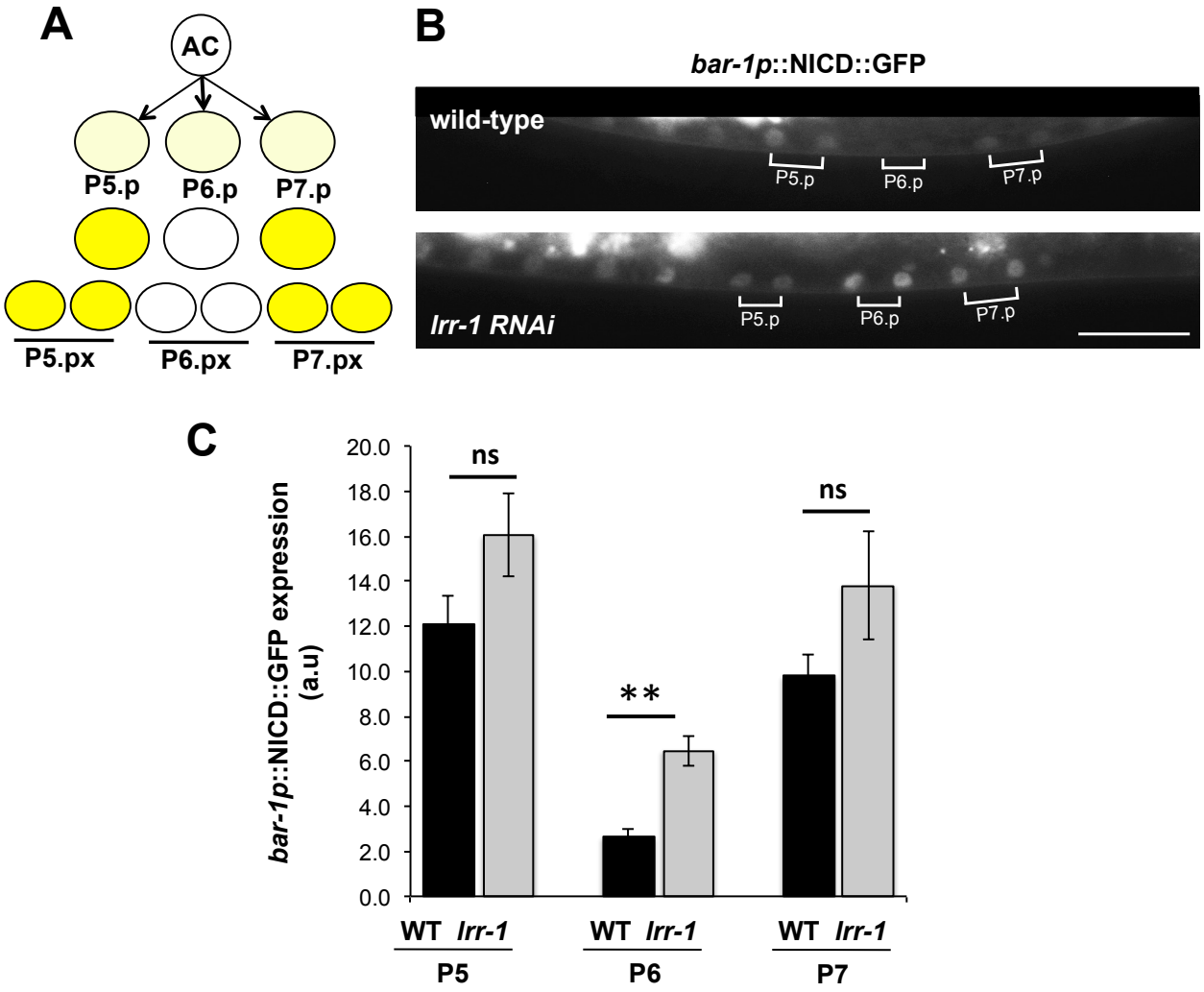

Figure 2.5 Expression of *bar-1p*:: NICD::GFP is elevated in P6.p in *lrr-1(RNAi)* animals.

(A) Schematic diagram of the wild type expression pattern of *bar-1p*::NICD::GFP. *bar-1p*::NICD::GFP expresses at low levels in all three VPC at early L3 stage. After the inductive signal, the expression in P6.p disappears but persists in P5.p and P7.p and their descendants (Nusser-Stein et al., 2012). (B) Fluorescent images showing *bar-1p*::NICD::GFP expression in Pn.px cells from wild type (top panel) and *lrr-1(RNAi)* mutants (bottom panel). NICD

expression is driven by the *bar-1* promoter, which has uniform expression in the three VPCs. P6.p descendants in *lrr-1(RNAi)* mutants show persistent elevated levels of NICD::GFP. (C) Quantification of *bar-1p*::NICD::GFP expression in P5.p, P6.p, and P7.p cells in wild type and *lrr-1(RNAi)* mutants.

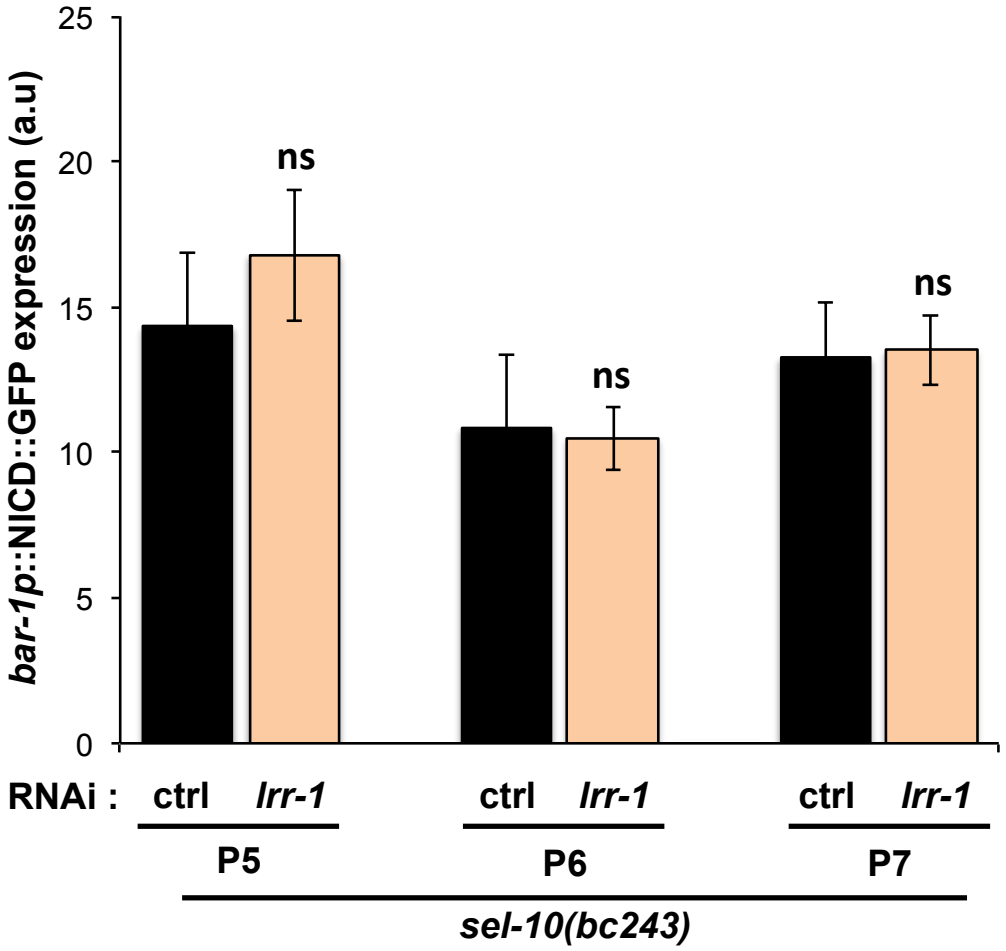

Figure 2.6. Inactivation of *lrr-1* does not further increase *bar-1p*::NICD::GFP levels in *sel-10(null)* mutants. Quantification of *bar-1p*::NICD::GFP expression in the descendants of P5.p, P6.p and P7.p in control RNAi and *lrr-1* RNAi in *sel-10(bc243)* mutants. Loss of *lrr-1* does not increase *bar-1p*::NICD::GFP levels in the VPCs of *sel-10* mutants. NICD expression is driven in all VPCs using a *bar-1* promoter (Nusser-Stein et al., 2012).

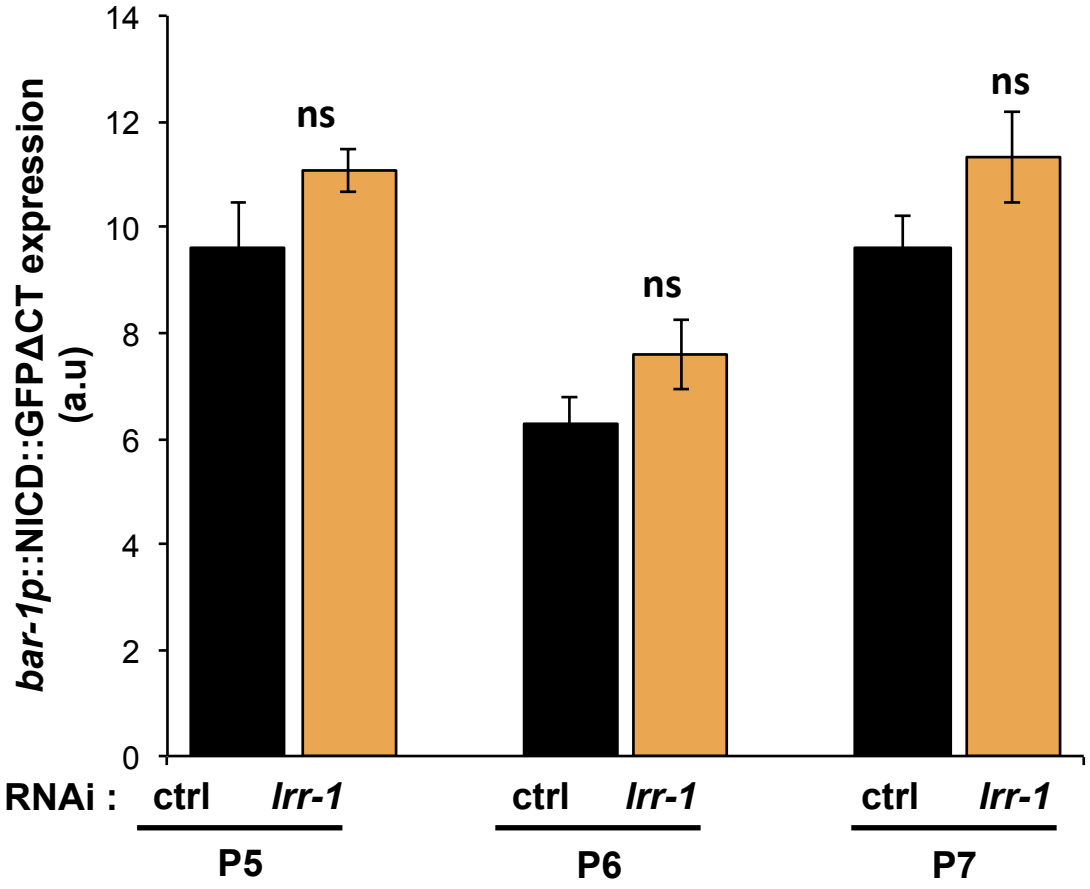

Figure 2.7 The NICD C-terminal domain is required *lrr-1(RNAi)* to increase NICD levels. Quantification of *bar-1p*::NICD::GFPΔCT levels in control and *lrr-1 (RNAi)* animals. NICD::GFPΔCT contains a C terminal deletion of 87 amino acids which includes the PEST domain. NICD::GFPΔCT expression is driven in the VPCs with a *bar-1* promoter (Nusser-Stein et al., 2012). Loss of *lrr-1* does not increase *bar-1p*::NICD::GFPΔCT levels compared to control animals.

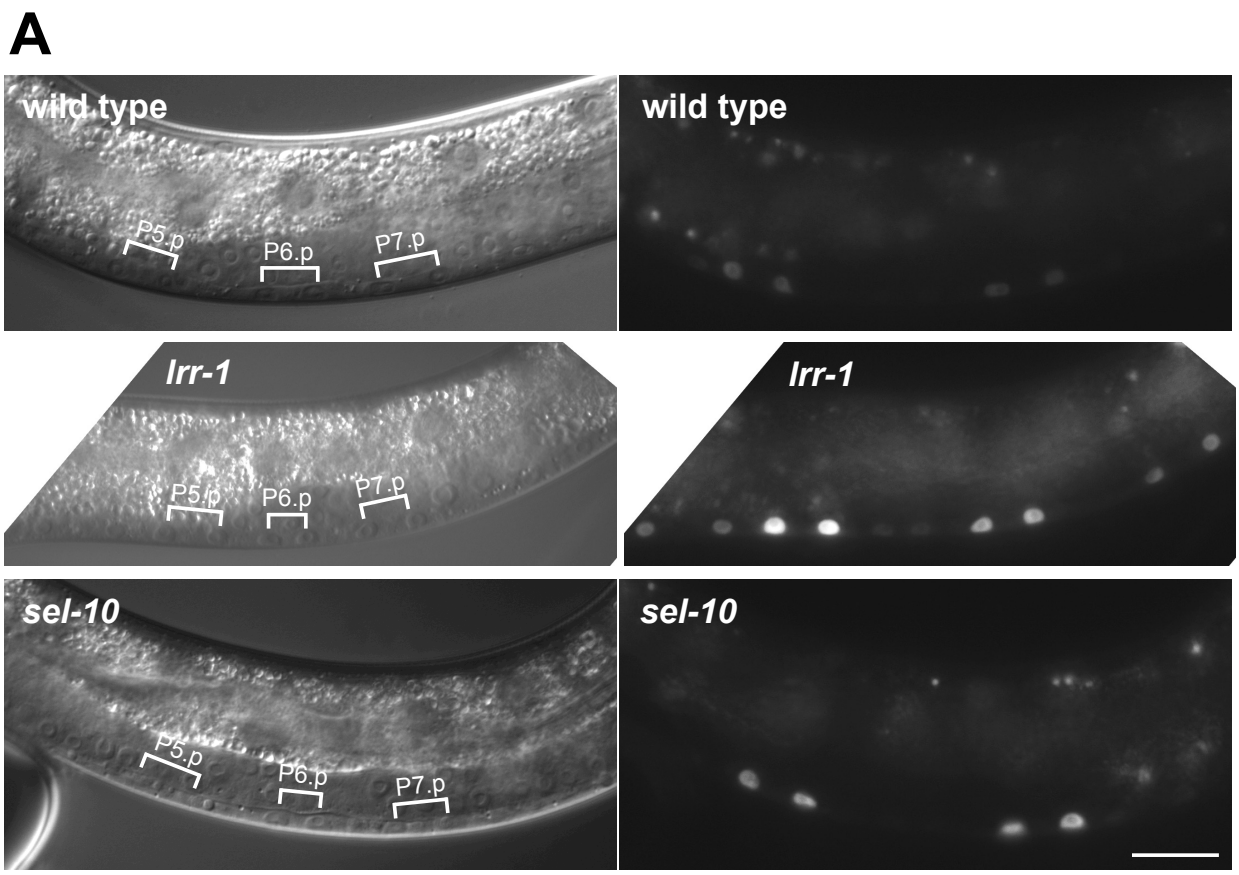
A
wild type
P5.p
P6.p
P7.p
wild type
lrr-1
P5.p
P6.p
P7.p
lrr-1
sel-10
P5.p
P6.p
P7.p
sel-10

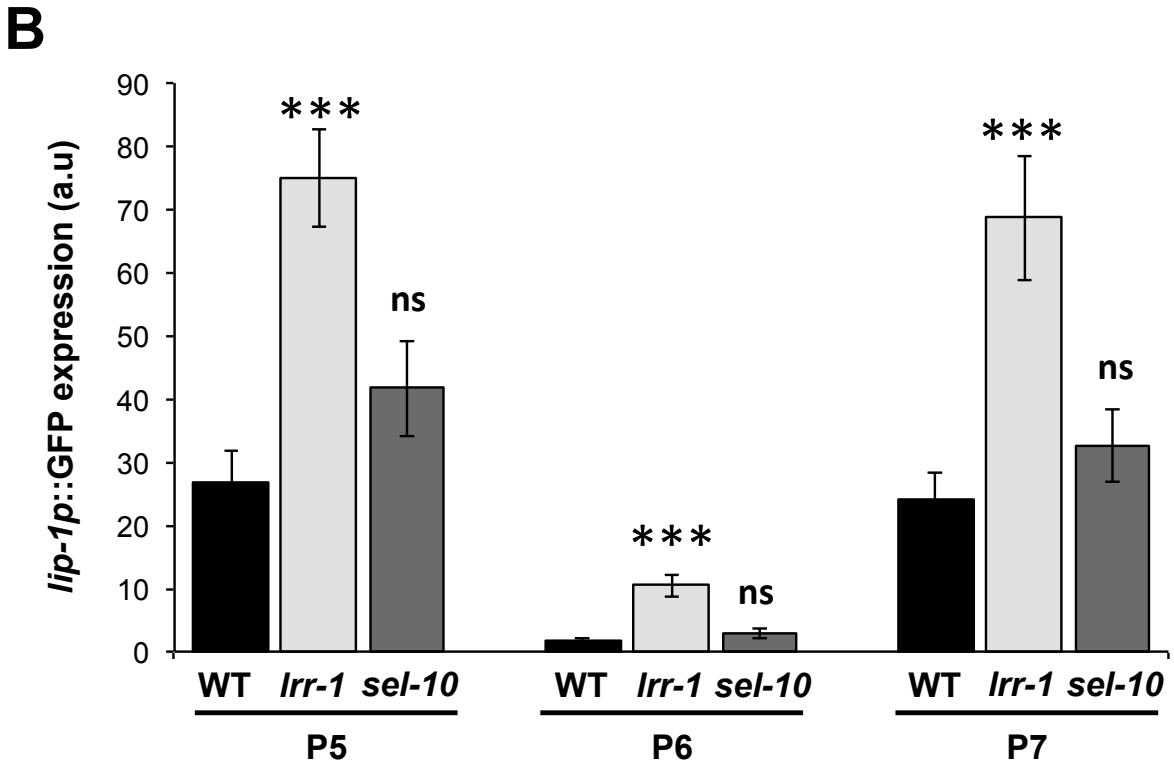
B
lip-1p::GFP expression (a.u)
90
80
70
60
50
40
30
20
10
0
***
ns
***
ns
***
ns
WT
lrr-1
sel-10
WT
lrr-1
sel-10
WT
lrr-1
sel-10
P5
P6
P7

Figure 2.8 *lrr-1* mutants have elevated levels of *lip-1p*::GFP while *sel-10(RNAi)* animals do not. (A) DIC (left panels) and fluorescent (right panels) images of wild-type, *lrr-1* mutants and *sel-10 (RNAi)* animals expressing *lip-1p*::GFP. Scale bar for all the images are 20 μM. (B) Quantification of *lip-1p*::GFP expression in the descendants of P5.p, P6.p and P7.p VPCS in wild type, *lrr-1(tm3543)*, and *sel-10 (RNAi)*.

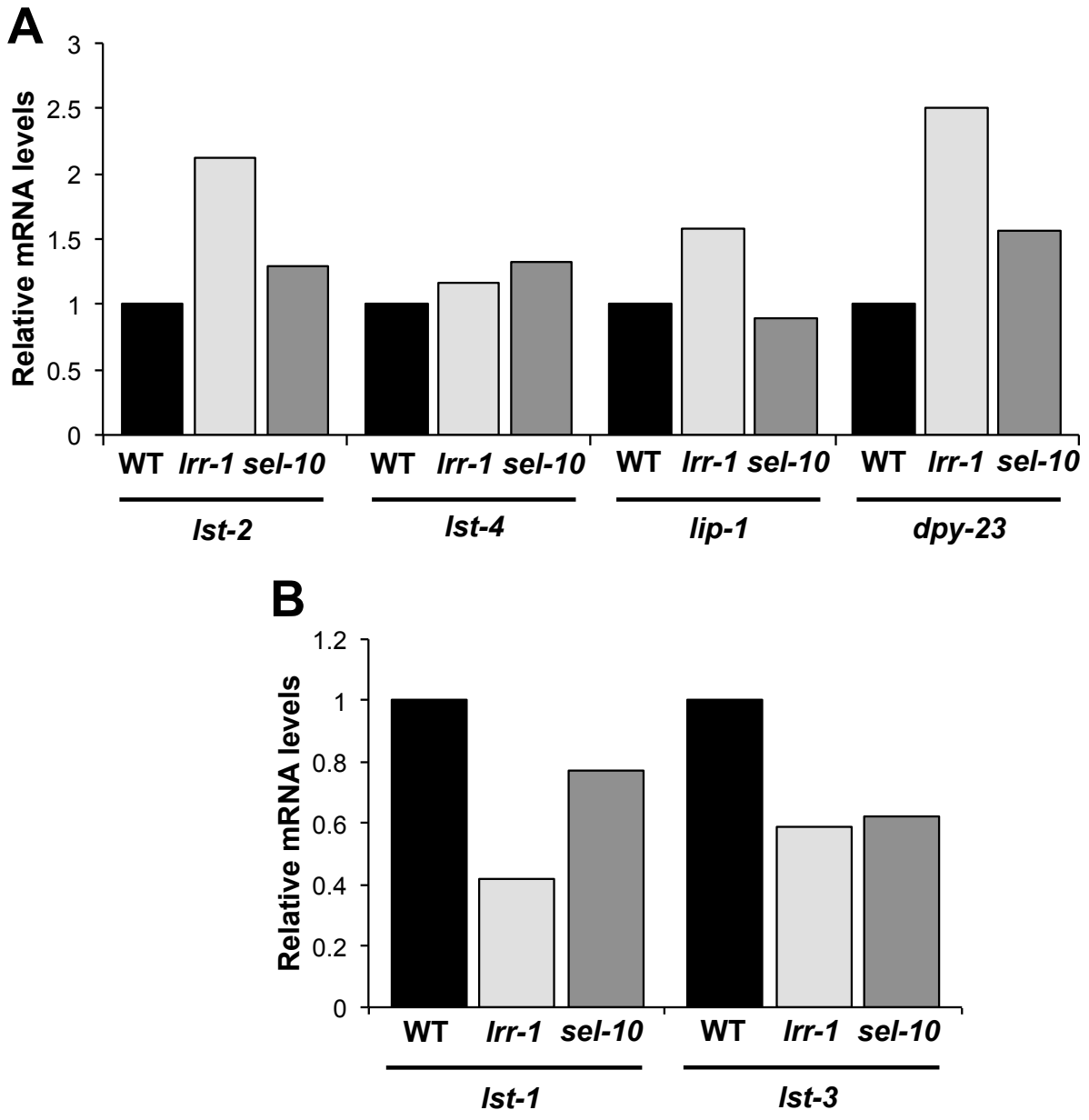

Figure 2.9 mRNA levels of *lst* genes are upregulated in *lrr-1(tm3543).* mRNA levels of L3-stage wild type, *lrr-1(tm3543)* mutants, and *sel-10 (bc243)* mutants as determined by qRT-PCR. Endogenous levels of *lst-2, lst-4, lip-1* and *dpy-23* (A) and *lst-1* and *lst-3* (B) were measured by qRT-PCR. Fold difference are relative to wild-type levels, which are set to 1 for each gene.

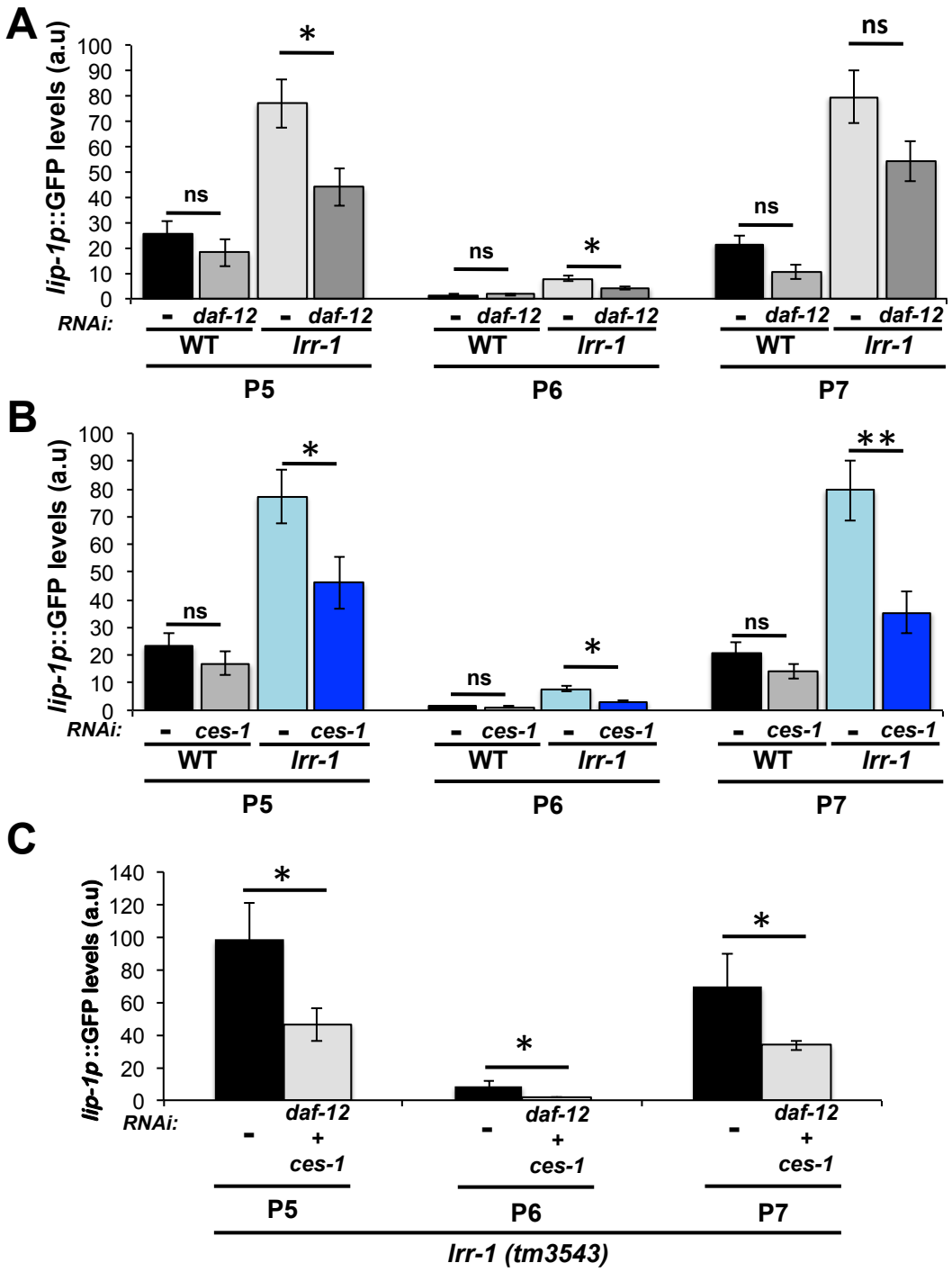

Figure 2.10 ***daf-12*** **and** ***ces-1*** **RNAi reduce the elevated levels of** ***lip-1p*****::GFP in** ***lrr-1(tm3543).*** Quantification of *lip-1p::*GFP expression in the descendants of P5.p, P6.p and P7.p

in wild type and *lrr-1(tm3543)* with control and *daf-12 RNAi* (A), or control and *ces-1 RNAi* (B) and (C) control and *daf-12* + *ces-1* double *RNAi*. (A) *daf-12 RNAi* reduces the levels of *lrr-1*; *lip-1p*::GFP significantly in P5.p and P6.p compared to *control RNAi*. (B) *ces-1 RNAi* reduces the levels of *lrr-1*; *lip-1p*::GFP significantly in P5.p, P6.p and P7.p compared to *control RNAi.* (C) Double knockdown of *daf-12* and *ces-1 (RNAi)* in *lrr-1; lip-1p::*GFP further reduces *lip-1p*::GFP levels in P6.p.

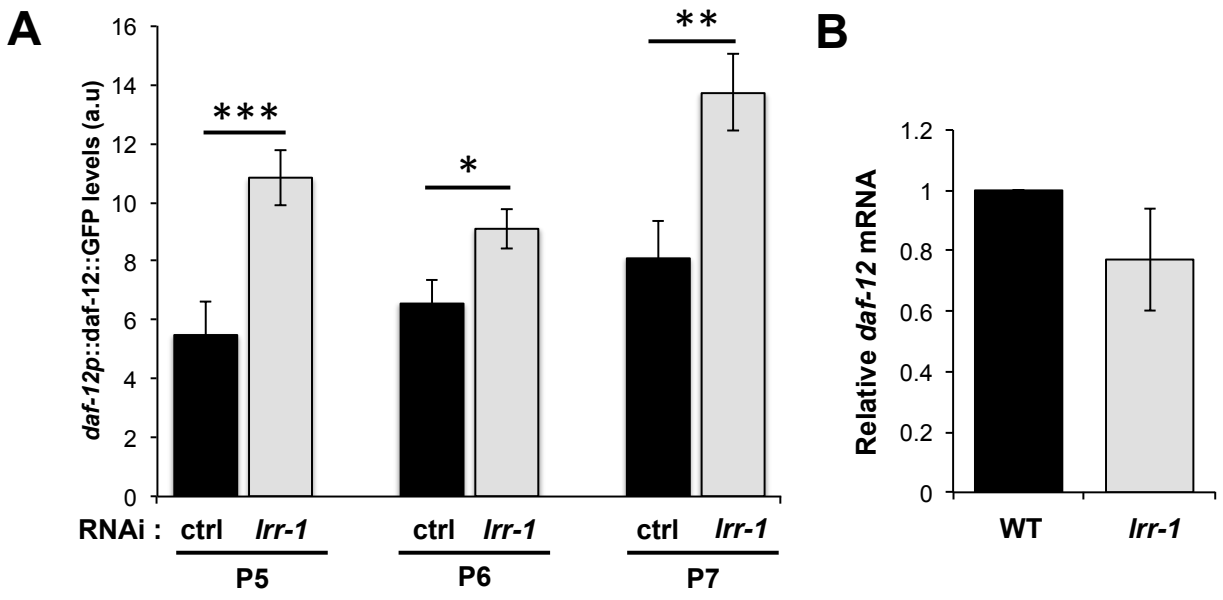

Figure 2.11 *daf-12p*::DAF-12::GFP expression is elevated in all three VPCs in *lrr-1(RNAi)*. (A) Quantification of *daf-12p*::DAF-12::GFP expression levels in the descendants of P5.p, P6.p and P7.p in control and *lrr-1* RNAi treatments. *daf-12p*::DAF-12::GFP is uniformly expressed in all three VPCs in control *RNAi* animals, and the levels are significantly elevated *lrr-1 (RNAi)* animals. (B) *daf-12* mRNA levels of L3-stage wild type and *lrr-1(tm3543)* mutants measured by qRT-PCR. *daf-12* mRNA levels are statistically unchanged in *lrr-1* mutants compared to wild-type.

Table 2.1: Genetic interaction between *lrr-1* and mutants in the Notch and Ras pathway.

Genotype	RNAi	Vul (%)	Muv (%)	n	P value
gap-1(ga133)	-	0	0	200	
gap-1(ga133)	*lrr-1*	0	2	150	§
ark-1(n3701)	-	0	0	200	
ark-1(n3701)	*lrr-1*	0	1.4	290	§
sli-1(n3538)	-	0	0	200	
sli-1(n3538)	*lrr-1*	0	0	200	§
lrr-1(tm3543)	-	0	0.9	700	
lrr-1(tm3543)	*unc-101*	0	0	100	§
lrr-1(tm3543)	*lst-2*		0	500	<0.05
lrr-1(tm3543)	*lst-3*		0.35	285	
lrr-1(tm3543)	*lst-4*		0.1	700	<0.05
lrr-1(tm3543)	*dpy-23*		0	185	§
let-23(sy1)	-	90	0.8	125	
let-23(sy1)	*lrr-1*	76	4.8	250	$<7 \times 10^{-11}$
let-60(n1046); mpk-1(n2521)	-	0	1	200	
let-60(n1046); mpk-1(n2521)	*lrr-1*	0	11.5	250	$<1 \times 10^{-56}$
lin-12(n302)	-	80.4	7.5	175	
lin-12(n302)	*lrr-1*	70	24.9	107	$<2 \times 10^{-20}$
sel-10(bc243)	-	0	0	130	
sel-10(bc243)	*lrr-1*	0	5.6	282	$<3 \times 10^{-31}$

§: More replicates will be obtained for statistical significance for publication.

Table 2.2: Transcription factors identified from modENCODE ChIP-seq database.

	Number of transcription factor binding sites in each lateral signal target (*lst*) gene					
Transcription factors	LST-1	LST-3	LST-4	LIP-1	LST-2	DPY-23
AHA-1	0	3	3	2	1	1
ALR-1	1	1	1	11	2	2
ALY-2	0	7	6	13	9	10
AMA-1	2	9	6	2	3	1
BLMP-1	4	2	2	10	2	2
C01B12.2	0	5	3	6	6	9
C16A3.4	1	3	3	0	3	6
CEH-14	1	1	1	0	3	3
CEH-26	2	3	3	2	4	6
CEH-30	1	3	4	3	2	4
CES-1	0	2	3	7	7	10
DAF-12	0	0	0	2	2	2
DAF-16	6	2	3	3	2	3
DPL-1	7	18	15	18	14	17
DPY-27	0	0	0	0	2	4
EFL-1	5	7	11	6	5	7
EGL-27	0	2	2	3	2	2
EGL-5	2	4	4	9	4	5
ELT-3	2	1	1	2	1	2
EOR-1	13	12	10	33	23	35
F16B12.6	0	2	2	0	1	1
F45C12.2	0	7	7	17	12	16
FOS-1	11	11	11	20	13	21
GEI-11	0	7	10	15	5	12
HLH-1	2	1	1	2	1	3
HLH-8	3	0	1	3	3	3
HPL-2	2	2	2	7	3	6

LIN-11	0	2	2	0	2	2
LIN-13	2	2	2	0	2	5
LIN-15B	0	9	9	5	5	7
LIN-35	2	6	5	8	8	14
LIN-39	0	2	2	7	5	8
MAB-5	2	2	2	2	4	8
MDL-1	2	3	3	7	5	7
MEF-2	0	2	2	2	2	2
MEP-1	3	2	3	2	3	5
NHR-116	1				2	
NHR-11	6	2	2	2	3	3
NHR-28	0	3	3	7	3	8
NHR-6	3	3	3	5	4	4
NHR-77	1	17	11	20	17	29
PES-1	33	4	4	0	5	9
PHA-4	1	12	11	24	23	33
PQM-1	2	1	1	2	3	2
R02D3.7	1	8	8	7	6	12
SEA-2	2	1	1	0	1	1
SKN-1	6	2	2	5	2	2
UNC-130	4	5	1	16	10	10
UNC-62	0	4	5	8	3	3
W03F9.2	4	6	4	12	13	13
ZAG-1		8	7	24	8	14
ZK377.2			6	0		4

CHAPTER 3

BACTERIAL FOLATES PROVIDE AN EXOGENOUS SIGNAL FOR *C. ELEGANS* GERMLINE STEM CELL PROLIFERATION [1]

---

[1] **Mukherjee M***., Chaudhari S.N*., Vagasi A.S., Bi G., Rahman M.M., Nguyen C., Paul L., Selhub J., and Kipreos E.T. 2016. *Developmental Cell.,* 38: 33-46

Reprinted here with permission of the publisher.

* These authors contributed equally to this work.

Summary

Here we describe an in vitro primary culture system for *C. elegans* germline stem cells. This culture system was used to identify a bacterial folate as a positive regulator of germ cell proliferation. Folates are a family of B-complex vitamins that function in one-carbon metabolism to allow the *de novo* synthesis of amino acids and nucleosides. We show that germ cell proliferation is stimulated by the folate 10-formyl-tetrahydrofolate-Glu_n both in vitro and in animals. Other folates that can act as vitamins to rescue folate deficiency lack this germ cell stimulatory activity. The bacterial folate precursor dihydropteroate also promotes germ cell proliferation in vitro and in vivo, despite its inability to promote one-carbon metabolism. The folate receptor homolog FOLR-1 is required for the stimulation of germ cells by 10-formyl-tetrahydrofolate-Glu_n and dihydropteroate. This work defines a folate and folate-related compound as exogenous signals to modulate germ cell proliferation.

Introduction

Animal germ stem cells (GSCs) are adult stem cell populations that provide reproductive cells to allow species propagation. *C. elegans* hermaphrodite GSCs proliferate in adult stem cell niches located in the distal regions of the two gonad arms (Hansen and Schedl, 2013). Primary cultures of *C. elegans* germ cells have not been previously reported. *C. elegans* embryonic cells can be cultured, but not propagated, in an L-15-based culture medium (Christensen et al., 2002). In this study, we describe a primary culture system for *C. elegans* germ cells that utilizes a culture medium with substantially different characteristics than L-15 medium. The in vitro culture system allows the analysis of relatively pure populations of germ cells that are isolated from germline tumorous mutant strains. Two external signals, Notch and Insulin/IGF-like, are known to promote the proliferation of GSCs (Hansen and Schedl, 2013; Michaelson et al., 2010). We used the in vitro culture system to identify bacterial folate as a new signal that promotes GSC proliferation.

Folates are a group of B vitamins whose canonical role is in one carbon transfer for the *de novo* synthesis of: thymidine; purines; methionine, and the methyl donor S-adenosylmethionine (Selhub, 2002) (Fig. 3.1A). Folates comprise moieties of a pteridine ring, para-aminobenzoic acid (PABA), and one or more glutamate residues (Glu_n) in g-linkages to the terminal glutamate (Fig. 3.1B). Folates differ from each other by: 1) the states of oxidation of the pteridine ring, i.e. dihydrofolate, DHF, or tetrahydrofolate, THF; 2) modification of the 5- and 10- position of the pteridine ring by substitution with formate (5-formyl-, 10-formyl-, and 5,10-methenyl-THF), formaldehyde (5,10-methylene-THF), or methanol (5-methyl-THF); and 3) the number of glutamate residues (Fig. 3.1B,C). The three forms of formylated THF are interconvertible: 5,10-

methenyl-THF, which is stable at acid pH (1.5-2.6), is converted to 5-formyl-THF at pH 4.0-5.5 and to 10-formyl-THF at neutral and higher pH, and vice versa (Stover and Schirch, 1992).

In mammals, there are three types of folate transporters. The reduced folate carrier, RFC, is a low-affinity, high-capacity transporter that brings folates into all cells of the body (Matherly et al., 2007). The proton-coupled folate transporter, PCFT, functions at low pH to transport folates from acidic pH environments, such as the mammalian small intestine (Desmoulin et al., 2012). Folate receptors, FRs, are high-affinity, low-capacity transporters that have been shown to function in the transcytosis of folates across polarized cell barriers (Grapp et al., 2013; Henderson et al., 1995; Selhub et al., 1987).

Folates are synthesized by bacteria, plants, fungi, and certain protozoa and archaea (Rossi et al., 2011). Folates cannot be synthesized *de novo* by animals, and hence are classified as vitamins that must be obtained from the animal's diet or microbiota. As is true for other animals, *C. elegans* requires folates for one-carbon metabolism. Inactivation of the *C. elegans* RFC homolog FOLT-1/RFC results in severely reduced germ cell numbers and sterility (Austin et al., 2010).

Our work demonstrates that a specific bacterial folate and pteroate (a folate-related compound) stimulate germ cell proliferation in a manner that can be distinguished from the canonical role of folates in one-carbon metabolism.

Experimental Procedures

CeM1 medium preparation

CeM1 medium was prepared with the ingredients listed in Table 3.S1. CeM1 was sterile filtered through 0.22 μm 150 ml filter units (Millipore). Three sequential treatments were performed on

the FBS prior to its inclusion in CeM1: heat inactivation; and treatments with Amberlite IRA 400-CL and charcoal-dextran (see Supplemental Experimental Procedures).

Germ cell isolation and primary culture

To obtain synchronous adult germline tumorous mutants, eggs were isolated by sodium hypochlorite treatment (Sulston and Hodgkin, 1988). The eggs were transferred to a 3xNGM plate (an NGM agar plate (Sulston and Hodgkin, 1988) with 3x peptone concentration) with a lawn of OP50 bacteria and grown at 25°C for four days to ensure that all animals became adults with germline tumors. The animals were washed four times with M9 salt solution (Sulston and Hodgkin, 1988) in 15 ml polystyrene tubes (Falcon) to remove live bacteria and transferred to a 12.5 cm^2 cell culture flask (Corning) containing 2.5 ml of M9 solution supplemented with: heat-killed OP50 bacteria; 200 units penicillin and 0.2 mg streptomycin per ml); 25 µg/ml tetracycline (Sigma-Aldrich, 87128); 34 µg/ml chloramphenicol (Research Products International); 50 µg/ml kanamycin; 0.02% normocin; and 5 µg/ml cholesterol. Animals were incubated overnight in the antibiotic-supplemented M9 solution. The next day, animals were washed four times with phosphate buffered saline (PBS) in 15 ml polystyrene tubes, washed one time with CeM1, and then resuspended in 2 ml of CeM1 in a 35 mm tissue culture dish (Falcon). Animals were transferred with a platinum wire to a 120 µl spot of CeM1 in another 35 mm culture dish. Germ cells were released by cutting animals into quarters using 31 gauge needles (Becton Dickinson). Cells were collected with three sequential washes with 1 ml of CeM1, collected into a 15ml polypropylene tube and spun at 300-1000 rpm for 1 min to pellet body parts and large cell aggregates. The supernatant was transferred to a new 15 ml tube and spun at 2000 rpm for 5 min to pellet individual cells. The cells were resuspended in full CeM1 (unless otherwise stated) and

transferred to a tissue culture dish. If multi-well tissue culture dishes were used, the outer wells were filled with PBS to keep the inner wells humidified, then sealed with parafilm to prevent loss of moisture, and incubated at 25°C.

Bacterial Extract

Bacteria were grown overnight in 2xYT medium that was either unsupplemented for OP50, or supplemented with 25 μg/ml tetracycline for HT115, or 100 μg/ml streptomycin for DA1877. The bacteria were collected by centrifugation at 4000 rpm for 30 min at 4°C, washed two times with sterile 0.9% NaCl, and the bacterial pellet was frozen at -80°C. Bacterial pellets were lyophilized under vacuum at room temperature. Crushed bacterial pellet was added at 0.08 g/ml to folate-extraction buffer (1% Na ascorbate, 20 mM phosphate buffer, pH 6.5), vortexed, and rotated at room temperature in the dark for 1 hr. The bacteria were spun out in a microcentrifuge at 13,300 rpm for 15 min. The supernatant was transferred to a new microcentrifuge tube and extracted once with 1:1 phenol:choloroform and three times with chloroform to remove proteins; spun out and transferred to a new tube to remove any residual chloroform, and then sterile filtered using a 0.2 μm syringe filter. The bacterial extract used in Fig. 3.2E was prepared with water instead of folate-extraction buffer and was used immediately after preparation.

Tumor frequency assay

Eggs isolated by sodium hypochlorite treatment were placed on 1x NGM plates seeded with live bacteria or heat-killed OP50 bacteria with the indicated experimental additives. Assays with live bacteria were performed at the semi-permissive temperature of 18°C; assays with heat-killed bacteria were performed at 20°C. L4-stage animals were transferred onto fresh plates, and the

percentages of adult animals with tumors were scored two days later by observation with a dissecting microscope. Tumor frequency assays were performed in triplicate with ~100 animals per replicate. Several tumor frequency assays were performed blind, including Figs 3.6B, 3.7D, 3.S5E, and 3.S5F. The supplements trimethoprim (cat. no. 92131) and PABA (100536) were from Sigma-Aldrich; vitamin B12 (103278) was from MP Biomedicals.

Counts of live isolated germ cells

Counts of live isolated germ cells were performed with the live-cell stain calcein-AM and dead-cell stain ethidium homodimer (Zhang et al., 2011). The numbers of live cells were obtained by counting cells stained with 1 μM calcein-AM (Sigma-Aldrich, C1359), 0.1 μM Ethidium homodimer (Sigma-Aldrich, E1903), and with or without 2 μg/ml Hoechst 33342 (Sigma-Aldrich, B2261). A minimum of three counts were made for each sample using a cellometer counting grid (CP2, Nexcelom Bioscience LLC) analyzed with an inverted fluorescence microscope (Zeiss Axio Observer.A1); cell count variation is presented as SEM. Typically, germ cells were isolated from 25 adult hermaphrodites for 0.5 ml/well of a 24-well plate.

Counts of germ cells in mid-L4-stage larvae

Counts of germ cells in mid-L4-stage larvae were performed with animals fixed with 95% ethanol for 10 min as described (Killian and Hubbard, 2005), and then stained with 2 μg/ml Hoechst 33342 in PBS. Germ cell counts were performed blind, with the identity of the treatment masked. The germ cells in one gonad arm per animal were counted. Mid-L4-stage larvae were identified based on vulva morphology. Larvae selected for germ cell counts had vulva morphologies categorized as L4.1 to L4.3 on the L4.0–L4.9 vulval morphology scale that has

been previously defined (Mok et al., 2015). For Fig. 3.7B, between 9 and 17 animals were analyzed per condition.

EdU-incorporation assay

Isolated germ cells from *glp-1(gf)*; *cki-2*; *daf-16* mutant adults were incubated in 80 µl of CeM1 in a 96-well plate, with the germ cells from approximately eight adults per well. 24 hr post-isolation, EdU was added to a concentration of 20 µM. At 48 hr post-isolation, cells were harvested and processed with the Click-iT Alexa Fluor 488 Imaging kit (Life Technologies), according to the manufacturer's instructions. Cells were subsequently stained with 2 µg/ml Hoechst 33342 DNA stain and analyzed by fluorescence microscopy for EdU staining of DNA, with images of EdU Alexa Fluor 488 staining taken initially, and then images of Hoechst staining taken subsequently. Typically, 150-200 cells were counted for each condition.

Folate analysis

Folates for chromatography analysis were prepared as follows. Lyophilized bacteria were resuspended at a concentration of 0.09-0.1 mg/ml in folate-extraction buffer (2% sodium ascorbate, 0.05 M 2-mercaptoethanol), boiled for 15 min, then spun in a centrifuge at 30,000xg for 30 min to remove insoluble components. Aliquots (2 ml) of the supernatants were mixed with 18 ml of potassium phosphate buffer containing 1% sodium ascorbate. Purified folates were isolated by passage through affinity columns (2.4 ml bed volume) containing purified milk folate-binding protein which was immobilized to a Sepharose matrix (Selhub et al., 1980).

For HPLC detection of folate species, 250 µl of the purified folate was mixed with 1% sodium ascorbate, 0.01 M potassium phosphate pH 7.5. A 0.9 ml aliquot was injected into a

4.6x250 mm Betasil Phenyl analytic column and eluted under acid conditions using acetonitrile gradient and detection by UV, fluorescence, and electrochemical signals (Bagley and Selhub, 2000) (data not shown). The use of multisignaling allowed better identification of the various peaks that were eluted from the column.

The microbial assay was used to determine folate concentration. Purified extract was treated with conjugase using the tri-enzyme system, as described (Poo-Prieto et al., 2006), and folate was then analyzed using 96 well plates, as described (Tamura et al., 1990).

Statistical analysis

Two-tailed Student's t-test was used to analyze the three replicates of tumor frequencies, the data for mitotic index, numbers of germ cell nuclei per proliferative zone, egg numbers per animal, and the number of germ cells per gonad arm. The chi-squares test was used to analyze the percentages of EdU positive cells. The nonparametric Mann-Whitney test was used to analyze the number of phosphohistone H3 positive cells per gonad arm. All error bars reflect standard error of the mean (Sempere et al.).

Additional methods are provided in the Supplemental Information.

Results

Cellularization of tumorous germ cells

In an effort to understand the regulation of GSC survival and proliferation, we sought to create a primary culture system for *C. elegans* germ cells. Wild-type germ cells are syncytial (Hansen and Schedl, 2013) and therefore cannot be isolated as viable cells. We found that germ cells can be isolated from the tumorous germline mutant strain *glp-1(ar202)*; *cki-2(ok2105)*; *daf-16(mu86)*

(hereafter *glp-1(gf)*; *cki-2*; *daf-16*) (Fig. 3.2A). Staining with the dye calcein-AM shows that the cells have intact plasma membranes, as calcein-AM is converted by cellular esterases to a fluorescent form that is unable to cross intact plasma membranes (Fig. 3.2A).

To determine the percentage of germ cells among the isolated cells, we compared the number of germ cells isolated from *glp-1(gf)*; *cki-2*; *daf-16* mutants and wild-type adult hermaphrodites. Wild-type germ cells are not cellularized and therefore would not survive in culture. *glp-1(gf)*; *cki-2*; *daf-16* mutants have increased numbers of germ cells, but appear to have approximately the same number of somatic cells as wild type. Therefore, any significant increase in the number of isolated cells from *glp-1(gf)*; *cki-2*; *daf-16* mutants can be attributed to germ cells. *glp-1(gf)*; *cki-2*; *daf-16* mutants released an average of 6023 ± 196 live cells per adult hermaphrodite, while wild type released an average of 37 ± 10 live cells per adult hermaphrodite (n = 3 and n = 6 sets of 25 animals, respectively). These results suggest that over 99% of the *glp-1(gf)*; *cki-2*; *daf-16* isolated cells are germ cells.

The *glp-1(gf)*; *cki-2*; *daf-16* strain contains: a temperature-sensitive, gain-of-function (gf) allele of the Notch receptor GLP-1, which promotes germ cell proliferation at the non-permissive temperature (Pepper et al., 2003); and loss-of-function mutations of the CDK-inhibitor CKI-2 and the FOXO transcription factor DAF-16, both of which inhibit GSC proliferation (Kalchhauser et al., 2011; Michaelson et al., 2010). In *glp-1(gf)*; *cki-2*; *daf-16* mutants, germ cell proliferation is not constrained to the distal stem cell niche but occurs throughout the gonad. This is demonstrated by the presence of cells in mitosis throughout the gonad, as shown by immunofluorescence staining with the mitotic marker anti-phosphohistone H3 (Ser10) antibody (Hendzel et al., 1997) (Fig. 3.S1). The addition of *cki-2(lf)* and *daf-16(lf)* mutations to the *glp-1(ar202)* mutation produced more mitotic proliferation, as demonstrated by the significantly

decreased region of the gonad in which the meiotic marker HIM-3 is present relative to *glp-1(ar202)* mutants alone (Hansen et al., 2004) (Fig. 3.S1).

Development of an in vitro culture medium for C. elegans germ cells

Embryonic *C. elegans* cells can be maintained, but not propagated, in L-15-based cell culture medium (Christensen et al., 2002). We observed that isolated germ cells die rapidly in the L-15 medium (Fig. 3.2B). After carrying out a systematic analysis of culture medium components, we prepared a medium optimized for germ cell culture called CeM1 (*C. elegans* medium 1) (Table 3.S1). Cell survival in CeM1 was extended relative to L-15 medium by altering: the base medium (3:1 Schneider's insect:L-15 medium); fetal bovine serum (FBS) concentration (8%); heat-inactivation of FBS at 65°C for 30 min; osmolality (390 mOsm/kg); and pH (6.5) (Fig. 3.S2). Additionally, the following CeM1 components contribute to germ cell survival: reduced L-glutathione; RPMI vitamins; the sugar trehalose; and cholesterol and heme, for which *C. elegans* are auxotrophic (Rao et al., 2005; Shim et al., 2002) (Fig. 3.2C).

We tested different FBS lots and observed a partial negative correlation between the levels of thyroxine (Atlanta Biologicals data sheets) and the ability of the FBS to support germ cell viability (data not shown). Steroid hormones, such as thyroxine, can be removed by exposing FBS to the anion-exchange resin Amberlite IRA 400-CL and charcoal-dextran (Leake et al., 1987; Wiedemann et al., 1972). Treatment of FBS with both reagents significantly increased germ cell survival (Fig. 3.2D). The full CeM1 medium can maintain the viability of a majority of isolated germ cells for a period of one month (Fig. 3.2).

Bacteria can differentially stimulate C. elegans germ cell proliferation

We considered the possibility that *C. elegans*' major dietary component, bacteria, could regulate germ cell proliferation. To test this, we created a bacterial extract of the *Escherichia coli* K-12 strain HT115(DE3) (hereafter HT115), which is used for feeding RNAi (Timmons and Fire, 1998). Addition of HT115 bacterial extract to CeM1 medium increased the number of germ cells over the first three days in culture, suggesting that bacterial component(s) induce germ cell proliferation (Fig. 3.2E). Heat-inactivation of the bacterial extract (60°C for 30 min) did not affect its ability to induce transient proliferation, suggesting that the active compound(s) are not particularly heat-sensitive (Fig. 3.2E).

In laboratory settings, *C. elegans* is propagated on a monoxenic diet of a single bacterial species. To assess the effects of extracts from different bacteria, we created extracts from two additional bacteria: *E. coli* B strain OP50, which is the standard laboratory diet; and *Comamonas aquatica* DA1877, which accelerates *C. elegans* growth (MacNeil et al., 2013). Bacterial extracts from the three strains were added to germ cells isolated from the tumorous mutant strain *glp-1(gf)*; *cki-2*; *daf-16* (hereafter referred to as "isolated germ cells"). Incorporation of the thymidine-analog EdU was used to follow DNA replication 24 to 48 hr post-isolation. Typically, 3-10% of the isolated germ cells incorporate EdU in the absence of bacterial extract. The addition of the bacterial extracts increased the percentage of cells incorporating EdU, with HT115 and DA1877 extracts having more activity than OP50 extract (Fig. 3.3A).

We tested the effect of diets of the three bacteria on germ cell proliferation in vivo by analyzing the frequency of germline tumor formation in the *glp-1(gf)*; *cki-2*; *daf-16* mutant strain grown at a semi-permissive temperature (Fig. 3.S3A). Hereafter, references to "tumor frequency" will imply that the assay was performed with *glp-1(gf)*; *cki-2*; *daf-16* mutants. Similar results

were obtained whether tumor frequency was scored blinded or non-blinded (see Experimental Procedures). Consistent with the EdU incorporation data, the frequency of visible tumors at the semi-permissive temperature of 18°C was higher with a diet of DA1877 or HT115 than with OP50 (Fig. 3.3B). Diets of the three bacteria appear to stimulate germ cell proliferation through a common pathway, as mixed diets of the different bacteria did not synergistically increase tumor formation (Fig. 3.S3B).

Bacterial folates stimulate germ cell proliferation

Several bacteria-derived compounds have been implicated in modulating *C. elegans* biological processes, including: folates, which reduce lifespan (Virk et al., 2012); tryptophan metabolite(s), which alter the expression of detoxification genes (Gracida and Eckmann, 2013); and vitamin B12, which accelerates growth (Watson et al., 2014). Supplementing bacteria with tryptophan or vitamin B12 did not stimulate germ cell proliferation (Fig. 3.S4). In contrast, our analysis of folates found that they are linked to the stimulation of germ cell proliferation.

Most bacteria are capable of the *de novo* synthesis of folate through a pathway that includes the condensation of the dihydropteridine ring with PABA, followed by the addition of one or more glutamates (Glu) (Fig. 3.1B). PABA can be rate-limiting for folate synthesis in bacteria (Sybesma et al., 2003). To test if increasing the level of bacterial folates increases germ cell proliferation, we supplemented bacteria with PABA. Diets of the three bacteria supplemented with PABA produced an increase in tumor frequencies (Fig. 3.3B). Similarly, adding extracts from bacteria supplemented with PABA to isolated germ cells increased the percentage of cells incorporating EdU (Fig. 3.3A). As expected, based on the inability of animals to use PABA to create folates, adding PABA directly to isolated germ cells had no affect on EdU incorporation

(Fig. 3.3A). Similarly, adding PABA to a diet of heat-killed bacteria, which cannot metabolize the PABA, had no stimulatory effect (Fig. 3.3C).

To further address the contribution of bacterial folates or folate-related compounds to germ cell proliferation, we used the antibiotic trimethoprim (TRI), which inhibits dihydrofolate reductase (DHFR) in bacteria to block the generation of THF. TRI reduces overall THF folate levels in *E. coli*; however, while the levels of poly-Glu_3 or higher THF folates become undetectable upon TRI exposure, the levels of mono- and di-Glu THF folates modestly increase (Kwon et al., 2008). We observed that incubating HT115 and DA1877 bacteria with 2.5 μg/ml TRI prior to creating extract reduced the extract's ability to stimulate EdU incorporation in isolated germ cells (Fig. 3.3D). Pretreatment of OP50 with TRI did not have an obvious effect on the extract's (normally lower) level of stimulating DNA replication (Fig. 3.3D). Similarly, feeding *glp-1(gf)*; *cki-2*; *daf-16* mutants a diet of HT115 or DA1877 grown on TRI reduced tumor frequency, while a diet of OP50 grown on TRI did not significantly reduce tumor frequency (Fig. 3.3E). The lack of effect of TRI on an OP50 diet or OP50 bacterial extract indicates that TRI by itself has no appreciable effect on germ cell proliferation, but rather mediates its effects via its action on specific bacteria.

We wanted to determine if the choice of bacterial diet and increasing bacterial folate production affects GSC proliferation in wild-type animals. Increases or decreases in mitotic proliferation of GSCs expand or contract the proliferative zone of the gonad to alter the number of germ cell nuclei in the zone (Michaelson et al., 2010). When wild-type hermaphrodites were fed a diet of HT115 or DA1877 bacteria, the number of germ cell nuclei in the proliferative zone was higher compared to an OP50 diet (Fig. 3.3F). Supplementing the bacteria with PABA increased the number of germ cell nuclei in the proliferative zone for OP50 and HT115 diets,

with a higher mitotic index for the HT115 diet, suggesting that a diet with increased levels of folates increases proliferative germ cell numbers (Figs 3.3F, 3.S5A). Incubation of the three bacteria with TRI reduced the numbers of mitotic germ cells per gonad arm in wild-type hermaphrodites fed a diet of DA1877, but had less effect on OP50 and HT115 diets (Fig. 3.S5B). Overall, these results suggest that increased levels of bacterial folates can increase mitotic germ cell proliferation in wild-type hermaphrodites.

To confirm that folates are the active bacterial component, folates were purified from bacteria and tested for their ability to induce germ cell proliferation. Total bacterial extract, purified folates, and folate-free, flow-through extract were tested on isolated germ cells for their effect on DNA replication. Total extract and purified folates increased the number of cells incorporating EdU when added to isolated germ cells (Fig. 3.4A; Table 3.S2). In contrast, the addition of the folate-free flow-through extract reduced EdU incorporation, suggesting that in the absence of folates, bacterial extract negatively impacts germ cell cultures. The addition of purified folates to a diet of heat-killed OP50 bacteria also increased tumor frequency (Fig. 3.4B).

To determine if purified folates increase the number of mitotic cells in wild-type animals, we added purified folates from OP50, DA1877, or HT115 to heat-killed OP50 bacteria and allowed wild-type animals to develop from eggs on these plates. The addition of purified folates from HT115 and DA1877 increased the number of nuclei in the proliferative zone, with the mitotic index statistically higher for DA1877 folates (Figs 3.4C, 3.S5C). These results indicate that bacterial folates promote GSC proliferation in wild-type hermaphrodites.

Our previous analysis used equal volumes of isolated purified folates. To compare the relative activity of the purified folates among the three bacteria, we added equal concentrations of purified folates (0.06 μM) to isolated germ cells. The purified folates from HT115 induced a

higher percentage of cells incorporating EdU than purified folates from OP50 and DA1877 (Fig. 3.4D). Folates purified from the mouse microbiota also have potent activity in stimulating EdU incorporation in isolated germ cells, suggesting that the active folate(s) are present in diverse microbial settings (Fig. 3.S5D).

10-formyl-THF-Glu$_n$ stimulates germ cell proliferation

CeM1 medium contains the synthetic folate folic acid at 2.8 μM, which is 40-fold higher than the concentration of purified folates that stimulate increased EdU incorporation in isolated germ cells. Therefore, bacterial folates provide a signal that is not provided by folic acid.

We tested the germ cell stimulatory activity of the reduced monoglutamyl forms of folates, including racemic (S,R) THF, 5-formyl-THF (folinic acid), and 5-methyl-THF, as well as the biologically active (S) isomer for the latter two folates. We found that these basic folates, which can promote one-carbon metabolism when added to other animal cells, were unable to stimulate germ cell DNA replication even at concentrations significantly higher than the purified bacterial folates (Fig. 3.4D). The addition of 5-methyl-THF and THF to a diet of heat-killed bacteria also did not have a major effect on tumor frequency (Fig. 3.4B).

In an effort to identify the active germ cell-stimulatory folate(s), we analyzed the folates from OP50, HT115, and DA1877 bacteria grown under normal or PABA-supplemented conditions. Ion-pair high performance liquid chromatography (HPLC) was used to separate the affinity-purified folates, which were then identified by their stereotypical UV absorbance spectra (Selhub et al., 1980). Four folate species were detected in the bacterial extracts: 10-formyl-THF-Glu$_n$; THF-Glu$_n$; 5-formyl-THF-Glu$_n$; and 5-methyl-THF-Glu$_n$ (Fig. 3.S6). The folates from DA1877 consisted predominantly of folates with three Glu residues, the most abundant of which

was 5-methyl-THF-Glu_3 (Fig. 3.S6C). In contrast, OP50 and HT115 had primarily formylated folates with 3-7 Glu residues (Fig. 3.S6A,B). Notably, the only folate species that increased upon growth with PABA in all three bacterial species was 10-formyl-THF-Glu_n.

We isolated individual DA1877 folate fractions using HPLC (Fig. 3.5A). The 5-methyl-THF-$Glu_{1,3}$ fractions lacked stimulatory activity, consistent with our analysis of pure folates. In contrast, the 10-formyl-THF-Glu_3 and 5,10-methenyl-THF-Glu_3 fractions stimulated EdU incorporation in isolated germ cells and increased tumor frequency assays when added to a diet of heat-killed bacteria (Fig. 3.5B,C). The activity of 5,10-methenyl-THF-Glu_3 is likely to be due to its conversion to 10-formyl-THF-Glu_3, which would occur because the assays were performed at neutral pH. The first peak from the chromatogram, whose molecular identity we could not determine, also exhibited stimulatory activity (data not shown). Overall, our results suggest that 10-formyl-THF-Glu_n can stimulate germ cell proliferation.

To clarify the importance of the number of glutamate residues, we converted purified OP50 bacterial folates from poly-Glu_{3-7} to mono-Glu by treatment with tri-enzyme (a mixture of chicken pancreas conjugase, alpha amylase, and pronase) (Martin et al., 1990). The conversion to mono-Glu folates abolished the stimulatory activity in EdU incorporation assays with isolated germ cells and tumor frequency assays (Fig. 3.6A,B). The stimulation of tumor frequency was also abolished when purified DA1877 bacterial folates were converted to mono-Glu using conjugase enzyme alone (Fig. 3.S5E).

To further confirm that poly-Glu contributes to germ cell stimulatory activity, we synthesized folates with 1, 3, or 6 Glu from folic acid-$Glu_{1,3,6}$: THF-$Glu_{1,3,6}$; 5-methyl-THF-$Glu_{1,3,6}$; 5,10-methenyl-THF-$Glu_{1,3,6}$; and 10-formyl-THF-$Glu_{1,3,6}$. We observed that folic acid, 5-methyl-THF, and THF were not active in stimulating increased tumor frequencies irrespective

of the number of Glu residues (Figs 3.6D; 3.S5F). In contrast, 10-formyl-THF and 5,10-methenyl-THF increased tumor frequency in vivo and EdU incorporation in isolated germ cells in vitro, with greater activity with higher numbers of poly-glutamates (Figs 3.6C,D; 3.S5F). Significantly, 10-formyl-THF-$Glu_{3,6}$ and 5,10-methenyl-THF-$Glu_{3,6}$ had activity even at the lowest concentration tested: 1 nM (Fig. 3.6C,D). The addition of 5,10-methenyl-THF-Glu_6 stimulated the transient proliferation of germ cells in vitro, similar to what we had observed with HT115 bacterial extract (Fig. 3.S5G). The ability of the synthetic folates 10-formyl-THF-Glu_n and 5,10-methenyl-THF-Glu_n to match the stimulatory activity of the folates isolated from bacteria confirms the identity of the bacterial stimulatory folates.

Folates stimulate germ cell proliferation independently of one-carbon metabolism

In other animals, multiple folates can act as single vitamin sources to reconstitute all of the folates required for one-carbon metabolism (Zhao et al., 2009). One potential model to explain the specificity of germ cell stimulation is that perhaps, unlike other animals, *C. elegans* can only utilize a single folate as a vitamin source. To address the role of folates as vitamins, we used the *folt-1* mutant as a means to deplete folate levels. *folt-1* is the *C. elegans* homolog of the mammalian RFC.

In mammals, the ubiquitously-expressed RFC transports the bulk of systemic folates into tissues (Zhao et al., 2009). In *C. elegans*, FOLT-1/RFC is required for ~80% of folate uptake into animals (Balamurugan et al., 2007). *folt-1(ok1467)* deletion mutants, when grown on a diet of OP50 bacteria, have severe defects in germ cell proliferation, with few germ cells per gonad arm (Austin et al., 2010). Strikingly, we found that providing *folt-1*/RFC mutants a diet of OP50 supplemented with PABA rescued the germ cell number defect, and allowed 100% of the *folt-*

1/RFC mutant adult hermaphrodites to become gravid (Fig. 3.7A). Therefore, the *folt-1*/RFC mutant is responsive to increased folate levels.

To further reduce the levels of folates, *folt-1*/RFC mutants were fed a diet of heat-killed, folate-depleted *pabC* mutant bacteria, which are unable to produce PABA (Roux and Walsh, 1993). To deplete folates in *pabC* mutants, the bacteria were incubated 24 hr in PABA-free minimal media. The resulting folate-depleted *pabC* bacteria had only 2.3% of the folate level of the parental *E. coli* K-12 strain (data not shown).

To test the ability of folates to rescue folate deficiency, heat-killed, folate-depleted *pabC* bacteria were supplemented with 10 μM of either the non-stimulatory folate S-5-formyl-THF-Glu_1 or the stimulatory folate 5,10-methenyl-THF-Glu_1. Both folates were able to rescue germ cell proliferation in the folate-depleted *folt-1*/RFC mutants, with the non-stimulatory S-5-formyl-THF-Glu_1 exhibiting more activity (Fig. 3.7B). Racemic 5-formyl-THF-Glu_1 (folinic acid) also rescues *C. elegans* sterility due to folate deficiency (Virk et al., 2016). These results suggest that the effectiveness of a folate to function as a vitamin does not correlate with its ability to stimulate germ cell proliferation under normal growth conditions.

To directly test if a folate-related compound can stimulate germ cell proliferation independently of one-carbon metabolism, we analyzed dihydropteroate. Pteroates are comprised of a pteridine ring and PABA moieties, but lack glutamates (Fig. 3.1B). Dihydropteroate is a precursor to all folate synthesis in bacteria. Animals are unable to convert pteroates to folates because they lack the enzyme (dihydrofolate synthase) that is required to add glutamate to pteroates (Fig. 3.1B). Animals therefore cannot utilize pteroates for one-carbon metabolism. As expected for a compound that cannot support one-carbon metabolism, dihydropteroate was

unable to rescue the folate deficiency of *folt-1*/RFC mutants grown on folate-depleted bacteria (Fig. 3.7B).

Significantly, dihydropteroate stimulated increased EdU incorporation in isolated germ cells and tumor frequency, although it was less active than 5,10-methenyl-THF-Glu_6 in inducing the proliferation of isolated germ cells (Figs 3.7C,D; 3.S5G). The ability of dihydropteroate to stimulate germ cell proliferation implies that the stimulation occurs independently of one-carbon metabolism.

The folate receptor homolog FOLR-1 is required for the stimulation of germ cell proliferation

The mammalian FRs, a, b, and g, transport folates, but have more restricted tissue expression than RFC (Zhao et al., 2009). Notably, mammalian FR can bind both folates and pteroates (Sodji et al., 2015). *C. elegans* contains an apparent ortholog of FR, *folr-1* (C17G1.1). Although FOLR-1/FR and human FRg proteins only share 12% identity and 25.5% similarity, they are the top scores in the two respective species using reciprocal psi-BLAST searches (Altschul et al., 1997). FOLR-1/FR has a predicted signal peptide and transmembrane domain that is compatible with cell surface localization (Cserzo et al., 2002; Petersen et al., 2011).

In contrast to *folt-1*/RFC mutants, RNAi depletion of *folr-1*/FR does not appear to affect the basal number of germ cells, and *folr-1(RNAi)* hermaphrodites lay the same number of eggs as wild type (Fig. 3.S7A). This suggests that unlike FOLT-1/RFC, FOLR-1/FR is not essential for the uptake of folates to function as vitamins. Strikingly, RNAi depletion of *folr-1*/FR abolishes the stimulatory effect of purified bacterial folates, 10-formyl-THF-Glu_6, 5,10-methenyl-THF-$Glu_{1,6}$, and dihydropteroate both in vivo (for tumor frequency) and in vitro (for EdU incorporation) (Figs 3.7E,F, 3.S7B). At the fully non-permissive temperature of 25°C, *folr-1*/FR

RNAi only modestly suppresses tumor formation in *glp-1(gf)*; *cki-2*; *daf-16* mutants, but blocks the response to PABA supplementation, indicating that it still blocks the stimulatory effect of folates (Fig. 3.S7C). These results suggest that both 10-formyl-THF-Glu_n and dihydropteroate stimulate germ cell proliferation through a FOLR-1-dependent pathway.

A folate-enriched diet increases cell number in somatic hyperplasia

We wanted to determine if bacterial folates could stimulate somatic cell division using the *cul-1* mutant, which exhibits hyperplasia of larval somatic cell lineages (Kipreos et al., 1996). *cul-1(e1756)* mutants expressing a hypodermal seam cell GFP marker were fed diets of OP50 or OP50 supplemented with 10 μM PABA. Both *cul-1* homozygous and heterozygous mutants exhibited increased seam cell numbers when on the diet supplemented with PABA (Fig. 3.3G). Notably, the hyperplasia in *cul-1* heterozygotes is a synthetic phenotype, as *cul-1* heterozygotes do not exhibit hyperplasia under normal growth conditions (Kipreos et al., 1996) and wild-type animals do not exhibit seam cell hyperplasia on a diet of OP50 supplemented with PABA (Fig. 3.3G).

We were unable to use heat-killed bacteria to assess the effect of pure folates or pteroates because *cul-1* homozygotes arrest development on heat-killed bacteria, and *cul-1* heterozygotes do not exhibit hyperplasia on heat-killed bacteria with added folates, potentially due to the sub-optimal diet (data not shown). Nevertheless, these results suggest that a diet with increased bacterial folates can stimulate the proliferation of a somatic cell lineage.

Discussion

In this study, we describe the first primary culture system for *C. elegans* germ cells. The CeM1 medium that we created differs markedly from the L-15-based medium used for *C. elegans* embryonic and larval cell cultures. CeM1 medium can maintain the viability of germ cells for up to one month, thereby providing an experimental platform for the study of nearly homogeneous populations of germ cells.

10-formyl-THF-Glu$_n$ is a germ cell-stimulatory folate

Our results show that bacterial folates act as an exogenous signal to stimulate an adult stem cell population. Surprisingly, many folate species (folic acid, THF, 5-formyl-THF, and 5-methyl-THF) are unable to stimulate germ cells under normal growth conditions, despite the fact that these folates are readily taken up by animals, including *C. elegans* (Balamurugan et al., 2007). Instead, we observed germ cell stimulatory activity only with the folates 10-formyl-THF-Glu$_n$ and 5,10-methenyl-THF-Glu$_n$, with increasing activity with larger numbers of poly-Glu. The ability of 5,10-methenyl-THF-Glu$_n$ to stimulate germ cells is unlikely to reflect its own activity, as it converts to 10-formyl-THF-Glu$_n$ within minutes at the neutral pH used in our experiments.

Bacterial folates and related compounds can stimulate C. elegans germ cells independently of one-carbon metabolism

We observed that the non-stimulatory folate S-5-formyl-THF-Glu$_1$ rescued the folate deficiency of folate-depleted *folt-1*/RFC mutant germ cells more effectively than the stimulatory folate 5,10-methenyl-THF-Glu$_1$. This suggests that the ability of a folate to act as a vitamin does not correlate with its ability to stimulate germ cell proliferation under normal growth conditions.

Additionally, 10-formyl-THF-Glu_n can stimulate *C. elegans* germ cell proliferation at a concentration of 1 nM, which is lower than the levels required for one-carbon metabolism in mammals (Geng et al., 2015; Neuhouser et al., 2011).

Dihydropteroate can also stimulate germ cell proliferation. Dihydropteroate is unable to function in one-carbon metabolism in animal cells, and consistently, its addition was unable to rescue folate deficiency in *C. elegans*. Significantly, the stimulation of germ cell proliferation by both dihydropteroate and 10-formyl-THF-Glu_n requires the presence of FOLR-1/FR. The mammalian homolog of FOLR-1/FR can bind both folates and pteroates (Sodji et al., 2015). These results suggest that dihydropteroate and 10-formyl-THF-Glu_n stimulate germ cell proliferation through a FOLR-1/FR-dependent pathway that is independent of one-carbon metabolism.

Dihydropteroate is present in all bacteria that are capable of *de novo* folate biosynthesis. However, we did not observe detectable levels of dihydropteroate by chromatography in extracts from the three bacteria (data not shown). This suggests that in these three bacteria, dihydropteroate is not the predominant germ cell stimulatory signal, with 10-formyl-THF-Glu_n and 5,10-methenyl-THF-Glu_n present at much higher levels. It is possible that in the wild, other bacteria produce higher levels of dihydropteroate that contribute to the stimulation of *C. elegans* germ cell proliferation.

One obvious question is why 10-formyl-THF and dihydropteroate, but not other folates, were selected during evolution to regulate germ cell proliferation. In this regard, it is notable that 10-formyl-THF and dihydropteroate are particularly unstable relative to other folates and folate-related compounds ((Blakley, 1969) Schircks Laboratories data sheets). Potentially, the labile

nature of these folate and folate-related compounds allows a tighter linkage between the presence of live bacteria and germ cell proliferation.

The folate receptor and signaling

The finding that FOLR-1/FR is required for the stimulation of *C. elegans* germ cell proliferation is interesting in light of recent mammalian cancer research. In many cancers, FRs are overexpressed, and this is associated with neoplastic progression and poor prognosis (Kelemen, 2006). FRa promotes proliferation, migration, and invasiveness of SKOV-3 ovarian cancer cells, which have high-level FRa expression; while surprisingly, RFC acts oppositely to reduce cell proliferation, migration, and invasiveness (Siu et al., 2012). Notably, FRa only contributes 20-30% of the uptake of folate in SKOV-3 and four other ovarian cancer cell lines, while RFC is responsible for ~70% of their folate uptake (Corona et al., 1998). Similarly, in *C. elegans*, FOLT-1/RFC is required for the majority of folate uptake to allow basal germ cell proliferation and fertility, while FOLR-1/FR is required for stimulatory folate signaling but is not essential for providing folates for basal germ cell proliferation.

Recent emerging evidence suggests the potential for human FR to function in cell signaling independently of one-carbon metabolism. The addition of folates to cells activates intracellular signaling pathways in a FR-dependent manner in time periods that are shorter than would be expected from changes in one-carbon metabolism. The addition of folic acid to mammalian cells has been reported to induce the phospho-activation of c-src tyrosine kinase, ERK kinase, and STAT transcription factor in a FRa-dependent manner within 2-5 minutes of stimulation (Hansen et al., 2015; Lin et al., 2012; Zhang et al., 2009). Additionally, FRa itself has been reported to translocate to the nucleus and function as a transcription factor in human tissue culture cells after

stimulation with 453 μM of folic acid (Boshnjaku et al., 2012). These studies used folic acid, a non-natural, synthetic folate, at elevated, non-physiological levels of 10 to 600 μM. These concentrations are orders of magnitude higher than the concentration of folates in human serum, which are 8.6 to 29.7 nM for the 5^{th}-95^{th} percentiles of an unsupplemented population (Hustad et al., 2000). This raises the question of the physiological relevance of the observations. In contrast, our results show biological effects with 1 nM of a specific, naturally-available folate.

Our work provides a direct link between microbial factors and the regulation of an adult stem cell population. The importance of the microbiota for animal health has recently been recognized (Clemente et al., 2012). Microbiota-derived folates are readily absorbed by the human host (Camilo et al., 1996). In diverse human populations, the initial colonization of the gut is enriched for microbes capable of *de novo* folate synthesis, indicating that humans harbor folate-synthesizing bacteria throughout their lifespan (Yatsunenko et al., 2012). We observed that folates isolated from mouse microbiota are potent stimulators of *C. elegans* germ cells, indicating that the active folates are present at high levels in the mammalian microbiota. Our work therefore suggests the possibility that microbiota-derived folates can act as signaling molecules, potentially to the host or to other organisms that may reside within the host, such as parasitic nematodes.

Author Contributions

Conceptualization, E.T.K. and J.S.; Methodology, E.T.K. and J.S.; Investigation, S.N.C., M.M., A.S.V., G.B., M.M.R., C.N., and E.T.K.; Resources, J.S.; Writing – Original Draft, E.T.K. and J.S.; Writing – Review and Editing, S.N.C., M.M., E.T.K., J.S., M.M.R., and L.P.; Visualization, M.M. and S.N.C.; Supervision, E.T.K., J.S., and L.P.; Funding Acquisition, E.T.K. and J.S.

Acknowledgements

We thank M.J. McEachern and members of the Kipreos lab for critical comments on the manuscript, M.C. Zetka, D.B. Hausman, and S. Dougan for reagents or resources. Some *C. elegans* strains were provided by the CGC, which is funded by NIH Office of Research Infrastructure Programs (P40 OD010440). This work was supported by grants from NSF (MCB-1138454) and NIH/NIGMS (1R01GM074212) (Zetka et al.), and support from United States Department of Agriculture cooperative agreement 51520-008-04S (JS). Any opinions, findings, conclusion, or recommendations expressed in this publication are those of the authors and do not necessarily reflect the view of the United States Department of Agriculture.

References

Altschul, S.F., Madden, T.L., Schaffer, A.A., Zhang, J.H., Zhang, Z., Miller, W., and Lipman, D.J. (1997). Gapped BLAST and PSI-BLAST: a new generation of protein database search programs. Nucleic Acids Res *25*, 3389-3402.

Austin, M.U., Liau, W.S., Balamurugan, K., Ashokkumar, B., Said, H.M., and LaMunyon, C.W. (2010). Knockout of the folate transporter folt-1 causes germline and somatic defects in C. elegans. BMC developmental biology *10*, 46.

Bagley, P.J., and Selhub, J. (2000). Analysis of folate form distribution by affinity followed by reversed- phase chromatography with electrical detection. Clinical chemistry *46*, 404-411.

Balamurugan, K., Ashokkumar, B., Moussaif, M., Sze, J.Y., and Said, H.M. (2007). Cloning and functional characterization of a folate transporter from the nematode Caenorhabditis elegans. American journal of physiology *293*, C670-681.

Blakley, R.L. (1969). The Biochemistry of Folic Acid and Related Pteridines (Amsterdam, Netherlands: North-Holland Publishing Company).

Boshnjaku, V., Shim, K.W., Tsurubuchi, T., Ichi, S., Szany, E.V., Xi, G., Mania-Farnell, B., McLone, D.G., Tomita, T., and Mayanil, C.S. (2012). Nuclear localization of folate receptor alpha: a new role as a transcription factor. Sci Rep *2*, 980.

Camilo, E., Zimmerman, J., Mason, J.B., Golner, B., Russell, R., Selhub, J., and Rosenberg, I.H. (1996). Folate synthesized by bacteria in the human upper small intestine is assimilated by the host. Gastroenterology *110*, 991-998.

Christensen, M., Estevez, A., Yin, X., Fox, R., Morrison, R., McDonnell, M., Gleason, C., Miller, D.M., 3rd, and Strange, K. (2002). A primary culture system for functional analysis of C. elegans neurons and muscle cells. Neuron *33*, 503-514.

Clemente, J.C., Ursell, L.K., Parfrey, L.W., and Knight, R. (2012). The impact of the gut microbiota on human health: an integrative view. Cell *148*, 1258-1270.

Corona, G., Giannini, F., Fabris, M., Toffoli, G., and Boiocchi, M. (1998). Role of folate receptor and reduced folate carrier in the transport of 5-methyltetrahydrofolic acid in human ovarian carcinoma cells. International journal of cancer *75*, 125-133.

Cserzo, M., Eisenhaber, F., Eisenhaber, B., and Simon, I. (2002). On filtering false positive transmembrane protein predictions. Protein Eng *15*, 745-752.

Desmoulin, S.K., Hou, Z., Gangjee, A., and Matherly, L.H. (2012). The human proton-coupled folate transporter: Biology and therapeutic applications to cancer. Cancer biology & therapy *13*, 1355-1373.

Geng, Y., Gao, R., Chen, X., Liu, X., Liao, X., Li, Y., Liu, S., Ding, Y., Wang, Y., and He, J. (2015). Folate deficiency impairs decidualization and alters methylation patterns of the genome in mice. Mol Hum Reprod *21*, 844-856.

Gracida, X., and Eckmann, C.R. (2013). Fertility and germline stem cell maintenance under different diets requires nhr-114/HNF4 in C. elegans. Curr Biol *23*, 607-613.

Grapp, M., Wrede, A., Schweizer, M., Huwel, S., Galla, H.J., Snaidero, N., Simons, M., Buckers, J., Low, P.S., Urlaub, H.*, et al.* (2013). Choroid plexus transcytosis and exosome shuttling deliver folate into brain parenchyma. Nat Commun *4*, 2123.

Hansen, D., Hubbard, E.J., and Schedl, T. (2004). Multi-pathway control of the proliferation versus meiotic development decision in the Caenorhabditis elegans germline. Dev Biol *268*, 342-357.

Hansen, D., and Schedl, T. (2013). Stem cell proliferation versus meiotic fate decision in Caenorhabditis elegans. Advances in experimental medicine and biology *757*, 71-99.

Hansen, M.F., Greibe, E., Skovbjerg, S., Rohde, S., Kristensen, A.C., Jensen, T.R., Stentoft, C., Kjaer, K.H., Kronborg, C.S., and Martensen, P.M. (2015). Folic acid mediates activation of the pro-oncogene STAT3 via the Folate Receptor alpha. Cell Signal *27*, 1356-1368.

Henderson, G.I., Perez, T., Schenker, S., Mackins, J., and Antony, A.C. (1995). Maternal-to-fetal transfer of 5-methyltetrahydrofolate by the perfused human placental cotyledon: evidence for a concentrative role by placental folate receptors in fetal folate delivery. J Lab Clin Med *126*, 184-203.

Hendzel, M.J., Wei, Y., Mancini, M.A., Van Hooser, A., Ranalli, T., Brinkley, B.R., Bazett-Jones, D.P., and Allis, C.D. (1997). Mitosis-specific phosphorylation of histone H3 initiates primarily within pericentromeric heterochromatin during G2 and spreads in an ordered fashion coincident with mitotic chromosome condensation. Chromosoma *106*, 348-360.

Hustad, S., Ueland, P.M., Vollset, S.E., Zhang, Y., Bjorke-Monsen, A.L., and Schneede, J. (2000). Riboflavin as a determinant of plasma total homocysteine: effect modification by the methylenetetrahydrofolate reductase C677T polymorphism. Clinical chemistry *46*, 1065-1071.

Kalchhauser, I., Farley, B.M., Pauli, S., Ryder, S.P., and Ciosk, R. (2011). FBF represses the Cip/Kip cell-cycle inhibitor CKI-2 to promote self-renewal of germline stem cells in C. elegans. EMBO J *30*, 3823-3829.

Kelemen, L.E. (2006). The role of folate receptor alpha in cancer development, progression and treatment: cause, consequence or innocent bystander? International journal of cancer *119*, 243-250.

Killian, D.J., and Hubbard, E.J. (2005). Caenorhabditis elegans germline patterning requires coordinated development of the somatic gonadal sheath and the germ line. Dev Biol *279*, 322-335.

Kipreos, E.T., Lander, L.E., Wing, J.P., He, W.W., and Hedgecock, E.M. (1996). cul-1 is required for cell cycle exit in C. elegans and identifies a novel gene family. Cell *85*, 829-839.

Kwon, Y.K., Lu, W., Melamud, E., Khanam, N., Bognar, A., and Rabinowitz, J.D. (2008). A domino effect in antifolate drug action in Escherichia coli. Nat Chem Biol *4*, 602-608.

Leake, R.E., Freshney, R.I., and Munir, I. (1987). Steroid response in vivo and in vitro. In Steroid hormones: a practical approach, B. Green, and R.E. Leake, eds. (Oxford, England: IRL Press Limited), pp. 205-218.

Lin, S.Y., Lee, W.R., Su, Y.F., Hsu, S.P., Lin, H.C., Ho, P.Y., Hou, T.C., Chou, Y.P., Kuo, C.T., and Lee, W.S. (2012). Folic acid inhibits endothelial cell proliferation through activating the cSrc/ERK 2/NF-kappaB/p53 pathway mediated by folic acid receptor. Angiogenesis *15*, 671-683.

MacNeil, L.T., Watson, E., Arda, H.E., Zhu, L.J., and Walhout, A.J. (2013). Diet-induced developmental acceleration independent of TOR and insulin in C. elegans. Cell *153*, 240-252.

Martin, J.I., Landen, W.O., Jr., Soliman, A.G., and Eitenmiller, R.R. (1990). Application of a tri-enzyme extraction for total folate determination in foods. Journal - Association of Official Analytical Chemists *73*, 805-808.

Matherly, L.H., Hou, Z., and Deng, Y. (2007). Human reduced folate carrier: translation of basic biology to cancer etiology and therapy. Cancer Metastasis Rev *26*, 111-128.

Michaelson, D., Korta, D.Z., Capua, Y., and Hubbard, E.J. (2010). Insulin signaling promotes germline proliferation in C. elegans. Development *137*, 671-680.

Mok, D.Z., Sternberg, P.W., and Inoue, T. (2015). Morphologically defined sub-stages of C. elegans vulval development in the fourth larval stage. BMC developmental biology *15*, 26.

Neuhouser, M.L., Nijhout, H.F., Gregory, J.F., 3rd, Reed, M.C., James, S.J., Liu, A., Shane, B., and Ulrich, C.M. (2011). Mathematical modeling predicts the effect of folate deficiency and excess on cancer-related biomarkers. Cancer epidemiology, biomarkers & prevention : a publication of the American Association for Cancer Research, cosponsored by the American Society of Preventive Oncology *20*, 1912-1917.

Pepper, A.S., Killian, D.J., and Hubbard, E.J. (2003). Genetic analysis of Caenorhabditis elegans glp-1 mutants suggests receptor interaction or competition. Genetics *163*, 115-132.

Petersen, T.N., Brunak, S., von Heijne, G., and Nielsen, H. (2011). SignalP 4.0: discriminating signal peptides from transmembrane regions. Nat Methods *8*, 785-786.

Poo-Prieto, R., Haytowitz, D.B., Holden, J.M., Rogers, G., Choumenkovitch, S.F., Jacques, P.F., and Selhub, J. (2006). Use of the affinity/HPLC method for quantitative estimation of folic acid in enriched cereal-grain products. The Journal of nutrition *136*, 3079-3083.

Rao, A.U., Carta, L.K., Lesuisse, E., and Hamza, I. (2005). Lack of heme synthesis in a free-living eukaryote. Proc Natl Acad Sci U S A *102*, 4270-4275.

Rossi, M., Amaretti, A., and Raimondi, S. (2011). Folate production by probiotic bacteria. Nutrients *3*, 118-134.

Roux, B., and Walsh, C.T. (1993). p-Aminobenzoate synthesis in Escherichia coli: mutational analysis of three conserved amino acid residues of the amidotransferase PabA. Biochemistry *32*, 3763-3768.

Selhub, J. (2002). Folate, vitamin B12 and vitamin B6 and one carbon metabolism. The journal of nutrition, health & aging *6*, 39-42.

Selhub, J., Ahmad, O., and Rosenberg, I.H. (1980). Preparation and use of affinity columns with bovine milk folate-binding protein (FBP) covalently linked to Sepharose 4B. Methods in enzymology *66*, 686-690.

Selhub, J., Emmanouel, D., Stavropoulos, T., and Arnold, R. (1987). Renal folate absorption and the kidney folate binding protein. I. Urinary clearance studies. The American journal of physiology *252*, F750-756.

Sempere, L.F., Freemantle, S., Pitha-Rowe, I., Moss, E., Dmitrovsky, E., and Ambros, V. (2004). Expression profiling of mammalian microRNAs uncovers a subset of brain-expressed microRNAs with possible roles in murine and human neuronal differentiation. Genome biology *5*, R13.

Shim, Y.H., Chun, J.H., Lee, E.Y., and Paik, Y.K. (2002). Role of cholesterol in germ-line development of Caenorhabditis elegans. Molecular reproduction and development *61*, 358-366.

Siu, M.K., Kong, D.S., Chan, H.Y., Wong, E.S., Ip, P.P., Jiang, L., Ngan, H.Y., Le, X.F., and Cheung, A.N. (2012). Paradoxical impact of two folate receptors, FRalpha and RFC, in ovarian cancer: effect on cell proliferation, invasion and clinical outcome. PloS one *7*, e47201.

Sodji, Q.H., Kornacki, J.R., McDonald, J.F., Mrksich, M., and Oyelere, A.K. (2015). Design and structure activity relationship of tumor-homing histone deacetylase inhibitors conjugated to folic and pteroic acids. Eur J Med Chem *96*, 340-359.

Stover, P., and Schirch, V. (1992). Synthesis of (6S)-5-formyltetrahydropteroyl-polyglutamates and interconversion to other reduced pteroylpolyglutamate derivatives. Analytical biochemistry *202*, 82-88.

Sulston, J., and Hodgkin, J. (1988). Methods. In The Nematode Caenorhabditis elegans, W.B. Wood, ed. (Cold Spring Harbor, New York: Cold Spring Harbor Laboratory), pp. 587-606.

Sybesma, W., Starrenburg, M., Tijsseling, L., Hoefnagel, M.H., and Hugenholtz, J. (2003). Effects of cultivation conditions on folate production by lactic acid bacteria. Applied and environmental microbiology *69*, 4542-4548.

Tamura, T., Freeberg, L.E., and Cornwell, P.E. (1990). Inhibition of EDTA of growth of Lactobacillus casei in the folate microbiological assay and its reversal by added manganese or iron. Clinical chemistry *36*, 1993.

Timmons, L., and Fire, A. (1998). Specific interference by ingested dsRNA. Nature *395*, 854.

Virk, B., Correia, G., Dixon, D.P., Feyst, I., Jia, J., Oberleitner, N., Briggs, Z., Hodge, E., Edwards, R., Ward, J.*, et al.* (2012). Excessive folate synthesis limits lifespan in the C. elegans: E. coli aging model. BMC biology *10*, 67.

Virk, B., Jia, J., Maynard, C.A., Raimundo, A., Lefebvre, J., Richards, S.A., Chetina, N., Liang, Y., Helliwell, N., Cipinska, M.*, et al.* (2016). Folate Acts in E. coli to Accelerate C. elegans Aging Independently of Bacterial Biosynthesis. Cell Rep *14*, 1611-1620.

Watson, E., MacNeil, L.T., Ritter, A.D., Yilmaz, L.S., Rosebrock, A.P., Caudy, A.A., and Walhout, A.J. (2014). Interspecies systems biology uncovers metabolites affecting C. elegans gene expression and life history traits. Cell *156*, 759-770.

Wiedemann, M., Raith, L., Wirtz, A., and Karl, H.J. (1972). Trennung von freien und proteingebundenen Steroiden mit Amberlite. Z Anal Chem *261*, 382-385.

Yatsunenko, T., Rey, F.E., Manary, M.J., Trehan, I., Dominguez-Bello, M.G., Contreras, M., Magris, M., Hidalgo, G., Baldassano, R.N., Anokhin, A.P.*, et al.* (2012). Human gut microbiome viewed across age and geography. Nature *486*, 222-227.

Zetka, M.C., Kawasaki, I., Strome, S., and Muller, F. (1999). Synapsis and chiasma formation in Caenorhabditis elegans require HIM-3, a meiotic chromosome core component that functions in chromosome segregation. Genes Dev *13*, 2258-2270.

Zhang, S., Banerjee, D., and Kuhn, J.R. (2011). Isolation and culture of larval cells from C. elegans. PloS one *6*, e19505.

Zhang, X.M., Huang, G.W., Tian, Z.H., Ren, D.L., and Wilson, J.X. (2009). Folate stimulates ERK1/2 phosphorylation and cell proliferation in fetal neural stem cells. Nutritional neuroscience *12*, 226-232.

Zhao, R., Matherly, L.H., and Goldman, I.D. (2009). Membrane transporters and folate homeostasis: intestinal absorption and transport into systemic compartments and tissues. Expert reviews in molecular medicine *11*, e4.

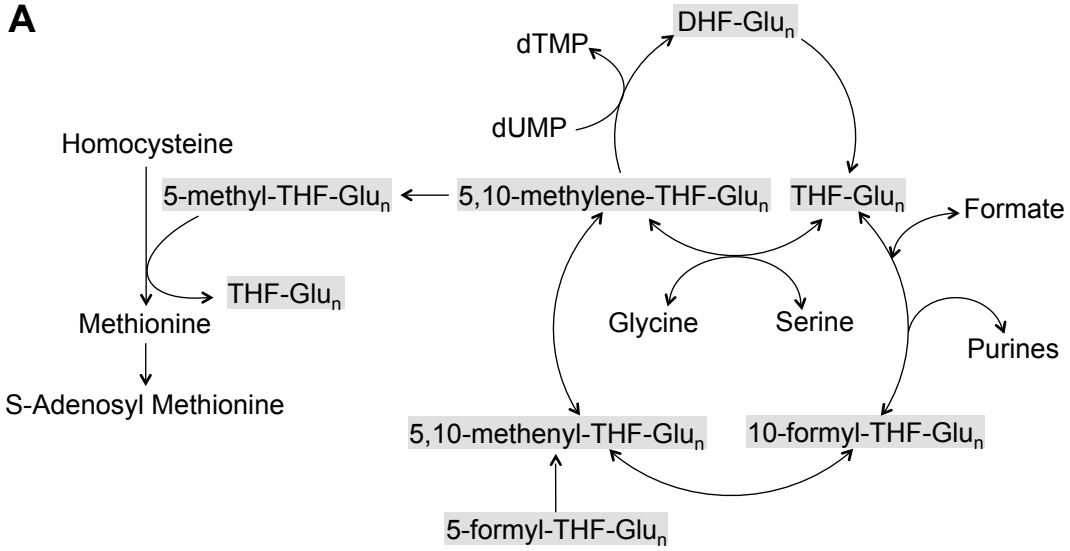
A
DHF-Glu$_n$
dTMP
dUMP
Homocysteine
5-methyl-THF-Glu$_n$
5,10-methylene-THF-Glu$_n$
THF-Glu$_n$
Formate
THF-Glu$_n$
Methionine
Glycine
Serine
Purines
S-Adenosyl Methionine
5,10-methenyl-THF-Glu$_n$
10-formyl-THF-Glu$_n$
5-formyl-THF-Glu$_n$

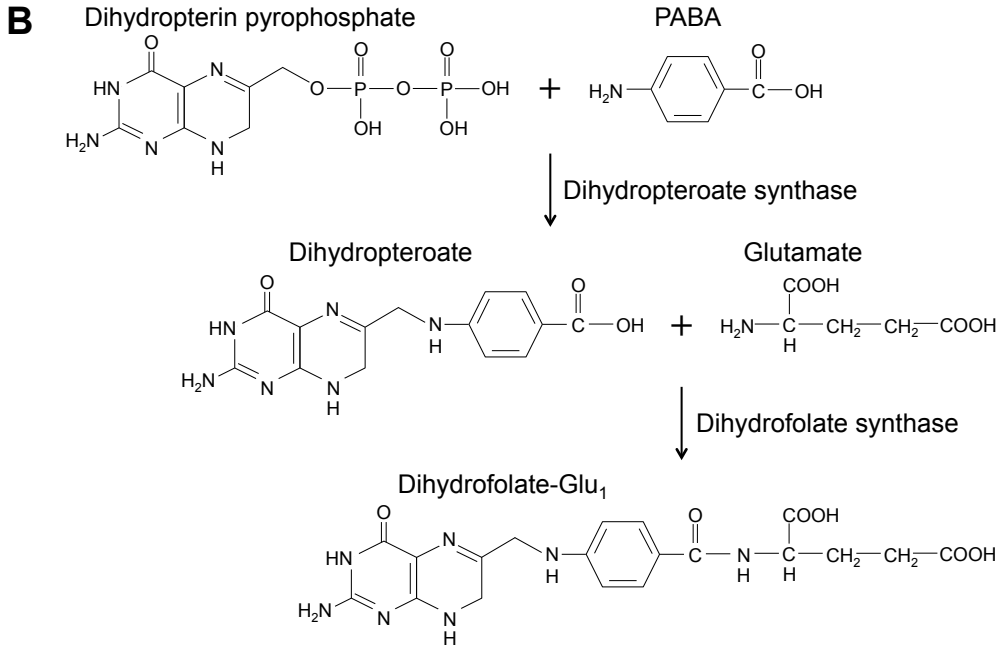
B
Dihydropterin pyrophosphate
PABA
Dihydropteroate synthase
Dihydropteroate
Glutamate
Dihydrofolate synthase
Dihydrofolate-Glu$_1$

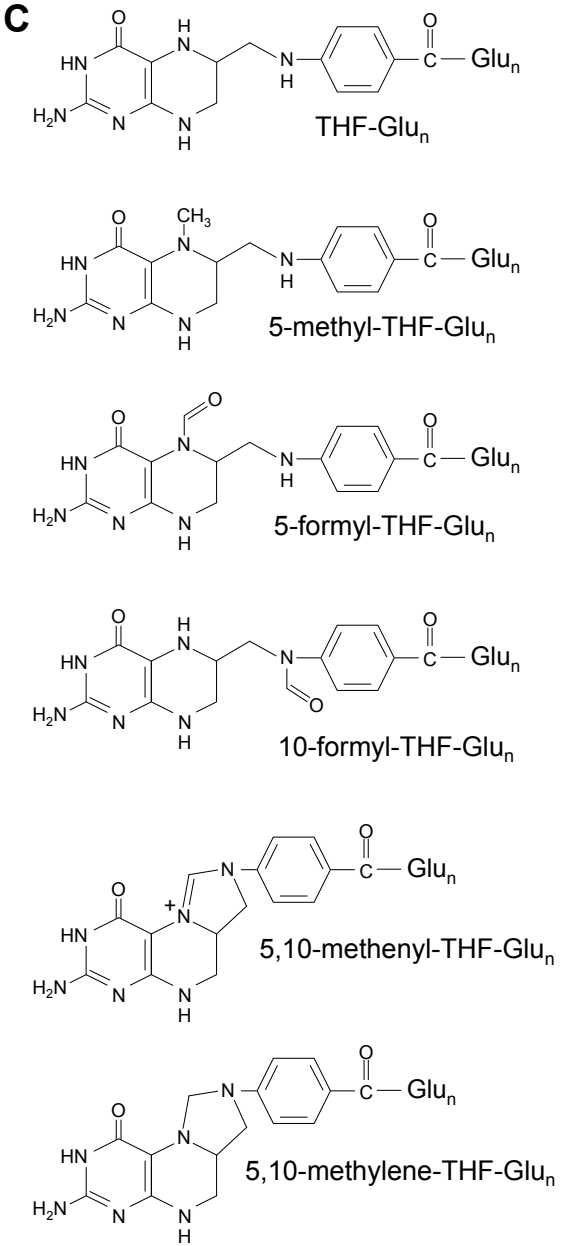
C
THF-Glu$_n$
5-methyl-THF-Glu$_n$
5-formyl-THF-Glu$_n$
10-formyl-THF-Glu$_n$
5,10-methenyl-THF-Glu$_n$
5,10-methylene-THF-Glu$_n$

Figure 3.1 Partial one-carbon metabolism cycle and folate structures.

(A) Diagram of partial one-carbon metabolism cycle; modified from (Zhao and Goldman, 2003).

(B) Schematic of the last stages of folate biosynthesis in bacteria. The enzymatic reactions to create dihydrofolate (DHF) only occur in organisms that are capable of *de novo* folate synthesis.

(C) Structures of one-carbon metabolism folates. The bonds linking the PABA and Glu are shown in-line.

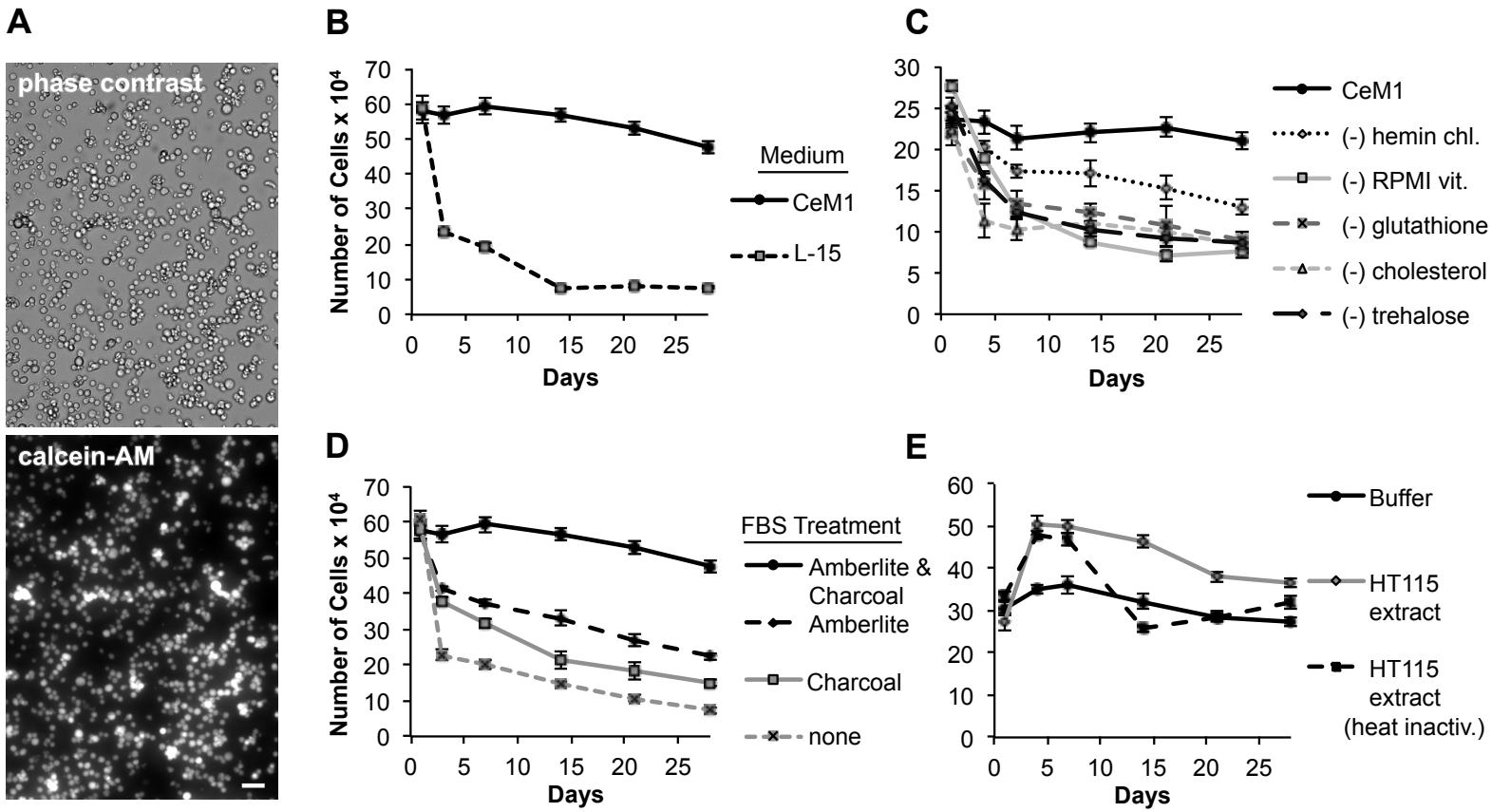
A
phase contrast
calcein-AM
B
Number of Cells x 10⁴
Days
Medium
CeM1
L-15
C
Days
CeM1
(-) hemin chl.
(-) RPMI vit.
(-) glutathione
(-) cholesterol
(-) trehalose
D
Number of Cells x 10⁴
Days
FBS Treatment
Amberlite & Charcoal
Amberlite
Charcoal
none
E
Days
Buffer
HT115 extract
HT115 extract (heat inactiv.)

Figure 3.2 Optimization of *C. elegans* germ cell culture conditions.

(A) Images of *glp-1(gf)*; *cki-2*; *daf-16* germ cells one-day post-isolation in CeM1 medium: phase contrast; and calcein-AM live-cell stain. Scale bar, 20 μm.

(B-E) Live cell counts for *glp-1(gf)*; *cki-2*; *daf-16* germ cells are shown for all panels. (B) CeM1 maintains germ cell viability more effectively than L-15 medium. (C) Germ cell viability decreases when CeM1 lacks the specified components. (D) Pretreatment of FBS with Amberlite IRA 400-CL and charcoal-dextran increases germ cell viability. (E) Bacterial extract (with or without heat inactivation at 60°C for 30 min) promotes initial germ cell proliferation. The same full CeM1 control was analyzed in (B) and (D), and is shown in each panel for comparison.

For all figures, error bars reflect standard error of the mean, SEM. See also Figures 3.S1 and 3.S2, and Table 3.S1.

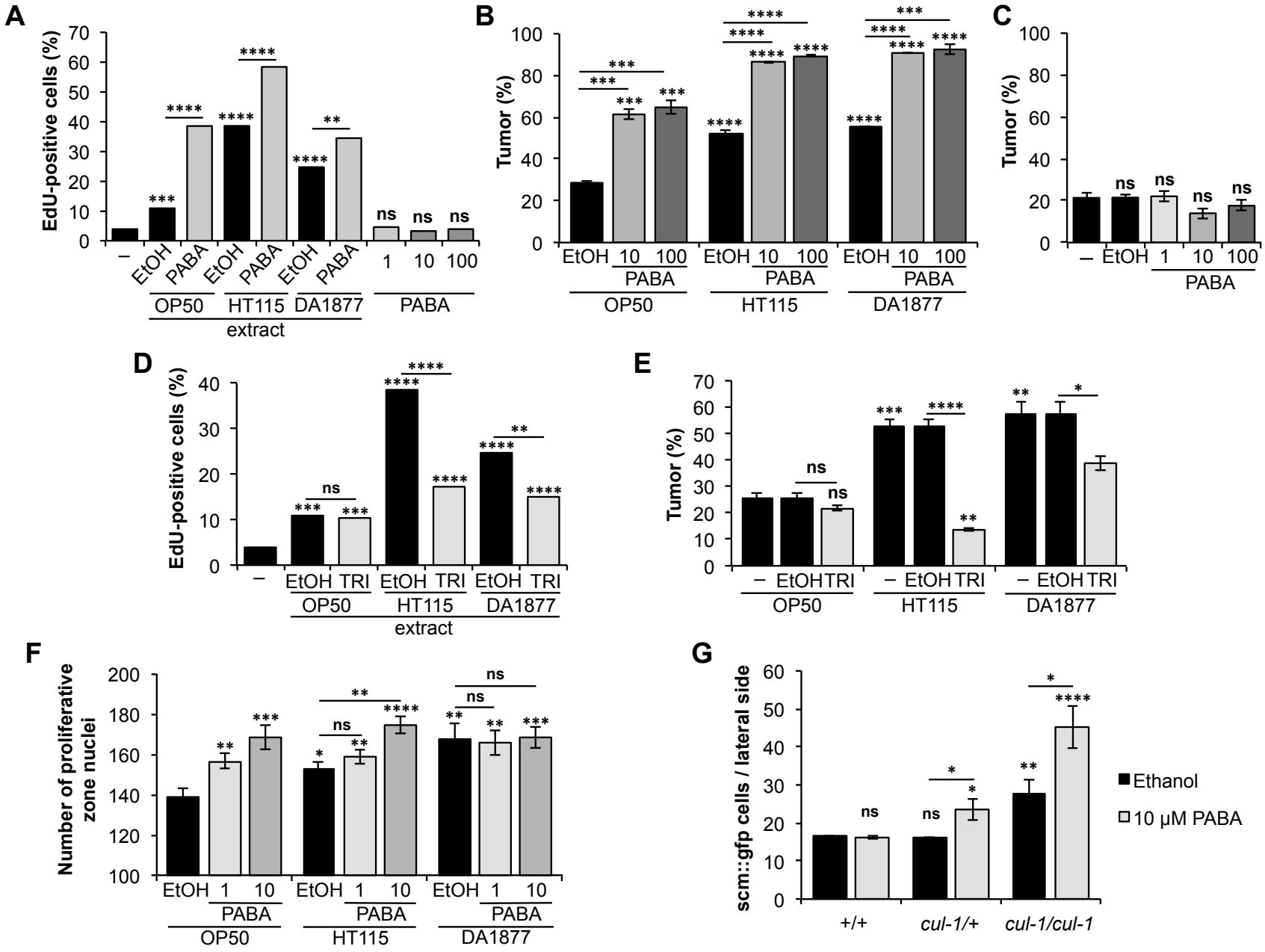
A
EdU-positive cells (%)
–
EtOH
PABA
OP50
HT115
DA1877
extract
1
10
100
ns
B
Tumor (%)
EtOH
10
100
PABA
OP50
HT115
DA1877
C
Tumor (%)
–
EtOH
1
10
100
PABA
D
EdU-positive cells (%)
TRI
E
Tumor (%)
F
Number of proliferative zone nuclei
G
scm::gfp cells / lateral side
Ethanol
10 μM PABA
+/+
cul-1/+
cul-1/cul-1

Figure 3.3 Bacterial folates stimulate germ cell proliferation in vitro and in vivo.

(A) EdU incorporation in isolated germ cells increases when CeM1 is supplemented with extract from bacteria grown with 2.5 mM PABA, but not from adding PABA alone at the indicated concentrations (in μM). Dash indicates buffer control.

(B) The percentages of germline tumors in *glp-1(gf)*; *cki-2*; *daf-16* mutants at 18°C increase on diets of live bacteria grown with PABA compared to ethanol carrier control (EtOH). The concentrations of PABA are in μM (for panels B, C, F).

(C) Tumor frequency with a diet of heat-killed OP50 bacteria supplemented with PABA at 20°C (the higher temperature compensates for the suboptimal diet of heat-killed bacteria). Dash indicates no addition.

(D) EdU incorporation in isolated germ cells using extracts from bacteria treated with the DHFR-inhibitor trimethoprim (TRI). Dash indicates buffer control. The concentration of TRI was 2.5 μg/ml (for panels D and E).

(E) Tumor frequency at 18°C with diets of bacteria treated with TRI. Dash indicates no addition.

(F) The number of germ cell nuclei in the proliferative zone of wild-type hermaphrodite gonads (analyzed 36 hr post-adulthood) when animals were fed diets of the indicated bacteria supplemented with PABA.

(G) The number of cells expressing seam cell marker scm::GFP per lateral side in *cul-1* homozygous and heterozygous mutants fed a diet of OP50 bacteria with or without PABA supplementation.

The same buffer and control bacterial extract samples were analyzed in (A) and (D), and are shown in each panel for comparison. For all figures, asterisks above bars denote statistical significance relative to the control, and asterisks above lines are for comparisons

below the lines: *P<0.05; **P<0.01; ***P<0.001; ****P<0.0001; ns = not significant. Statistics are described in the Experimental Procedures section. See also Figures 3.S3–3.S5.

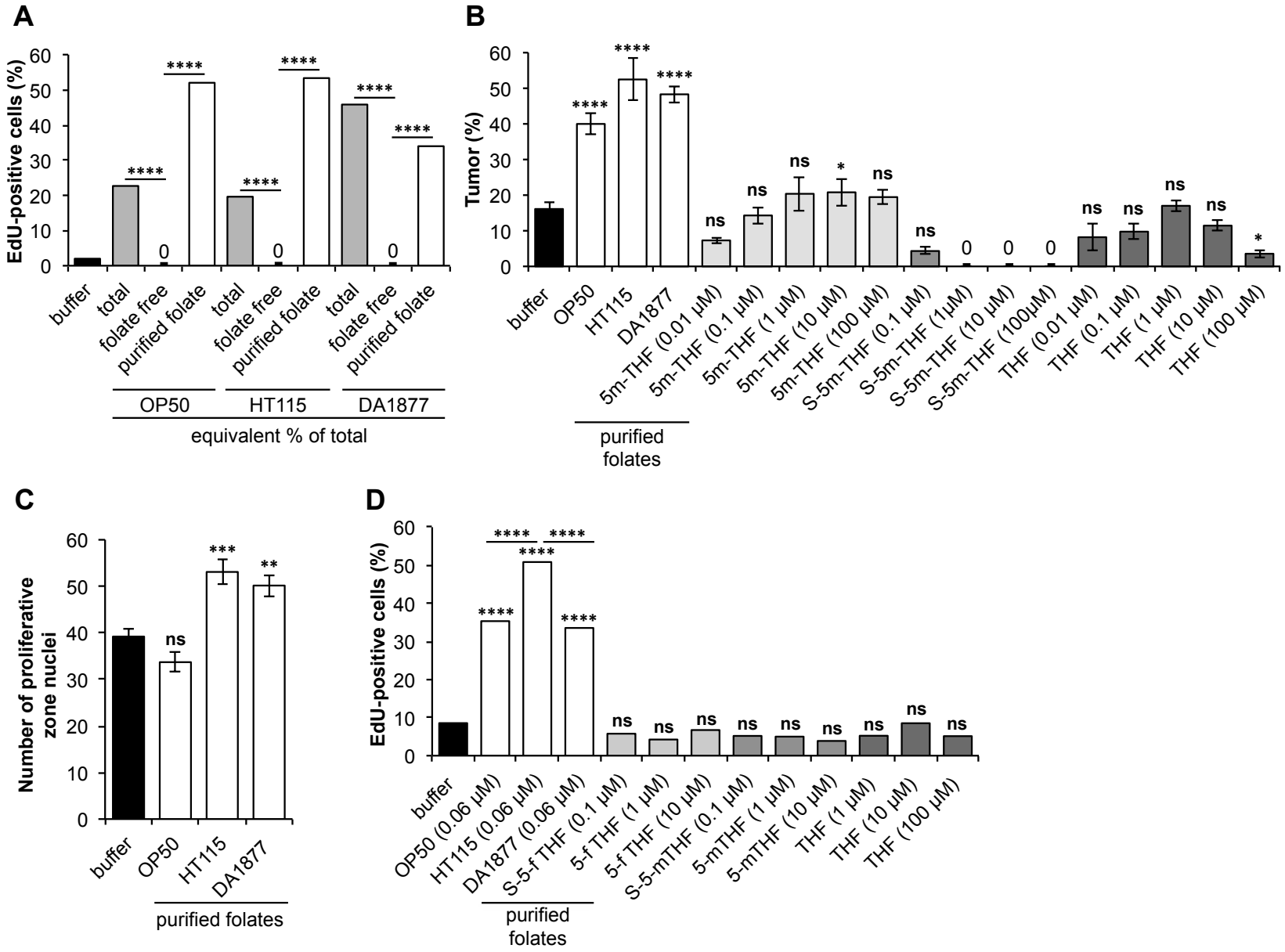
A
EdU-positive cells (%)
buffer
total
folate free
purified folate
OP50
HT115
DA1877
equivalent % of total
B
Tumor (%)
buffer
OP50
HT115
DA1877
5m-THF (0.01 μM)
5m-THF (0.1 μM)
5m-THF (1 μM)
5m-THF (10 μM)
5m-THF (100 μM)
S-5m-THF (0.1 μM)
S-5m-THF (1μM)
S-5m-THF (10 μM)
S-5m-THF (100μM)
THF (0.01 μM)
THF (0.1 μM)
THF (1 μM)
THF (10 μM)
THF (100 μM)
purified folates
C
Number of proliferative zone nuclei
buffer
OP50
HT115
DA1877
purified folates
D
EdU-positive cells (%)
buffer
OP50 (0.06 μM)
HT115 (0.06 μM)
DA1877 (0.06 μM)
S-5-f THF (0.1 μM)
5-f THF (1 μM)
5-f THF (10 μM)
S-5-mTHF (0.1 μM)
5-mTHF (1 μM)
5-mTHF (10 μM)
THF (1 μM)
THF (10 μM)
THF (100 μM)
purified folates

Figure 3.4 Purified folates stimulate germ cell proliferation.

(A) Germ cell stimulatory activity segregates with purified folates during affinity purification. Equal percentages of total bacterial extract; folate-free extract (post-folate purification); or folates purified from the extract were added to isolated germ cells and EdU incorporation was assessed. The concentrations of the purified folates were: 0.063 μM (OP50); 0.038 μM (HT115); and 0.055 μM (DA1877).

(B) The effect of purified folates and the reduced folates shown on tumor frequency at 20°C when added to heat-killed bacteria. Equal volumes of purified folates were used; the concentrations of purified folates for experiments (B) and (C) were: 0.21 μM (OP50); 0.13 μM (HT115); and 0.18 μM (DA1877).

(C) The number of germ cell nuclei in the proliferative zone of wild-type hermaphrodite gonads for animals fed a diet of heat-killed OP50 supplemented with purified folates from the indicated bacteria.

(D) Purified folates from the indicated bacteria stimulate EdU incorporation at 0.06 μM, while the basic reduced folates, 5-methyl-THF (5m-THF), 5-formyl-THF (5f-THF), and THF, are not active at concentrations of 0.1 to 100 μM.

See also Figure 3.S5 and Table 3.S2.

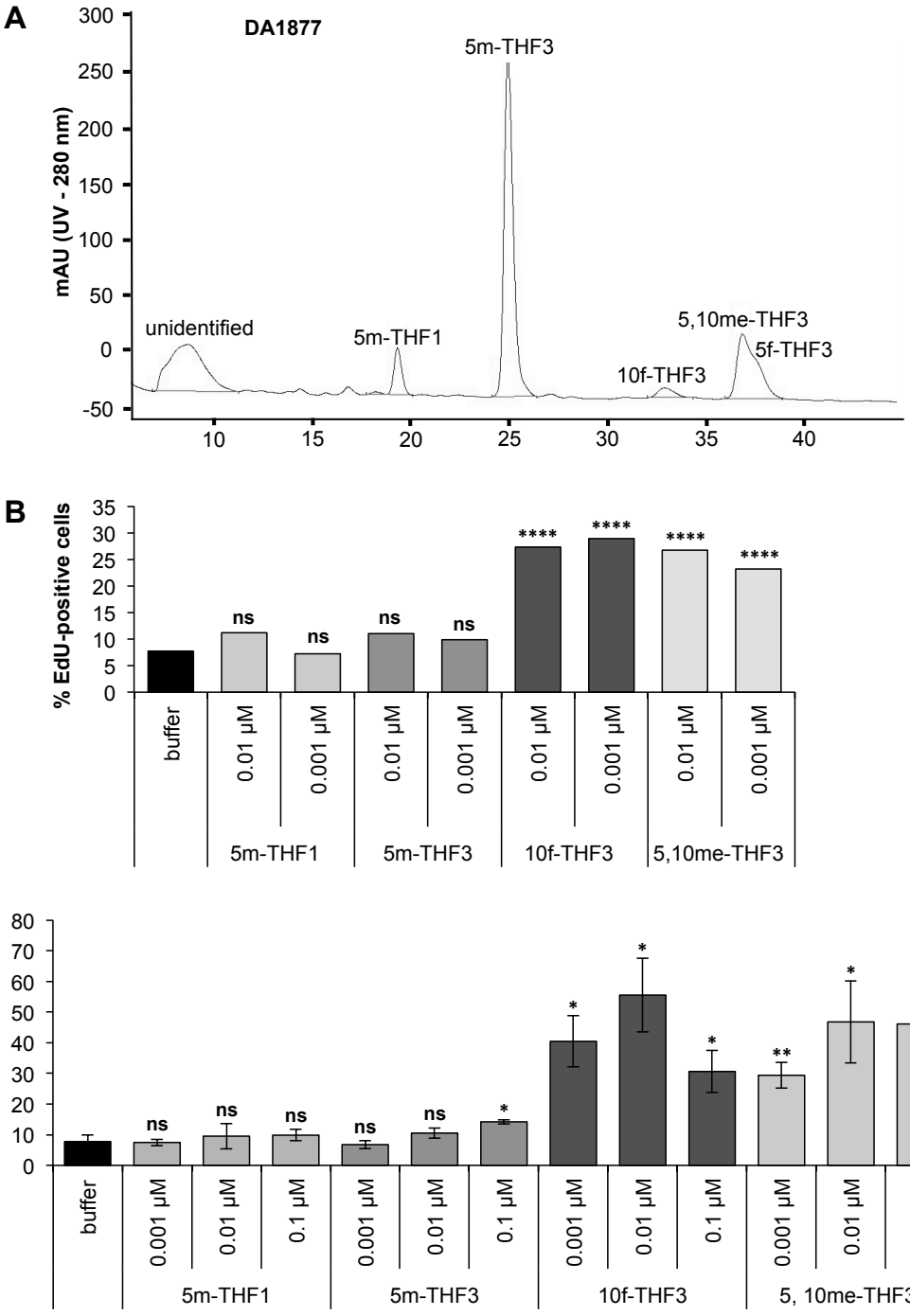
A
DA1877
5m-THF3
mAU (UV - 280 nm)
unidentified
5m-THF1
10f-THF3
5,10me-THF3
5f-THF3
B
% EdU-positive cells
ns
****
buffer
0.01 µM
0.001 µM
5m-THF1
5m-THF3
10f-THF3
5,10me-THF3
C
Tumor (%)
*
**
0.1 µM
5, 10me-THF3

Figure 3.5 10-formyl-THF and 5,10-methenyl-THF isolated from bacteria stimulate germ cells.

(A) Chromatogram showing UV absorbance (milli-absorbance units) of affinity-purified DA1877 folates separated by ion-pair chromatography. Folate species identified by UV spectra are labeled.

(B and C) Affinity-purified folate fractions, containing the indicated folates, were isolated from DA1877 bacteria grown with PABA supplementation and tested for their ability to induce DNA replication (EdU incorporation) in isolated germ cells (B) or increase tumor frequency at 20°C with a diet of heat-killed bacteria (C). 10-formyl-THF (10f-THF); 5,10-methenyl-THF (5,10me-THF). See also Figure 3.S6.

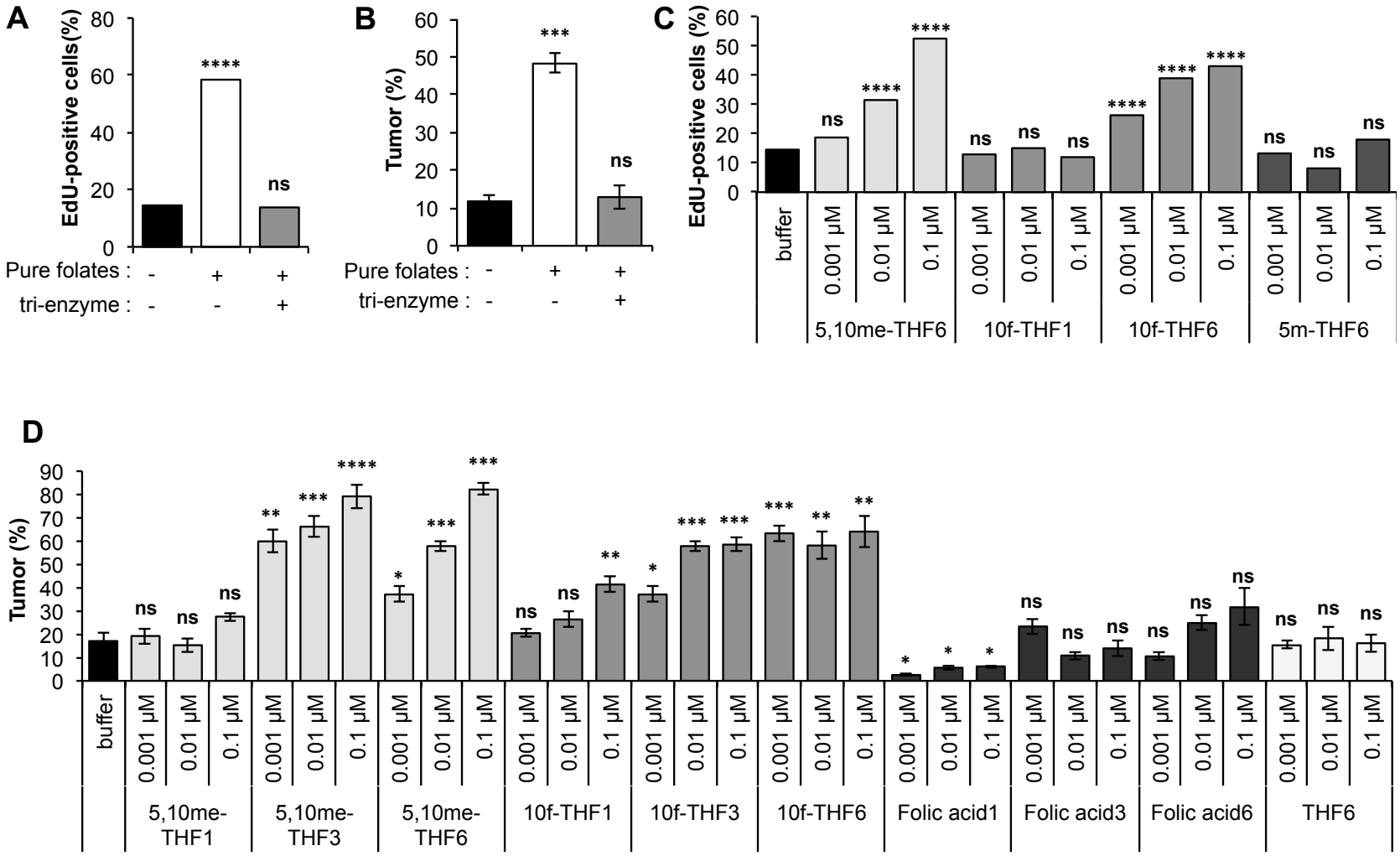
A
EdU-positive cells(%)
Pure folates :
tri-enzyme :
B
Tumor (%)
Pure folates :
tri-enzyme :
C
EdU-positive cells (%)
buffer
5,10me-THF6
10f-THF1
10f-THF6
5m-THF6
D
Tumor (%)
buffer
5,10me-THF1
5,10me-THF3
5,10me-THF6
10f-THF1
10f-THF3
10f-THF6
Folic acid1
Folic acid3
Folic acid6
THF6

Figure 3.6 Poly-glutamate increases 10-formyl-THF-Glu$_n$ germ cell stimulatory activity. (A and B) Purified folates from OP50 were treated with tri-enzyme to convert poly-Glu folates to mono-Glu folates. Germ cell stimulatory activity was assessed by analyzing EdU incorporation in isolated germ cells (A) and tumor frequency at 20°C with a diet of heat-killed bacteria (B). The concentration of purified folates was 0.06 μM for (A) and 0.12 μM for (B).

(C and D) Comparison of the activity of synthetic folates with 1, 3, 6 Glu residues in the EdU incorporation assay with isolated germ cells (C) and tumor frequency assay at 18°C (D).

See also Figure 3.S5.

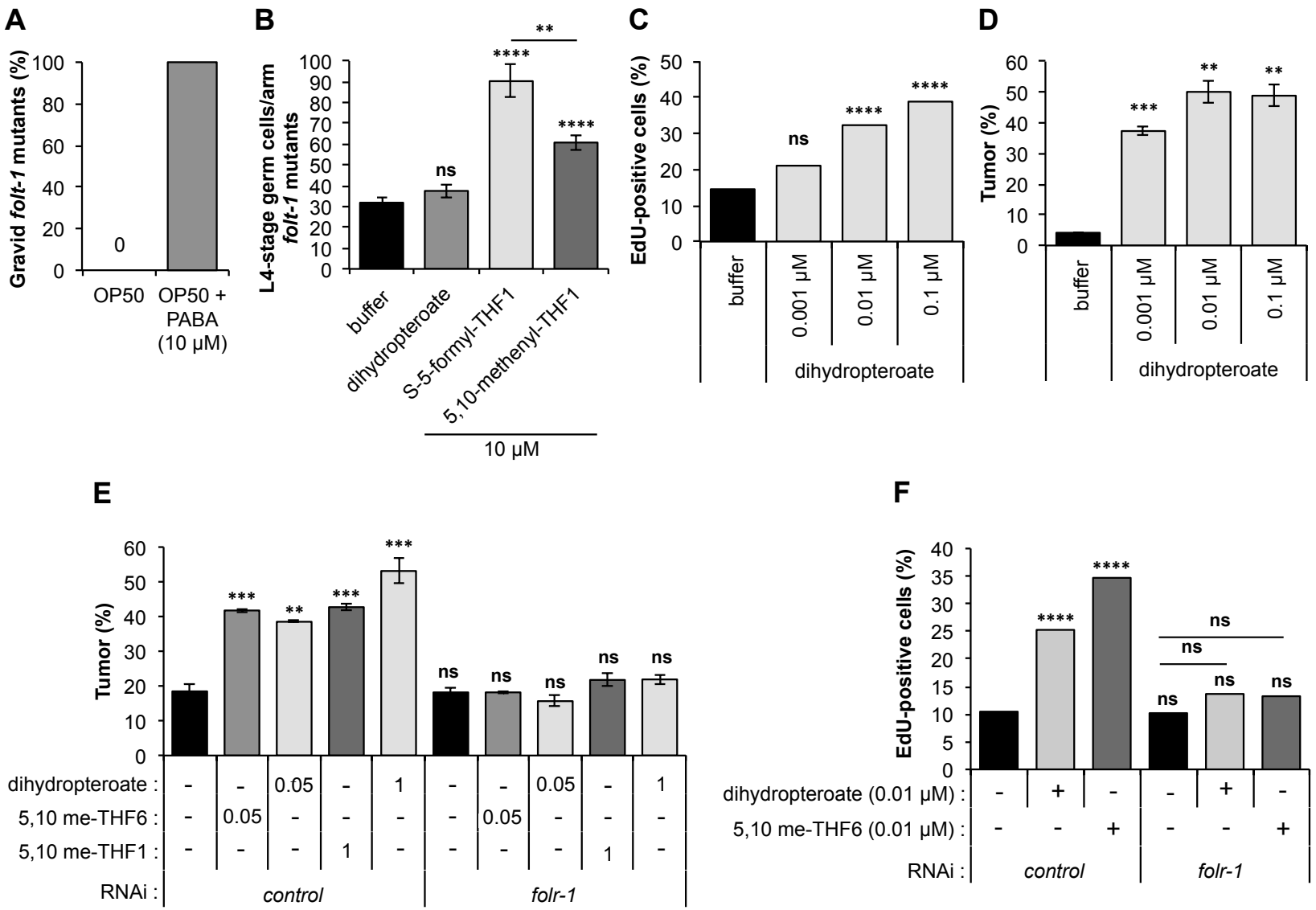
A
Gravid folt-1 mutants (%)
100
80
60
40
20
0
0
OP50
OP50 + PABA (10 µM)
B
L4-stage germ cells/arm folt-1 mutants
100
90
80
70
60
50
40
30
20
10
0
ns
****
****
**
buffer
dihydropteroate
S-5-formyl-THF1
5,10-methenyl-THF1
10 µM
C
EdU-positive cells (%)
50
40
30
20
10
0
ns
****
****
buffer
0.001 µM
0.01 µM
0.1 µM
dihydropteroate
D
Tumor (%)
60
50
40
30
20
10
0
***
**
**
buffer
0.001 µM
0.01 µM
0.1 µM
dihydropteroate
E
Tumor (%)
60
50
40
30
20
10
0
***
***
**
***
***
ns
ns
ns
ns
ns
dihydropteroate : - - 0.05 - 1 - - 0.05 - 1
5,10 me-THF6 : - 0.05 - - - - 0.05 - - -
5,10 me-THF1 : - - - 1 - - - - 1 -
RNAi : control folr-1
F
EdU-positive cells (%)
40
35
30
25
20
15
10
5
0
****
****
ns
ns
ns
ns
ns
dihydropteroate (0.01 µM) : - + - - + -
5,10 me-THF6 (0.01 µM) : - - + - - +
RNAi : control folr-1

Figure 3.7. Folates and pteroates stimulate germ cell proliferation independently of a role as vitamins. (A) *folt-1(ok1467)* mutant sterility is rescued by growth on OP50 supplemented with PABA. The percentage of gravid animals is shown (n = 20 each).

(B) Stimulatory and non-stimulatory folates can rescue folate deficiency, but dihydropteroate cannot. *folt-1(ok1467)* mutants were fed heat-killed, folate-depleted *pabC* mutant bacteria with the indicated folates or folate-related compounds (10 μM). Germ cell numbers per gonad arm from mid/late L4-stage larvae were scored blindly.

(C and D) Dihydropteroate stimulates EdU incorporation in isolated germ cells (C) and tumor frequency at 18°C (D). For (C), the experiment was performed at the same time as Fig. 3.6C, and the same control is shown for comparison.

(E) *folr-1*/FR RNAi blocks the stimulatory effect of dihydropteroate, 5,10-methenyl-THF_6, and 5,10-methenyl-THF_1 on tumor frequency at 18°C. The concentrations are in μM.

(F) *folr-1*/FR RNAi blocks the stimulatory effect of dihydropteroate and 5,10-methenyl-THF-Glu_6 on EdU incorporation in isolated germ cells.

See also Figure 3.S7.

Supplemental Figures

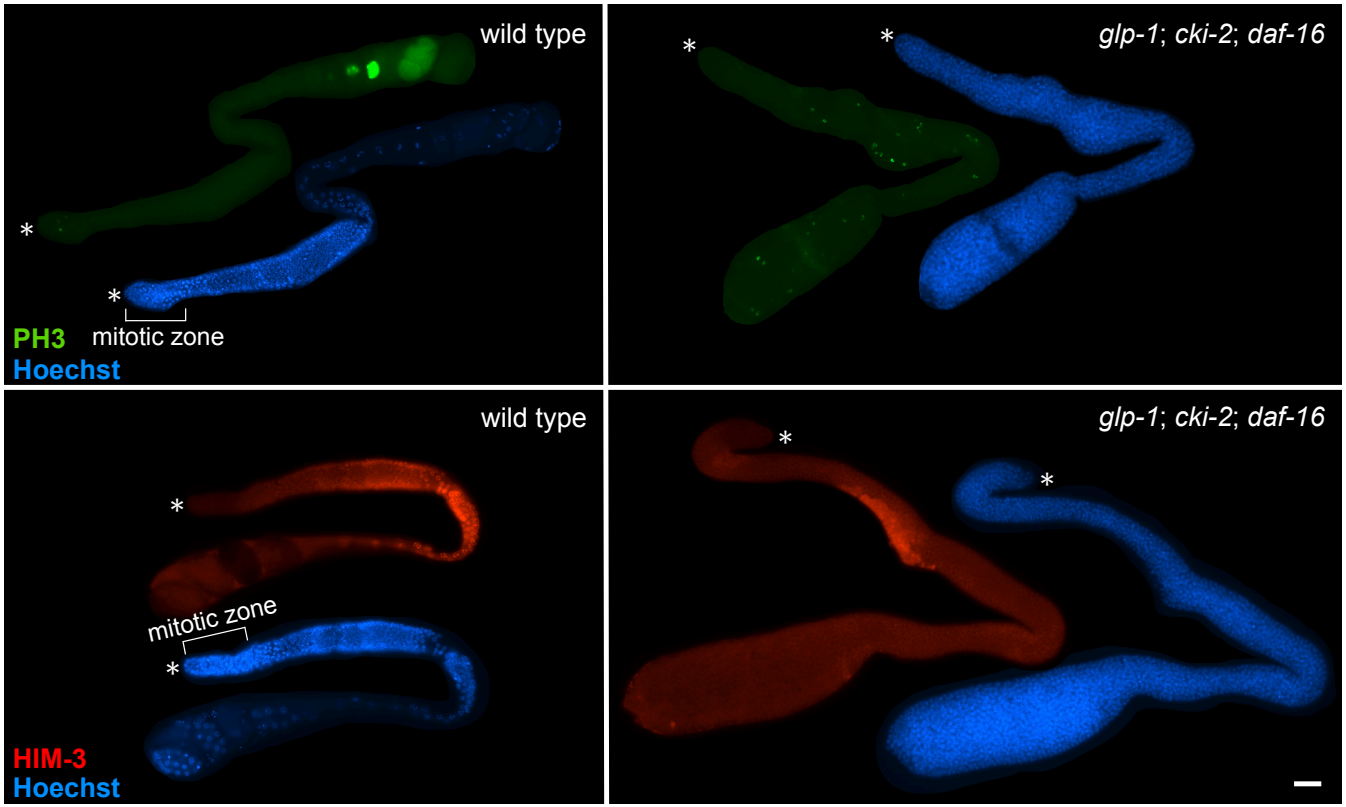

Figure 3.S1, related to Figure 3.2A. Tumorous gonads from *glp-1(gf)*; *cki-2*; *daf-16* mutants. Images of *glp-1(gf)*; *cki-2*; *daf-16* and wild-type dissected gonads stained with the mitotic marker anti-phosphohistone H3 (Ser10) antibody (green, top), the meiotic marker anti-HIM-3 antibody (red, bottom), and Hoechst 33342 DNA stain (blue). Image z-sections were merged for the anti-phosphohistone H3 staining to show mitotic cells throughout the gonad. Asterisks mark the distal end of the gonad. Scale bar, 20 μm.

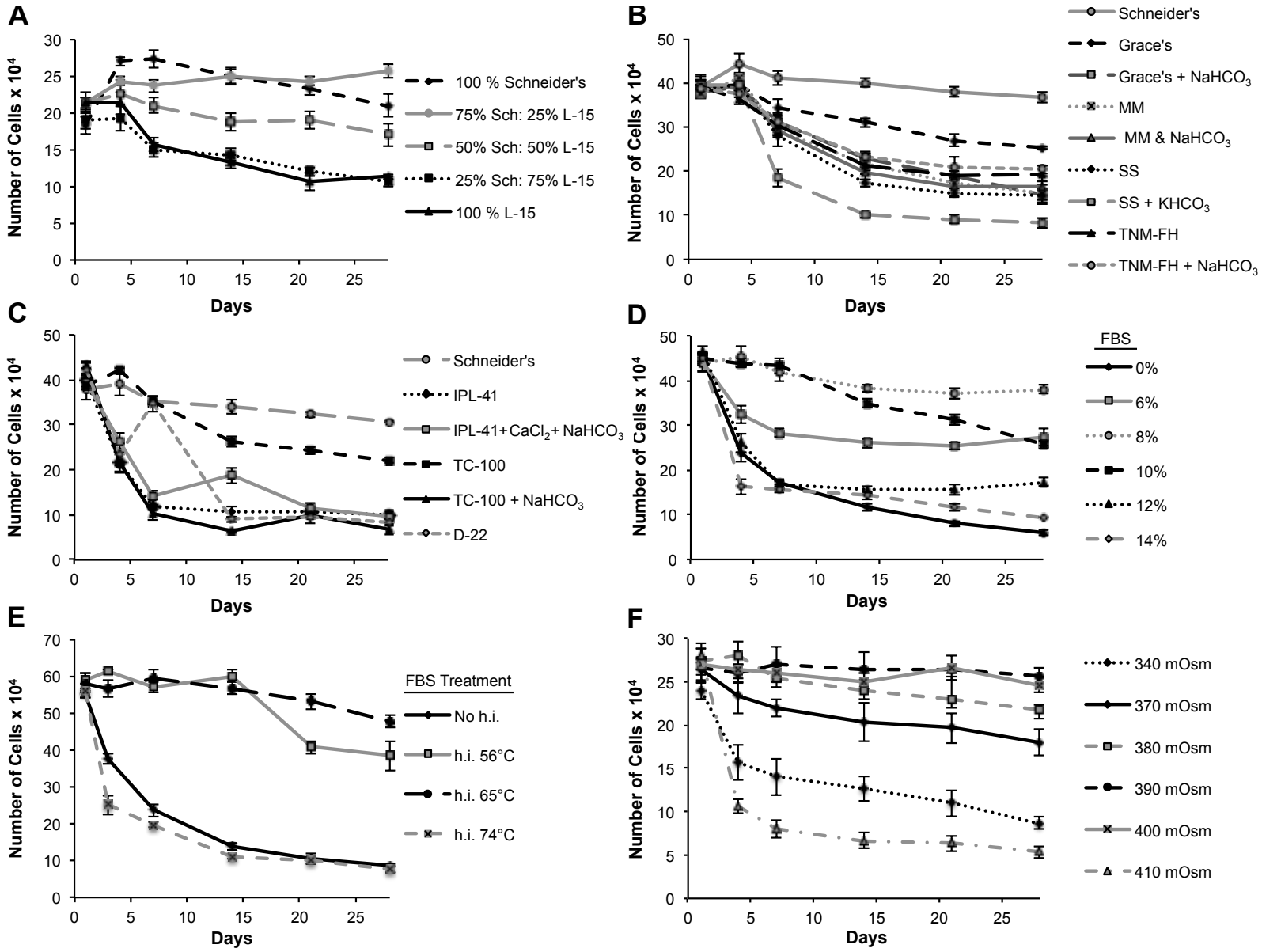
A
Number of Cells x 10⁴
Days
100 % Schneider's
75% Sch: 25% L-15
50% Sch: 50% L-15
25% Sch: 75% L-15
100 % L-15
B
Number of Cells x 10⁴
Days
Schneider's
Grace's
Grace's + NaHCO3
MM
MM & NaHCO3
SS
SS + KHCO3
TNM-FH
TNM-FH + NaHCO3
C
Number of Cells x 10⁴
Days
Schneider's
IPL-41
IPL-41+CaCl2+ NaHCO3
TC-100
TC-100 + NaHCO3
D-22
D
Number of Cells x 10⁴
Days
FBS
0%
6%
8%
10%
12%
14%
E
Number of Cells x 10⁴
Days
FBS Treatment
No h.i.
h.i. 56°C
h.i. 65°C
h.i. 74°C
F
Number of Cells x 10⁴
Days
340 mOsm
370 mOsm
380 mOsm
390 mOsm
400 mOsm
410 mOsm

Figure 3.S2, related to Figure 3.2B-E. Comparison of media components for germ cell culture. (A-F) Live germ cell counts for cultures with: (A) different ratios of Schneider's insect medium and L-15 medium; (B and C) different base insect media (MM, Mitsuhashi and Maramorosch medium; SS, Shields and Sang medium); (D) CeM1 prepared with different FBS concentrations; (E) CeM1 prepared with FBS that was heat inactivated at different temperatures for 30 min, or no heat inactivation. The 65°C heat-inactivated FBS sample is the complete CeM1 medium, and this sample was analyzed at the same time as the experiments shown in Fig. 2B and 2D; the curve is shown here for comparison. (F) CeM1 media adjusted to different osmolalities.

A

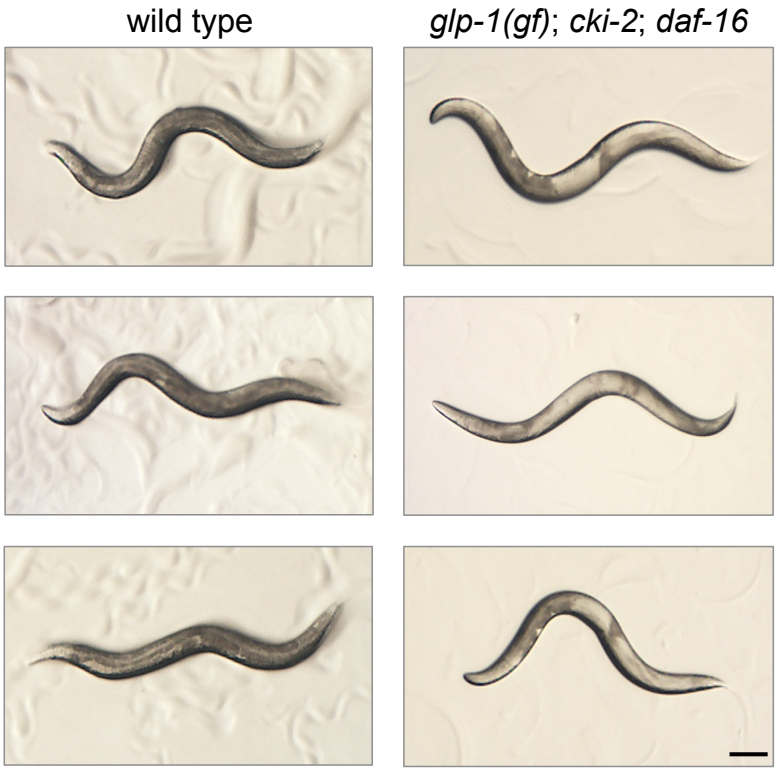
wild type
glp-1(gf); cki-2; daf-16

B

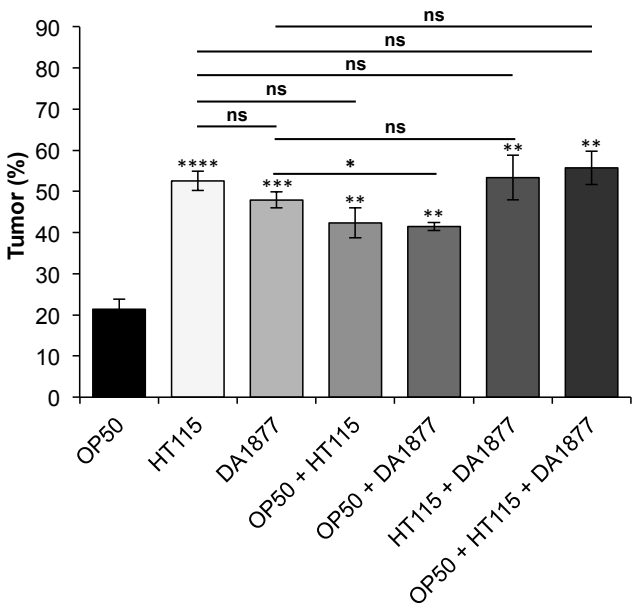
Tumor (%)
90
80
70
60
50
40
30
20
10
0
ns
ns
ns
ns
ns
ns
*
****
***
**
**
**
**
OP50
HT115
DA1877
OP50 + HT115
OP50 + DA1877
HT115 + DA1877
OP50 + HT115 + DA1877

Figure 3.S3, related to Figure 3.3. Images of germline tumors and the lack of synergistic effects from mixing bacterial diets on tumor frequency. (A) Bottom-illuminated stereomicroscope images of three wild-type adult hermaphrodites with no tumors and three *glp-1(gf)*; *cki-2*; *daf-16* adult hermaphrodite mutants exhibiting tumors that are visible as white regions within the body. Scale bar, 100 μm. (B) Tumor frequency of *glp-1(gf)*; *cki-2*; *daf-16* mutants grown at 18°C and fed diets of the indicated live bacteria, or 1:1 or 1:1:1 mixtures of live bacteria.

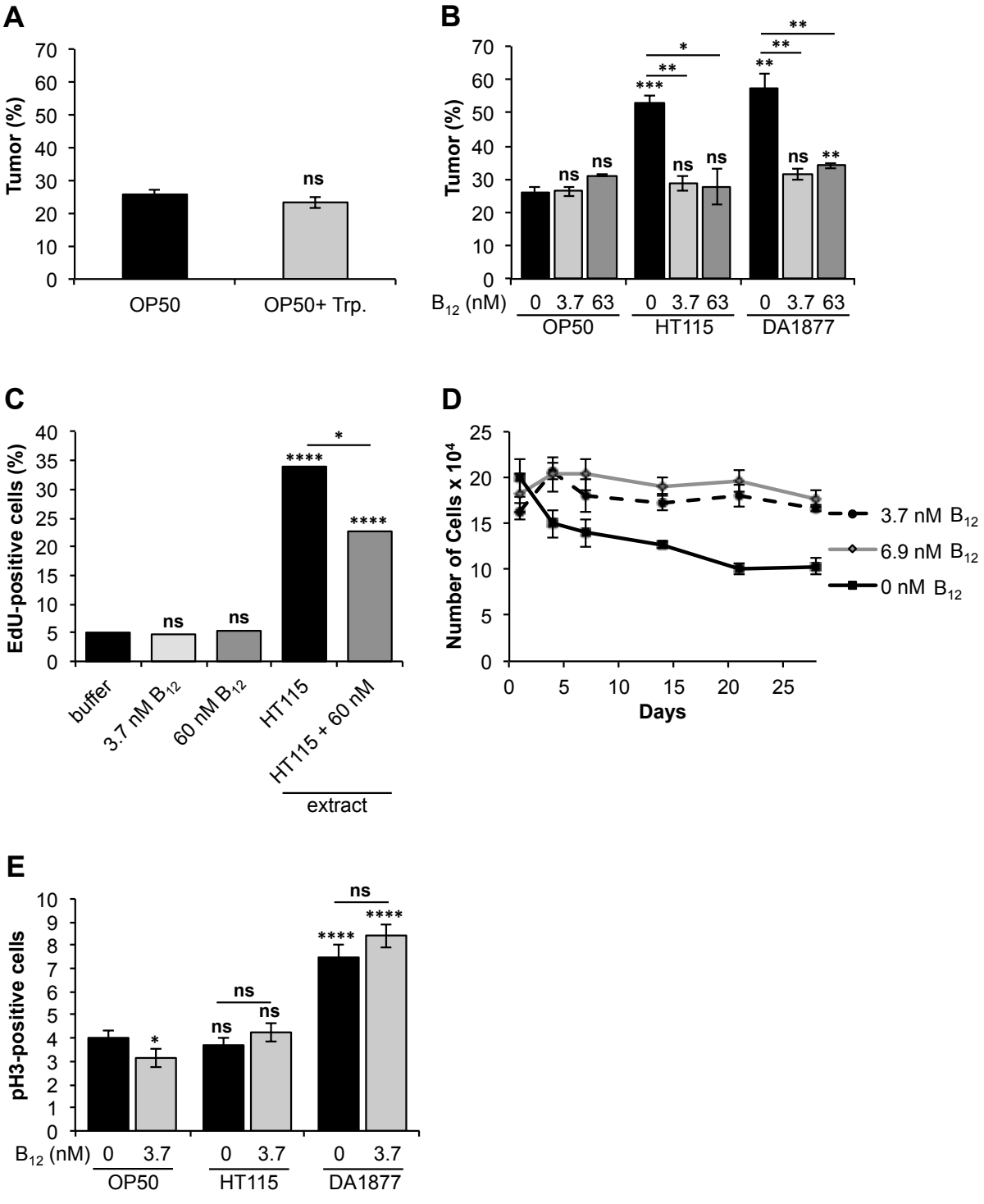
A
Tumor (%)
ns
OP50
OP50+ Trp.
B
Tumor (%)
B12 (nM) 0 3.7 63 0 3.7 63 0 3.7 63
OP50
HT115
DA1877
C
EdU-positive cells (%)
buffer
3.7 nM B12
60 nM B12
HT115
HT115 + 60 nM
extract
D
Number of Cells x 10^4
Days
3.7 nM B12
6.9 nM B12
0 nM B12
E
pH3-positive cells
B12 (nM) 0 3.7 0 3.7 0 3.7
OP50
HT115
DA1877

Figure 3.S4, related to Figure 3.3. Increased supplementation with tryptophan or vitamin B12 does not increase germ cell proliferation. (A and B) Tumor frequencies for *glp-1(gf)*; *cki-2*; *daf-16* mutants grown at 18°C on a diet of OP50 with or without 0.15 mM tryptophan (A); or in different concentrations of vitamin B12 with the indicated bacteria (B). (C) The percentage of isolated germ cells that incorporated EdU into genomic DNA 24-48 hr post-isolation when supplemented with the indicated amount of vitamin B12 and HT115 bacterial extract. (D) Counts of live germ cells cultured with CeM1 containing the following concentrations of vitamin B12: 3.7 nM (the normal CeM1 medium); 6.9 nM; or 0 nM. (E) The number of mitotic phosphohistone H3 Ser10-positive cells per gonad arm for wild-type adults grown on a diet of the bacterial strains listed with the indicated concentrations of vitamin B12. These results suggest that the concentration of vitamin B12 in CeM1 medium is sufficient to maintain cell viability, and that increased levels of vitamin B12 or tryptophan metabolites do not stimulate germ cell proliferation.

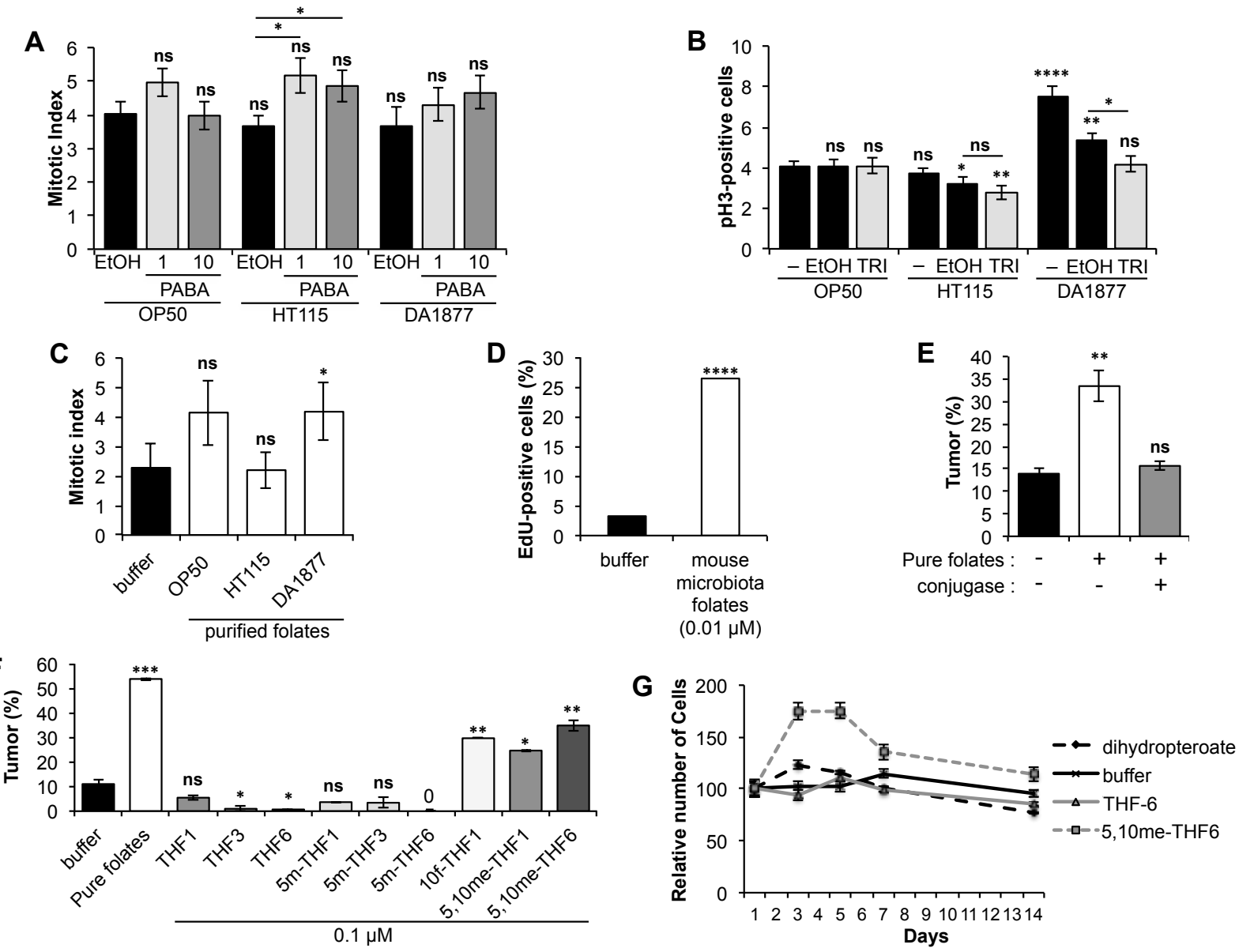
A
Mitotic Index
EtOH 1 10 EtOH 1 10 EtOH 1 10
PABA PABA PABA
OP50 HT115 DA1877
B
pH3-positive cells
– EtOH TRI – EtOH TRI – EtOH TRI
OP50 HT115 DA1877
C
Mitotic index
buffer OP50 HT115 DA1877
purified folates
D
EdU-positive cells (%)
buffer
mouse microbiota folates (0.01 µM)
E
Tumor (%)
Pure folates : - + +
conjugase : - - +
F
Tumor (%)
buffer Pure folates THF1 THF3 THF6 5m-THF1 5m-THF3 5m-THF6 10f-THF1 5,10me-THF1 5,10me-THF6
0.1 µM
G
Relative number of Cells
Days
dihydropteroate
buffer
THF-6
5,10me-THF6

Figure 3.S5, related to Figures 3.3, 3.4, and 3.6. Wild-type germ cell proliferation is increased by bacterial folates; poly-Glu increases folate stimulatory activity; and 5,10-methenyl-THF-Glu_n stimulates germ cell proliferation. (A,C) Mitotic index of wild-type hermaphrodite proliferative zone germ cells fed a diet of the indicated bacteria supplemented with PABA at the indicated concentrations in μM or ethanol control (EtOH) (A), or purified folates at 0.21 μM (OP50), 0.13 μM (HT115), and 0.18 μM (DA1877) (C). (B) The number of mitotic, phosphohistone H3-positive germ cells per gonad arm in wild-type adult hermaphrodite fed a diet of live bacteria supplemented with 2.5 μg/ml TRI or ethanol control. (D) Purified folates (0.01 μM) from a mouse microbiota increase EdU incorporation in isolated germ cells. (E) Tumor frequencies at 20°C on heat-killed bacteria supplemented with DA1877 purified folates (0.043 μM) treated with or without conjugase. (F) Tumor frequencies with the indicated synthetic folates (0.1 μM) or purified folates from OP50 bacteria (0.21 μM) on a diet of heat-killed bacteria at 20°C. (G) 5,10-methenyl-THF-Glu_6 supports initial germ cell proliferation in vitro. Numbers of live isolated germ cells supplemented with 0.1 μM of the indicated supplements. The graph is the average of two experiments; cell numbers are set to 100 on day 1.

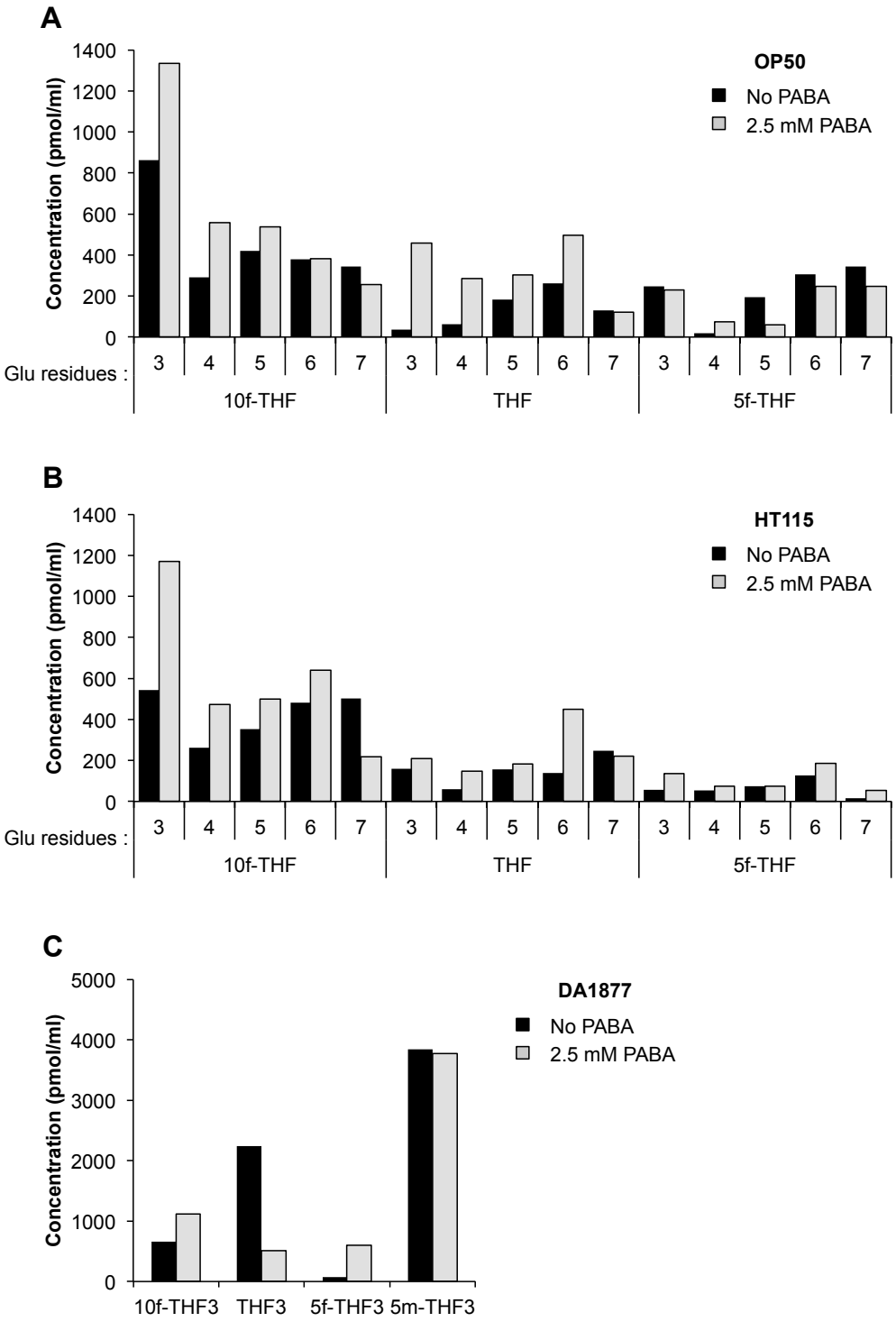
A
OP50
No PABA
2.5 mM PABA
Concentration (pmol/ml)
1400
1200
1000
800
600
400
200
0
Glu residues :
3 4 5 6 7 3 4 5 6 7 3 4 5 6 7
10f-THF
THF
5f-THF
B
HT115
No PABA
2.5 mM PABA
Concentration (pmol/ml)
1400
1200
1000
800
600
400
200
0
Glu residues :
3 4 5 6 7 3 4 5 6 7 3 4 5 6 7
10f-THF
THF
5f-THF
C
DA1877
No PABA
2.5 mM PABA
Concentration (pmol/ml)
5000
4000
3000
2000
1000
0
10f-THF3
THF3
5f-THF3
5m-THF3

Figure 3.S6, related to Figure 3.5. 10-formyl-THF-Glu$_n$ is increased upon supplementing bacteria with PABA. (Flatt et al.) Graph of folate species identified by affinity chromatography with detection by UV absorption spectra for OP50 (A), HT115 (B), and DA1877 (C) bacterial strains grown with or without PABA supplementation.

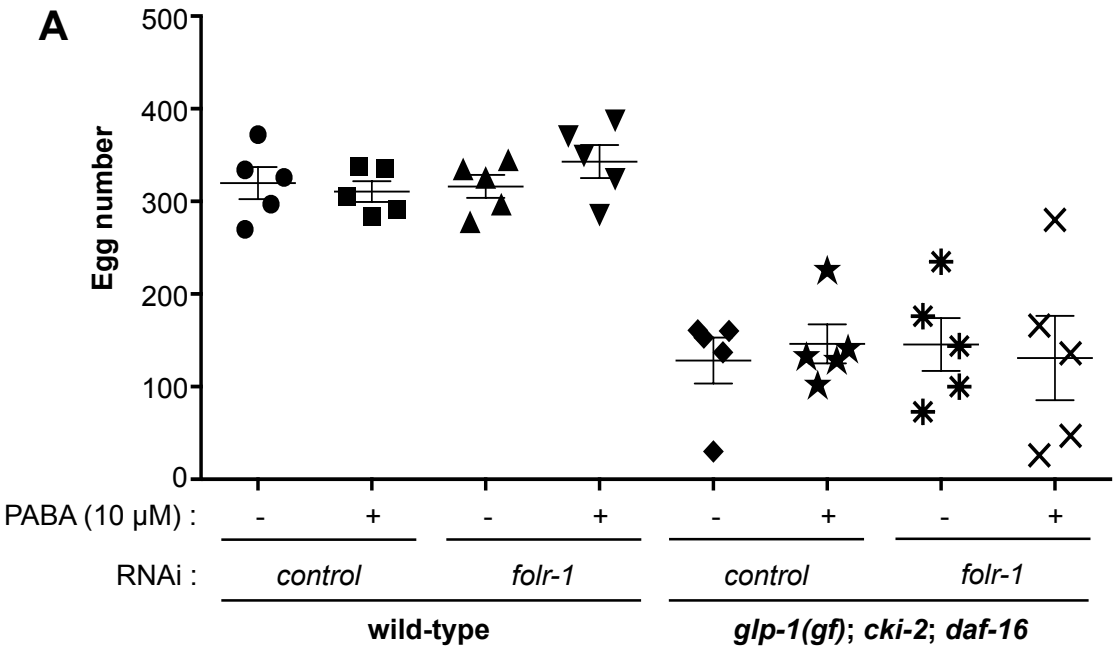
A
Egg number
500
400
300
200
100
0
PABA (10 μM) :
- + - + - + - +
RNAi :
control
folr-1
control
folr-1
wild-type
glp-1(gf); cki-2; daf-16

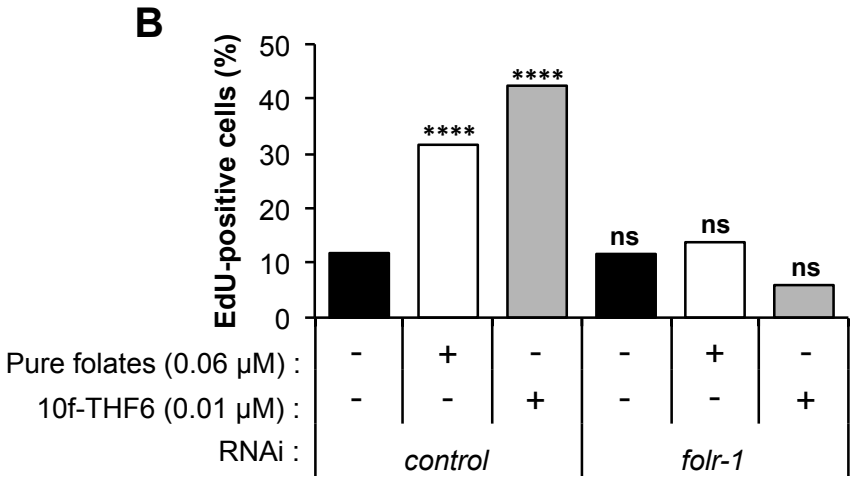
B
EdU-positive cells (%)
50
40
30
20
10
0
****
****
ns
ns
ns
Pure folates (0.06 μM) :
10f-THF6 (0.01 μM) :
RNAi :
control
folr-1

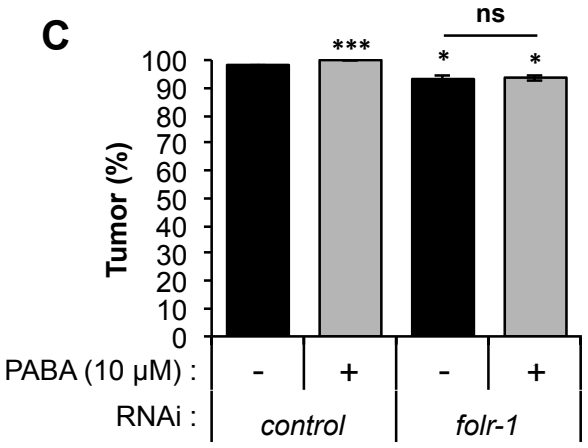
C
Tumor (%)
100
90
80
70
60
50
40
30
20
10
0
***
ns
*
*
PABA (10 μM) :
RNAi :
control
folr-1

Figure 3.S7, related to Figure 3.7. *folr-1*/FR RNAi does not affect egg number but blocks the stimulatory effect of PABA supplementation of OP50 at the fully non-permissive temperature. (A) *folr-1*/FR RNAi and control RNAi gives comparable numbers of eggs for wild type and *glp-1(gf)*; *cki-2*; *daf-16* mutants grown at 18°C. Note that *glp-1(gf)*; *cki-2*; *daf-16* mutants have lower egg numbers due to the inhibition of egg formation by tumors at the semi-permissive temperature. Within each genotype, no pairwise comparison is statistically significant. (B) *folr-1*/FR RNAi blocks the stimulatory effect of 10-formyl-THF-Glu_6 and purified bacterial folates on EdU incorporation in isolated germ cells. (C) Tumor frequency of *glp-1(gf)*; *cki-2*; *daf-16* mutants grown on live HT115 bacteria expressing control RNAi or *folr-1*/FR RNAi constructs with or without 10 μM PABA supplementation at 25°C.

Table 3.S1, related to Figure 3.2. CeM1 medium components.

Component (attribute)	CeM1 medium	L-15 medium
Schneider's Insect medium (Life Technologies, 21720-024)	67.2%	–
Leibovitz's L-15 medium without phenol red (Life Technologies, 21083-027)	22.4%	90%
Fetal Bovine Serum (lot G11012, Atlanta Biologicals, Inc.)	8% (heat-inactivated; treat Amberlite IRA-400 & charcoal dextran)	10%
penicillin–streptomycin (Sigma-Aldrich, P4333)	1x	1x
hemin chloride[a] (MP Biomedicals, 0219402501)	0.2%	–
RPMI vitamins (Sigma-Aldrich, R7256)	1%	–
L-glutathione, reduced (Sigma-Aldrich, G4251)	0.6 mg/ml	–
normocin (InvivoGen)	0.1%	–
cholesterol[b] (J.T. Baker, 1580-01)	0.1%	–
trehalose[c] (Sigma-Aldrich, T0167)	to 390 mOsm/kg	–
(pH)[d]	NaOH added to pH 6.5	~pH 7.2
sucrose	–	to 340 mOsm/kg

[a]Hemin chloride was added from a 2 mM stock solution freshly prepared in 0.1 N NaOH.

[b]Cholesterol was added from a 10 mg/ml stock solution in ethanol.

[c]The medium was adjusted to 390 mOsm/kg by adding trehalose using a freezing point osmometer for osmolality measurements (Advanced Digimatic Osmometer 3DII from Advanced Instruments Inc.).

[d]The medium was adjusted to pH 6.5, using NaOH.

Table 3.S2, related to Figure 3.4A. Affinity purification and quantification of bacterial folates.

Sample	Total folate (no conjugase) (µg folate/g lyoph. bact.)	Total folate (post conjugase) (µg folate/g lyoph. bact.)	Percent recovery of purified folates (post conjugase)[a]
OP50 bacterial extract	19.9	49.8	
HT115 bacterial extract	5.9	19.6	
DA1877 bacterial extract	42.2	98.7	
OP50 purified folates	12.4	55.5	111%
HT115 purified folates	2.9	33.2	169%
DA1877 purified folates	29.7	54.6	55%
OP50 folate-free extract	undetectable	undetectable	
HT115 folate-free extract	undetectable	undetectable	
DA1877 folate-free extract	undetectable	undetectable	

[a]The percent recovery can be over-estimated if the post-purification folates are better able to stimulate growth in the microbial folate assay that is used to determine concentration.

Supplemental Experimental Procedures

Treatment of FBS prior to inclusion in CeM1 medium

Three sequential treatments were performed on FBS prior to its inclusion in CeM1 medium. FBS was heat inactivated by incubation at 56°C or 65°C for 30 minutes. The FBS was then incubated with 50 mg/ml of the strongly basic resin Amberlite IRA 400-CL (Sigma-Aldrich, 247669) that had been prewashed in water, on a rotator for 4-6 hours at room temperature. The FBS was separated from the beads by centrifugation, transferred to a fresh tube, and incubated with a second round of 50 mg/ml Amberlite IRA 400-CL beads overnight at 4°C. After separating the FBS from the Amberlite IRA 400-CL beads, the FBS was rotated with 100 mg/ml charcoal-dextran (Sigma-Aldrich, C6241) overnight at 4°C. The charcoal-dextran was removed by two sequential centrifugations at 3500 rpm for 30 min, 4°C. For all experiments, unless otherwise specified, FBS was heat-inactivated and treated with Amberlite IRA 400-CL and charcoal-dextran. We have observed differences in the performance of FBS lots, similar to what is observed in the cell culture of many other species (data not shown).

C. elegans and bacterial strains

The following *C. elegans* strains were used: wild type (N2), *glp-1(ar202)* (GC143); *glp-1(ar202)*; *cki-2(ok2105)*; *daf-16(mu86)* (ET507); *unc-119(e2498::Tc1)*; *wIs51*[scm::GFP; *unc-119(+)*] (JR667); *cul-1(e1756)*/*unc-69(e587)*; *him-5(e1490)*; *wIs51* (ET350); and *folt-1(ok1460)*/nT1 [*qIs51*] (VC959). Strains with *glp-1(ar202)* mutants were maintained at 16°C; wild-type animals were maintained at 20°C, using established methods (Sulston and Hodgkin,

1988). Unless otherwise stated, eggs for experiments came from hermaphrodites grown on live OP50 bacteria.

The following bacteria were acquired from the *Caenorhabditis* Genetics Center: *E. coli* OP50; *E. coli* HT115(DE3) [*F-, mcrA, mcrB, IN(rrnD-rrnE)1, rnc14::Tn10(DE3 lysogen: lavUV5 promoter -T7 polymerase*]; and *Comamonas aquatica* DA1877. HT115(DE3) is tetracycline resistant. DA1877 is streptomycin resistant. The following bacteria strains were obtained from the *Coli* Genetics Stock Center: JW1082-7 [F-, *Δ(araD-araB)567, ΔlacZ4787(::rrnB-3), λ⁻, ΔpabC760::kan, rph-1, Δ(rhaD-rhaB)568, hsdR514*]; and BW25113 [F-, *Δ(araD-araB)567*, *ΔlacZ4787*(::rrnB-3), *λ⁻*, *rph-1*, *Δ(rhaD-rhaB)568*, *hsdR514*]. Growth of *pabC* mutants (JW1082-7) under folate-deficient conditions utilized glucose minimal medium (Shehata and Marr, 1970).

Preparation of animals for germ cell isolation

To obtain synchronous adult germline tumorous mutants, eggs were isolated by sodium hypochlorite treatment (Sulston and Hodgkin, 1988). The eggs were transferred to a 3xNGM plate (an NGM agar plate (Sulston and Hodgkin, 1988) with 3x peptone concentration) with a lawn of OP50 bacteria and grown at 25°C for four days to ensure that all animals became adults with germline tumors. The animals were washed four times with M9 salt solution (Sulston and Hodgkin, 1988) in 15 ml polystyrene tubes (Falcon) to remove live bacteria and transferred to heat-killed OP50 bacteria plates, which were created by placing OP50-seeded 3xNGM plates at 62-67°C for 24 hr. After two (or more) hours on the heat-killed bacteria plate, the animals were transferred to a 12.5 cm^2 cell culture flask (Corning) containing 2.5 ml of M9 solution supplemented with: heat-killed OP50 bacteria; 200 units penicillin and 0.2 mg streptomycin per

ml); 25 μg/ml tetracycline (Sigma-Aldrich, 87128); 34 μg/ml chloramphenicol (Research Products International); 50 μg/ml kanamycin; 0.02% normocin; and 5 μg/ml cholesterol. Animals were incubated overnight in the antibiotic-supplemented M9 solution.

Folate analysis

After passage of bacterial extract onto the folate-binding protein affinity column (described in Methods), effluents were collected separately and the column was subsequently washed with one volume of 0.1 M potassium phosphate buffer pH 7.4, and the effluent was added to the first effluent. The column was subsequently washed with 10 volumes of the same buffer, then with 5 volumes of 2 mM potassium phosphate buffer pH 7.4 to rid the column of the high salt buffer. Folate bound to the columns was then eluted with 20 mM trifluoroacetic acid into tubes that contained 10 μl of 10 mM dithiothreitol (Midttun et al.) and 1 M dipotassium phosphate to neutralize the acid and protect the eluted folate from oxidation.

The affinity chromatography utilizes the high affinity (Kd = 10^{-9} - 10^{-11} M) folate binding protein, which was purified to almost homogeneity (Selhub et al., 1980; Selhub and Franklin, 1984; Selhub and Grossowicz, 1973) to purify and concentrate biological folate. The affinity column has been used to purify folates from: diverse tissues from different animals (liver, kidney, brain, blood, etc.) that were exposed to different conditions; more than 100 food products; and blood and plasma (for examples, see (Poo-Prieto et al., 2006; Rong et al., 1991; Selhub et al., 1991). When sufficient concentration permitted, subsequent fractionation of these affinity-purified extracts was accompanied by detection of peak activities by UV absorption, which revealed spectra that were specific for folate; there were no other peaks. When the concentration did not permit the use of UV absorption, we used an ESA CoulArray electrochemical detector

consisting of four flow-through, porous-carbon graphite coulometric electrodes, each set at incrementally higher potentials. The different potentials allowed us to distinguish between different forms of folates, and at the same time increase the sensitivity of detection by more than one order of magnitude. We used this method to analyze thousands of human plasma samples to detect unmetabolized folic acid and other folates. In these analyses, only two activity peaks were detected, 5-methyl-THF and folic acid, no other peaks were detected by the electrochemical detector, UV absorbance, fluorescence, or other means (Kalmbach et al., 2011; Morris et al., 2010). These results suggest that it is highly unlikely that other compounds coelute with folate at significant levels from the affinity column.

The following basic folates and pteroates were used: 5-formyl-5,6,7,8-tetrahydrofolic acid (Sigma); (6S)-5-formyl-5,6,7,8-tetrahydrofolic acid (Schircks Laboratories); 5-methyl-5,6,7,8-tetrahydrofolic acid (Merck); (6S)-5-methyl-5,6,7,8-tetrahydrofolic acid (Schircks Laboratories); 5,6,7,8-tetrahydrofolic acid (Merck); and 7,8-dihydropteroic acid (Schircks Laboratories). 5,10-methenyl-5,6,7,8-tetrahydrofolic acid and 10-formyl-5,6,7,8-tetrahydrofolic acid were synthesized from 5-formyl-5,6,7,8-tetrahydrofolic acid as described (Stover and Schirch, 1992). The creation of Glu1, 3, and 6 folate derivatives is described in the section below. For consistency, we will refer to the number of Glu in all folates by a subscript number, so for example, folic acid-Glu_3 contains three Glu residues. For tumor frequency assays, the folates and other compounds were added to the agar plates when the plates were poured, after allowing the agar to cool to ~47°C prior to addition.

Interconversion of folates during analysis

In the analysis of bacterial folate species shown in Fig. 3.S6, the folates were isolated from bacteria at pH 7.0 and separated by ion-pair chromatography, also at pH 7.0. At this neutral pH, 5,10-methenyl-THF will convert predominantly to 10-formyl-THF, and to some extent 5-formyl-THF. For the separation (and subsequent purification) of folates from DA1877 (Fig. 3.5A), folates were isolated from bacteria at neutral pH and then purified by ion-pair chromatography at neutral pH. This isolated mixture of folates was then separated by reverse-phase chromatography at acid pH to allow the isolation of individual folates. In the initial purification with ion-pair chromatography, 5,10-methenyl-THF would convert predominantly to 10-formyl-THF (with potential conversion to 5-formyl-THF). In the subsequent reverse-phase chromatography at acid pH, 10-formyl-THF and 5-formyl-THF would convert to 5,10-methenyl-THF. In all chromatographic analyses undertaken, 5,10-methylene-THF, if present in the bacterial extract, may have converted to THF as a result of the chromatography process (Horne, 2001).

Synthesis of reduced monoglutamyl and polyglutamyl folates

Reduced folates were prepared as described previously (Selhub, 1989). Aliquots of 50 nmoles in 800 µl water of pteroylglutamates (folic acids) with 1, 3, and 6 glutamate residues ($PteGlu_1$, $PteGlu_3$, and $PteGlu_6$, Schircks Laboratories, Switzerland), were reduced to the corresponding tetrahydro-pteroylglutamates ($H_4PteGlu_n$) by potassium borohydride in presence of PtO as a catalyst. 0.3 ml aliquots from these solutions were used to synthesize the corresponding 5-methyl$H_4PteGlu_n$ after incubation with formaldehyde and reduction with potassium borohydride for 1 hr at 37°C. Second 0.3 ml aliquots were used for the synthesis of the corresponding 10-

formylH_4PteGlu_n. These were mixed with 2 ml formic acid (88%) in the presence of 0.1 M DTE and incubated under nitrogen for 1 hr at 37°C. Excess formic acid was removed by vacuum evaporation, and an aliquot of the remaining solution was brought to pH 8.3 for converting the 5,10-methenylH_4PteGlu_n to the corresponding 10-formyl- derivatives. The purity of the products was determined by ion-pair HPLC and spectral analysis with a diode array detector (Selhub, 1989).

Isolation of individual folate species from bacteria

Lyophilized DA1877 bacteria were heat extracted by boiling for 15 min in 2% sodium ascorbate. After centrifugation, folates in the supernatant were purified by affinity chromatography using highly-purified milk folate binding protein bound to Sepharose (Selhub et al., 1988). The affinity purified folate was then fractionated by ion-pair chromatography, which separates folates into clusters each with the same number of glutamate residues (Selhub, 1989). Fractions from same cluster were combined, vacuum evaporated to remove acetonitrile, and passed through a C18 Sep Pack cartridge, which retains all folates in the combined fractions. The cartridge was then washed with 5 ml of acid (pH 3.0) solution, and then eluted from the cartridge with 1 ml of methanol containing 10 mM dithioerythritol, DTE. The eluate was evaporated to dryness, reconstituted with a pH 7.0 buffer solution containing 10 mM DTE, and fractionated with HPLC using an acetonitrile gradient elution at acid pH (2.6) (Bagley and Selhub, 2000). In this method, folates are separated on the basis of their pteridine ring structure (Fig. 3.5A) thus allowing the collection of separate forms of folate.

RNA interference

Feeding RNAi was performed as described (Kamath and Ahringer, 2003). Feeding-RNAi constructs, expressed in HT115(DE3) bacteria, were obtained from the Ahringer library (Kamath et al., 2003). Overnight cultures of RNAi-feeding bacteria in LB medium were induced the next day on NGM agar plates containing 1mM IPTG and 100 μg/ml carbenicillin. Eggs or synchronized L1 larvae were placed on the RNAi plates and adults were scored for tumor frequency assay or harvested for analysis of mitotic germ cell numbers, or EdU incorporation assays with isolated germ cells.

Immunofluorescence and analysis of mitotic germ cell numbers

For the analysis of mitotic germ cell numbers, eggs were isolated by sodium hypochlorite treatment (Sulston and Hodgkin, 1988) of gravid adults. Synchronized L1-stage larvae were isolated by placing the eggs in M9 solution with 0.5 μg/ml cholesterol and incubating overnight at 25°C. The L1 larvae were placed on NGM agar plates with the indicated additives and live or heat-killed bacteria at 20°C. Plates seeded with heat-killed OP50 bacteria contained 100 μg/ml carbenicillin and 25 μg/ml tetracycline to prevent growth of any possible bacterial contaminants. After development to the young adult stage, hermaphrodites (without eggs) were segregated onto new plates and cultured for 36 hr. Gonads were dissected from animals 36 hr-post adulthood. To harvest gonads, adults were placed in 20 μl of PBS containing 0.875 mM tetramisole (Sigma). Animals were cut behind the pharynx using 21g syringe needles to extract the gonad. Using a glass Pasteur pipette, extracted gonads were collected in 1.5 ml pre-lubricated micro-centrifuge tubes and fixed by incubation with 3% formaldehyde in 0.1 M K_2HPO_4 (pH 7.2) buffer for 1 hr at room temperature. Following fixation, the gonads were permeabilized by incubation with -

20°C 100% methanol for 5 min. Gonads were blocked in PBT (PBS + 0.1% Tween-20) with 0.5% bovine serum albumin (BSA, Fisher) for 30 min at room temperature, and then incubated with anti-phosphohistone H3 (Ser10) antibody (Cell Signaling; 1:200 dilution) in PBT + 0.5% BSA overnight at 4°C. Samples were washed 3 times in PBT; incubated with Dylight 488 Goat anti-rabbit secondary antibody (Thermo Scientific Pierce; 1:500) in PBT + 0.5% BSA for 2 hr at room temperature; then washed 3 times with PBT. DNA was stained with 1 µg/ml Hoechst 33342. Extracted gonads were mounted on slides with 90% glycerol and 1 mg/ml p-phenylenediamine (Sigma) and visualized using a Zeiss Axioskop microscope. The number of nuclei in the proliferative zone was determined by counting mitotic nuclei based on morphology (Michaelson et al., 2010), using image stacks of dissected gonads stained with Hoechst 33342. The Image J plugin program Point Picker was used to assist in germ cell counts (http://bigwww.epfl.ch/thevenaz/pointpicker/).

For Figure 1B, wild-type and *glp-1(gf)*; *cki-2*; *daf-16* mutant animals were harvested by hypochlorite treatment and eggs were placed on 1X NGM plates and grown at 25°C for 3 days. Gonads were dissected and fixed as described above. Gonads were incubated with anti-phosphohistone H3 (Ser-10) antibody (Cell Signaling; 1:200) and anti-HIM-3 antibody (Zetka et al., 1999) (the kind gift of Monika C. Zetka; 1:200) in PBT + 0.5% BSA overnight at 4°C and processed as described above.

Analysis of seam cell numbers

Eggs from the strains JR667 and ET350 were isolated by sodium hypochlorite treatment and placed on live bacteria with 10 µM PABA or ethanol control. After 4 days at 20°C, adult hermaphrodites were analyzed for seam cell numbers. *cul-1(e1756)* homozygotes (strain ET350)

do not become adults and were also analyzed as 4-day old larvae. Seam cell numbers were determined based on GFP epifluorescence on one lateral side of each of 10 animals per condition.

Supplemental References

Bagley, P.J., and Selhub, J. (2000). Analysis of folate form distribution by affinity followed by reversed- phase chromatography with electrical detection. Clinical chemistry *46*, 404-411.

Flatt, T., Min, K.J., D'Alterio, C., Villa-Cuesta, E., Cumbers, J., Lehmann, R., Jones, D.L., and Tatar, M. (2008). Drosophila germ-line modulation of insulin signaling and lifespan. Proc Natl Acad Sci U S A *105*, 6368-6373.

Horne, D.W. (2001). High-performance liquid chromatographic measurement of 5,10-methylenetetrahydrofolate in liver. Analytical biochemistry *297*, 154-159.

Kalmbach, R., Paul, L., and Selhub, J. (2011). Determination of unmetabolized folic acid in human plasma using affinity HPLC. The American journal of clinical nutrition *94*, 343S-347S.

Kamath, R.S., and Ahringer, J. (2003). Genome-wide RNAi screening in Caenorhabditis elegans. Methods *30*, 313-321.

Kamath, R.S., Fraser, A.G., Dong, Y., Poulin, G., Durbin, R., Gotta, M., Kanapin, A., Le Bot, N., Moreno, S., Sohrmann, M.*, et al.* (2003). Systematic functional analysis of the Caenorhabditis elegans genome using RNAi. Nature *421*, 231-237.

Michaelson, D., Korta, D.Z., Capua, Y., and Hubbard, E.J. (2010). Insulin signaling promotes germline proliferation in C. elegans. Development *137*, 671-680.

Midttun, O., Hustad, S., and Ueland, P.M. (2009). Quantitative profiling of biomarkers related to B-vitamin status, tryptophan metabolism and inflammation in human plasma by liquid chromatography/tandem mass spectrometry. Rapid communications in mass spectrometry : RCM *23*, 1371-1379.

Morris, M.S., Jacques, P.F., Rosenberg, I.H., and Selhub, J. (2010). Circulating unmetabolized folic acid and 5-methyltetrahydrofolate in relation to anemia, macrocytosis, and cognitive test performance in American seniors. The American journal of clinical nutrition *91*, 1733-1744.

Poo-Prieto, R., Haytowitz, D.B., Holden, J.M., Rogers, G., Choumenkovitch, S.F., Jacques, P.F., and Selhub, J. (2006). Use of the affinity/HPLC method for quantitative estimation of folic acid in enriched cereal-grain products. The Journal of nutrition *136*, 3079-3083.

Rong, N., Selhub, J., Goldin, B.R., and Rosenberg, I.H. (1991). Bacterially synthesized folate in rat large intestine is incorporated into host tissue folyl polyglutamates. The Journal of nutrition *121*, 1955-1959.

Selhub, J. (1989). Determination of tissue folate composition by affinity chromatography followed by high-pressure ion pair liquid chromatography. Analytical biochemistry *182*, 84-93.

Selhub, J., Ahmad, O., and Rosenberg, I.H. (1980). Preparation and use of affinity columns with bovine milk folate-binding protein (FBP) covalently linked to Sepharose 4B. Methods in enzymology *66*, 686-690.

Selhub, J., Darcy-Vrillon, B., and Fell, D. (1988). Affinity chromatography of naturally occurring folate derivatives. Analytical biochemistry *168*, 247-251.

Selhub, J., and Franklin, W.A. (1984). The folate-binding protein of rat kidney. Purification, properties, and cellular distribution. J Biol Chem *259*, 6601-6606.

Selhub, J., and Grossowicz, N. (1973). Chemical fixation of folate binding protein to activated sepharose. FEBS Lett *35*, 76-78.

Selhub, J., Seyoum, E., Pomfret, E.A., and Zeisel, S.H. (1991). Effects of choline deficiency and methotrexate treatment upon liver folate content and distribution. Cancer Res *51*, 16-21.

Shehata, T.E., and Marr, A.G. (1970). Synchronous growth of enteric bacteria. Journal of bacteriology *103*, 789-792.

Stover, P., and Schirch, V. (1992). Synthesis of (6S)-5-formyltetrahydropteroyl-polyglutamates and interconversion to other reduced pteroylpolyglutamate derivatives. Analytical biochemistry *202*, 82-88.

Sulston, J., and Hodgkin, J. (1988). Methods. In The Nematode Caenorhabditis elegans, W.B. Wood, ed. (Cold Spring Harbor, New York: Cold Spring Harbor Laboratory), pp. 587-606.

Zetka, M.C., Kawasaki, I., Strome, S., and Muller, F. (1999). Synapsis and chiasma formation in Caenorhabditis elegans require HIM-3, a meiotic chromosome core component that functions in chromosome segregation. Genes Dev *13*, 2258-2270.

CHAPTER 4

THE STEROID HORMONE DAFACHRONIC ACID INHIBITS GERMLINE STEM CELL PROLIFERATION IN *C. ELEGANS* [1]

---

[1] **Mukherjee M***, Chaudhari S.N*., Vagasi A.S, and Kipreos E.T. 2016. To be submitted to *Developmental Biology.*

* These authors contributed equally to this work

Abstract

Dafachronic acid (DA) is a steroid hormone that is responsible for controlling dauer formation and regulating lifespan in *C. elegans*. In this work, we describe DA as an inhibitor of *C. elegans* germ stem cell proliferation. Using the *C. elegans* germ cell primary culture system described in Chapter 3, we show that DA restricts proliferation of isolated germ cells in culture. DA also inhibits tumor formation in a tumorous germline mutant in vivo and decreases the proliferation of wild-type germ cells. Conversely, the loss of DAF-9 cytochrome P450 (CY450), which is responsible for the production of DA, increases tumor frequencies in germline tumorous mutants and increases the number of mitotic germ cells in wild-type animals. We demonstrate that DA requires its canonical receptor DAF-12 to mediate the inhibition of germline stem cell proliferation both in vivo and in vitro.

Introduction

Steroid-hormone signaling in *C. elegans* enables the nematode to progress through development, maintain homeostasis, and regulate longevity (Aguilaniu et al., 2016; Wollam and Antebi, 2011). This is generally accomplished by binding of the steroid hormones to nuclear hormone receptors (NHRs) to regulate their transcriptional activity (Wollam and Antebi, 2011). The nematode can sense unfavorable conditions, such as shortage of food, crowding and turn on developmental programs that lets it enter a mode of growth suspension called the Dauer larval stage, where it remains non-reproductive and stress-resistant (Aguilaniu et al., 2016). Under replete conditions, where food is abundant, insulin (IIS) and TGFβ signaling pathways converge on *daf-9*/cytochrome P450 (CY450) leading to the production of 3-keto bile acid like steroids called dafachronic acids (DA) (Antebi, 2013b; Mahanti et al., 2014; Motola et al., 2006). The cytochrome P450 family of genes is responsible for detoxification of xenobiotic compounds and synthesis and degradation of steroid hormones (Gerisch et al., 2007). *daf-9*/CY450 catalyzes the last step in converting two distinct precursor molecules into Δ^4- and Δ^7-DAs (Motola et al., 2006). In addition to Δ^4- and Δ^7-DAs, several other physiological DAs have since been identified (Mahanti et al., 2014). DAs bind to the NHR DAF-12, which then activates reproductive programs, whereas the un-liganded DAF-12 (not bound to DA) forms a heterocomplex with the co-repressor DIN-1/SHARP, leading to larval arrest and entry into dauer phase (Fig. 4.1) (Aguilaniu et al., 2016; Ludewig et al., 2004).

DAF-12 and DA regulate adult lifespan in a complex manner. DAF-12 that is not bound by DAs promotes adult lifespan at low temperatures (Gerisch et al., 2007; Jia et al., 2002), but shortens lifespan at high temperatures (Gerisch et al., 2007; Gerisch et al., 2001; Hsin and Kenyon, 1999; Jia et al., 2002). Additionally, DA-bound DAF-12 promotes longevity in animals

that lack the germline (Gerisch et al., 2007; Gerisch et al., 2001; Hsin and Kenyon, 1999). Loss of the germline precursor cells in the L1 stage results in animals that lack all germ cells, and these mutants have extended lifespan by almost 60% (Hsin and Kenyon, 1999). However, animals lacking both the germline and somatic gonad do not show extended lifespan, suggesting that lifespan extension depends on signals from the somatic gonad (Aguilaniu et al., 2016; Yamawaki et al., 2010). Removal of the germline causes heightened production of DAs (Shen et al., 2012) that activates DAF-12, which then mediates the transcription of microRNAs *mir-84* and *mir-241* (Boehm and Slack, 2005). These microRNAs facilitate the nuclear localization of the FOXO transcription factor DAF-16, by negatively regulating inhibitors of DAF-16 (Berman and Kenyon, 2006; Boehm and Slack, 2005; Gerisch et al., 2007). DAF-16/FOXO is a key mediator of longevity and the IIS pathway regulates its activity, however in germline-mediated longevity, its activity appears to be independent of IIS signaling (Antebi, 2013a). DAF-12 along with DAF-16, are required to transcribe key lifespan extension genes in regulating germline-mediated longevity (McCormick et al., 2012).

Dietary restriction (DR), induced by a reduction of caloric intake, extends lifespan in *C. elegans*, *Drosophila*, yeast, and other eukaryotes (Masoro, 2005). DR results in a reduction of germ cell numbers in the proliferative zone in wild-type *C. elegans* (Thondamal et al., 2014). The same study also showed that DR increased the transcription of *daf-9* as well as the production of Δ^7-DA by several-fold in wild-type adult worms (Thondamal et al., 2014). However, the lifespan extension under DR was not dependent on DAF-12, but on a different NHR called NHR-8 (Thondamal et al., 2014). NHR-8 is a non-canonical NHR that regulates cholesterol homeostasis and bile acid metabolism in *C. elegans* (Magner et al., 2013). Using a weak *nhr-8* deletion allele that has a deletion in the ligand-binding domain, Thondamal et. al

showed that NHR-8 acts downstream of Δ^7-DA to promote lifespan extension in *C. elegans* under DR conditions (Thondamal et al., 2014). They also show that under DR conditions, NHR-8 is required to reduce the levels of mTOR/*let-363* signaling, which is in turn is known to regulate germline proliferation in the proliferative zone in the *C. elegans* gonad (Korta et al., 2012). These observations tie together nutrient sensing and germline plasticity to adult lifespan control (Thondamal et al., 2014).

Thondamal et al. proposed that NHR-8, which is a close homolog of DAF-12, directly mediates DA signaling in response to DR (in their hands, complete starvation). They showed that DA was required for DR-mediated loss of germ cells by showing that a daf-9 mutant (which is incapable of making DA) did not have a decrease in germ cells upon DR, but the decrease in germ cells could be restored by exogenously adding DA. *nhr-8* mutants (which similarly do not make DA) also did not exhibit a decrease in germ cell numbers in response to DR, but, significantly, there was still no decrease upon adding exogenous DA (Thondamal et al., 2014). This suggested that NHR-8 is required for DA to affect germ cell numbers. While the authors proposed that NHR-8 may directly bind DA and mediate its effects on germ cells, there are critical evidence that was not shown to support this. For example, it was not shown that DA or NHR-8 functioned cell autonomously in the germ cells to mediate the response to DA, or that NHR-8 could bind or be directly activated by DA. The role of the canonical DA receptor DAF-12 was also not analyzed for its effects on germ cells (although it was shown to not be required for the effect of DA on DR-mediated lifespan extension).

In this work, we demonstrate that DA is a cell-autonomous inhibitor of germ stem cell proliferation by using an isolated germ cell culture system. We use a tumorous germline mutant *glp-1(ar202)*; *cki-2(ok2105)*; *daf-16(mu86)* described in Chapter 3, to demonstrate the effects of

DA on isolated germ cells. The germ cells isolated from this strain can live for over a month in a specialized germ cell culture medium, CeM1, which has also been described in Chapter 3. We show that the addition of DA inhibits germ cell survival in culture and this is dependent on the canonical NHR DAF-12. We also show that under normal feeding conditions, exogenous DA is able to inhibit tumor formation in the tumorous germline mutant and as well as decrease the number of mitotic germ cells in the wild-type germline in a DAF-12 dependent manner.

Materials and methods

C. elegans and bacterial strains

C. elegans strains used for this study were: wild-type (N2), *glp-1(ar202)* (GC143), *glp-1(ar202)*; *cki-2(ok2105)*; *daf-16(mu86)* (ET507), *daf-12(rh61rh412)* (AA18), and *glp-1(ar202)*; *cki-2(ok2105)*; *daf-16(mu86)*; *daf-12(rh61rh411)* (ET526). Strains with *glp-1(ar202)* mutants were maintained at 16°C; wild-type animals were maintained at 20°C, using established methods (Sulston and Hodgkin, 1988). The following bacteria were used: *E. coli* OP50; *E. coli* HT115(DE3) [*F-, mcrA, mcrB, IN(rrnD-rrnE)1, rnc14::Tn10(DE3 lysogen: lavUV5 promoter -T7 polymerase*]. HT115(DE3) is tetracycline resistant. All bacteria strains were obtained from the *Caenorhabditis* Genetics Center.

Dafachronic acids

Δ^4- and Δ^7-dafachronic acids were purchased from Cayman Chemicals. Stock solution of 1mM dafachronic acid was made in 100% Ethanol; and ethanol was used as carrier control.

Culture of C. elegans germ cells in CeM1 medium

CeM1 medium was prepared as described in Chapter 3. Animals were prepared and germ cells were isolated from the *glp-1(ts); cki-2; daf-16* mutants as described in Chapter 3. Bacterial extract and folates used to stimulate germ cell proliferation were prepared as described in Chapter 3.

EdU-incorporation assay

After germ cells were incubated 24 hrs in CeM1 medium (as described in Chapter 3), EdU was added to a concentration of 20 μM. 24 hrs after addition of EdU, cells were harvested and processed with the Click-iT Alexa Fluor 488 Imaging kit (Life Technologies), according to the manufacturer's protocol. 2 μg/ml Hoechst 33342 was used to stain DNA and cells were analyzed by epifluorescence microscopy. Images of EdU Alexa Fluor 488 staining were taken initially, and then images of Hoechst staining were taken subsequently. At least 150 cells were counted for each condition.

RNA Interference

RNAi was performed as described (Kamath et al., 2003). Feeding-RNAi constructs of *daf-9*, *nhr-8*, and empty vector expressed in HT115(DE3) bacteria, were obtained from the Ahringer library (Kamath et al., 2003). Overnight cultures of RNAi-feeding bacteria in 2XYT medium were induced the next day on NGM agar plates containing 1mM IPTG and 100 μg/ml carbenicillin. Eggs or synchronized L1 larvae were placed on the RNAi plates and adults were scored for: tumor frequency; mitotic germ cell numbers in adults that were 36 hrs post young-adulthood; or EdU incorporation with isolated germ cells.

Assay for germ cell viability

Live/dead cell counts were carried out to test the viability of germ cells under varying dafachronic acid conditions over the course of a month. The live-cell stain calcein-AM (Sigma-Aldrich, C1359; 1 μM), and the dead-cell stain ethidium homodimer (Sigma-Aldrich, E1903; 0.1 μM) were used (Zhang et al., 2011). Three counts were made for each sample using a cellometer counting grid (CP2, Nexcelom Bioscience LLC) and analyzed using an inverted fluorescence microscope (Zeiss Axio Observer.A1); cell count variation is presented as SEM. Germ cells were isolated from 25 adult hermaphrodites for 0.5 ml/well of a 24-well plate.

Tumor frequency assay

Eggs isolated by sodium hypochlorite treatment were placed on 1x NGM plates seeded with either OP50 bacteria or HT115 containing RNAi vector or empty vector, and with or without dafachronic acid supplementation. Tumor frequencies were analyzed at the semi-permissive temperature of 18°C. After synchronized growth from eggs to L4-stage larvae (see below), the L4 larvae were transferred to fresh plates with or without RNAi and dafachronic acids (~100 larvae/plate; 3 plates per condition). On the second day after transfer, the percentages of adult animals with tumors were scored on each of the plates. Average tumor frequencies were derived from the triplicate measurements.

Immunofluorescence and analysis of mitotic germ cell numbers

To obtain populations of synchronized L1-stage larvae, eggs were isolated by sodium hypochlorite treatment (Sulston and Hodgkin, 1988) of gravid adults and placed in M9 buffer with 0.5 μg/ml cholesterol overnight at 25ºC. The next day, the L1 larvae were placed on 1X

NGM agar plates with the indicated additives. Young adult-stage hermaphrodites (without eggs) were segregated onto new plates. Animals were placed on DA and ethanol control plates 12 hrs post young-adulthood, and maintained on these treatments for 24 hrs prior to harvesting the gonads. Gonads were dissected from animals 36 hrs-post young-adulthood. To dissect gonads, adults were placed in 20 µl of phosphate buffered saline (PBS) containing 0.875 mM tetramisole (Sigma). Animals were cut behind the pharynx using 21g syringe needles to extract the gonad. A glass Pasteur pipette was used to transfer gonads to 1.5 ml pre-lubricated micro-centrifuge tubes. The gonads were fixed by incubation with 3% formaldehyde in 0.1 M K_2HPO_4 (pH 7.2) buffer for 1 hr at room temperature. After fixation, the gonads were permeabilized in -20°C 100% methanol for 5 min. Gonads were then blocked by incubation for 30 min at room temperature with PBT (PBS + 0.1% Tween-20) with 0.5% bovine serum albumin (BSA, Fisher).

Anti-phosphohistone H3 (Ser10) antibody (Cell Signaling) was diluted (1:2000) in PBT + 0.5% BSA and incubated with the gonads overnight at 4°C. The next day, samples were washed 3 times in PBT; incubated with Dylight 488 Goat anti-rabbit secondary antibody (Thermo Scientific Pierce; 1:500) in PBT + 0.5% BSA for 2 hrs at room temperature; then washed 3 times with PBT. DNA was stained by incubation for 5 mins with 2 µg/ml Hoechst 33342 in PBT. Samples were mounted on slides with 90% glycerol and the anti-bleach agent 1 mg/ml p-phenylenediamine (Sigma). Samples were visualized using a Zeiss Axioskop microscope with ORCA ER CCD camera. Phosphohistone H3 (Ser10) marks mitotic germ cells (Hendzel et al., 1997). The number of mitotic germ cells in the proliferative zone was determined (Michaelson et al., 2010)by counting mitotic germ cells based on Hoechst staining morphology as described by (Michaelson et al., 2010). Z- stacks of dissected gonads were obtained at 0.5 µM intervals using a Ludl hardware controller and shutters controlled with Openlab Automation software.

Image z-stacks were analyzed with Image J software (Schindelin et al., 2015) using the Point Picker plugin (http://bigwww.epfl.ch/thevenaz/pointpicker/).

Statistical Analysis

Two-tailed Student's t-test was used to analyze the three replicates of tumor frequencies, the data for mitotic index, numbers of germ cell nuclei in the proliferative zone. Chi-squares test was used to analyze the percentages of EdU positive cells. The nonparametric Mann-Whitney test was used to analyze the number of phosphohistone H3 positive cells per gonad arm. Error bars reflect standard error of the mean (s.e.m)

Results

Dafachronic acid inhibits C. elegans germ cell proliferation in a cell-autonomous manner

The germ cell culture system described in Chapter 3 can be used to test physiologically active compounds and their effects on germ cell survival and proliferation. Under nutrient deprived conditions DA levels increase in *C. elegans*, which leads to a reduction in the number of germ cells in the proliferative zone in the gonad (Thondamal et al., 2014). We wanted to determine if adding DA exogenously had a similar effect on the survival and proliferation of in vitro culture of germ cells isolated from the tumorous mutant *glp-1(ts)*; *cki-2*; *daf-16*. We found that the addition of physiological concentrations of Δ^7-DA (Motola et al., 2006) had deleterious effects on isolated germ cells: causing them to die more rapidly with increasing concentration (Fig 4.2).

Dafachronic acid inhibits C. elegans germ cell proliferation in a DAF-12 dependent manner

As described in Chapter 3, the addition of specific bacterial folates increases germ stem cell proliferation in vitro. We wanted to determine whether the addition of DA reduced DNA replication in germ cells obtained from *glp-1(ts)*; *cki-2*; *daf-16* tumorous germline mutants. As a measure of DNA replication, we determined the percentage of cells incorporating the thymidine analog EdU. Consistent with our observations from the germ cell survival data (Fig. 4.2), we found that the addition of the 1 μM Δ^4-DA reduced EdU incorporation in *glp-1(ts)*; *cki-2*; *daf-16* germ cells provided with bacterial extracts containing stimulatory folates (Fig 4.3A).

To determine the role of the canonical DA binding receptor DAF-12 in the inhibition of EdU incorporation, we combined a *daf-12* null allele (*rh61rh411*) with the *glp-1(ts)*; *cki-2*; *daf-16* mutant alleles. The *daf-12 (rh61rh411)* used here contains mutations in both the DNA and ligand bind domains of DAF-12 (Antebi et al., 2000). Germ cells isolated from the *glp-1(ts)*; *cki-2*; *daf-16*; *daf-12* quadruple mutant strain were not affected by the addition of 1 μM Δ^4-DA (Fig 4.3A). These results suggest that dafachronic acid inhibits germ cell cycle progression and/or DNA replication in a DAF-12-dependent and cell-autonomous manner.

To determine if dafachronic acid inhibits germ cell proliferation in vivo, we added 1 μM Δ^7-dafachronic acid to *glp-1(ts)*; *cki-2*; *daf-16* mutants at the semi-permissive temperature (18ºC) and analyzed their tumor frequency. Indeed, the addition of Δ^7-DA significantly reduced the frequency of animals displaying tumors. Introducing the *daf-12* loss-of-function allele significantly increased the percentage of animals that had tumors in the *glp-1(ts)*; *cki-2*; *daf-16* mutants at 18ºC. Addition of Δ^7-DA was not able to inhibit tumor formation in the quadruple *glp-1(ts)*; *cki-2*; *daf-16; daf-12* mutant, suggesting that functional DAF-12 is necessary for DA to inhibit germ cell proliferation (Fig 4.3B).

Δ^4-DA also negatively impacts the number of mitotic germ stem cells in wild-type gonads. We measured by the number of mitotic cells per gonad arm using the mitotic cell marker anti-phospho-histone H3 (pH3) staining (Hendzel et al., 1997). We observed that addition of 1 μM Δ^4-DA significantly reduced the number of pH3-positive cells per gonad arm in the wild type (Fig. 4.3C). The inhibition of wild-type germ cell proliferation was similarly ameliorated by a mutation in *daf-12*, indicating that DAF-12 mediates the inhibitory effects of DA in wild-type germ cells (Fig 4.3C). Addition of 1 μM Δ^4-DA also showed a significant reduction in the total number of germ cell nuclei in the proliferative gonadal region of wild-type animals, which was not observed when Δ^4-DA was added to the *daf-12(rh61rh412)* null mutant (Fig 4.3D and E). These results suggest that DA is able to inhibit mitotic and proliferating germ cells in wild-type background in a DAF-12 dependent manner.

daf-9 RNAi increases germ cell proliferation

daf-9 encodes for a cytochrome P450/CY450 that catalyzes the final step in synthesizing both Δ^4-and Δ^7-DAs (Antebi, 2013b). RNAi depletion of *daf-9* increased tumor formation in *glp-1(ts)*; *cki-2*; *daf-16* mutants and the number of mitotic pH3-positive cells in wild-type gonads (Fig 4.4A, B), suggesting that abolishing DA production increases germline tumor formation as well as mitotic germ cell proliferation.

Dafachronic acid inhibits germ cell proliferation independent of nhr-8

The steroid hormone receptor NHR-8 has been implicated in mediating the effect of DA on reducing germ cell proliferation under starvation conditions (Thondamal et al., 2014). Notably, the role of DA and NHR-8 in regulating normal cell proliferation has not been studied. We

wanted to determine whether the germ cell inhibitory effect of DA was mediated soley by DAF-12, or if NHR-8 also was required for the inhibition. We used RNAi to deplete *nhr-8* in *glp-1(ts)*; *cki-2*; *daf-16* mutants and asked whether the isolated germ cells were still inhibited by added DA. To stimulate germ cell proliferation, the stimulatory folate 5,10 methynele-THF-Glu_6 (described in Chapter 3) was added and the effect of DA was assessed. We observed that 1μM Δ^4-DA was able to reduce the stimulatory effect of 5,10 methynele THF_6 on germ cell proliferation even in *nhr-8(RNAi)* germ cells (Fig. 4.5). This suggests that NHR-8 is not required for Δ^4-DA to mediate its effect of inhibiting germ cell proliferation, but rather DA appears to mediate its effects on germ cells soley through its canonical receptor DAF-12.

Discussion

Using our primary germ cell isolation and culture system, we have identified a novel germ cell inhibitory signal that works cell-autonomously to prevent germ cell proliferation. We have shown that dafachronic acids (Δ^4 and Δ^7) can inhibit isolated germ cell proliferation in culture in a DAF-12-dependent and NHR-8-independent manner. We have also demonstrated these effects in vivo. DAs can inhibit tumor formation in intact tumorous worms of the *glp-1(ts)*; *cki-2*; *daf-16* background at the semi-permissive temperature, and this is dependent on the presence of a functional DAF-12 receptor. RNAi inhibition of *daf-9*, which is responsible for synthesizing DAs in *C. elegans*, increases the percentage of tumorous mutants. This implies that the normal physiological generation of DA constitutively inhibits germ cell proliferation.

The inhibitory effect of DAs on germ cells is not limited to tumorous mutants. Addition of Δ^4-DA to wild-type animals significantly reduces the number of germ cells in the proliferative zone, as well as the number of mitotic germ cells as visualized by pH3 staining. This effect is

similarly dependent on the presence of a functional DAF-12 receptor, as providing exogenous Δ^4-DA to the *daf-12(rh61rh412)* null mutant fails to reduce the number of germ cells or pH3 positive cells in an otherwise wild-type background.

Dietary restriction (DR) of *C. elegans* has been shown to increase the amount of *daf-9* mRNA as well DA levels in *C. elegans* (Thondamal et al., 2014). *C. elegans* is normally maintained in the laboratory by culturing the animals on an agar surface with a lawn of *E.coli* OP50 as food source (Hosono et al., 1989). DR or bacterial deprivation is achieved by reducing the amount of bacterial lawn present on the NGM surface (Greer et al., 2007) or by growing the animals for a certain portion of their life without any bacteria (Thondamal et al., 2014). DR drastically reduced the number of germ cells in the proliferative zone in wild-type *C. elegans*. However, when *daf-9* mutants were subjected to DR, they did not show any reduction in germ cell numbers in the proliferative zone (Thondamal et al., 2014). This effect of the *daf-9* mutation appears to be due to a failure to make DA, as addition of exogenous DA under DR conditions reintroduced the germ cell deficit phenotype (Thondamal et al., 2014). An *nhr-8* mutant that lacked the ligand-binding domain blocked the decrease in germ cell numbers under DR conditions, even when exogenous DA was provided to the *nhr-8* mutants. This led the authors to propose that under DR conditions, DA mediates its inhibitory effects on germ cell proliferation through NHR-8, and the authors proposed the NHR-8 functions as the DA receptor for this role (Thondamal et al., 2014). Notably, the authors did not demonstrate that NHR-8 directly binds DA, and did not directly test the role of DAF-12 in regulating germ cell numbers in response to DA. Therefore, it is still possible that under DR conditions, both NHR-8 and DAF-12 are required to allow DA to inhibit germ cell proliferation. In this regard, it should be noted that NHR-8 controls the production of DAs by regulating the metabolism of its sterol precursor

molecule, (Magner et al., 2013), but it may also regulate production of other hormones besides DA. So it is possible that the *nhr-8* may mediate its effects under DR conditions via DA independent mechanisms.

We described in Chapter 3 that bacterial folates increase germ stem cell proliferation in culture as well as in vivo. Insulin signaling (IIS) and TGFβ are two other systemic signals that promote germ stem cell proliferation (Dalfo et al., 2012; Michaelson et al., 2010). Notably, DA and bacterial folates, as well as insulin signaling control lifespan in *C. elegans*. Both IIS and bacterial folates inhibit lifespan but increase germ cell proliferation (Antebi, 2013a; Kenyon, 2010; Virk et al., 2012; Virk et al., 2016), whereas DA extends lifespan but decreases germ cell proliferation (Gerisch et al., 2007; Yamawaki et al., 2010). These inverse relationships may reflect a trade-off between reproductive lifestyle and long-life: the availability of abundant food is relayed to GSCs by bacterial folates and insulin/IGF-like signaling leading to increased GSC proliferation in order to maximize offspring production; conversely, scarcity of optimal food leads to the inhibition of GSC proliferation and the activation of lifespan extension pathways.

Author Contributions

M.M performed phosphohistone H3 staining, mitotic germ cell counts and analyzed EdU experiment for Fig 4.5. S.N.C performed tumor assays. A.S.V performed cell viability assay. E.T.K performed EdU incorporation assay for Fig 4.3A and provided overall guidance for the paper. M.M and E.T.K wrote the paper.

Acknowledgements

Some *C. elegans* strains were provided by the CGC, which is funded by NIH Office of Research Infrastructure Programs (P40 OD010440). This work was supported by grants from NSF (MCB-1138454) and NIH/NIGMS (1R01GM074212) (Zetka et al.).

References

Aguilaniu, H., Fabrizio, P., and Witting, M. (2016). The Role of Dafachronic Acid Signaling in Development and Longevity in Caenorhabditis elegans: Digging Deeper Using Cutting-Edge Analytical Chemistry. Frontiers in endocrinology *7*, 12.

Antebi, A. (2013a). Regulation of longevity by the reproductive system. Experimental gerontology *48*, 596-602.

Antebi, A. (2013b). Steroid regulation of C. elegans diapause, developmental timing, and longevity. Current topics in developmental biology *105*, 181-212.

Antebi, A., Yeh, W.H., Tait, D., Hedgecock, E.M., and Riddle, D.L. (2000). daf-12 encodes a nuclear receptor that regulates the dauer diapause and developmental age in C. elegans. Genes Dev *14*, 1512-1527.

Berman, J.R., and Kenyon, C. (2006). Germ-cell loss extends C. elegans life span through regulation of DAF-16 by kri-1 and lipophilic-hormone signaling. Cell *124*, 1055-1068.

Boehm, M., and Slack, F. (2005). A developmental timing microRNA and its target regulate life span in C. elegans. Science (New York, NY *310*, 1954-1957.

Dalfo, D., Michaelson, D., and Hubbard, E.J. (2012). Sensory regulation of the C. elegans germline through TGF-beta-dependent signaling in the niche. Curr Biol *22*, 712-719.

Gerisch, B., Rottiers, V., Li, D., Motola, D.L., Cummins, C.L., Lehrach, H., Mangelsdorf, D.J., and Antebi, A. (2007). A bile acid-like steroid modulates Caenorhabditis elegans lifespan through nuclear receptor signaling. Proc Natl Acad Sci U S A *104*, 5014-5019.

Gerisch, B., Weitzel, C., Kober-Eisermann, C., Rottiers, V., and Antebi, A. (2001). A hormonal signaling pathway influencing C. elegans metabolism, reproductive development, and life span. Dev Cell *1*, 841-851.

Greer, E.L., Dowlatshahi, D., Banko, M.R., Villen, J., Hoang, K., Blanchard, D., Gygi, S.P., and Brunet, A. (2007). An AMPK-FOXO pathway mediates longevity induced by a novel method of dietary restriction in C. elegans. Curr Biol *17*, 1646-1656.

Hendzel, M.J., Wei, Y., Mancini, M.A., Van Hooser, A., Ranalli, T., Brinkley, B.R., Bazett-Jones, D.P., and Allis, C.D. (1997). Mitosis-specific phosphorylation of histone H3 initiates primarily within pericentromeric heterochromatin during G2 and spreads in an ordered fashion coincident with mitotic chromosome condensation. Chromosoma *106*, 348-360.

Hosono, R., Nishimoto, S., and Kuno, S. (1989). Alterations of life span in the nematode Caenorhabditis elegans under monoxenic culture conditions. Experimental gerontology *24*, 251-264.

Hsin, H., and Kenyon, C. (1999). Signals from the reproductive system regulate the lifespan of C. elegans. Nature *399*, 362-366.

Jia, K., Albert, P.S., and Riddle, D.L. (2002). DAF-9, a cytochrome P450 regulating C. elegans larval development and adult longevity. Development *129*, 221-231.

Kamath, R.S., Fraser, A.G., Dong, Y., Poulin, G., Durbin, R., Gotta, M., Kanapin, A., Le Bot, N., Moreno, S., Sohrmann, M.*, et al.* (2003). Systematic functional analysis of the Caenorhabditis elegans genome using RNAi. Nature *421*, 231-237.

Kenyon, C.J. (2010). The genetics of ageing. Nature *464*, 504-512.

Korta, D.Z., Tuck, S., and Hubbard, E.J. (2012). S6K links cell fate, cell cycle and nutrient response in C. elegans germline stem/progenitor cells. Development *139*, 859-870.

Ludewig, A.H., Kober-Eisermann, C., Weitzel, C., Bethke, A., Neubert, K., Gerisch, B., Hutter, H., and Antebi, A. (2004). A novel nuclear receptor/coregulator complex controls C. elegans lipid metabolism, larval development, and aging. Genes Dev *18*, 2120-2133.

Magner, D.B., Wollam, J., Shen, Y., Hoppe, C., Li, D., Latza, C., Rottiers, V., Hutter, H., and Antebi, A. (2013). The NHR-8 nuclear receptor regulates cholesterol and bile acid homeostasis in C. elegans. Cell metabolism *18*, 212-224.

Mahanti, P., Bose, N., Bethke, A., Judkins, J.C., Wollam, J., Dumas, K.J., Zimmerman, A.M., Campbell, S.L., Hu, P.J., Antebi, A.*, et al.* (2014). Comparative metabolomics reveals endogenous ligands of DAF-12, a nuclear hormone receptor, regulating C. elegans development and lifespan. Cell metabolism *19*, 73-83.

Masoro, E.J. (2005). Overview of caloric restriction and ageing. Mechanisms of ageing and development *126*, 913-922.

McCormick, M., Chen, K., Ramaswamy, P., and Kenyon, C. (2012). New genes that extend Caenorhabditis elegans' lifespan in response to reproductive signals. Aging Cell *11*, 192-202.

Michaelson, D., Korta, D.Z., Capua, Y., and Hubbard, E.J. (2010). Insulin signaling promotes germline proliferation in C. elegans. Development *137*, 671-680.

Motola, D.L., Cummins, C.L., Rottiers, V., Sharma, K.K., Li, T., Li, Y., Suino-Powell, K., Xu, H.E., Auchus, R.J., Antebi, A.*, et al.* (2006). Identification of ligands for DAF-12 that govern dauer formation and reproduction in C. elegans. Cell *124*, 1209-1223.

Schindelin, J., Rueden, C.T., Hiner, M.C., and Eliceiri, K.W. (2015). The ImageJ ecosystem: An open platform for biomedical image analysis. Molecular reproduction and development *82*, 518-529.

Shen, Y., Wollam, J., Magner, D., Karalay, O., and Antebi, A. (2012). A steroid receptor-microRNA switch regulates life span in response to signals from the gonad. Science (New York, NY *338*, 1472-1476.

Sulston, J., and Hodgkin, J. (1988). Methods. In The Nematode Caenorhabditis elegans, W.B. Wood, ed. (Cold Spring Harbor, New York: Cold Spring Harbor Laboratory), pp. 587-606.

Thondamal, M., Witting, M., Schmitt-Kopplin, P., and Aguilaniu, H. (2014). Steroid hormone signalling links reproduction to lifespan in dietary-restricted Caenorhabditis elegans. Nat Commun *5*, 4879.

Virk, B., Correia, G., Dixon, D.P., Feyst, I., Jia, J., Oberleitner, N., Briggs, Z., Hodge, E., Edwards, R., Ward, J.*, et al.* (2012). Excessive folate synthesis limits lifespan in the C. elegans: E. coli aging model. BMC biology *10*, 67.

Virk, B., Jia, J., Maynard, C.A., Raimundo, A., Lefebvre, J., Richards, S.A., Chetina, N., Liang, Y., Helliwell, N., Cipinska, M.*, et al.* (2016). Folate Acts in E. coli to Accelerate C. elegans Aging Independently of Bacterial Biosynthesis. Cell Rep *14*, 1611-1620.

Wollam, J., and Antebi, A. (2011). Sterol regulation of metabolism, homeostasis, and development. Annual review of biochemistry *80*, 885-916.

Yamawaki, T.M., Berman, J.R., Suchanek-Kavipurapu, M., McCormick, M., Gaglia, M.M., Lee, S.J., and Kenyon, C. (2010). The somatic reproductive tissues of C. elegans promote longevity through steroid hormone signaling. PLoS Biol *8*.

Zetka, M.C., Kawasaki, I., Strome, S., and Muller, F. (1999). Synapsis and chiasma formation in Caenorhabditis elegans require HIM-3, a meiotic chromosome core component that functions in chromosome segregation. Genes Dev *13*, 2258-2270.

Zhang, S., Banerjee, D., and Kuhn, J.R. (2011). Isolation and culture of larval cells from C. elegans. PloS one *6*, e19505.

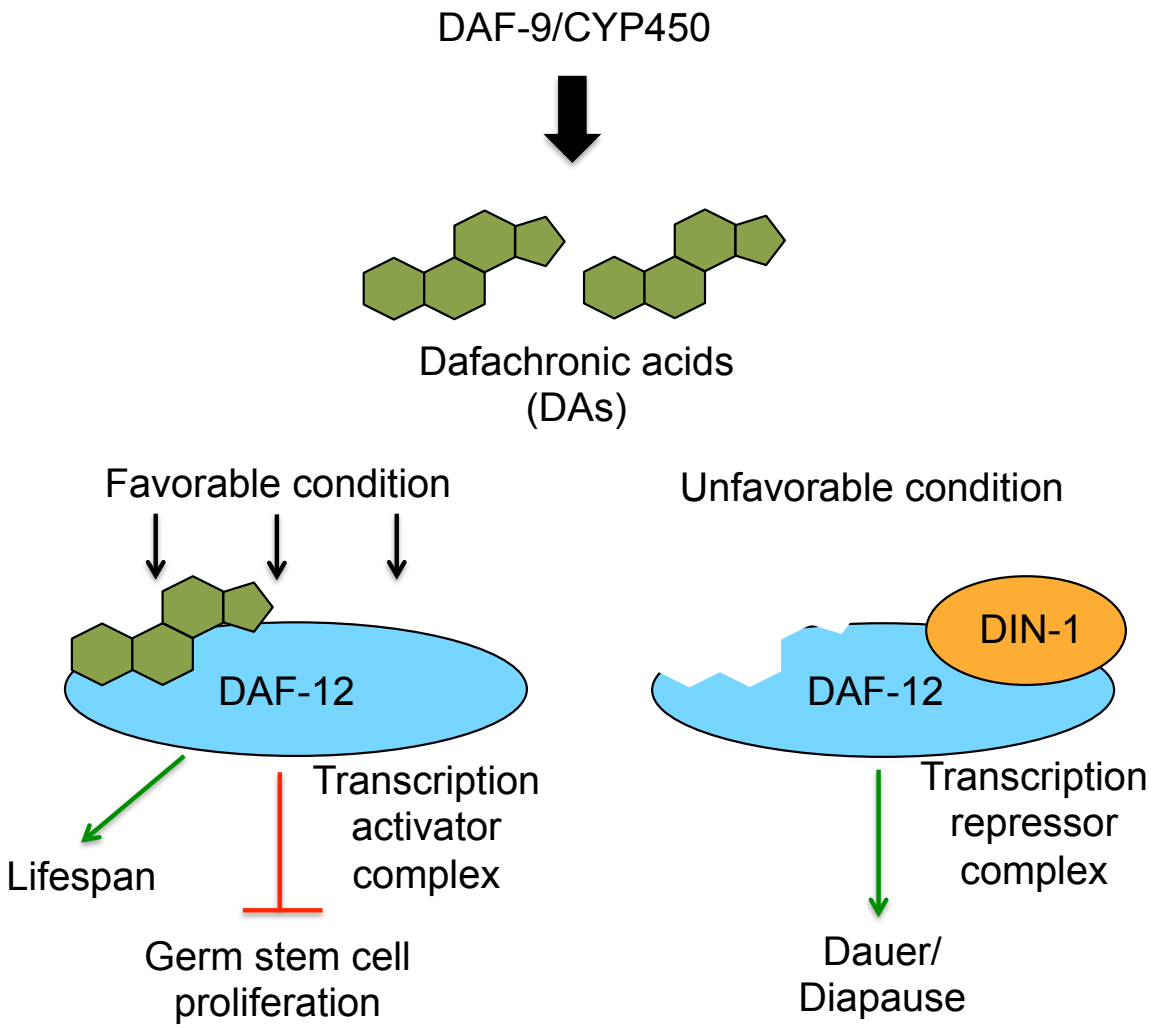

Figure 4.1 Diagram showing dafachronic acid (DA) and DAF-12 modulating heterochronic decisions and germ cell regulation.

DAF-9/ CY450 synthesizes the steroid hormone Dafachronic acids (DA). Under favorable conditions (i.e when food is abundant), DA binds to the nuclear hormone receptor DAF-12 and inhibits germ stem cell proliferation. Under unfavorable conditions, DAF-12 is bound by its co-repressor DIN-1S/SHARP and allows Dauer/ Diapause programs to initiate.

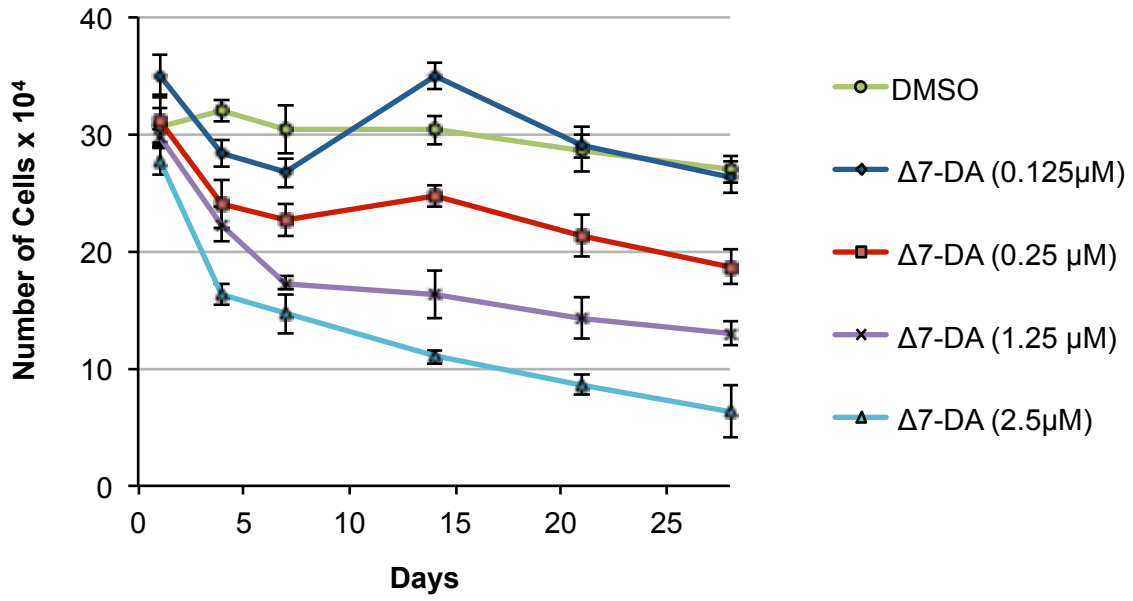

Figure 4.2. Dafachronic acid inhibits germ cell survival and proliferation in vitro.

The addition of Δ^7-dafachronic acid (at the indicated concentrations) is deleterious to isolated germ cells from *glp-1(ts)*; *cki-2*; *daf-16* mutants, as demonstrated by a decrease in live germ cell counts over time.

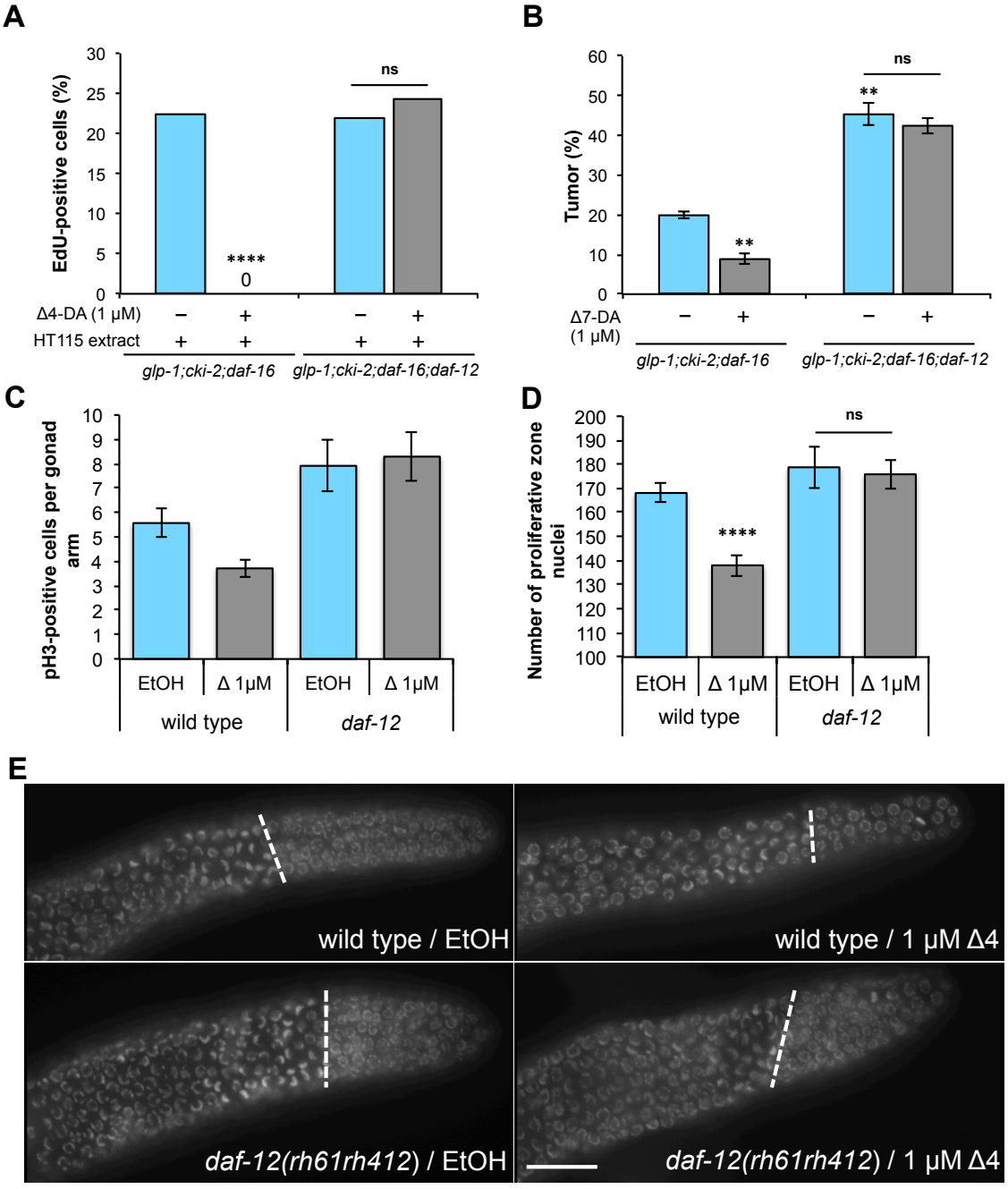

Figure 4.3. The inhibition of germ cell proliferation is dependent on the nuclear hormone receptor DAF-12. (A) Percentage of cells showing EdU incorporation for *glp-1(ts)*; *cki-2*; *daf-16* germ cells as well as *glp-1(ts)*; *cki-2*; *daf-16; daf-12(rh61rh411)* germ cells growth with

HT115 bacterial extract (to stimulate EdU incorporation) and with either 1 μM Δ4-DA or ethanol control.

(B, C, D and E) Δ^7- and Δ^4-dafachronic acid, respectively, inhibit tumor formation (B), mitotic GSCs numbers in wild-type and (C), and the number of germ cell nuclei in the proliferative zone in wild-type (D) in a DAF-12-dependent manner. (E) Merged Z-stacks of Hoechst stained dissected gonads of wild-type (top panels) and *daf-12 (rh61rh412)* (bottom panels) mutant animals marking the proliferative zone with a dotted red line. Left panels are gonads treated with ethanol carrier (EtOH) control and right panels are gonads treated with 1 μM Δ^4-DA. Scale bar, 20 μM.

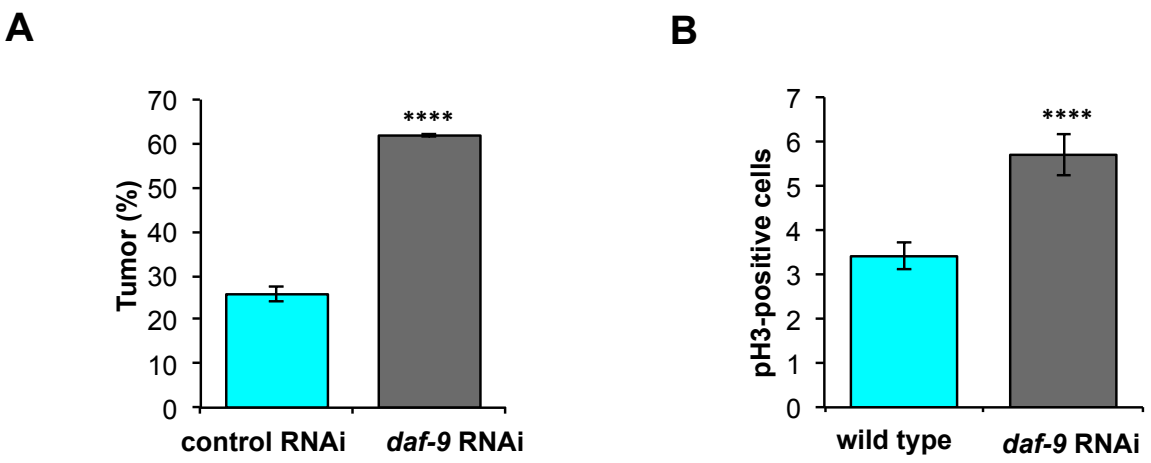

Figure 4.4. *daf-9* RNAi increases germ cell proliferation. Blocking dafachronic acid formation in vivo with *daf-9* RNAi increases tumor formation in *glp-1(ts)*; *cki-2*; *daf-16* mutants (A), and the number of mitotic GSCs per gonad arm in wild-type animals (B).

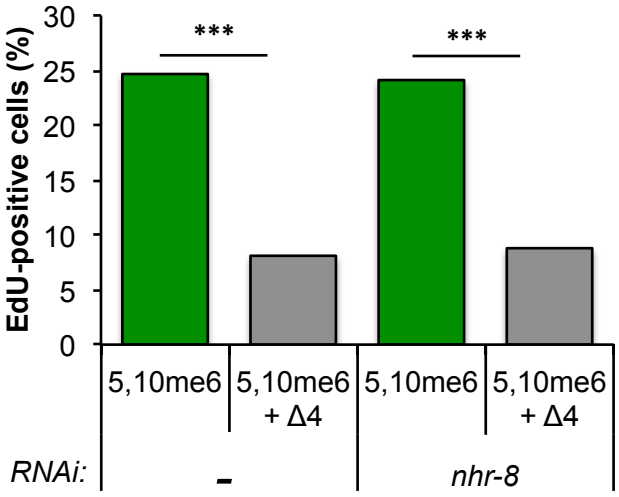

Figure 4.5. NHR-8 is not required for dafachronic acid-mediated germ cell inhibition. Percentage of cells showing EdU incorporation when cells were isolated from *glp-1(ts)*; *cki-2*; *daf-16* grown under control RNAi or *nhr8 RNAi*. The germ cell stimulatory folate 5, 10 methynele-THF-Glu_6 was added to each condition along with either ethanol carrier control (EtOH) or 1 μM Δ^4-DA.

CHAPTER 5

CONCLUSIONS AND DISCUSSION

Regulation of Notch signaling by CRL2^{LRR-1}

In Chapter 2 we described CRL2^{LRR-1} as a novel negative regulator of LIN-12/Notch signaling during *C. elegans* vulval development. Loss of LRR-1 leads to an impenetrant (~1%) Muv phenotype, which we have confirmed is due to a failure in negatively regulating LIN-12/Notch signaling. Although *lrr-1* has an impenetrant Muv phenotype, its Muv phenotype is exacerbated in sensitized backgrounds that enhance LIN-12/Notch activity, as well as genetic backgrounds that decrease Ras–MAPK activity. The modest phenotype of *lrr-1* mutant alone is emblematic of many regulators of both Ras–MAPK and LIN-12/Notch involved in *C. elegans* vulva development, which have no abnormal phenotypes on their own, but in combination with loss-of-function mutations for other pathway regulators, display abnormal vulval phenotypes. For example, loss-of-function in the negative regulators of the Ras–MAPK pathway *ark-1*, *sli-1*, *gap-1*, and *unc-101* do not have Muv phenotypes on their own, but display Muv in combination with each other as well as other components of the Ras–MAPK pathway (Berset et al., 2001; Berset et al., 2005; Sundaram, 2006). In addition, *sel-10*, an SCF ubiquitin ligase that binds to and degrades NICD (Gupta-Rossi et al., 2001; Hubbard et al., 1997; Oberg et al., 2001; Wu et al., 2001) was discovered as a suppressor of *lin-12* hypomorphs (Sundaram and Greenwald, 1993), but does not have a Muv phenotype on its own (Hubbard et al., 1997; Jager et al., 2004). SEL-10 also plays a role in other developmental aspects in *C. elegans* where LIN-12/Notch participates.

sel-10 null mutants suppress the 2 AC phenotype associated with *lin-12* hypomorphs (Sundaram and Greenwald, 1993); *sel-10* mutants enhance the 0 AC phenotype caused by over-active *lin-12* (Hubbard et al., 1997); enhance the egg-laying defect (Koegl et al.) caused by overexpression of *lin-12*; and enhance the gonad migration (Mig) defect associated with increased LIN-12/Notch activity in males (Hubbard et al., 1997). It will be interesting to analyze if $CRL2^{LRR-1}$ is involved in regulating LIN-12/Notch signaling with respect to these other developmental processes.

We identified DAF-12 and CES-1 as transcription factors that bind to regulatory regions of Notch transcriptional targets. RNAi elimination of DAF-12 or CES-1 causes reduction in the elevated *lip-1p*::GFP levels in *lrr-1* mutants. Although we do not know whether LRR-1 affects CES-1 levels, we have shown that DAF-12 protein levels are negatively regulated by LRR-1. We showed that LRR-1 does not affect *daf-12* mRNA levels, indicating that DAF-12 is regulated by LRR-1 at the post-transcriptional or post-translational level. The exact mechanism by which DAF-12 protein levels are affected by $CRL2^{LRR-1}$ is subject to further research.

Our studies show LRR-1 is a negative regulator of LIN-12/Notch levels, both the full-length receptor as well NICD levels. The downstream Notch target genes (*lst-2, lst-4, dpy-23*, and *lip-1*) are also elevated in *lrr-1* mutants. However *sel-10* mutants do not show elevated levels of all Notch target genes. These results point towards a key difference in the mechanism of regulation of LIN-12/Notch signaling by these two genes. Our results imply that LRR-1 acts downstream of SEL-10, at the level of regulating Notch target gene transcription, which in turn may work via a positive feedback loop to to stabilize LIN-12 full-length as well as NICD protein levels in the VPCs in *lrr-1* mutants.

Humans and other mammals have four Notch proteins (Notch1-4), that although very similar to each other, have differences in their extracellular and cytoplasmic domains as well as

five different ligands belonging to the Delta (DLL1, 3 and 4) and Serrate (Jagged1, Jagged 2) family (Capaccione and Pine, 2013). Notch is known to positively regulate itself in certain cancerous cell lines. Mutations in the C-terminal domain of Notch that prevent NICD degradation, are often found together with mutations in Fbw7 (human homolog of SEL-10) in T-cell acute lymphoblastic leukemia (T-ALL), suggesting that increased levels of NICD contribute to this cancer (O'Neil et al., 2007; Thompson et al., 2007). In T-ALL cell lines, the intracellular domain of Notch homolog Notch3 (NICD3) activates the micro RNA *mir-233*, which represses Fbw7 levels (Borggrefe et al., 2016; Kumar et al., 2014). Therefore, via the regulation of *mir-233*, Notch ensures that its intracellular cleaved product has a longer half-life in tumorous cells. Prolyl isomerase 1 (Pin1) is a direct transcriptional target of Notch1 which was shown to positively reinforce Notch signaling in breast cancer cells by enhancing the γ-secretase mediated cleavage of Notch1 (Rustighi et al., 2009). Pin1 directly binds to phosphorylated Notch1 at conserved serine/threonine rich (STR) region to possibly bring about a conformational change in the Notch1 receptor so that γ-secretase can efficiently cleave it and release NICD1 (Rustighi et al., 2009). Pin1 proteins are cis/trans isomerase enzymes that carry out the catalytic conversion of specific phosphorylated serine/threonine-proline (STP) motifs and induces conformational changes that are sometimes required for full activity of certain proteins and is involved in cross-talk of a number of oncogenic signaling pathways in breast cancer and other cancers (Liou et al., 2011; Wulf et al., 2005). Using a mouse model, Pin1 was later shown to be a regulator of stem cell feature of both normal stem cells and cancer stem cells (CSCs) in the mammary gland (Rustighi et al., 2014). Besides assisting γ-secretase to cleave NICD1 (Rustighi et al., 2009), Rustighi et. al have also shown that following isomerization by Pin1, Notch1 (and possibly Notch4) gets de-phosphorylated by PP2A phosphatase thereby escaping Fbwx7α (Fbw7)

dependent ubiquitination and degradation (Rustighi et al., 2014). Therefore by negatively regulating the Notch inhibitor Fbw7, Pin1 ensures CSC self-renewal and replicative potential (Rustighi et al., 2014). Notch regulates a multitude of target genes during development, and in certain cancerous cell lines, a few Notch target genes are able to fuel a feed-forward cycle that ensures Notch can continue to signal (Borggrefe et al., 2016; Rustighi et al., 2009; Rustighi et al., 2014). In this light, further work is important to determine whether human $CRL2^{LRR1}$-mediated regulation of Notch signaling that we show in *C. elegans* vulva development, is conserved in humans. Human $CRL2^{LRR1}$ could similarly be involved in a feed-forward mechanism in regulating Notch signaling in certain cancerous or non-cancerous cells.

Notch signaling has been shown to play opposite roles as either an oncogenic influence or as a tumor suppressor depending on the cancer type (Miele and Osborne, 1999). Notch signaling pathway components, including receptors and its ligands, are overexpressed in a variety of cancers such as cervical, colon, lung, prostrate, renal carcinoma, pancreas, and large cell lymphomas; whereas the role of Notch as a tumor suppressor is seen in fewer instances such as in hepatocellular carcinoma and small cell lung cancer (Wang et al., 2010). Identification of components or regulators of Notch signaling under these vastly different contexts is of utmost importance for the development of targeted therapeutics and drugs.

Bacterial folates stimulate and Dafachronic acid inhibits germ stem cell proliferation

In Chapter 3, we describe a novel method to obtain and maintain *C. elegans* germ stem cells in culture. The optimized media, CeM1, can maintain live *C. elegans* germ stem cells for a period of over one month. *C. elegans* embryonic cells have been isolated and maintained in culture, but with poor survival (Christensen et al., 2002; Strange et al., 2007). This is the first known system

that has been able to propagate isolated *C. elegans* germ cell cultures, and using this system as a tool we have discovered novel factors that affect the proliferation of these stem cells. We identified specific folates from the bacteria that *C. elegans* eat, 10-formyl-THF-Glu_n and 5,10-methenyl-THF-Glu_n, as signals that affect germ stem cell proliferation. Other folate species, folic acid, THF, 5-formyl-THF, and 5-methyl-THF, did not have any germ cell stimulatory ability. The two stimulatory folate species show increasing germ cell proliferation with larger numbers of poly-Glu. Significantly, the stimulatory folates activate germ stem cell proliferation independent of the one-carbon metabolism cycle. The stimulatory folate 5,10-methenyl-THF-Glu_1 is able to rescue the one-carbon metabolism deficiency of the *folt-1*RFC mutants less effectively than the non-stimulatory folate S-5-formyl-THF-Glu_1. Further, the bacterial folate precursor dihydropteroate can also stimulate germ cell proliferation in *C. elegans*. This result is particularly notable, because *C. elegans*, like other animals, does not have the enzyme required to convert pteroates to folates (dihydrofolate synthase), and therefore dihydropteroate cannot participate in one-carbon metabolism. As expected, dihydropteroate fails to rescue *folt-1*/RFC deficiency.

We have demonstrated that the stimulatory folates as well as dihydropteroate require the human folate receptor (FR) homolog FOLR-1 to stimulate germ cell proliferation. Our work implicates bacterial folates as ligands that signal germ stem cell proliferation via the FR homolog. Future work is required to determine whether these stimulatory folates as well as dihydropteroate bind FOLR-1 and if so with what affinity. Although FRs are not widely expressed in human tissues, FRα, β, and γ are overexpressed in a variety of cancerous tissues such as those in the ovary, uterus, kidney, pancreas, leukemic blasts in chronic myelogenous leukemia (CML), and acute myelogenous leukemia (Antony, 1996; Kelemen, 2006; Ledermann et al., 2015; Parker et

al., 2005). In most cell studied, FRα is not the major carrier of folates. In ovarian cancer cells, FRα contributes to only 20% uptake of folates, whereas the major carrier RFC brings in about 70% of folates into the cell (Corona et al., 1998). Yet, RFC activity is not linked to cancer. In fact, overexpressing RFCs in ovarian cancer cells leads to reduction in proliferation, migration and invasiveness of the cancer (Siu et al., 2012).

Studies in human cells implicate FRs in signaling independent of one-carbon metabolism. Antibodies that bind to cell surface receptors can activate signaling independently of ligand binding. Anti-FR antibodies significantly increase cell proliferation in erythropoiesis, without being able to increase the intracellular folate levels (Antony et al., 1987). In ovarian carcinoma cell lines, incubation with an anti-FRα antibody increases the physical association of FRα with the non-receptor tyrosine kinase Lyn (Miotti et al., 2000). Downstream signaling pathways such as non-receptor tyrosine kinase c-src and ERK as well as phospho-STAT are activated via FRα in endothelial cells, colon cancers cells and neural stem cells (Kuo et al., 2015; Lin et al., 2012; Zhang et al., 2009). Overexpression of FRα was also shown to increase Notch3 expression and activity in a mouse gonadotroph cell line (Yao et al., 2009). It will be of significant interest to determine if the germ cell stimulatory folates 10-formyl-THF-Glu_n and dihydropteroate can activate downstream signaling molecules such as ERK, STAT as well as non-receptor tyrosine kinases in *C. elegans*, and characterize the mechanism by which folates are able to stimulate activation of these signaling pathways.

We also identified the steroid hormone dafachronic acid (DA) as a negative regulator of germ stem cell proliferation (Chapter 4). We show that the Δ^4-DA and Δ^7-DA inhibit germ cell proliferation of isolated germ cells in vitro, as well as tumor formation and the number of mitotic germ cells in intact wild-type animals. We demonstrate that DA requires the nuclear hormone

receptor DAF-12 to negatively regulate germ cells. RNAi elimination of the DA synthesis enzyme DAF-9 leads to increased tumor production in a temperature sensitive germline tumor mutant, as well as increased mitotic cell numbers in wild-type animals. This suggests that DA acts normally in both tumorous mutants and wild-type animals to inhibit germ cell proliferation.

Dietary restriction (DR) has been shown to increase *daf-9* mRNA levels as well as accumulation of DAs in *C. elegans*, which leads to a reduction in the number of proliferative germ cell in wild-type gonads (Thondamal et al., 2014). A non-canonical nuclear hormone receptor NHR-8 was shown to be required for mediating DR-induced reduction in germ cell numbers (Thondamal et al., 2014). However, the involvement DAF-12 in DR-mediated germ cell number reduction was not tested. While DA is known to bind to DAF-12 (Motola et al., 2006), there is no evidence that DA is able to bind to NHR-8. DAs bind to DAF-12 similar to how bile acids bind to the mammalian DAF-12 homolog FXR (Zhi et al., 2012). Although it is known that *C. elegans* DA binds to DAF-12 (Motola et al., 2006), we do not know the exact mechanism by which DA inhibits germ cell proliferation. Being a nuclear hormone receptor, DAF-12 has both ligand binding and DNA binding domains, and DA can bind to DAF-12 and regulate its transcriptional targets (Antebi, 2006). Identification of the mRNAs upregulated or downregulated in a DAF-12-dependent manner in germ cells upon DA binding will provide insights into the mechanisms by which DA regulates germ cell development.

References

Antebi, A. (2006). Nuclear hormone receptors in C. elegans. WormBook, 1-13.

Antony, A.C. (1996). Folate receptors. Annual review of nutrition *16*, 501-521.

Antony, A.C., Bruno, E., Briddell, R.A., Brandt, J.E., Verma, R.S., and Hoffman, R. (1987). Effect of perturbation of specific folate receptors during in vitro erythropoiesis. J Clin Invest *80*, 1618-1623.

Berset, T., Hoier, E.F., Battu, G., Canevascini, S., and Hajnal, A. (2001). Notch inhibition of RAS signaling through MAP kinase phosphatase LIP-1 during C. elegans vulval development. Science *291*, 1055-1058.

Berset, T.A., Hoier, E.F., and Hajnal, A. (2005). The C. elegans homolog of the mammalian tumor suppressor Dep-1/Scc1 inhibits EGFR signaling to regulate binary cell fate decisions. Genes & development *19*, 1328-1340.

Borggrefe, T., Lauth, M., Zwijsen, A., Huylebroeck, D., Oswald, F., and Giaimo, B.D. (2016). The Notch intracellular domain integrates signals from Wnt, Hedgehog, TGFbeta/BMP and hypoxia pathways. Biochimica et biophysica acta *1863*, 303-313.

Capaccione, K.M., and Pine, S.R. (2013). The Notch signaling pathway as a mediator of tumor survival. Carcinogenesis *34*, 1420-1430.

Christensen, M., Estevez, A., Yin, X., Fox, R., Morrison, R., McDonnell, M., Gleason, C., Miller, D.M., 3rd, and Strange, K. (2002). A primary culture system for functional analysis of C. elegans neurons and muscle cells. Neuron *33*, 503-514.

Corona, G., Giannini, F., Fabris, M., Toffoli, G., and Boiocchi, M. (1998). Role of folate receptor and reduced folate carrier in the transport of 5-methyltetrahydrofolic acid in human ovarian carcinoma cells. International journal of cancer *75*, 125-133.

Gupta-Rossi, N., Le Bail, O., Gonen, H., Brou, C., Logeat, F., Six, E., Ciechanover, A., and Israel, A. (2001). Functional interaction between SEL-10, an F-box protein, and the nuclear form of activated Notch1 receptor. The Journal of biological chemistry *276*, 34371-34378.

Hubbard, E.J., Wu, G., Kitajewski, J., and Greenwald, I. (1997). sel-10, a negative regulator of lin-12 activity in Caenorhabditis elegans, encodes a member of the CDC4 family of proteins. Genes & development *11*, 3182-3193.

Jager, S., Schwartz, H.T., Horvitz, H.R., and Conradt, B. (2004). The Caenorhabditis elegans F-box protein SEL-10 promotes female development and may target FEM-1 and FEM-3 for degradation by the proteasome. Proceedings of the National Academy of Sciences of the United States of America *101*, 12549-12554.

Kelemen, L.E. (2006). The role of folate receptor alpha in cancer development, progression and treatment: cause, consequence or innocent bystander? International journal of cancer *119*, 243-250.

Koegl, M., Hoppe, T., Schlenker, S., Ulrich, H.D., Mayer, T.U., and Jentsch, S. (1999). A novel ubiquitination factor, E4, is involved in multiubiquitin chain assembly. Cell *96*, 635-644.

Kumar, V., Palermo, R., Talora, C., Campese, A.F., Checquolo, S., Bellavia, D., Tottone, L., Testa, G., Miele, E., Indraccolo, S.*, et al.* (2014). Notch and NF-kB signaling pathways regulate miR-223/FBXW7 axis in T-cell acute lymphoblastic leukemia. Leukemia *28*, 2324-2335.

Kuo, C.T., Chang, C., and Lee, W.S. (2015). Folic acid inhibits COLO-205 colon cancer cell proliferation through activating the FRalpha/c-SRC/ERK1/2/NFkappaB/TP53 pathway: in vitro and in vivo studies. Sci Rep *5*, 11187.

Ledermann, J.A., Canevari, S., and Thigpen, T. (2015). Targeting the folate receptor: diagnostic and therapeutic approaches to personalize cancer treatments. Ann Oncol *26*, 2034-2043.

Lin, S.Y., Lee, W.R., Su, Y.F., Hsu, S.P., Lin, H.C., Ho, P.Y., Hou, T.C., Chou, Y.P., Kuo, C.T., and Lee, W.S. (2012). Folic acid inhibits endothelial cell proliferation through activating the cSrc/ERK 2/NF-kappaB/p53 pathway mediated by folic acid receptor. Angiogenesis *15*, 671-683.

Liou, Y.C., Zhou, X.Z., and Lu, K.P. (2011). Prolyl isomerase Pin1 as a molecular switch to determine the fate of phosphoproteins. Trends in biochemical sciences *36*, 501-514.

Miele, L., and Osborne, B. (1999). Arbiter of differentiation and death: Notch signaling meets apoptosis. Journal of cellular physiology *181*, 393-409.

Miotti, S., Bagnoli, M., Tomassetti, A., Colnaghi, M.I., and Canevari, S. (2000). Interaction of folate receptor with signaling molecules lyn and G(alpha)(i-3) in detergent-resistant complexes from the ovary carcinoma cell line IGROV1. Journal of cell science *113 Pt 2*, 349-357.

Motola, D.L., Cummins, C.L., Rottiers, V., Sharma, K.K., Li, T., Li, Y., Suino-Powell, K., Xu, H.E., Auchus, R.J., Antebi, A.*, et al.* (2006). Identification of ligands for DAF-12 that govern dauer formation and reproduction in C. elegans. Cell *124*, 1209-1223.

O'Neil, J., Grim, J., Strack, P., Rao, S., Tibbitts, D., Winter, C., Hardwick, J., Welcker, M., Meijerink, J.P., Pieters, R.*, et al.* (2007). FBW7 mutations in leukemic cells mediate NOTCH pathway activation and resistance to gamma-secretase inhibitors. The Journal of experimental medicine *204*, 1813-1824.

Oberg, C., Li, J., Pauley, A., Wolf, E., Gurney, M., and Lendahl, U. (2001). The Notch intracellular domain is ubiquitinated and negatively regulated by the mammalian Sel-10 homolog. The Journal of biological chemistry *276*, 35847-35853.

Parker, N., Turk, M.J., Westrick, E., Lewis, J.D., Low, P.S., and Leamon, C.P. (2005). Folate receptor expression in carcinomas and normal tissues determined by a quantitative radioligand binding assay. Analytical biochemistry *338*, 284-293.

Rustighi, A., Tiberi, L., Soldano, A., Napoli, M., Nuciforo, P., Rosato, A., Kaplan, F., Capobianco, A., Pece, S., Di Fiore, P.P.*, et al.* (2009). The prolyl-isomerase Pin1 is a Notch1 target that enhances Notch1 activation in cancer. Nature cell biology *11*, 133-142.

Rustighi, A., Zannini, A., Tiberi, L., Sommaggio, R., Piazza, S., Sorrentino, G., Nuzzo, S., Tuscano, A., Eterno, V., Benvenuti, F.*, et al.* (2014). Prolyl-isomerase Pin1 controls normal and cancer stem cells of the breast. EMBO molecular medicine *6*, 99-119.

Siu, M.K., Kong, D.S., Chan, H.Y., Wong, E.S., Ip, P.P., Jiang, L., Ngan, H.Y., Le, X.F., and Cheung, A.N. (2012). Paradoxical impact of two folate receptors, FRalpha and RFC, in ovarian cancer: effect on cell proliferation, invasion and clinical outcome. PloS one *7*, e47201.

Strange, K., Christensen, M., and Morrison, R. (2007). Primary culture of Caenorhabditis elegans developing embryo cells for electrophysiological, cell biological and molecular studies. Nature protocols *2*, 1003-1012.

Sundaram, M., and Greenwald, I. (1993). Suppressors of a lin-12 hypomorph define genes that interact with both lin-12 and glp-1 in Caenorhabditis elegans. Genetics *135*, 765-783.

Sundaram, M.V. (2006). RTK/Ras/MAPK signaling. WormBook : the online review of C elegans biology, 1-19.

Thompson, B.J., Buonamici, S., Sulis, M.L., Palomero, T., Vilimas, T., Basso, G., Ferrando, A., and Aifantis, I. (2007). The SCFFBW7 ubiquitin ligase complex as a tumor suppressor in T cell leukemia. The Journal of experimental medicine *204*, 1825-1835.

Thondamal, M., Witting, M., Schmitt-Kopplin, P., and Aguilaniu, H. (2014). Steroid hormone signalling links reproduction to lifespan in dietary-restricted Caenorhabditis elegans. Nat Commun *5*, 4879.

Wang, Z., Li, Y., and Sarkar, F.H. (2010). Notch signaling proteins: legitimate targets for cancer therapy. Current protein & peptide science *11*, 398-408.

Wu, G., Lyapina, S., Das, I., Li, J., Gurney, M., Pauley, A., Chui, I., Deshaies, R.J., and Kitajewski, J. (2001). SEL-10 is an inhibitor of notch signaling that targets notch for ubiquitin-mediated protein degradation. Molecular and cellular biology *21*, 7403-7415.

Wulf, G., Finn, G., Suizu, F., and Lu, K.P. (2005). Phosphorylation-specific prolyl isomerization: is there an underlying theme? Nature cell biology *7*, 435-441.

Yao, C., Evans, C.O., Stevens, V.L., Owens, T.R., and Oyesiku, N.M. (2009). Folate receptor alpha regulates cell proliferation in mouse gonadotroph alphaT3-1 cells. Experimental cell research *315*, 3125-3132.

Zhang, X.M., Huang, G.W., Tian, Z.H., Ren, D.L., and Wilson, J.X. (2009). Folate stimulates ERK1/2 phosphorylation and cell proliferation in fetal neural stem cells. Nutritional neuroscience *12*, 226-232.

Zhi, X., Zhou, X.E., Melcher, K., Motola, D.L., Gelmedin, V., Hawdon, J., Kliewer, S.A., Mangelsdorf, D.J., and Xu, H.E. (2012). Structural conservation of ligand binding reveals a bile acid-like signaling pathway in nematodes. J Biol Chem *287*, 4894-4903.